FTIR Investigations of Whey Protein Interactions in Relation to Model Food Systems

A thesis submitted to McGill University in partial fulfillment of the requirements of the degree of Ph.D.

By Diana Valtierra

Department of Food Science and Agricultural Chemistry

Macdonald Campus of McGill University

Short title:

FTIR studies of high-protein model food systems

ABSTRACT

The research presented in this thesis is centered on one of the most important food proteins, the bovine whey protein β-lactoglobulin. Thermal stability studies of the two main genetic variants of β-lactoglobulin (A and B) as well as AB mixtures from different sources, investigations of their interactions with glycomacropeptide (GMP) and the study of the interactions of β-lactoglobulin with other ingredients in a "high-protein cookie" model food system were conducted by Fourier transform infrared (FTIR) spectroscopic techniques. Although variants A and B of β-lactoglobulin differ from each other only at two amino-acid positions (64 and 118, where Asp and Val in the A variant are substituted by Gly and Ala, respectively, in the B variant), variable-temperature (VT)-FTIR studies in conjunction with two-dimensional correlation (2D-COS) spectroscopy demonstrated these differences had a much larger impact on β-lactoglobulin's thermal behavior than differences in the conditions that the protein had been subjected to during the isolation and purification procedures. Furthermore, VT-FTIR studies of β-lactoglobulin AB from different sources (undefined mixtures of variants A and B originating from pooled milk samples) yielded inconsistent results which is attributable not only to the different thermal behavior of the two variants but also to their interactions to form AA, BB, and AB dimers. Extension of these VT-FTIR studies to binary mixtures of GMP and β-lactoglobulin A, B, and AB from the different sources and at different ratios showed variable effects of protein-GMP interactions on the protein's thermal behavior. In the case of β-lactoglobulin A, its denaturation temperature in the mixtures with GMP was lower than that of the pure protein whereas the opposite trend was observed for β-lactoglobulin B and the AB mixtures. To study the interactions of β-lactoglobulin with other food ingredients, a "high-protein cookie" model food system was formulated in consultation with the R&D center of a leading manufacturer of high-protein nutritional products. The spatial distribution of the protein, lipid, and carbohydrate ingredients in unbaked and baked model cookies was examined on the micron scale by employing focal-plane-array (FPA)-FTIR imaging microscopy in the attenuated total reflectance (ATR) mode, representing the first application of this "chemical imaging" technique to the study of a model food system. As such it was necessary to develop a multi-step protocol enabling the extraction of relevant information from hyperspectral data sets comprising thousands of spatially resolved FTIR spectra of each imaged sample. In addition, films cast from binary mixtures of β-lactoglobulin and each of the other ingredients at the concentration

ratio employed in the "high-protein cookie" formulation were examined by FPA-FTIR imaging microscopy before and after heating in order to investigate the effects of their interactions with β-lactoglobulin on the protein's secondary structure and thermal stability. These studies suggest the potential future role of FPA-FTIR imaging microscopy as a practical technique for use by the food industry to gain a better understanding of the behavior and interactions of food components that ultimately have a major impact on the quality of food products.

RESUME

La présente recherche porte sur l'étude d'une des plus importantes protéines alimentaires, la β-lactoglobuline de source bovine. La stabilité thermique des deux principales variantes génétiques de la β-lactoglobuline (A et B) ainsi que des mélanges AB provenant de différentes sources, leurs interactions avec les glycomacropeptides (GMP) ainsi que l'application de la β-lactoglobuline dans un modèle de biscuit hyper-protéiné y sont étudiés par la spectroscopie infrarouge à transformée de Fourier (IRTF). Même si les variantes A et B de la β-lactoglobuline ne diffèrent qu'aux positions 64 et 118 où l'Asp et la Val dans la variante A sont respectivement substituées par de la Gly et Ala dans la variante B; leurs analyses par la spectroscopie IRTF à température variable (IRTF-TV) ainsi que par corrélation bidimensionnelle des résultats spectroscopiques (2D-COS) il a été démontré que le type de variante a un impact plus important sur le comportement thermique de la β-lactoglobuline que la méthode d'isolation même. De plus, des études de IRTF-TV de la β-lactoglobuline AB de différentes sources ont rendus des résultats inconsistants attribuables non seulement aux différents comportements thermiques des deux variantes mais aussi à leurs interactions sous formes de dimères AA, BB et AB. L'application de ces études sur des mélanges binaires de GMP et β-lactoglobuline A, B et AB de différentes sources et sous différents ratios ont démontrés des effets variables de l'interaction GMP-protéine sur le comportement thermique de cette protéine. Dans le cas de la β-lactoglobuline A, sa température de dénaturation, lorsque mélangée avec le GMP est inférieure à celle de la protéine seule, l'effet inverse est observé avec les β-lactoglobuline B et AB. Le développement de la matrice d'un « biscuit protéiné » modèle fut effectué en collaboration avec le centre R&D d'une société spécialisée dans la conception et manufacture de produits hyper-protéinés. L'imagerie IRTF par matrice à plan focal (FPA-FTIR) ainsi que des techniques complémentaires furent utilisées pour examiner la distribution spatiale à l'échelle du micron des protéines, lipides, et glucides dans des biscuits de modèle crues ou cuites au four. Cette nouvelle application d' « imagerie chimique » dans l'étude d'un modèle alimentaire a nécessité le développement d'un protocol multi-étapes pour l'extraction d'information à partir données hyperspectrales. De plus, des films obtenus de mélanges binaires de β-lactoglobuline et chacun des autres ingrédients utilisés dans le « biscuit protéiné » furent aussi examinés par microscopie FPA-FTIR avant et après cuisson afin de mieux comprendre leurs effets respectifs sur la structure secondaire de la β-lactoglobuline ainsi que sa

stabilité thermique. Ces études présentent un potentiel futur du rôle de l'imagerie FPA-FTIR dans l'étude du comportement ainsi que des interactions de divers composants alimentaires.

ACKNOWLEDGEMENTS

I would like to give my most sincere gratitude to all the people responsible for making this possible.

First of all, I would like to thank the Consejo Nacional de Ciencia y Tecnología (CONACYT) for awarding me with three and a half years of scholarship, without CONACYT and the support of the Mexican government to education programs this would have not happened.

I would like to thank my parents for all their financial and moral support; mom, dad, without your encouragement, your example and your help I would have never dreamt of studying a Ph. D., thank you for believing in me, thank you for your patience and your help, I know this took much, much longer than expected and I apologize for that. Dad, thanks for being the perfect example of hard work and perseverance, you never ever give up! Mom, you are my rock, the perfect guide and the best mother anyone could ask for! I love you both and God bless you always, I literally can´t repay you for everything you have done for me but I hope you´re proud of me.

I would like to thank Dr. Ismail, for his brilliant help, for his vast knowledge and guidance, thank you for the always evolving input over the past years, thank you for not only being a supervisor but also for being a great human being. I would like to give an immense thank you to Dr. Jacqueline Sedman, as Dr. Van de Voort once said "Jacqueline is the hidden jewel in the IR department", without her sagacious editing skills and her great knowledge this would have not been accomplished.

I would like to give a very big thanks to Bariatrix Nutrition Inc., M. Sc. Ziad Khoury and Vivekanand Dwivedy for their brilliant and invaluable help and expertise in developing the food model and for teaching me how proteins actually work in real food products and how difficult it is to develop these types of products.

I would like to thank the University of Concordia, Dr. Turnbull for allowing me to use the CD equipment and a huge thanks to Alain Tessier for his vast help with the ESI-MS research. I would also like to thank the QANUC NMR Facility and Dr. Sameer Al-Abdul-Wahid; the NMR

experiments were recorded at the Québec/Eastern Canada High Field NMR Facility, supported by NSERC, FQRNT and McGill University.

I would like to thank my lab mates: Dr. Pedro Alvarez, Dr. Laura Carranza, Dr. Alexandra Grygorczyk, Dr. Ahmed Gomaa, Dr. Andrew Ghetler, Dr. Frances Nsonzi, M. Sc. Alexander Enfield and Marianna Aboulhosn for passing on the knowledge, for their input and their help during my research and the great moments in and out of the lab.

I would like to thank my siblings Sofia, Acereth and Salvador for their love and moral support. I would like to thank my friends for also making the road much more pleasant: Laura, Lily, Diana, Paula, Félix, Plamen, Anja, Alfredo, Emilio, Maribel, Martín and Pablo. And last but not least, I would like to thank Mikiko Ichihashi for her enourmous support, covering for me at work and making food for me while I wrote my last drafts.

CONTRIBUTIONS OF AUTHORS

Chapters 3, 4 and 5 are being prepared for publication. The author of the thesis is responsible for developing the ideas and concepts presented and for the analysis of all the data in these studies. Dr. Ashraf A. Ismail, the thesis supervisor, provided guidance and support throughout the course of this research. Dr. Jacqueline Sedman provided vital advice and editing support for this thesis.

Chapter 3: Examination of the secondary structure and thermal behavior of β-lactoglobulin variants A and B obtained from different sources

Chapter 4: Study of binary mixtures of GMP and β-lactoglobulin A, B, and AB from different sources

Chapter 5: Interactions of β-lactoglobulin with other ingredients in a "high-protein cookie" model food system

CONTRIBUTIONS TO KNOWLEDGE

The following are considered to be the primary contributions to knowledge resulting from the research presented in this thesis.

1. Impact of protein isolation method on conformational mobility and thermal unfolding of β-lactoglobulin

β-Lactoglobulin is among the most well-studied food proteins and has been the subject of several FTIR investigations reported in the literature; but there are many discrepancies in the results obtained by different research groups. The present study is the first to investigate the impact of the conditions to which the protein had been subjected during its isolation and purification on its FTIR spectroscopic behavior by directly comparing β-lactoglobulin samples obtained from different sources: food-grade β-lactoglobulin (a mixture of genetic variants A and B), including samples of the individual genetic variants separated by ion-exchange chromatography; variant A isolated in the laboratory from the milk of a homozygous cow; and research-grade β-lactoglobulin A, B, and AB from a commercial supplier (studied as received, no separation performed). For each of the individual genetic variants, samples from different sources were generally found to differ in their denaturation temperature and extent of aggregation but not in the sequence of unfolding events determined by two-dimensional correlation (2D-COS) spectroscopy. Thus, the results of these studies demonstrate that discrepancies noted in the literature on the conformational stability of β-lactoglobulin, including studies of the individual genetic variants, may be attributed in part to the protein isolation/purification history of the samples.

2. Differences in conformational mobility and thermal unfolding and aggregation pathways of β-lactoglobulin variants A and B

Although β-lactoglobulin A and B had been previously studied individually by FTIR spectroscopy under various physicochemical conditions, the detailed analysis of the variable-temperature FTIR (VT-FTIR) spectra of samples from several sources (recorded in D_2O solutions) through the application of differential and 2D correlation spectroscopy provided new insight. In particular, spectral changes at relatively low temperatures (30-60^oC), attributed to H-D exchange of particular

sub-populations of amide groups within β-sheet structure, yielded the first FTIR spectroscopic evidence that the B variant has substantially more conformational mobility than the A variant.

3. Effects of glycomacropeptide (GMP) on the thermal unfolding and aggregation of β-lactoglobulin

VT-FTIR studies of binary mixtures of GMP and β-lactoglobulin A, B, and AB from different sources and at different ratios showed variable effects of protein-GMP interactions on the protein's thermal behavior, such that the denaturation temperature of β-lactoglobulin A in the mixtures with GMP was lower than that of the pure protein whereas the opposite trend was observed for β-lactoglobulin B and the AB mixtures.

4. First demonstration of the infrared imaging of the spatial distribution of components in a model food by focal-plane-array-FTIR (FPA-FTIR) spectroscopy

The spatial distribution of the protein, lipid, and carbohydrate ingredients in a "high-protein cookie" model food was examined on the micron scale by employing focal-plane-array (FPA)-FTIR imaging microscopy in the attenuated total reflectance (ATR) mode. This work represents the first application of this "chemical imaging" technique to the study of model food systems and entailed the development of a multi-step protocol enabling the extraction of relevant information from the hyperspectral data.

5. Examination of protein secondary structure in the presence of a variety of other food ingredients under baking (heating) conditions to gain a better understanding of the behavior and interactions of the components of a model food system

FPA-FTIR spectroscopy was employed to assess the changes in the secondary structure of β-lactoglobulin in the presence of each of the other components of a model food system under baking (heating) conditions. This study represents the first attempt to exploit the detailed information on protein secondary structure provided by FTIR spectra for the purpose of examining the interactions of a food protein with a variety of other food ingredients, including sugars, fats, lecithins, polyols and carbohydrate gums.

TABLE OF CONTENTS

LIST OF TABLES

TABLE **PAGE**

LIST OF FIGURES

FIGURE **PAGE**

CHAPTER 1. INTRODUCTION

1.1. GENERAL INTRODUCTION

Food proteins have been thoroughly studied for many decades in order to understand their behavior and their functional properties as components of foods or as ingredients employed in processed food formulations. For example, whey proteins, which comprise approximately 20% of the proteins in milk, are highly important in food processing owing to their functional properties (e.g., emulsification, water-holding capacity, gelation), and extensive research has been carried out by food scientists to gain a better understanding of their structure-functionality relationships and thereby obtain information that may assist the food industry in making better use of these proteins. Owing to the complexity of most food systems, much of this type of research has involved the study of individual food proteins or, more commonly, food protein commodities such as whey protein concentrate (WPC) and whey protein isolate (WPI). However; the behavior and properties of proteins when they are present in a complex food matrix (such as a finished food product) are often not the same as those observed in these types of laboratory studies. This disparity, which has been termed the "food protein paradox", reflects the sensitivity of proteins to their environment and their interactions with numerous other components present in foods. Therefore, there is an increased tendency to use model food systems in conjunction with sophisticated research tools, where the formulation and processing of a given model food system in the laboratory are designed to resemble those used for the food product (Harper, 2009; Owusu-Apenten, 2004).

Food scientists have a large variety of spectroscopic and non-spectroscopic methods available to them for the study of model food systems. Among these, Fourier transform infrared (FTIR) spectroscopy has several unique advantages including the possibility to perform *in situ* analysis of food matrices in liquid, solid or even gaseous state and to obtain both qualitative and quantitative compositional information (Sedman *et al.*, 2010; Delaunay *et al*., 2008; Sørensen, 2003). Another important advantage in relation to the study of protein-containing model food systems is the well-established utility of FTIR spectroscopy as a technique for the study of protein secondary structure (Barth, 2007). Infrared imaging is a rather new technology that combines the information content of FTIR spectroscopy with spatial resolution on the micron scale, thereby

providing a vast amount of information on heterogeneous samples. Within the food science domain, infrared imaging is considered to be a promising technique for studies of network microstructures in foods at a molecular level, and it has also made its way into the food industry as a quality control technology (Li-Chan *et al*., 2010).

The research presented in this thesis was directed toward the formulation and study of a "high-protein cookie" model food system. The elaboration of the "cookie" model food system was done in consultation with the Product Development team of a leading manufacturer of high-protein products intended to help people achieve weight loss and weight maintenance. In addition to being formulated as a high-protein nutritional product, the "high-protein cookie" is also a model for a baked food product that addresses the growing market demand for gluten-free products. While gluten-free baked products generally lack the desirable textural characteristics that the gluten proteins in wheat flour impart to baked goods, this problem can be overcome, to a certain extent, through the use of emulsifiers, humectants and bulking agents such as lecithin, sorbitol, and polydextrose (Gallagher *et al*., 2005; Zoulias *et al*., 2000; Conforti and Lupano, 2004; Ranhotra *et al*., 1980). There have been previous studies from different research groups on partial substitution of wheat flour with non-wheat proteins, such as soy flour or rice flour, in order to improve the protein quality and content of wheat-based baked products; however, there are no studies involving the complete replacement of wheat proteins with another food protein (Pérez *et al*., 2008; Mohsen *et al*., 2009; Conforti and Lupano, 2004). In more general terms, most previous research on high-protein food systems has focused on nutritional aspects (Veldhorst *et al*., 2008; Booth *et al*., 1970; Bensaïd *et al*., 2002; Vandewater and Vickers, 1996).

Various types of proteins such as whey protein, soy protein, caseinates and gelatin are commonly employed in formulating high-protein nutritional products. Among these, whey protein concentrates (WPCs) and whey protein isolates (WPIs) are widely used in high-protein beverages and nutritional bars owing to their high nutritional value and excellent functional properties (Holsinger *et al*., 1974; Grygorczyk, 2009). β-Lactoglobulin is the major whey protein in cows' milk, constituting ~50% of the protein content of bovine whey, and is the predominant contributor to the functional properties of whey protein concentrates and whey protein isolates.

Bovine β-lactoglobulin has been extensively studied by FTIR spectroscopy, in large part because its highly structured amide I' band provides a wealth of information concerning the conformational changes that this protein undergoes in response to changes in its environment. As such, the availability of food-grade β-lactoglobulin afforded us the possibility of formulating a "high-protein cookie" using β-lactoglobulin as the sole protein source to serve as a model food system ideally suited for study by FTIR spectroscopy and infrared imaging.

1.2 OBJECTIVES

The research presented in this thesis had three primary objectives:

- To examine the thermal behavior of the main variants of β-lactoglobulin by FTIR spectroscopy, with particular attention to the effects of differences in protein isolation conditions;
- To investigate the interactions of β-lactoglobulin with glycomacropeptide (GMP), the casein-derived peptide present in sweet whey;
- To study the interactions of β-lactoglobulin with other food components in a "high protein cookie" model food system.

These objectives were addressed by exploring several experimental approaches with the following specific objectives:

1. To study the conformational mobility, thermal stability, and unfolding pathway of β-lactoglobulin (AB as well as variants A and B individually) from different sources by variable-temperature FTIR (VT-FTIR) and two-dimensional correlation (2D-COS) spectroscopy
2. To probe the interactions of β-lactoglobulin A, B, and AB with GMP by studying the conformational mobility thermal stability and unfolding pathway of the protein in mixtures with GMP by VT-FTIR and 2D-COS and comparing the results directly with those obtained in the absence of GMP
3. To develop "high protein cookie" model food systems using β-lactoglobulin, GMP and β-lactoglobulin/GMP as the protein sources
4. To apply texture, water activity and moisture content analyses in the examination of the model food systems

5. To apply focal-plane-array-FTIR (FPA-FTIR) imaging and variable-pressure-scanning electron microscopy (VP-SEM) to examine the distribution of the components in the model food systems
6. To examine the thermal stability of β-lactoglobulin (under baking conditions) in the presence of individual components of the model food system (carbohydrates, fats, and emulsifiers) as well as in baked model cookies

CHAPTER 2: LITERATURE REVIEW

2.1. AN INTRODUCTION TO MILK PROTEINS

Milk is a secretion of the mammary glands of female mammals and its main function is to nourish their young. Milk contains many essential nutrients as well as hormones, modulators and growth factors. The main constituents of milk are listed in Table 2.1.

Lactose is the main carbohydrate present in milk, which is a disaccharide, composed of D-glucose and D-galactose; lactose is a reducing sugar which can react with the γ–amino group of lysine residues in proteins (Maillard reaction); this can occur during long storage or during heating, resulting in browning (desired depending on the product), loss of nutritive value and off-flavors. Most fat in milk is present as fat globules made up largely of triacylglycerols (95-96%) which can be quite complex since the component fatty acids can vary in chain length, from 2 to 20 carbon atoms, and in unsaturation, from 0 to 4 double bonds (Belitz, 2009; Walstra *et al.*, 1999, Walstra *et al.*, 2006). The nitrogen content in milk is distributed between proteins (~95%) and non-protein compounds (~5%). The protein composition is shown in Table 2.2 (Walstra *et al.*, 2006; Alhaj *et al.*, 2007, Yalçin, 2006; Robbins *et al*., 1999). There are two main protein fractions in milk: the caseins and the whey proteins; all the proteins listed below caseins in Table 2.2 belong to the whey protein fraction.

Table 2.1. Milk composition (Walstra *et al.*, 2006).

Component	Average content in milk (%w/w)
Water	87.1
Solids non-fat	8.9
Sugar (mainly lactose)	4.8
Fat	4.0
Protein (casein micelles and soluble whey proteins)	3.3
Mineral substances	0.7
Organic acids	0.17
Miscellaneous	0.15

Table 2.2. Concentrations of milk proteins (Walstra *et al.*, 2006).

Protein	Concentration (g/L)
Caseins	22.5
β-Lactoglobulin	3.2
α-Lactalbumin	1.2
Bovine serum albumin	0.4
Immunoglobulins	0.7
Glycomacropeptide	1.2
Lactoferrin	0.1
Lactoperoxidase	0.03
Lysozyme	0.0004

2.1.1. Caseins

Caseins constitute 80% of the protein present in milk and they are a mixture of four different types of casein molecules: α_{s1}- (10 g/kg), α_{s2}- (2.6 g/kg), β- (9.3 g/kg) and κ-casein (3.3 g/kg). Unlike whey proteins, caseins are not globular proteins and they are organized as "micellar"

structures. The casein micelles contain colloidal calcium phosphate, hence they contain 77% of calcium present in milk; either bound directly to the casein or as solid calcium phosphate within the micelle structure. Caseins have an isoelectric point (pI) of ~4.6, hence they can be precipitated from milk at pH 4.6. However; even though all caseins can precipitate at pH 4.6 both α–casein and β–casein can also precipitate in the presence of calcium ions while κ–casein does not. Nevertheless, during the cheese making process κ-casein can be easily attacked by rennet giving as a result the curdling of milk (Yalçin, 2006; Robbins *et al*., 1999; Farrell *et al*., 1996; Walstra 2006).

2.1.1.1. α_{s1}-Casein (α_{s1}-CN). Consists of 199 amino acid residues with discernible hydrophobic regions, contains a high concentration of phosphoseryl residues, enabling it to bind Ca^{2+} (Belitz *et al*., 2009; Malin *et al.,* 2001; Walstra, 2006).

2.1.1.2. α_{s2}-Casein (α_{s2}-CN). Contains 207 amino acid residues, it is the most hydrophilic fraction of caseins and it is also extremely sensitive to ionic strength due to its distinct domain of high net charge (Belitz *et al*., 2009).

2.1.1.3. β-Casein (β-CN). Constitutes 35-45% of the casein fraction in milk, three-fourths of its residues are hydrophobic making it the hydrophobic fraction of caseins (Belitz *et al*., 2009; Walstra, 2006; Kumosinski *et al*., 1993).

2.1.1.4. κ-Casein (κ-CN). There are three known genetic variants of κ-CN: A, B, and C. κ-CN is the stabilizing portion of the casein micelle held together by intermolecular disulfide bonds and it is the only glycosylated casein fraction. The presence of κ-CN on the surface of the casein micelle (~30% of the micellar surface) creates a hairy, sterically stabilizing layer around the casein micelle preventing other casein micelles from approaching too closely. It has been said by previous researches that individual κ-CN molecules crosslink into disulfide-bonded polymers projecting the hydrophilic tails into the milk serum while the hydrophobic regions are attached to the micelle core (Belitz *et al*., 2009; Farrel *et al*., 1996; Creamer *et al*., 1998).

2.1.2. Whey proteins (serum proteins)

Whey is the fluid that remains after coagulation of the caseins (curd) and it retains about 55% of the total milk nutrients, being proteins among those nutrients; however, in the past whey was discarded into rivers since it was only considered as a by-product of cheese production (Fitzsimons *et al*., 2007). There are two types of whey: acid whey (pH ≤ 5.1) which occurs when the curd is produced by direct acidification of milk, as in cottage cheese manufacture; and sweet whey (pH ≥ 5.6) which is obtained after rennet-coagulation, as in most cheese making processes. The main components of whey are shown in Table 2.3. As indicated by their name, whey proteins are present in whey and there are several factors which determine their concentration, such as the type of whey, the source of milk (e.g. bovine), the type of feed for the cattle, the stage of lactation and the quality of processing (Madureira *et al.*, 2007).

Table 2.3. Main components of bovine whey.

Component	Concentration (g/L)
Lactose	45-50
Soluble proteins: ➢ β-Lactoglobulin (~50%) ➢ α-Lactalbumin (~25%) ➢ Glycomacropeptide (sweet whey) (~15-20%) ➢ Bovine serum albumin (~8-10%) ➢ Minor components: Immunoglobulins	6-8
Lipids	4-5
Mineral salts (NaCl, KCl), calcium salts	0.8
Lactic and citric acids	0.5

Whey proteins are globular proteins with a relatively high hydrophobicity and their amino acid chains are compactly folded and the stability of their structure is maintained by non-covalent interactions and by covalent disulfide bonds. Whey proteins have a substantial α-helical content, in which the acidic/basic and hydrophobic/hydrophilic amino acids are distributed in a more or

less balanced way. Given their globular nature, most of the reactive non-polar amino acids are buried in the hydrophobic core of the protein and the polar side chains are exposed on the exterior of the protein (Madureira *et al*., 2007; Lee *et al*., 2007).

2.1.2.1. β-Lactoglobulin

Bovine β-lactoglobulin (β-lg) is the major protein in the whey fraction of cows´ milk (~50%); thus, its physicochemical properties tend to dominate in whey protein preparations. β-Lactoglobulin has a molecular weight of 18 kDa in its monomeric state, its polypeptide chain consists of 162 amino acids, it has two intramolecular disulphide bridges at Cys 66–Cys 160 (strand D and C-terminal, respectively) and at Cys 106–Cys 119 (strand G-strand H, respectively), and one free thiol group at Cys 121 (strand H) (Cavallieri *et al*., 2008; Edwards *et al*., 2002).

β-Lactoglobulin is a member of the family of lipocalins (lipocalycins). These are proteins with capacity to carry small lipophilic molecules such as vitamins, hormones and fatty acids. Lipocalins may have very different amino acid sequences but their common feature is to have eight β-strands folding into four antiparallel β-sheets to form a "β-barrel" ("basket-like structure"), thus generating a hydrophobic core. In the native state (Figure 2.1), β-lactoglobulin consists of one α-helix and nine β-strands, forming a flattened β-barrel core, providing a binding site for a wide variety of amphiphilic or hydrophobic molecules and a number of simple and complex ions (Dufour *et al*., 1999, Zhang and Keiderling, 2006; García *et al.*, 2007; Martins *et al*., 2008; Perez and Calvo, 1995).

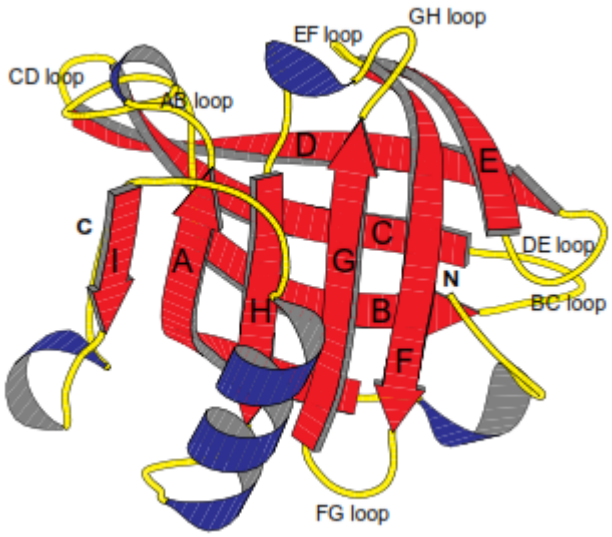

Figure 2.1. Ribbon diagram of β-lactoglobulin. The nine strands that form the β–barrel structure of β-lactoglobulin are labeled from A to I (red), the loops (yellow) between the strands are indicated, and the main α–helical (blue) structure is shown at the front of the figure. Reprinted, with permission, from Brownlow *et al.*, 1997.

There are eight genetic variants of β-lactoglobulin; in ruminants the predominant variants are A, B and C for Jersey dairy cattle breed, and variant D of the Montbeliarde dairy cow; nevertheless, the most important and abundant variants in cows are A and B. β-Lactoglobulin A and B differ from each other only at positions 64 and 118, where Asp and Val in the A variant are substituted by Gly and Ala, respectively, in the B variant. These seemingly minor differences result in a slightly different isoelectric point of the two variants and they have a profound effect on the physicochemical properties of the protein, including structural flexibility, solubility, self-association properties, and pressure and temperature stability (Belitz *et al*., 2009; Meza-Nieto *et al*., 2007; Boye *et al*., 1997; Boye *et al*., 2004; Taulier and Chalikian, 2001).

β-Lactoglobulin exists in various states (monomer, dimer and octamer) as a function of pH, temperature, concentration, and genetic variant. It is present in its dimeric form in milk and at pH values between 7 and 5.2, which is tightly bound by hydrophobic interactions. The octamer occurs at pH values from 5.2 to 3.5 with variant A, but not with variants B and C; while the monomer occurs at a pH below 3, or above 8.0. The dimer dissociates into monomers when it is subjected to a pH < 3 preserving its native conformation. The protein undergoes irreversible denaturation at a

pH > 8.6, as well as when it is heated or when the partially unfolded protein is in the presence of Ca^{2+} ions (Taulier and Chalikian, 2001; Meza-Nieto *et al*., 2007; Boye *et al*., 1997; Bhattacharjee *et al*., 2005; D´Alfonso *et al*., 2002). When the free -SH group from Cys 121 is exposed on partial denaturation, it can participate either in protein dimerization via disulfide bridge formation or in reactions with other milk proteins, especially κ-casein and α-lactalbumin, during the heating of milk (Belitz *et al*., 2009; Meza-Nieto *et al*., 2007).

The "Tanford transition" is a conformational change that occurs at a pH between 7.1 and 8.2 when Glu 89 (naturally buried at pH 6.2), located in the E-F loop, is protonated and exposed, driving some of the loops connecting the β-strands towards the entrance to the hydrophobic calyx, thereby closing it (Martins *et al*., 2008). Previous authors demonstrated that upon heating β-lactoglobulin in solution (pH 6.7), all the α-helix and up to a fifth of the β-sheet structure were lost when reaching 70 °C. It was suggested that the state of β-lactoglobulin above 65 °C is not that of a classical molten globule (a compact state that has a largely native secondary structure), at least at low concentrations where dissociation of the dimer occurs below the denaturation temperature, to expose and destabilize the elements of secondary structure nearest to the homodimer interface (Qi *et al*., 1997).

Heat treatment of milk at 70 °C causes denaturation of β-lactoglobulin as well as other whey proteins and formation of complexes with casein micelles. Whey proteins interact with κ-casein, via hydrophobic interactions, through the formation of intermolecular disulfide bonds and calcium bridges; the result is a co-polymerization of the proteins. The extent of interaction between β-lactoglobulin and κ-casein depends on time and temperature of heating, concentration of the protein, pH value and if there are salts in the solution. Another fact is that the higher the concentration of the whey proteins, the more disruption of casein micelles is observed (Lucey *et al*., 1998; Vasbinder and De Kruif, 2001; Dalgleish *et al*., 1997; Elfagm and Wheelock, 1978; Donato *et al.*, 2007; Harte *et al*., 2007).

2.1.2.2. α-Lactalbumin

α-Lactalbumin is the second major whey protein and makes up 25% of total bovine whey protein. It is a 123-residue protein and there are two variants: A and B (Gln → Arg). The native structure consists of two domains: a large α-helical domain containing three major α-helices and two short 3_{10}-helices; and a β-domain containing three-stranded antiparallel β-pleated sheets. The two domains are connected by a calcium binding loop, the cysteine bridge between residues 73 and 91; and at the same time they are divided by a deep cleft between them, which is a second disulfide bridge between residues 61 and 77. Besides these two disulfide bridges, the tertiary structure of the protein is also stabilized at pH values in the range of 5.4- 9.0 by two additional disulfide bridges between residues 6 and 120 and residues 28 and 111, (Bushmarina *et al*., 2006; Permyakov and Berliner, 2000; Kundu and Kishor, 2004; Troullier *et al*., 2000).

Besides being a calcium-binding protein that enhances calcium absorption, α-lactalbumin is also a rich source of lysine, leucine, threonine and tryptophan. α-Lactalbumin is produced in the mammary epithelial cells during lactation and plays a key role in milk synthesis; it is one of the two components of lactose synthase, an enzyme which catalyzes the final step in lactose biosynthesis in the mammary gland. It is also one of the few proteins that remain intact upon pasteurization (Permyakov and Berliner, 2000; Yalçin, 2006; Noyelle and Van Dael, 2002; McGuffey *et al*., 2005).

α-Lactalbumin has a molten globule state conformation at acidic pH and in the apo-state at high temperatures; this conformational state may facilitate the insertion of proteins in membranes. The thermally denatured state of α-Lactalbumin has been found to share common characteristics with the molten globule state; the unfolding temperature is about 65°C for the native structure of the protein. When the bound Ca^{2+} is removed (apo-state), the unfolding temperature decreases to about 35°C due to the loss of tertiary structural stability. At pH 2.0, much secondary structure is retained but a complete loss of the characteristic thermal transition occurs. This suggests that the molten globule is thermodynamically indistinguishable from the thermally unfolded states while maintaining primarily native-like secondary structure (Permyakov and Berliner, 2000; McGuffey *et al*., 2005; Mizuguchi *et al*., 1997).

2.1.2.3. Bovine serum albumin (BSA)

Bovine serum albumin is a relatively large globular protein (66 kDa) with an amino acid sequence of 583 residues. It accounts for approximately 8–10% of the proteins of whey and its physiochemical properties have been well characterized. BSA binds free fatty acids, other lipids and flavor compounds, which can alter the heat denaturation of the protein. The BSA molecule is predominantly α–helical and consists of three homologous domains (I, II, III), which are divided into nine loops by 17 disulfide bonds. BSA is also considered as a soft protein, implying that the molecules have a high potential to undergo structural rearrangements upon adsorption onto interfaces (Baier and McClements, 2001; López-Fandiño, 2006).

2.1.2.4. Glycomacropeptide (GMP)

In the cheese-making process, κ–casein is acted upon by chymosin and is hydrolyzed into para-κ-casein (residues 1-105) which becomes part of the curd, and GMP (residues 106-169) which remains in the whey and constitutes 15–20% of the whey protein. GMP is present in sweet whey, due to the cleavage of κ-casein by rennin, but is absent from acid whey, which is produced when caseins are precipitated by lowering the pH to 4.6. GMP is highly glycosylated and thus, although it consists of only 64 amino acid residues its molecular weight can range up to 30 kDa. It is soluble in acid owing to its low isoelectric point (pI ~ 2.8), forms gels or foams and has good heat stability (Lim *et al*., 2007; Brody, 2000).

GMP is a stimulator of cholecystokinin (appetite-suppressing hormone); this hormone plays an essential role in gastrointestinal function. Pure GMP has a unique amino acid profile with elevated amounts of threonine and isoleucine and no aromatic amino acids. Thus, GMP is ideally suited to the phenylketonuria (PKU) diet as a potential substitute for phenylalanine-free amino acid based formulas. GMP was reported to enhance the chocolate flavor used in a beverage with the added feature that chocolate flavor helped to mask the dairy flavor of GMP (Lim *et al*., 2007; Brody, 2000).

2.2. WHEY PROTEIN PRODUCTS AS FOOD INGREDIENTS

The use of whey proteins to substitute part of the fat in food products has become a common practice due to their functional properties and high nutritional value (Sibel *et al*., 2008; Singha *et al*., 2007; Livney, 2010; Zoulias *et al*., 2000). Whey proteins, either as pure material or as whey powder, are widely used in the food industry in products such as processed meats, bakery products, pasta, ice cream, confectionery, infant foods, spreads, dips and beverages. Whey proteins can play many different roles in a food product, for example enhancing nutritional value while serving as emulsifiers or as foaming agents (Lucena *et al*., 2006; López-Fandiño, 2006; Lee *et al*., 2008; Djuric *et al*., 2004; Herceg *et al.*, 2007). Important functional properties of whey proteins are listed in Table 2.4.

There have been many advances in whey processing technology, making whey-derived products valuable food ingredients and there are several treatments whey can go through, thus giving rise to whey products with different and specific profiles of proteins. Membrane-based separation technologies are used to concentrate proteins, such as ultrafiltration (UF); and to remove most lactose, minerals and low molecular weight components, such as diafiltration (DF). These treatments are employed to produce whey protein concentrates (WPCs) of widely varying compositions with protein contents ranging from 30 to 80% (Madureira *et al*., 2007) and containing substantial amounts of lactose and minerals. Whey protein isolate (WPI) is a purer material that is produced using ion-exchange resins or by ultrafiltration. The protein content of WPI is above 85% on a dry basis (Alvarez *et al*., 2007; Lucena *et al*., 2006; Lim *et al*., 2008).

Table 2.4. Functional properties of whey proteins (Onwulata and Huth, 2008).

Functionality	Properties of whey proteins
Water binding	Water binding capacity increases with denaturation of protein.
Solubility	Soluble at all pH levels. If denatured, insoluble at pH 5.
Viscosity	Low for native protein, higher if denatured.
Gelation	Heat gelation at 70° C or higher and influenced by pH and salts.
Emulsification	Good except at pH 4-5, if heat denatured.
Foaming	Good foam/overrun, β-lactoglobulin better than α-lactalbumin.
Flavor binding	Retention varies with degree of denaturation.

Variations in whey protein manufacturing processes and conditions (from producer-to-producer and from batch-to-batch) result in differences in composition (content and relative ratios of the different protein species, minerals, lactose, residual lipids, small peptides) as well as varying degrees of protein denaturation, glycosylation, and oxidation (particularly oxidation of methionine residues to methionine sulfoxide). This variability is disadvantageous for the food industry in that allegedly identical products may display different behavior in a given food formulation (Hau and Bobetto, 2001).

2.3. PROTEIN INTERACTIONS

2.3.1. Protein - protein interactions: General aspects of gelation and aggregation

As shown in Table 2.4, whey proteins have a number of functional properties; among these, gelation plays a key role in relation to the use of whey proteins as food ingredients. Gels are a form of matter intermediate between a solid and a liquid. In food gels, the molecular network consists of proteins and/or polysaccharides. The properties of the gel are a function of the complex interactions between the solvent and the molecular network. The polymer network holds the solvent (in most cases water), resulting in the formation of a gel (Damodaran and Paraf, 1997; Turgeon and Beaulieu, 2001). There are three major influences that determine the nature of protein gels: [1] environmental conditions, such as pH, ionic strength, and mineral content; [2] protein

composition, extent of denaturation and concentration; and [3] processing conditions, such as heating and cooling rates. When gelation is thermally induced; heat-denatured proteins aggregate through intermolecular interactions and produce a gel network when the aggregates develop into a continuous three-dimensional structure that entraps and restricts the motion of solvent. These aggregates of heat-denatured protein molecules can be formed through intermolecular hydrophobic interactions, disulphide bonds, hydrogen bonds, or electrostatic interactions (Turgeon and Beaulieu, 2001; Yan *et al*, 2008; Fitsimons *et al*., 2007; Hines and Foegeding, 1993; Creusot *et al*., 2006).

Interactions that occur in a food system during processing and storage of many food products can alter the functional properties of food proteins, among them gelation. When gel formation occurs, there is a competition between gel formation and phase separation. Interaction of globular proteins with each other and/or with other food hydrocolloids can lead to phase separation, precipitation or syneresis depending on their structure and physicochemical properties, thus affecting the texture of the food product (Semenova *et al*., 2002; Ngarize *et al*., 2005; Ngarize *et al*., 2004).

2.3.1.1. Whey proteins and their interactions

There are several factors that influence and control the functional properties of whey proteins and determine the attractive/repulsive forces in protein-protein interactions including size, conformation, pI, flexibility, hydrophilic/hydrophobic balance, surface hydrophobicity, presence of free thiol groups; environmental and compositional conditions (Sánchez *et al*., 2002; Pelegrine and Gasparetto, 2005; Law and Leaver, 2000; Labropoulus and Hsu, 1996). A protein is least soluble at its isoelectric point (pI), at which the net charge of the protein is zero, because the electrostatic repulsions between protein molecules is at a minimum and less water is able to interact with the protein molecules. For a large number of proteins, including whey proteins, pI values are in the range of 3.5-6.5, and therefore, the protein molecules have a net negative charge at neutral pH. When proteins are under extreme acidic or basic pH values, a protein may unfold, exposing the buried hydrophobic groups that are generally located in the core of the protein. Thus, non-covalent protein-protein interactions are favored near the isoelectric points of the whey proteins,

whereas neutral and alkaline pH values favor the formation of intermolecular disulfide bonds (Cavallieri and da Cunha, 2008; Ikeda, 2003; Ikeda and Foegeding, 1999).

Denaturation of the whey proteins results in an increase in intermolecular interactions as the native protein unfolds and the side chain groups that were buried within the protein become exposed. Aggregation of the unfolded protein molecules can occur through thiol-disulfide interchange reactions, hydrophobic interactions and ionic linkages, resulting in a gel network under certain conditions. To form a gel network, the following three factors are involved: [1] a critical minimum concentration of molecules, [2] a critical minimum time for the reaction to happen, and [3] a minimal temperature to cause structural changes (Oldfield *et al*., 1998; Rich and Foegeding, 2000; Ikeda and Foegeding, 1999). In heat-treated milk, whey protein aggregates are formed by interactions between β-lactoglobulin molecules or between β-lactoglobulin and other cysteine-containing whey proteins, such as α-lactalbumin and BSA. The addition of β-lactoglobulin A, B, or an AB mixture to milk prior to heat treatment results in larger aggregate structures that, on acidification, can lead to a greater extent of cross-linking and a firmer gel structure than the smaller aggregate structures formed during the heating of milk (Vasbinder and De Kruif, 2001; Meza-Nieto *et al*., 2007).

When whey proteins in aqueous solutions are heated above 65–75°C, they may precipitate due to the formation of insoluble aggregates or at higher protein concentrations set to form viscoelastic gels. In the latter case, whey proteins may form a particulate or a fine-stranded (or filamentous) gel network. Particulate gels are opaque and contain large aggregates; on the other hand, fine-stranded gels tend to be transparent and contain "flexible strands or more rigid fibrils" (Zhou *et al*., 2008). When gels are formed at the protein´s pI for prolonged times, the gels tend to be bigger, stronger and more deformable. Under these conditions, the repulsive electrostatic interactions are minimal (pI) which intensifies the bond formation between aggregates and gel strength (Cavallieri and da Cunha, 2008).

Previous research suggests that when whey protein concentrate (WPC) is heated at 75°C, disulfide-bonded strands are formed in the following order: first the unfolding of bovine serum albumin followed by β-lactoglobulin, then by the aggregation of α-lactalbumin with itself and by

the aggregation of α-lactalbumin with β-lactoglobulin (Havea *et al*., 1998). In a later study, the same researchers investigated the effect of heat on the model system of bovine serum albumin and α-lactalbumin in whey protein concentrate permeates and concluded that bovine serum albumin aggregates catalyze the formation of disulfide-bonded α-lactalbumin dimers. Moreover, adding bovine serum albumin or α-lactalbumin to a solution of β-lactoglobulin increased the rigidity of the resultant gels and disulfide bonds were formed between β-lactoglobulin and bovine serum albumin or α-lactalbumin (Havea *et al*., 2001).

In the particular case of β-lactoglobulin, the major whey protein, previous studies have shown that gelation is associated with a pronounced change in the protein's secondary structure leading to the formation of intermolecular hydrogen bonds between β-sheet structures, thus confirming that β-sheets may be essential for the formation of a gel network (Allain *et al*., 1999). Heat-induced gelation of β-lactoglobulin is believed to involve three events: [1] the activation of the molecule to a reactive structural form, [2] formation of linear "string of beads" polymers via sulfhydryl-disulfide interchange reaction; and [3] setting of the "string of beads" strands into a gel network formed through hydrophobic interactions, hydrogen bonds and van der Waals interactions (Prabakaran and Damodaran, 1997). When β-lactoglobulin is heated, the free thiol group is exposed due to conformational changes of the molecule, this group is very reactive and readily forms disulfide links with other proteins having a reactive thiol group or through thiol-disulfide bridge exchange reactions; thus, the process of denaturation and subsequent aggregation of bovine β-lactoglobulin resembles a polymerization process (Hoffman and van Mil, 1997). The critical change in β-lactoglobulin´s conformation apparently occurs at 61-65 °C since the initiation of sulfhydryl-disulfide exchange reactions in β-lactoglobulin occurs in that temperature range. The reactive monomer initially reacts with another monomer to form a reactive dimer via sulfhydryl-disulfide exchange reaction; a polymerization reaction starts when the reactive dimer concentration reaches a critical level (Prabakaran and Damodaran, 1997). At temperatures up to 90°C the B variant of β-lactoglobulin denatures more rapidly than the A variant and forms smaller and soluble aggregates, while the A variant will mainly form insoluble aggregates. Another important difference between the two variants is that at neutral pH values (room temperature), the B variant has a lower net charge than the A variant due to the substitution of an Asp residue in the A variant by a Gly residue (Parris *et al*., 1993).

Besides thermal treatments, high pressure is also known to denature proteins, resulting in aggregation and gelation (Ngarize *et al*., 2005). Pressure-induced denaturation of proteins involves rupture of hydrophobic and electrostatic interactions as a result of the decrease in volume of the protein solution while heat denaturation of the protein is caused by violent movement of molecules that can destroy heat-labile hydrogen bonds (Ngarize *et al*., 2005, Fertsch *et al*., 2003). Applied hydrostatic pressure causes partial protein unfolding that can lead to the irreversible process of gelation and thus high-pressure (HP) processing can provide a means of altering the functional properties of proteins. The nature of the protein, its concentration, the level of pressure applied, the holding time, the number of pressure cycles, temperature, pH, and ionic strength all play significant roles in the rate and extent of protein denaturation and the rheological properties of pressure-induced gels (Alvarez *et al*., 2007; Huppertz and De Kruif, 2007).

As important as protein-protein interactions are, in real food systems proteins interact with other type of molecules such as lipids and carbohydrates; hence, it is vital to consider and to study protein-lipid and protein-polysaccharide interactions.

2.3.2. Protein – lipid interactions

In food systems, protein-lipid interactions occur naturally during processing and/or during storage. For example, it has been shown that products of lipid oxidation formed during peanut storage interact with proteins, forming complexes. Protein-lipid interactions affect the physicochemical properties of proteins and the organoleptic quality of food products, as well as having an effect on protein functional properties. Likewise as with protein-protein interactions, these types of interactions are affected by temperature, pH and ionic strength, among other factors (Alzagtat and Alli, 2002; Damodaran and Paraf, 1997).

The following five types of interactions can occur between proteins and lipids:

1. Electrostatic interactions between negatively/positively charged groups of amino acids (e.g. glutamate) and positively/negatively charged groups of phospholipids (e.g. choline).

For example; at neutral pH, both the proteins and phospholipids are negatively charged and there is a higher electrostatic repulsion impeding their interactions (Alzagtat and Alli, 2002).

2. Covalent bonds between proteins and lipids. These interactions seem to be of higher relevance in amino acid transport than in the structural organization of lipid-protein complexes (Alzagtat and Alli, 2002).
3. Hydrogen bonds. They may be formed between the hydroxyl group of a fatty acid or a mono/diglyceride and the carbonyl groups of the amino acid residues. An example of this type of interactions is found in milk fat globules between the phospholipids and many glycoproteins, preventing coalescence of fat globules (Walstra *et al*., 2006; Alzagtat and Alli, 2002).
4. Hydrophobic interactions at an oil-water interface lead to partial protein unfolding, creating a membrane with high viscoelastic properties. These types of interactions are important in the stability of protein-lipid complexes (Alzagtat and Alli, 2002).
5. Dispersion interactions (van der Waals forces); in general these short-range forces between dipoles, adjacent atoms or adjacent molecules are very sensitive to intermolecular distances. For example, the attraction of $–CH_2$ groups from proteins with $–CH_2$ groups from phospholipids, being both non-polar groups (Alzagtat and Alli, 2002).

Research has been done using BSA and diglycerides and free fatty acids, and it was found that both of them (on their own) antagonize the adsorption of proteins. On the other hand, when using natural olive oil the protein-olive oil adsorbed at the interface forming mixed films with a high viscoelasticity (Damodaran and Paraf, 1997).

2.3.2.1. Protein-stabilized emulsions

Food product stability and emulsion formation are aided in many cases by proteins; since they diffuse and adsorb at the oil–water interface, also by forming a membrane (film) around oil droplets that prevents the oil droplets from coalescing. Nevertheless, the efficiency of proteins to stabilize emulsions depends heavily on the density and structure of the protein adsorption layers on the drop surface (Kulmyrzaev *et al*., 2000; Lee *et al*., 2007; Damodaran and Paraf, 1997).

Protein-stabilized emulsions are affected by several factors, however ionic strength and pH are considered the most important when determining the stability of protein-stabilized emulsions. As an example, many protein-stabilized food emulsions are supplemented with minerals, such as sports drinks and beverages (Kulmyrzaev and Schubert, 2004; Kulmyrzaev *et al*., 2000).

Protein molecules have the ability to stabilize emulsion films, and this stabilization is usually attributed to two mechanisms: [1] formation of adsorption layers with a certain mechanical stability that act to protect the film from rupture and/or [2] the creation of a barrier in the disjoining pressure (force per unit area of the film) which prevents the film from thinning and allowing direct contact of two opposite film surfaces (Tcholakova *et al*., 2006).

There are several factors which play a crucial role in these two mechanisms: electrostatic repulsions, steric interactions and van der Waals forces have the most important roles, however rheological properties of the adsorption layers (such as viscosity and interfacial elasticity) are also considered to be important (Tcholakova *et al*., 2006).

2.3.3. Proteins and low-molecular-weight carbohydrates

Proteins and carbohydrates in food products contribute to food stability, texture and shelf life. Since most food products contain both, the interactions between them have a significant effect on the stability of the whole food system (Doublier *et al*., 2000).

Low-molecular-weight sugars are extensively used as sweeteners in a wide variety of food products. The type and content of sugars have a huge effect on the properties of aqueous solutions and therefore have an effect on protein structure. There are several research works about how the conformational and thermal stability of proteins is increased in the presence of sugars (Semenova *et al*., 2002).

A variety of effects of sucrose on the gelation behaviour of globular proteins have been described: [1] it increases the protein gelation temperature, [2] it possibly lowers the gelation rate

due to a higher viscosity, [3] it increases the rigidity of the protein gel after being heated beyond the irreversible denaturation temperature and/or for a long period of time (e.g. merengue), and [4] it causes weaker gels when the protein is heated below the denaturation temperature and/or during short periods of time (Semenova *et al*., 2002). Since sucrose is an osmolyte (osmoprotectant) these phenomena have been called "the osmolyte effect". Osmolytes in biological systems are known to be small molecules that protect cells from external osmotic stress conditions such as dehydration, a variation in temperature and/or pH, freezing, and high salt concentrations; these osmolytes stabilize protein conformation without affecting the protein functionality. There are different types of osmolytes and among them we find polyhydric alcohols (polyols) like glycerol and sucrose (Saadati and Bordbar, 2008).

Herceg *et al*. (2007) studied the interaction between carbohydrates and whey protein isolate, whey protein concentrate and β-lactoglobulin. They found that foam stability and emulsifying properties improved with the addition of mono- and disaccharides (glucose and sucrose, respectively) whereas emulsion stability was reduced by addition of polysaccharides such as starch and inulin.

2.3.4. Protein-polyol interactions

In recent years, the influence polyols have on the stability of globular proteins during processing and during storage has become a topic of interest in relation to protein emulsions because polyols have the ability to increase both the viscosity of a solution and the repulsive colloidal interactions, thereby decreasing the collision frequency of the droplets making up the dispersed phase within an emulsion (McHugh *et al*., 1994). Another important property of polyols is their ability to act as plasticizers since they have the ability to reduce internal hydrogen bonding while increasing intermolecular spacing. As an example, both sorbitol and glycerol have become of interest in recent research because it was demonstrated that they can reduce droplet aggregation in protein emulsions (McHugh *et al*., 1994; McHugh and Krochta, 1994).

2.3.5. Protein-polysaccharide interactions

There are different types of interactions between macromolecules: specific; non-specific; attractive (i.e. hydrophobic, hydrogen bonds, disulfide bonds); repulsive (i.e. electrostatic, hydration, steric repulsions); strong (i.e. hydrophobic, hydration, steric repulsions) or weak (i.e. hydrogen bonds, van der Waals), (Semenova *et al*., 2002; Turgeon *et al*., 2003; 148, Samant *et al*., 1993; Samhouri *et al*., 2009; Doublier *et al*., 2000; Miyawaki, 2007).

When proteins and polysaccharides are mixed together in an aqueous medium (Figure 2.2), many factors influence whether they will be compatible or not including pH, protein/polysaccharide ratio, ionic strength and the nature of the polymer (net charge, molecular weight, flexibility, etc.). When they are incompatible, they may remain co-soluble in a single phase, however when the repulsion between a protein and a polysaccharide with the same net charge is stronger than their interactions with the solvent, separation of a colloidal solution into two liquid phases may occur (coacervation) (Benichou *et al*., 2002). On the other hand when the protein has a net positive charge while the polysaccharide remains anionic, the two polymers cease to be incompatible and protein-polysaccharide complexation via electrostatic attraction may occur. Again, a single-phase or a two-phase system may result depending on the strength of the protein-polysaccharide interactions, which is governed by numerous factors including the nature of the protein and the polysaccharide, their concentrations, the pH and ionic strength of the solution. When the protein-polysaccharide interactions are stronger than the interactions with the solvent complex coacervation may occur, whereby the protein-polysaccharide complexes form a separate concentrated phase in equilibrium with a dilute phase. Three different behaviours may be observed: [1] complex coacervation, [2] co-solubility, or [3] incompatibility (Benichou *et al*., 2002; Semenova *et al*., 2002; Samant *et al*., 1993).

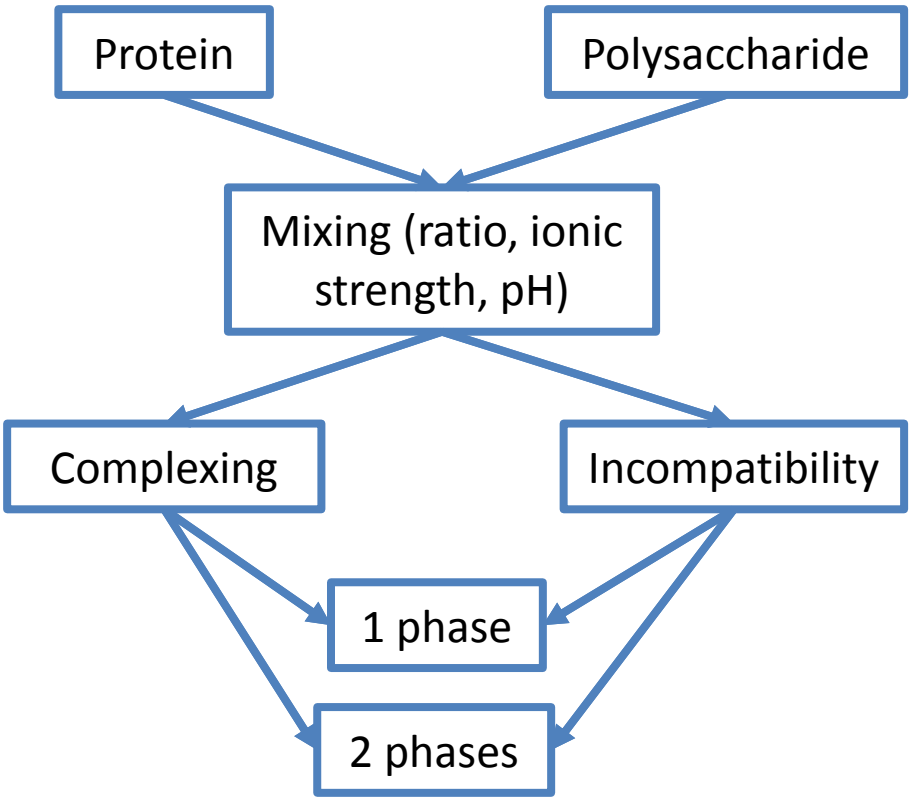

Figure 2.2. Possible interactions between a protein and a polysaccharide in an aqueous medium (adapted from Benichou *et al*., 2002).

2.4. INSTRUMENTAL METHODS FOR THE STUDY OF PROTEIN STRUCTURE AND INTERACTIONS

2.4.1. Fourier transform infrared spectroscopy

Fourier transform infrared (FTIR) spectroscopy is a well-established method for the study of proteins due to the high content of information within an infrared spectrum. The strengths of FTIR spectroscopy include the following: it is a rapid non-destructive method that can detect a wide range of functional groups and is sensitive to changes in molecular structure, it can be applied to small soluble proteins as well as to large membrane proteins, the infrared spectrum of a protein encodes information about protein backbone conformation, side chain structure and environment and it requires little or no sample preparation (Barron *et al*., 2005; Barth and Zscherp, 2000; Khurana *et al*., 2008; Kirkwood *et al*., 2004; Iñón *et al*., 2004; Sivakesava *et al*., 2001). Because

FTIR spectra of proteins are highly sensitive to changes in protein secondary structure, FTIR spectroscopy is a valuable tool for the investigation of protein folding/unfolding and the dynamics of these and other processes have been monitored with time-resolutions down to nanoseconds (Barth, 2007; Kötting and Gerwert, 2005; Fabian *et al*., 1993, Barth, 2000; Barth, 2000(a); Schultz, 2000).

FTIR spectroscopy is not limited by protein size (the largest water-soluble protein studied to date is fibrinogen, which has a molecular weight of 340,000 Da) or the presence of other types of molecules such as lipids or carbohydrates. The latter can also be the object of simultaneous study, thus providing information on the lipid-protein and/or protein-carbohydrate interactions (Arrondo and Goni, 1999; Sivakesava *et al*., 2001; Schultz, 2000). FTIR spectroscopy has also been used to detect changes in secondary structure of protein molecules upon adsorption, heating and storage of solutions and emulsions (Tcholakova *et al*., 2006). Some other applications of FTIR spectroscopy can be mentioned such as the study of polysaccharide-whey protein complexes (Zaleska *et al.,* 2000).

The infrared spectra of proteins and polypeptides exhibit nine amide bands (Table 2.5). The amide I, II and III bands are all useful for the study of protein conformation with the amide I band being the most widely used (Lefèvre and Subirade, 1999; Fabian and Vogel, 2002; de Jongh *et al*., 1996; Slayton and Anfinrud, 1997).

Table 2.5. Protein and polypeptide amide bands

Amide band	Vibrational mode
A	N-H Stretching
B	N-H Stretching
I	C=O Stretching (primarily), C-N Stretching, N-H Bending
II	N-H Bending, C-N Stretching
III	C-N Stretching, N-H Bending, C=O Stretching
IV	O=C-N
V	N-H Bending
VI	C=O Bending
VII	C-N Torsion

Amide I band. Appears between 1600 and 1700 cm^{-1} with a maximum for most proteins at around 1654–1674 cm^{-1}.The amide I band arises primarily from the stretch vibration of the peptide C=O group which is coupled slightly with CN stretching, CCN deformation and NH bending. Since H_2O exhibits strong absorption in the same region of the spectrum it is frequently necessary to dissolve the protein in D_2O, which leads to a shift of the amide I band (amide I') between 2 and 9 cm^{-1} to lower frequencies depending on the protein of interest (Baello *et al*, 2000; Susi *et al*., 1967; Timasheff *et al*., 1967; Iloro and Pastrana-Ríos, 2006; Byler and Susi, 1986; Rahmelow *et al*., 1998; Jung, 2000).

The amide I band can be used to determine quantitative and qualitative data about the secondary structure of proteins under various conditions allowing accurate measurements of conformational changes in proteins. This capability arises because of the sensitivity of the amide I band frequency to the extent of hydrogen bonding of the C=O groups which varies among

secondary structure elements, so that the amide I band covers a multitude of single bands with slightly different frequencies. These components can generally be assigned in the following way: components between 1649 and 1658 cm^{-1} are assigned to α-helices, those between 1620 and 1635 cm^{-1} to intramolecular β-sheets and those between 1665 and 1690 cm^{-1} to β-turns. β-Sheets also show weak high-frequency component at around 1672 cm^{-1} and aggregated proteins show bands due to intermolecular antiparallel β-sheets around 1614-1624 and at 1684 cm^{-1} (Barth, 2007; Nara and Tanokura, 2008; Bandekar and Krimm, 1979; Gerwert, 1993; Jung, 2000; Kubelka and Keiderling, 2001).

FTIR spectroscopy is one of the few techniques that can be used to determine the protein structure under interfacial conditions, recent studies have been done in emulsion systems using this technique in order to examine conformational changes in proteins after adsorption at the oil/water interface in the emulsion (Chirgadze and Brazhnikov, 1974; Fairbrother *et al*., 1991; Lee *et al*., 2007; Smith, 1996).

Amide II band. The amide II band arises from N-H bending coupled with C-N stretching, the band is observed around 1550 cm^{-1} in H_2O and shifts to about 1450 cm^{-1} in D_2O. A large shift of the amide II band occurs upon deuteration, this band is frequently used to monitor hydrogen/deuterium exchange between the protein core and the solvent during unfolding of the protein structure induced by various perturbations such as temperature or pressure (Iloro and Pastrana-Ríos, 2006; Jung, 2000; Rahmelow *et al*., 1998; Gerwert, 1993).

Amide III band. The amide III band is found in the range between 1220 and 1330 cm^{-1} and results from N-H bending and C-N stretching. The band position is very sensitive to secondary structure as follows: α-helix 1293-1328 cm^{-1}, β-sheet 1225-1250 cm^{-1} and unordered structures 1257-1288 cm^{-1}. However because of its lower intensity it is generally less used than the amide I band (Rahmelow *et al*., 1998; Jung, 2000; Van der Ven *et al*., 2002).

A protein with different types of secondary structural elements should give rise to a number of discrete amide band components. Since the bands are typically broad and lie close together, they overlap and give rise to an amide contour with undefined features. These can be further analyzed

with resolution-enhancement techniques such as Fourier self-deconvolution and derivatization, allowing the quantitative determination of different secondary structural elements in proteins and the reliable examination of even marginal changes in protein conformation underlying the amide band contours. Fourier self-deconvolution reduces the bandwidth of component bands by altering the function that encodes line shape and line width in the Fourier domain. Fourier self-deconvolution requires specialized software and the control of three independent parameters by the operator: [1] line shape, [2] line width and [3] resolution enhancement factor (Fabian *et al*., 1993; de Jongh *et al*., 1996; Barth, 2000(a)).

Another technique used to enhance spectral resolution is two-dimensional correlation spectroscopy (2D-COS). 2D-COS spreads the overlapped peaks in a second dimension and also allows the sequence of events occurring during an experiment to be determined (Alvarez *et* al., 2007; Iloro and Pastrana-Ríos, 2006). Two types of 2D correlation plots are generated: synchronous and asynchronous which represent in-phase and out-of-phase variations, respectively, between spectral components to an applied perturbation such as temperature, pH, etc. The asynchronous contour plot combined with the synchronous plot provides details on the sequence of events following an applied perturbation (Iloro and Pastrana-Ríos, 2006; Filosa *et al*., 2001; Wang *et al*., 2006).

2.4.1.1. Attenuated total reflectance (ATR-FTIR) spectroscopy

Attenuated total reflectance (ATR) is a special sampling technique often applied in FTIR studies of biological systems. In ATR-FTIR spectroscopy the IR beam is directed into an internal reflection element (IRE), which is a high-refractive-index crystal that is transparent to IR radiation in the frequency range of interest. Above a critical angle, which depends on the IRE, the light beam undergoes total internal reflection when it touches the surface of the IRE giving rise to an evanescent wave that penetrates into the sample and decays exponentially as it propagates through the sample (Fabian and Vogel, 2002; Khurana and Fink, 2000; Vigano *et al*., 2001; Allain *et al*., 1999). The distance at which the amplitude of the evanescent wave has decayed to 1/e of its initial amplitude, termed the depth of penetration, is wavelength-dependent and also depends on several other factors (the IRE material, the angle of incidence of the IR beam, and the refractive index of

the sample) but is generally on the order of microns. ATR-FTIR spectroscopy is an advantageous method due to the shallow depth of penetration (and hence short effective pathlength) since the spectra do not depend on the thickness of the material deposited and the spectra of aqueous samples are not masked by water absorption bands (Siebert, 1995; Vigano *et al*., 2001; Beullens *et al*., 2006).

ATR-FTIR spectroscopy is finding a wide variety of applications in the area of food science, including quantitative quality control applications in the food analysis field. It provides a simple and reproducible means of handling products in the form of liquids and pastes and has two great advantages: [1] the analyses are non-destructive and [2] the sampling takes less than 5 min. In combination with chemometric techniques, ATR-FTIR spectroscopy has been successfully used for the detection of adulteration of fruit juices, honey, and oils (Vardin *et al*., 2001; Sivakesava *et al*., 2001) and to determine nutritional parameters in commercially available yogurts (energetic value, the carbohydrate, protein and calcium contents) (Moros *et al*., 2005; Moros *et al*., 2006).

2.4.2. Circular dichroism

Optical activity of asymmetric molecules can be measured using two interrelated phenomena: circular dichroism (CD) and optical rotary dispersion (ORD). While CD measures the unequal absorption of left- and right-handed circularly polarized light by optically active molecules, ORD measures the ability of molecules to rotate the plane of linearly polarized light as a function of the wavelength. There are two spectral regions in which CD spectra of proteins are measured: the near-UV region (250 to 300 nm) where the bands measured originate from aromatic amino acids and the far-UV region (170 to 250 nm), also known as the amide region, where the bands measured originate from the peptide bonds. While the amide region can be used to characterize the secondary structure of a protein, particularly the α-helical portion, the near-UV region can be used as a fingerprint of the native conformation of the protein. In other words, the far-UV region can be used to study changes in secondary structure and the near-UV region can be used to study changes in tertiary structure (Yada *et al*., 1994). One of the strengths of CD consists in the fact that it can be employed to explore protein structure under a large variety of conditions such as: high protein concentrations, slightly acid pH and high temperatures (Kelly *et al*., 2005).

2.4.3. Fluorescence

When an electron is excited and returns from the first excited state to the ground state, fluorescence emission is observed. The characteristics of this emission, including its wavelength and intensity, are much more sensitive to changes in the microenvironment of the chromophore than light absorption is. The fluorescence spectra of proteins in aqueous solutions at room temperature exhibit maxima in the range of 331-343 nm. Fluorescence in proteins originates from the aromatic amino acid residues (phenylalanine, tyrosine and tryptophan) but is dominated by the Trp residues since both their UV absorption and their quantum yield of emission are greater than those of Tyr and Phe. Measuring the fluorescence of the Trp residues is very useful when it is important to understand the polarity of the microenvironment (Burstein *et al*., 1973; Sakuno *et al*., 2008).

2.4.4. Surface plasmon resonance (SPR)

Surface plasmon resonance (SPR) is a technique allowing for the study of binding affinity interactions of biological molecules in a multiplexed format. This approach is being widely applied to monitor DNA–DNA, DNA–RNA, peptide–protein and protein–protein interactions as well as surface enzyme reactions. This label-free technique relies on the robust attachment of biomolecules in an array format on a gold-coated surface. When a beam of light impinges on this gold-coated surface under conditions of total internal reflection, the photons can interact with free electrons from the metal layer causing a dip in the intensity of the light reflected to the detector. The angle at which a dip in the intensity of the light reaching the detector occurs will depend on the refractive index of the sample attached to the gold surface and the amount of material bound to the surface (Hiep *et al*., 2007; Grygorczyk, 2009; Smith *et al*., 2003). The binding of a ligand to the sample attached to the gold surface will change its refractive index, causing a shift in the angle of the light, in this manner, binding interactions may be studied by SPR. A schematic representation of a biosensor based on this principle is presented in Figure 2.3.

The utility of SPR for the study of protein interactions is exemplified by biomolecular interaction analysis (BIA). BIA is a technology that monitors molecular binding processes in real time on the surface of a specially prepared biosensor chip without the use of fluorescent,

enzymatic, or radioactive tags (Grygorczyk, 2009; Marchesseau *et al*., 2002; Smith *et al*., 2003; Seol *et al*., 2003).

SPR has been applied for the measurement of the α-lactalbumin content of consumer milk, colostrums, whey proteins and infant formulae (Indyk, 2009); and of the casein content in raw milk samples (Hiep *et al*., 2007; Muller-Renaud *et al*., 2004). It has also been employed to study the apparent hydrophobicity of caseins and to characterize casein-casein interactions at the molecular level (Marchesseau *et al*., 2002).

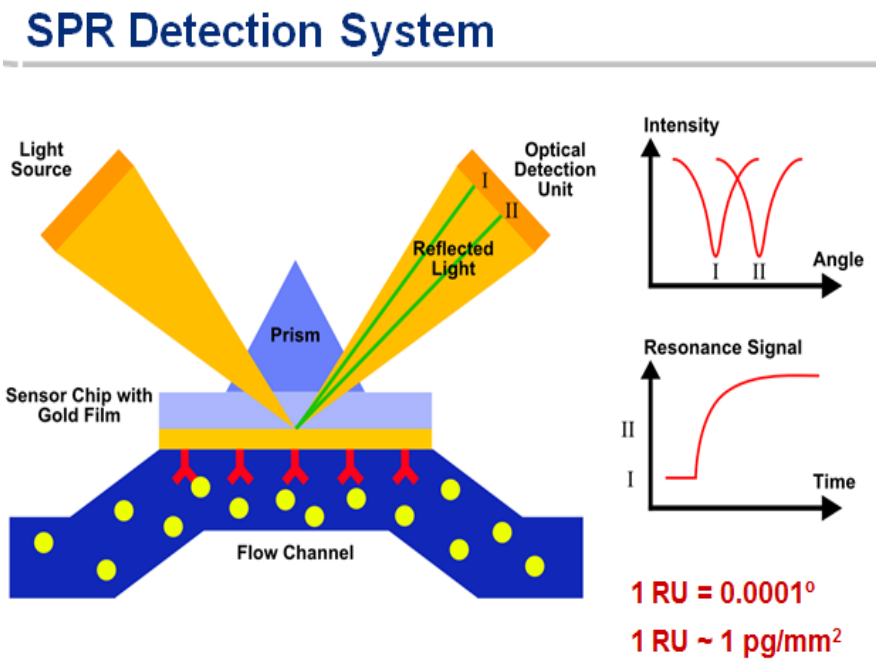

Figure 2.3. Surface plasmon resonance biosensor© (Biacore™); used with permission of GE Healthcare.

2.4.5. Electrospray ionization-mass spectrometry (ESI-MS)

Mass spectrometry combined with electrospray ionization (ESI-MS) has become very popular since it can accurately measure protein molecular masses up to 100,000 Da or more and provides structural information. A schematic representation of the ionization process is presented in Figure 2.4. The sample in solution is injected into a capillary, to which a high electrical voltage is applied (Alvarez *et al*., 2007; Careri and Mangia, 2003; Tilleman *et al*., 2005). Mass spectrometry is then used to analyze the population of charged species formed by the ionization process.

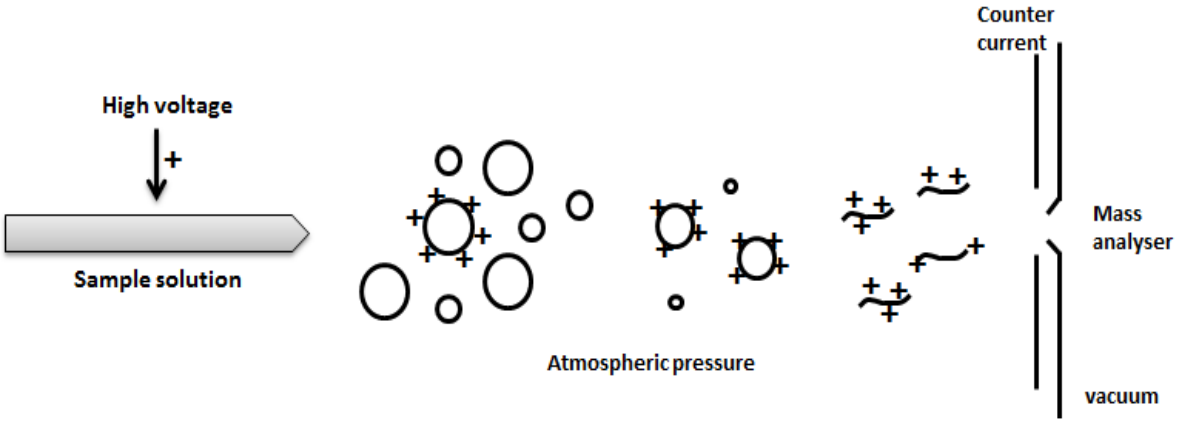

Figure 2.4. The electrospray ionization-mass spectrometry process. A sample in solution (for example a protein) is injected into a capillary, a high electrical voltage is applied and the mass spectrometer analyzes the population of charged species initially formed by the ionization process. Adapted from Tilleman *et al.* (1995).

As ESI-MS can be employed to determine the molecular mass of proteins it can be utilized to detect modifications of proteins by insertion, deletion or modification of amino acids, to identify genetic variants and to examine post-transcriptional modifications such as glycosylation and phosphorylation (Tilleman *et al*., 2005). In addition, the ease of ionization of ionizable groups in a protein depends on the flexibility of the protein: the more flexible a protein is, the easier it is to charge the groups buried in the interior. Accordingly, measurements of the charged-state distribution by ESI-MS can be employed to probe changes in tertiary structure (Alvarez *et al*., 2007).

2.4.6. Focal-plane-array Fourier transform infrared (FPA-FTIR) spectroscopy

Infrared imaging is a relatively new technology which allows the characterization of heterogeneous samples and it has found its way to be applied in the medical, agricultural and food science fields among others. Infrared imaging systems have a multichannel detector (MCD) which is composed of individual elements (pixels) in a linear array (LA) or in a two-dimensional grid (focal plane array: FPA), when the IR beam exits the spectrometer and strikes the detector, the signal measured by each individual detector (pixel) corresponds to a specific spatial location on the sample. For microimaging, an IR microscope is used to focus the IR beam onto a smaller

sampling area providing a spatial resolution on the order of microns, the spatial resolution attained depends on the pixel dimensions and the magnification of the sampling area but is ultimately restricted by the diffraction limit which is approximately 5.6 μm at 1000 cm^{-1} for transmission measurements (Sedman *et al*., 2010; Enfield, 2010).

As illustrated in Figure 2.5, an FPA-FTIR imaging system consists of an FTIR spectrometer, an infrared microscope with a FPA detector and a CCD (charge-coupled device) camera to acquire a visible image of the sampling area. A MCT (mercury cadmium telluride) FPA detector is commonly employed in this type of system and must be cryogenically cooled with liquid N_2 to reduce thermal noise. The wavenumber cut-off for an MCT FPA detector is approximately 900 cm^{-1} (Sedman *et al*., 2010; Enfield, 2010).

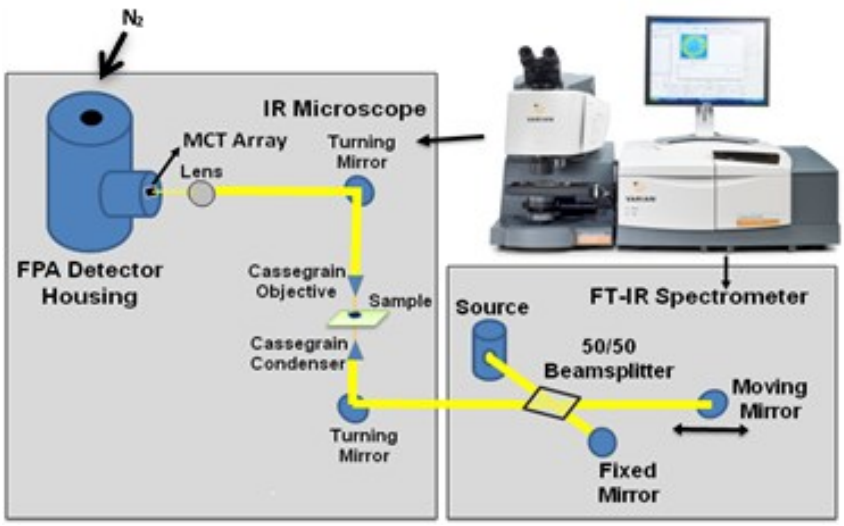

Figure 2.5. Focal-plane-array FTIR (FPA-FTIR) spectrometer integrated with an infrared microscope. Reprinted, with permission, from Sedman et al. (2010).

Figure 2.6 shows a schematic illustration of the spectral data "hypercube" acquired by an FPA-FTIR spectrometer. A full spectrum is associated with each spatial location (x, y) in the array extending along the third dimension (z). At each of the wavenumbers plotted along the z axis the spectral intensity at each pixel in the array is scaled and mapped to a color [red= high; blue= low]. A "chemical image" corresponds to a slice through the data hypercube at a wavenumber at which

a particular component in the sample is known to absorb and represents the spatial localization of that component of the sample (Sedman *et al*., 2010; Enfield, 2010).

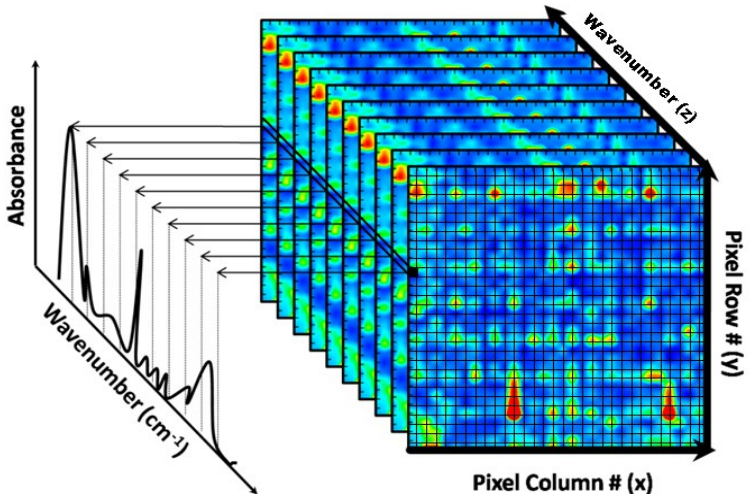

Figure 2.6. Hyperspectral data cuboid. Each point along the z-axis represents the intensity at a particular wavenumber plotted in the spatial (x, y) plane as a color (red=high and blue=low. Reprinted, with permission, from Sedman *et al*. (2010).

An advantage of FPA/FTIR imaging is the speed of image acquisition; as mentioned above, each pixel is an individual detector therefore allowing simultaneous acquisition of n^2 (commonly for FPA arrays = 32^2, 64^2, 128^2; n = number of detector elements in each row/of the array) spectra in approximately the same time a single spectrum is acquired by conventional FTIR microspectrometry. Another advantage of this system is the ability to obtain a "snap-shot" of the area that is being sampled. The images can be acquired by three different modes: transmission, transmission-reflection or ATR. In order to acquire an image in the transmission or the transmission-reflection mode the sample cannot be thicker than ten micrometers, limiting these modes of image acquisition to samples that are either inherently very thin or can be microtomed. On the other hand, ATR allows imaging of samples of any thickness due to the short effective pathlength with the extra advantage of allowing for higher spatial resolution than can be attained in the transmission or transmission-reflection mode (Sedman *et al*., 2010; Enfield, 2010).

2.4.7. Nuclear magnetic resonance (NMR)

NMR can be used to study the structure, chemical kinetics and dynamics of many biochemical systems. A great asset of NMR spectroscopy is the possibility to detect molecular motion in proteins, hence providing information on the dynamics of many sites of the protein over a wide range of time scales. NMR spectroscopy is also applicable to the study of molecular interactions, e.g. protein-protein interactions (Rule and Hitchens, 2006). As described by Edwards *et al*. (2002), NMR can be used to monitor hydrogen-deuterium exchange of each amino acid residue of a protein in D_2O solutions, making it possible to detect which residues remain unexchanged after the protein is exposed to heating and thereby allowing the researcher to elucidate which portion of the protein is unfolding at a given temperature. For these types of experiments, the temperature must be accurately controlled as any fluctuation in temperature can cause changes in the chemical shifts (Rule and Hitchens, 2006).

2.4.8. Scanning electron microscopy (SEM)

Scanning electron microscopy (SEM) is a useful technique to view and image the structure of many types of samples over a wide range of keV (kiloelectronvolt) and magnification power, food samples included. Aranyi and Hawrylewi (1968) described the principle of this technique and its application in the characterization of flours and doughs. A SEM image is acquired by detecting the electrons emitted as the surface of the sample is scanned with an electron beam; accordingly, SEM is a nondestructive technique that allows for direct imaging of the sample with a very large depth of focus and at different magnifications. Whereas conventional SEM requires that nonconductive samples be coated with a layer of evaporated metal to prevent artifacts resulting from the buildup of electrons from the electron beam on the sample's surface, the development of variable-pressure SEM technology (VP-SEM) operated under low-vacuum conditions has eliminated this requirement. VP-SEM allows the analysis of wet or oily food samples in their original state, thereby eliminating sample preparation steps such as dehydration and/or freezing that can alter food structure (Ohu *et al.*, 2000; James, 2009).

2.5. HIGH-PROTEIN MODEL FOOD SYSTEM

This thesis addresses the study of a "high-protein cookie" model food system in which interactions of whey proteins with carbohydrates, fats and emulsifiers will be studied. The development of the "cookie" model food system was done in collaboration with Bariatrix Nutrition, a leading food company dedicated to the elaboration of high-protein products with the mission to help people achieve weight loss and weight maintenance. It is long known that cooperation between universities and the food industry can be very fulfilling for both parts. A classic example is the case of tinned foods, fruit of the collaboration between the Underwood Company and MIT, which led to the production of safe canned foods (Graf and Saguy, 1991).

Various types of proteins such as whey protein, soy protein, caseinates and gelatin are commonly employed in formulating high-protein nutritional products. Among these, whey protein concentrate (WPC) and whey protein isolate (WPI) are widely used in high-protein beverages and nutritional bars owing to the high nutritional value and excellent functional properties of whey proteins (Holsinger *et al*., 1974; Grygorczyk, 2009).

2.5.1. High-protein beverages

Much research has been done in the high-protein beverages field since it is a convenient product for people with a busy life style who want to eat something fast without much preparation and keeping a healthy diet (Holsinger *et al*., 1974). Given the fact that high protein beverages are very complex food systems, studies are still being carried out in order to understand the behavior of proteins and their interactions in beverages with other food components (Smithers, 2008; Grygorczyk, 2009). Therefore a great variety of ingredients have been applied to beverages with high protein contents to minimize the impact of different mixes of proteins on the beverage such as sweeteners, emulsifying agents, stabilizers, fat sources, vitamins and minerals, and even specific types of packaging (Childs *et al*., 2008; Temelli *et al*., 2004). Hence there is a clear necessity of studying processing and storage defects which can occur in high-protein product with the proper consideration to food sensory quality which is quite challenging for producers (Iordache and Jelen, 2003; Smithers, 2008; Childs *et al*., 2008; Lee and Vickers, 2008; Koffi *et al*., 2005; Grygorczyk, 2009).

β-Lactoglobulin aggregation/gelation with casein (calcium caseinate, α-CN, β-CN and κ–CN) in high protein UHT-treated beverages was recently studied by the McGill IR group to elucidate and try to solve this problem, nevertheless the complexity of the system just made possible to understand part of it (Grygorczyk, 2009). As mentioned previously, GMP is present in sweet whey at a concentration of approximately of 20%, nevertheless very few studies have been published related to GMP interactions with other whey proteins. However GMP is getting attention from the food industry thanks to its unique amino acid profile and to its ability to stimulate cholecystokinin (Martinez *et al*., 2009; Brody, 2000, Lim *et al.*, 2007, Yalçin, 2006).

2.5.2. High-protein baked products

Previous work has been done in the formulation of bread and biscuits/cookies in order to maximize the protein content (Conforti and Lupano, 2004; Ranhotra *et al*., 1980; Mohsen *et al*., 2009). There are many studies about partial substitution of wheat flour by other types of flour such as soy flour or rice flour, in order to improve the protein quality and content of wheat-based baked products; one of the reasons soy flour is used is its high lysine content (Pérez *et al*., 2008; Mohsen *et al*., 2009).

Other researchers studied the effect of replacing up to 35% of the fat in a cookie formulation with polydextrose, maltodextrins, β-glucans, pectin or a blend of microparticulated whey proteins with emulsifiers; it was found that even when the physical and flavour characteristics of the cookies were similar to the control, the cookies were always much harder. They also found that the best combinations were polydextrose with maltodextrins and polydextrose with microparticulated whey proteins (Zoulias *et al*., 2000).

Another growing market and therefore growing research field is the elaboration of gluten-free products. Patients with celiac disease have a strong immune response to certain amino acid sequences (aromatic amino acid residues) found in the protein from wheat, barley and rye having as a consequence a serious damage of the small intestine mucosa. The main problem resides in the fact that celiac disease is one of the most common genetic diseases: 1 of 130 to 300 of the global population (Sabanis *et al.*, 2009).

The main issue of supplementing cookies with soy flour is the strong and unappealing flavour from soy, therefore there is a great field of opportunity for milk derived proteins such as whey proteins. Soy protein isolate has a high lysine content of 6.5 g per every 100 g of total protein, however whey proteins like β-lactoglobulin and α-lactalbumin have 12 g per 100 g of total protein while soy protein isolate has 1 g of tryptophan per 100 g of protein and α-lactalbumin has a content of 4.8 g per 100 g of protein which is higher than that of meat proteins (Pérez *et al*., 2008; DAVISCO FOODS).

A common problem encountered when using whey protein in baked products is the hardness conferred to the final product, thus the use of emulsifiers, humectants and bulking agents such as sorbitol, polydextrose, glycerine, lecithin, etc. becomes very useful in the development of these types of products (Gallagher *et al*., 2005; Zoulias *et al*., 2000; Conforti and Lupano, 2004; Ranhotra *et al*., 1980).

2.5.2.1. Emulsifiers in the baking industry

Emulsifiers are commonly used to disperse oil in water (O/W) or water in oil (W/O), however they have a very particular use in the bakery industry and they are classified by HLB numbers which refer to the ratio of hydrophilic to lipophilic components (amphiphilic) present in the emulsifier (Edwards, 2007). The most important categories of emulsifiers used in the bakery industry are briefly described below.

2.5.2.1.1. Lecithins

Lecithins are a naturally occurring mixture of phospholipids, which consist of one polar head and two neutral chains. Lecithin, mainly obtained from soybeans, is the most extensively used emulsifier in the food industry. The main phospholipids in lecithin are phosphatidylcholines (PC), phosphatidylethanolamine (PE), and phosphatidylinositol (PI) (Kuligowski *et al*., 2008; Edwards, 2007).

The lecithins used in the bakery industry may be either fluid or de-oiled, the latter being more expensive due to the fact that they have a neutral taste, they are easier to handle and they have less impact on the color of the baked product; nevertheless both fluid and de-oiled lecithins have similar functionality. Commercially available lecithins can also be hydrolyzed or enriched. The choice of the lecithin to be employed in a particular formulation will depend on the cost, the interactions with the components of the formulation, the functionality during processing and the effects on the shelf life of the product (Whitehurst, 2004; Edwards, 2007).

Lecithins are used in cakes, pastries and biscuits for different purposes such as an improved distribution of the ingredients, uniform browning, among other advantages (Whitehurst, 2004).

2.5.2.1.2. Mono- and diglycerides

Mono and diglycerides are emulsifiers that find their major application in the bakery industry, their advantages include their dispersability properties during mixing and enhancement of crumb softness by forming a complex with starch amylose. These emulsifiers can be added in combination with other emulsifiers, when they are combined with ionic emulsifiers it increases the stability of the monoglyceride (Whitehurst, 2004).

2.5.2.1.3. Di-acetyl tartaric esters of monoglycerides (DATEM)

DATEM are glycerol derivatives obtained through the esterification of glycerol with fatty acids and mono- and diacetyl tartaric acids, they are ionic emulsifiers and are easily dispersible in either hot or cold water. DATEMs are permitted in all bread types and they can improve consistency, viscosity, texture and taste; DATEM interacts with (wheat) flour proteins in a very similar way to protein-lipid interactions (Whitehurst, 2004).

In trying to extract DATEM from bread, it was found that DATEM interacts very strongly with the proteins and that the strength of the interaction increases with increasing input of mechanical energy into the system. The DATEM-protein complex is stabilized through formation of hydrogen bridges with the amidic groups of the protein and through hydrophobic bonds, in this way the emulsifier protects the protein from denaturation as shown in Figure 2.7 (Whitehurst, 2004).

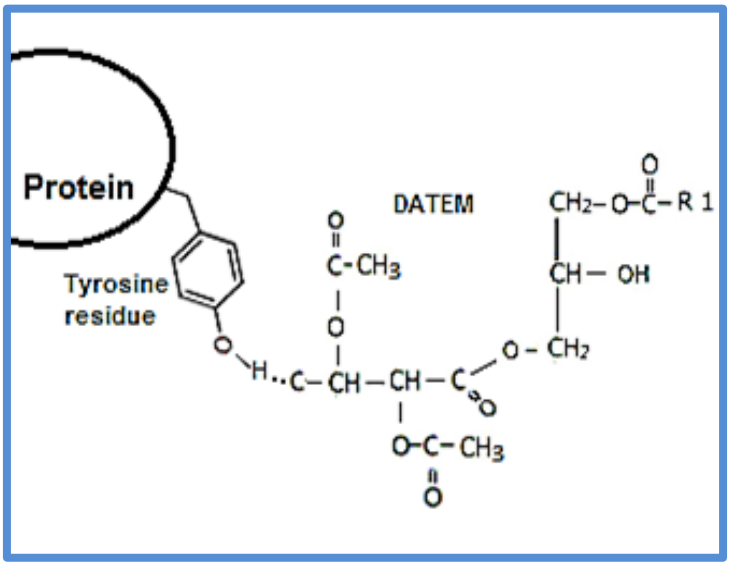

Figure 2.7. Protein-emulsifier interaction in dough resulting in improved mixing tolerance and volume. The figure shows the interaction of the emulsifier DATEM with the non-charged polar residues of the protein through the formation of hydrogen bonds and hydrophobic interactions. Adapted from Whitehurst (2004).

2.5.2.1.4. Polysorbates (Tween)

In practical applications, better emulsifying properties are often obtained by mixing two different emulsifiers. Polysorbates are extremely water soluble and when a small amount of them is added to water the interfacial tension decreases dramatically. Weight for weight, polysorbates have a far better potential to reduce interfacial tension than proteins do, their molecular weight is about 1 part in 24 parts (1 / 25th) of the molecular weight of a protein. Thus they can reach the interphase faster and displace the proteins from the interface. Also when exposed to high temperatures (approximately 80ºC), polysorbates form reverse micelles and swell with water (Whitehurst, 2004; Kunieda and Nakamura, 1991).

Chapter 3. Examination of the Secondary Structure and Thermal Behavior of β-Lactoglobulin Variants A and B Obtained from Different Sources

3.1. INTRODUCTION

Bovine β-lactoglobulin has been extensively studied by FTIR spectroscopy over the past few decades (Casal *et al*., 1988; Boye *et al*., 1996; Dong *et al*., 1996; Boye *et al*., 1997; Qi *et al*., 1997; Lefevre and Subirade, 1999), however the effects that the conditions employed in the isolation of the protein from milk and in any subsequent purification or processing steps may have on its secondary structure and thermal behavior have not been fully examined, although it was found in previous research in our laboratory that samples obtained from a single commercial supplier were not consistent from batch-to-batch in terms of their thermal stability, as monitored by FTIR spectroscopy (unpublished data). Furthermore, other researchers have noted that the commercially available products commonly contain a certain amount of aggregated protein (Qi *et al.*, 1995).

Within this context, the studies presented in this chapter were undertaken to characterize the FTIR spectroscopic behavior of β-lactoglobulin samples from several different sources, including the food-grade β-lactoglobulin employed in the subsequent development of a "high protein cookie" model food system. For this purpose, the two genetic variants present in food-grade β-lactoglobulin (variants A and B) were separated by ion-exchange chromatography; although variants A and B differ in their primary structure at only two positions they exhibit differences in their thermal stability, conformational mobility and association properties and accordingly have been investigated as separate entities in several FTIR studies reported in the literature (Dong *et al*., 1996; Boye *et al*., 1997). To obtain "reference" samples of known history, protein isolation from fresh whole milk produced by a cow homozygous for variant A was performed in our laboratory. Research-grade samples of β-lactoglobulin A and β-lactoglobulin B as well as an AB mixture were also acquired from a commercial supplier (Sigma). All samples were subjected to detailed examination by variable-temperature FTIR (VT-FTIR) spectroscopy in D_2O solution from room temperature up to 95^oC, allowing for the monitoring of slow H-D exchange processes, thermal unfolding, and aggregation through analysis of the amide I' band profile. As is typically done in FTIR studies of proteins, resolution enhancement by Fourier self-

deconvolution (FSD) was performed to reduce the overlap of individual amide I' band components assigned to particular secondary-structure elements. Interpretation of the Fourier self-deconvolved VT-FTIR spectra was further aided by the use of differential spectroscopy to isolate thermally induced spectral changes from the overall amide I' band profile and by the application of generalized two-dimensional correlation spectroscopy (2D-COS) to elucidate the sequence of thermally induced spectral changes. These techniques, which have not been previously employed in studies of β-lactoglobulin variants A and B, provide new evidence contributing to the understanding of the differing FTIR spectroscopic behavior of the two variants and lay the foundation for the research presented in Chapter 4.

3.2. MATERIALS AND METHODS

3.2.1. Protein samples

β-Lactoglobulin A, β-lactoglobulin B and β-lactoglobulin AB mixture were purchased from Sigma Aldrich (Oakville, ON, Canada) and used without further purification. Food-grade β-lactoglobulin (consisting of variants A and B) was obtained from Davisco Foods International Inc. (Le Sueur, MN, USA).

3.2.2. Separation of β-lactoglobulin variants A and B by ion-exchange chromatography

Food-grade β-lactoglobulin (consisting of variants A and B) was subjected to linear-gradient anion-exchange chromatography to separate variant A (pI = 5.1) from variant B (pI = 5.2). The procedure employed was that of Piez *et al.* (1961) with some modifications. A slurry of diethylaminoethyl (DEAE)-cellulose was prepared in 0.1 M NaOH and poured into a glass column (15 mm × 20 cm). The adsorbent was washed with 10 volumes of 0.1 M NaOH and then with 10 volumes of 0.1 M HCl. The column was equilibrated overnight at room temperature with sodium phosphate buffer (0.05 M, pH 5.8) and washed with 10 volumes of 0.01M NaOH after use. A sample of 250 mg in 5 mL of buffer was dialyzed against the equilibration buffer for 18 h prior to chromatography at 4° C. A linear gradient elution was performed with a mixture of two buffers (buffer A: 0.05 M sodium phosphate, pH 5.2; buffer B: 0.05 M sodium phosphate in 0.08 M NaCl). Fractions of approximately 5 mL were collected and analyzed by an Evolution UV-visible

spectrophotometer (Thermo Electron Corporation, Waltham, MA, USA) at 280 nm. The fractions for variant A and the fractions for variant B were collected and dialyzed separately at 4 °C against distilled water (replaced every 6 h) over a period of 48 h. The samples were then freeze-dried and refrigerated at 4 °C (Labconco Lyph Lock 4.5 Freeze Dryer, Kansas City, MO, USA).

3.2.3. Separation of β-lactoglobulin from acid whey obtained from whole milk using trichloroacetic acid (TCA)

Milk samples were obtained from different cows at the McGill Macdonald Campus Dairy Complex for the purpose of identifying a cow homozygous for β-lactoglobulin variant A. The method employed for protein separation from the milk was that reported by Fox *et al.* (1967) with some modifications in the procedure. The milk was left to stand at refrigeration (4 °C) and freezing temperatures (-10 °C) in order to be able to scoop out the cream. It was then centrifuged at 5000 × g for 30 min in a refrigerated Sorval centrifuge (Sorval RC-5B, Thermo Scientific, Waltham, MA, USA) to remove the remaining fat. The skim milk was acidified to pH 4.6 by adding approximately 50 mL of 1 M HCl per liter of milk with constant stirring in order to precipitate the caseins and then filtered through new Miracloth. Approximately 130 g of TCA was dissolved in the minimum amount of water possible with continuous stirring, the solution was slowly added to the acid whey again with continuous stirring. The resulting solution was left to stand at room temperature for 30 min and then centrifuged at 8000 × g in a refrigerated Sorval centrifuge in order to separate the precipitated whey proteins from the β-lactoglobulin, which remained in solution. The remaining solution was then filtered through a coarse-pore Buchner funnel under vacuum. The filtered solution was dialyzed against distilled water at 4 °C until tests for chloride ions were negative. Finally, the dialyzed solution was freeze-dried and stored at 4 °C. The yield was approximately 270 mg per liter of milk, which is approximately 15% of the yield reported by Fox *et al*. (1967).

Following isolation of β-lactoglobulin from the acidified whey, ESI-MS was used in ascertain whether the cow from which the sample was taken was homozygous for β-lactoglobulin variant A. β-Lactoglobulin solutions for ESI-MS analysis were prepared as described by Alvarez *et al.* (2007) and Gomaa (2010). A 10-mg/mL protein solution was prepared by dissolving β-lactoglobulin in 0.1% formic acid (1:1 water/methanol) and 5 μL of the solution was injected in a Waters Micromass Q-TOF Ultima mass spectrometer (Micromass; Manchester, UK). The gas flow

rate was approximately 20 μL min^{-1}. The sample was directed into the mass spectrometer in the positive ionization mode (+ESI) at 3.8 kV. The spectrometer was operated at a cone voltage of 80 V, with an inter-scan delay of 0.1 s and a scan range of 600-2400 m/z.

3.2.4. Study of the secondary structure and thermal behavior of β–lactoglobulin A, β–lactoglobulin B and β–lactoglobulin AB by FTIR spectroscopy, variable-temperature (VT)-FTIR and two-dimensional correlation spectroscopy (2D-COS)

Samples of β-lactoglobulin A, β–lactoglobulin B and β–lactoglobulin AB were dissolved in D_2O (Cambridge Isotope Laboratories, Inc., Andover, MA) at a concentration of 15% (w/v), all solutions were prepared in triplicate. FTIR spectra were recorded with an Agilent FTIR spectrometer equipped with a deuterated triglycine sulfate (DTGS) detector and purged with dry air from a Balston dryer (Balston, Lexington, MA). All spectra were collected by co-addition of 256 scans at a resolution of 2 cm^{-1}. For VT-FTIR experiments, a 10-μL aliquot of the protein solution was placed between two CaF_2 windows separated by a 15-μm Teflon spacer in a temperature-controlled cell. The temperature of the sample was raised in 5°C increments up to 95°C, with a hold time of 10 min at each temperature during which time the infrared spectrum was acquired. The FTIR spectra were subjected to Fourier self-deconvolution (FSD) (k = 2.4, w = 24 cm^{-1}) and baseline-corrected. The deconvoluted VT-FTIR spectra were normalized and analyzed by 2D-COS employing a program written by Y. Wang (Wang *et al*., 2006).

3.2.5. Study of H-D exchange of β–lactoglobulin A using ^1H 2D-NMR spectroscopy

A sample for progressive H→D exchange NMR analysis was prepared by dissolving 11 mg of bovine β-lactoglobulin variant A from cow's milk in 700 μL of D_2O and adjusted to pD 2.0. The NMR experiments were conducted at the Québec/Eastern Canada High Field NMR Facility. NMR spectra were collected on a Varian Unity Inova 500-MHz spectrometer equipped with a triple-resonance cold probe. TOCSY spectra employed a mixing time of 50 ms and a spin-lock field of 5000 Hz, and a WATERGATE read pulse was used to minimize the signal from H_2O. Spectra were collected with 320 and 768 complex time-domain points in F1 and F2, respectively, spanning 6000 Hz in both dimensions; 8 scans were collected for each indirect time point, with a

'steady-state' pulse preceding the inter-scan delay of 1.1 s, for a total acquisition time of 112 min per spectrum. TOCSY spectra were acquired for time zero and after 48 hours. Data were processed using the NMR Pipe processing package. In both dimensions, a shifted-squared-sine bell window function was applied to the time-domain data and data were zero-filled prior to Fourier transformation. In the direct dimension, a polynomial solvent filter was applied to minimize signals from H_2O. In the indirect dimension, linear prediction was used to double the number of points prior to apodization. The correlations between backbone H_N and Hα were made by reference to the assignments reported by Uhrínová *et al.* (1998).

3.3. RESULTS AND DISCUSSIONS

3.3.1. Verification of purity of β-lactoglobulin variants A and B separated by ion-exchange chromatography

The first source of β-lactoglobulin variant A employed in the present study was a commercial food-grade β-lactoglobulin (consisting of a mixture of variants A and B) which was subjected to ion-exchange chromatography to separate variants A and B, as described above. Subsequent to the chromatographic separation of the two variants, ESI-MS analysis was performed to verify their purity (Figure 3.1), the molecular weight for variants A and B being 18363 and 18277 daltons, respectively. As seen in Figure 3.1a, the mass spectrum of the chromatographically purified variant A showed the presence of a small amount (~10%) of variant B.

(a)

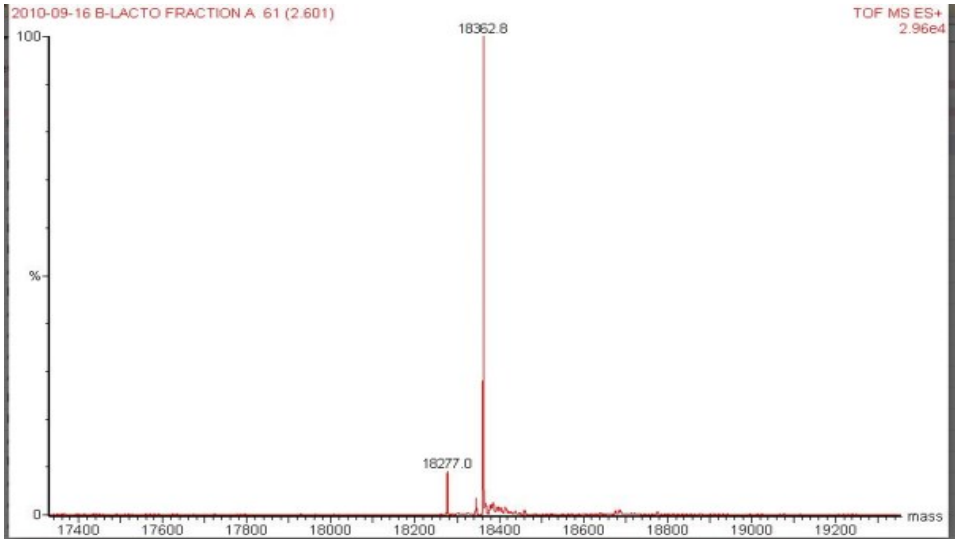

(b)

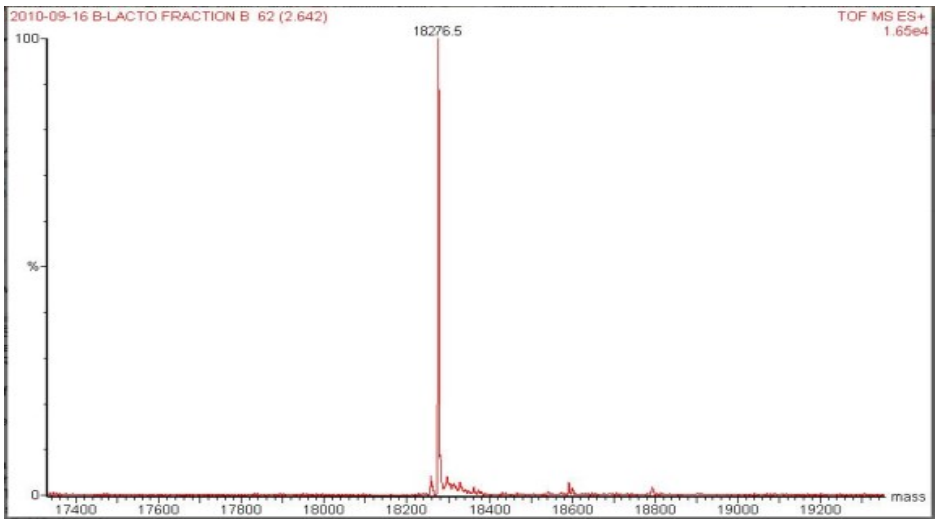

Figure 3.1. Electrospray ionization-mass spectrometry (ESI-MS) results for fractions obtained from ion-exchange chromatography of a sample of commercial food-grade β-lactoglobulin: (a) variant A (b) variant B.

3.3.2. ESI-MS analysis of β-lactoglobulin separated from whole milk using TCA

To obtain a second source of β-lactoglobulin variant A, milk samples were obtained from several cows at the McGill Macdonald Campus Dairy Complex for the purpose of identifying a homozygous cow for β-lactoglobulin variant A. Following isolation of β-lactoglobulin from the acid whey obtained from these samples, as described above, ESI-MS analysis was performed to

ascertain whether the cow from which the sample was taken was homozygous for β-lactoglobulin variant A. For purposes of comparison, the mass spectra of β-lactoglobulin obtained from two of the milk samples are presented in Figures 3.2 and 3.3. The presence of two peaks in Figure 3.2 indicates that both variants A and B are present in the whole milk sample from the Ayrshire cow (code 8322), which is therefore heterozygous for β-lactoglobulin. On the other hand, Figure 3.3 shows a single peak assigned to variant A, revealing the Canadienne cow (code 68015) to be homozygous for β-lactoglobulin A.

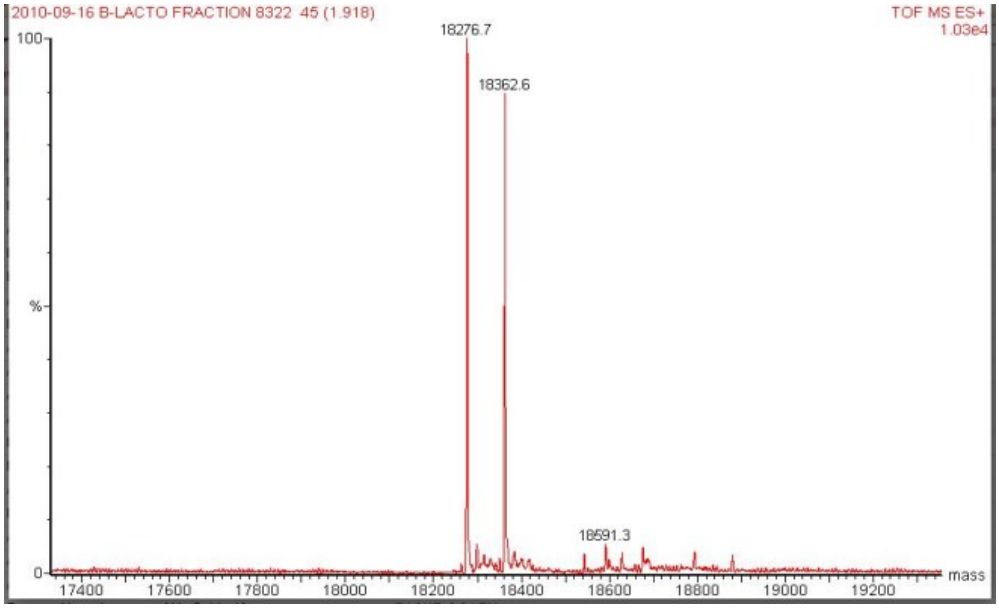

Figure 3.2. Electrospray ionization-mass spectrometry (ESI-MS) of β-lactoglobulin obtained from the milk of an Ayrshire cow (code 8322).

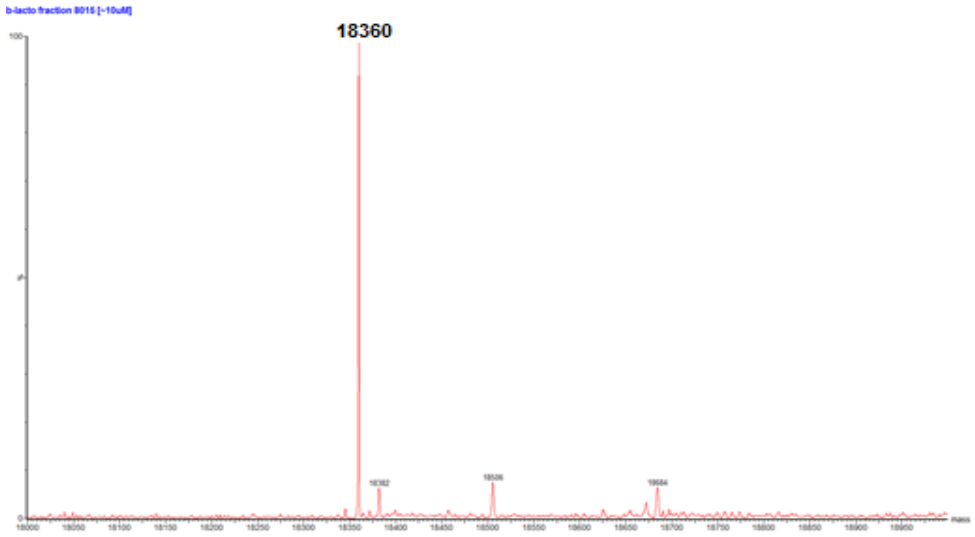

Figure 3.3. Electrospray ionization-mass spectrometry (ESI-MS) of β-Lactoglobulin obtained from the milk of a Canadienne cow (code 6815). The presence of a single peak characteristic of variant A allowed the identification of this cow as homozygous for β-lactoglobulin Variant A.

3.3.3. Study of the secondary structure and thermal behavior of β–lactoglobulin A by FTIR spectroscopy

Figure 3.4 shows the Fourier self-deconvoluted amide I' region in the FTIR spectra of β-lactoglobulin A obtained as described in Sections 3.2.2 and 3.2.3 as well as β-lactoglobulin A purchased from a commercial supplier (Sigma). In all cases the FSD-FTIR spectra of β-lactoglobulin A show six amide I' bands, which have been previously assigned by Boye *et al.* (1996, 1997) (Table 3.1). On examination of the spectra in Figure 3.4, differences among the samples from the three sources are apparent in the bands below 1640 cm^{-1}. In particular, the relative intensities of the bands at ~1627 and ~1637 cm^{-1} differ among the three spectra, with the absorbance ratio A_{1627}/A_{1637} being highest in the spectrum of the sample obtained from Sigma and lowest in the sample separated from the food-grade β-lactoglobulin AB mixture; in the latter spectrum, a slight band shift from ~1627 to ~1625 cm^{-1} is also observed. The bands in this region originate from β-lactoglobulin's nine β-strands (Boye *et al.,* 1996*,* 1997), eight of which form the β-barrel characteristic of the lipocalin family of proteins while the ninth participates in dimer formation. In previous studies of the FTIR spectra of β-lactoglobulin (a mixture of variants A and

B), Lefevre and Subirade (1999) reported that the observation of two components between 1620 cm^{-1} and 1635 cm^{-1} indicates the presence of the dimeric form, which is the form present in solution at neutral pH, while a single component indicates the presence of the monomeric form of β-lactoglobulin. Accordingly, the differences seen in Figure 3.4 could reflect changes in secondary structure that alter the hydrogen bonding between amide groups in some of the β-strands (thereby altering the amide I' frequencies) or they might be associated with differences in the monomer-dimer equilibrium among the three different samples of β-lactoglobulin A. In addition, differences in tertiary structure, although seldom considered to be manifested in FTIR spectra, have been reported to affect the spectrum of β-lactoglobulin by exposing amide groups to the solvent (Boye *et al.,* 1996; Gomaa *et al.,* 2013). In lipocalins such as β-lactoglobulin, the interior of the β-barrel forms a hydrophobic core while the outer surface of the barrel is exposed to the solvent. Accordingly, upon dissolution of the protein in D_2O, H-D exchange of the amide groups will proceed more readily on the outer surface of the β-barrel than in the interior. Indeed, in an FTIR study by Boye *et al.* (1996), in which the spectrum of β-lactoglobulin AB in D_2O solution was monitored as a function of temperature, mild heating resulted in spectral changes attributed to H-D exchange of previously buried β-sheets, suggesting loosening of the tertiary structure (Gomaa *et al.,* 2013). Given the potential roles of differences in secondary, tertiary, and quaternary structure (i.e., dissociation of β-lactoglobulin dimers), the spectral differences among the three β-lactoglobulin A samples in Figure 3.4 could not be readily explained and will be further discussed after presenting the results of VT-FTIR experiments.

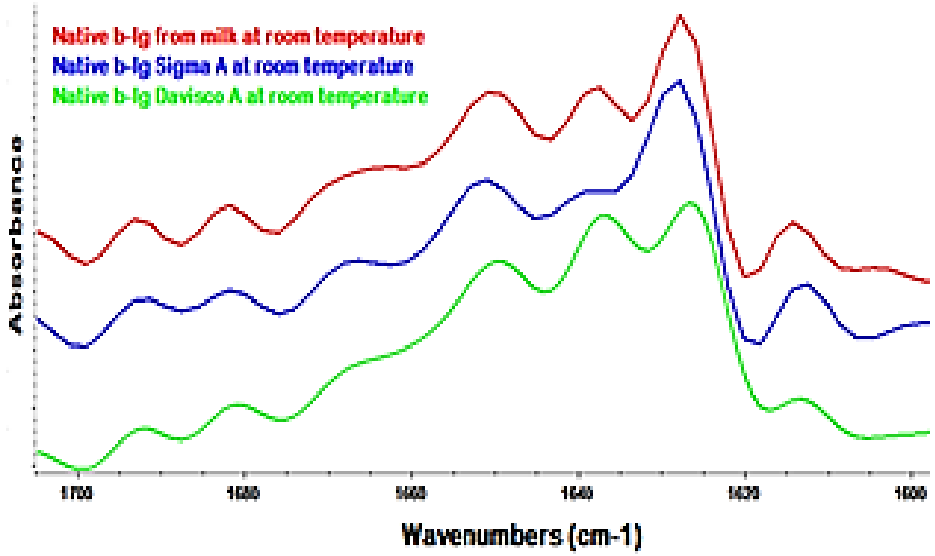

Figure 3.4. Deconvoluted spectra in the amide I´ region of β-lactoglobulin A purchased from Sigma (blue), separated from variant B by ion-exchange chromatography of food-grade β-lactoglobulin (Davisco) (green), and isolated from whole milk (red) at 25° C.

Table 3.1. β-lactoglobulin amide I' band assignments (Boye *et al.*, 1996, 1997)

Amide I' band assignment	β-lactoglobulin AB	β-lactoglobulin A	β-lactoglobulin B
Buried intramolecular β-sheet (antiparallel) (high-frequency band)	1691-1693	1692	1692
Solvent-exposed intramolecular β-sheet (antiparallel) (high-frequency band)	1687-1684	1681-1676	1681-1680
Loops & turns	1670-1666	1669-1664	1669 (shoulder)
α-Helix	1650-1649	1649-1647	1649-1647
Solvent-exposed intramolecular β-sheet (antiparallel) (low-frequency band)	1636-1632	1637-1635	1636-1635
β-Structure	1625-1623	1629-1625	1628-1624

The effects of heat treatment on β-lactoglobulin A obtained from the three sources were examined by VT-FTIR spectroscopy over the temperature range of 25-95ºC. Figure 3.5 shows the spectra recorded after 10 min of holding time at 95ºC, representing the end of the heating cycle. It is evident that the β-lactoglobulin A isolated from whole milk in our laboratory and that obtained from Sigma underwent extensive aggregation as indicated by the very strong band at 1618 cm^{-1} and the weak band at ~1684 cm^{-1}, both of which are associated with the formation of intermolecular β-sheets (Boye *et al.*, 1997). In contrast, the spectrum of β-lactoglobulin A obtained by ion-exchange chromatography of food-grade β-lactoglobulin AB exhibits a broad, largely featureless amide I' band that indicates extensive loss of secondary structure but little formation of intermolecular β-sheets. Figures 3.6-3.8 show the plotted absorbance at 1618 cm^{-1} as a function of temperature for β-lactoglobulin A from the three different sources, showing that β-lactoglobulin A isolated from whole milk in our laboratory and the product obtained from Sigma are similar, exhibiting a quite sharp increase in the absorbance at 1618 cm^{-1} and a defined transition to a denatured state between 75 and 85ºC, whereas the β-lactoglobulin A derived from food-grade β-lactoglobulin AB shows a very different behavior characterized by a gradually increasing absorbance with no defined transition from a native to a denatured state. These differences may be attributed to the differences in the methods by which the proteins were originally isolated. According to its manufacturer (Davisco Foods), the food-grade β-lactoglobulin AB is isolated from sweet whey by large-scale ion-exchange chromatography followed by a proprietary mild thermal treatment (between 40ºC and 50ºC) prior to spray drying. In contrast, in the isolation of β-lactoglobulin A from whole milk in our laboratory, the protein was never subjected to heat treatment and a powdered sample was obtained by freeze drying. Given the apparently much more extensive aggregation of the latter upon heating to 95ºC, it may be concluded that the proprietary mild thermal treatment employed in the production of food-grade β-lactoglobulin AB results in a "non-native" structure that has less propensity to aggregate in the preparation of thermally processed foods. As far as the samples obtained from the commercial supplier of β-lactoglobulin A are concerned, the VT-FTIR results showed very similar behavior to β-lactoglobulin A isolated from whole milk.

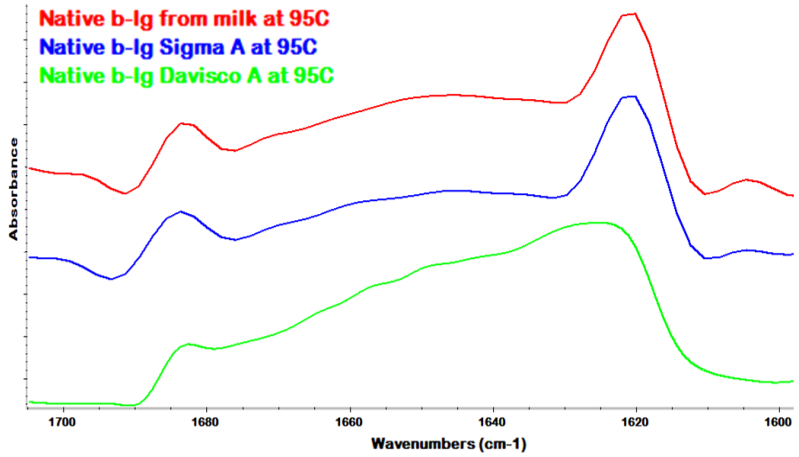

Figure 3.5. Deconvoluted spectra in the amide I´ region of D_2O solutions of β-lactoglobulin variant A held for 10 min at 95±1°C: β-lactoglobulin A acquired from a commercial supplier (blue), separated from variant B by ion-exchange chromatography of food-grade β-lactoglobulin (Davisco) (green), and isolated from whole milk (red).

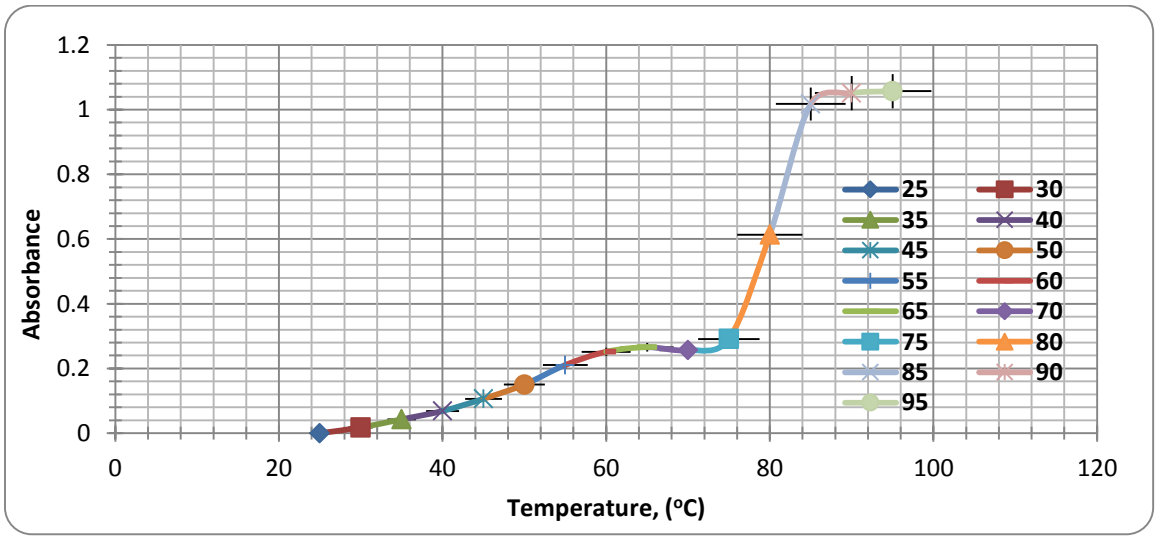

Figure 3.6. Aggregation of β-lactoglobulin variant A isolated from whole milk as a function of temperature, as monitored by the absorbance at 1618 cm^{-1}, assigned to intermolecular β -sheets and indicative of irreversible protein denaturation.

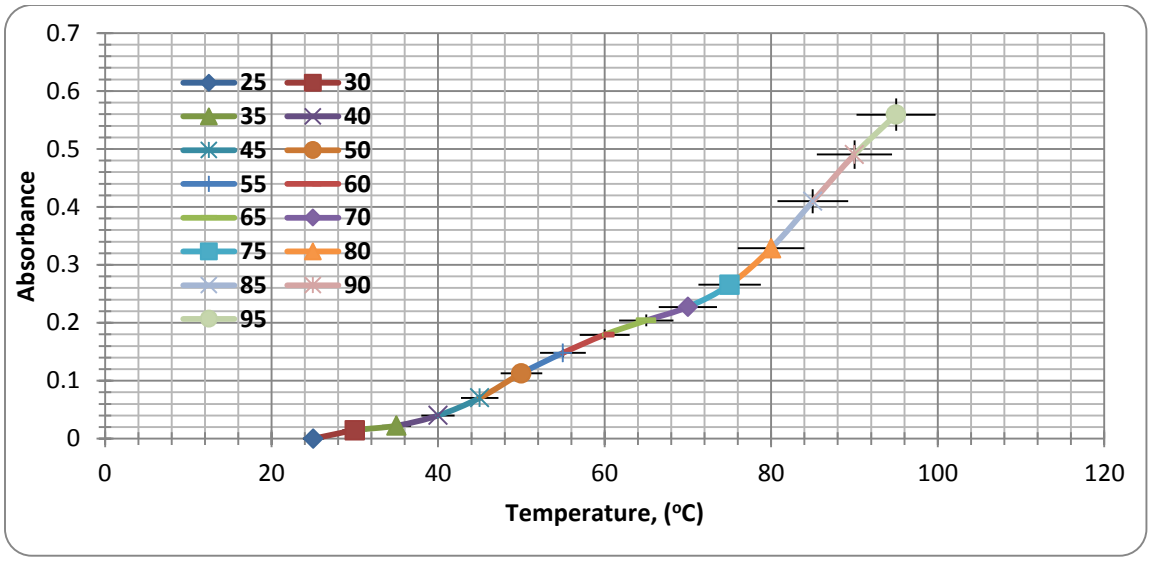

Figure 3.7. Aggregation of β-lactoglobulin variant A obtained by ion-exchange chromatography of food-grade β-lactoglobulin AB, as monitored by the absorbance at 1618 cm^{-1}, assigned to intermolecular β-sheets and indicative of irreversible protein denaturation.

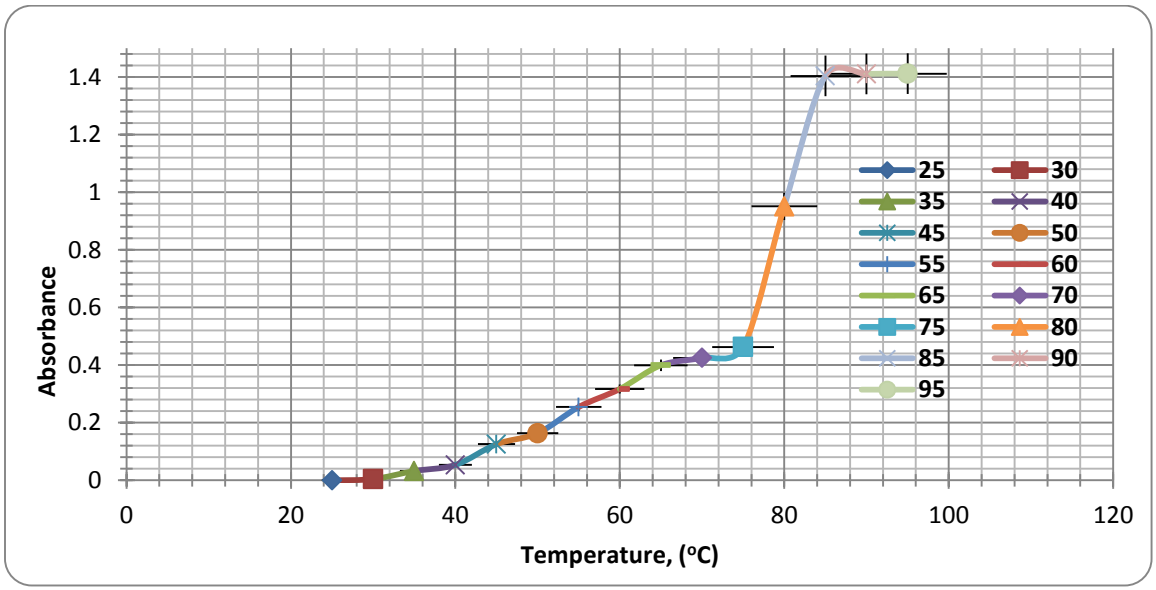

Figure 3.8. Aggregation of β-lactoglobulin variant A from Sigma as a function of temperature, as monitored by the absorbance at 1618 cm^{-1}, assigned to intermolecular β-sheets and indicative of protein denaturation.

The thermal unfolding of β-lactoglobulin A from the three different sources prior to aggregation was further studied through the application of 2D correlation spectroscopy (2D-COS) to the amide I' region in the VT-FTIR spectra collected over the temperature range of 30-75°C.

The synchronous and asynchronous contour maps generated from the VT-FTIR spectra of the sample of β-lactoglobulin A isolated from whole milk are presented in Figure 3.9, and the 2D correlation table based on the examination of the 2D contour maps is presented in Table 3.2, the corresponding results for the other two samples are presented in Tables 3.3 and 3.4. The results in Tables 3.2-3.4 were employed to elucidate the sequence of events occurring during thermal treatment of the protein samples on the basis of the principles of 2D correlation analysis established in the literature (Filosa *et al*., 2001; Wang *et al*., 2006), which may be summarized as follows. Referring to Figure 3.9 and the corresponding correlation table (Table 3.2), the wavenumbers listed in the top row and the left-hand column of the table correspond to positions on the x-axis and y-axis, respectively, of the contour maps in the figure, and the vertical arrows after the wavenumbers indicate whether the absorbance at that wavenumber increased (↑) or decreased (↓) as the temperature was raised during the VT-FTIR experiment. The + and – signs in the cells of the table correspond to the signs of cross-peaks above the diagonal in the synchronous (Figure 3.9, left-hand panel) and asynchronous (Figure 3.9, right-hand panel) maps; an entry of 0 indicates the absence of a cross-peak. A positive cross-peak on the synchronous map (solid line on map; +/ in the table) indicates that the absorbances at the corresponding (x, y) wavenumbers either both increased or both decreased as the temperature was raised, whereas a negative cross-peak on the synchronous map (dashed line on map; -/ in the table) indicates that the absorbances at the corresponding (x, y) wavenumbers changed in opposite directions.

Comparison with the signs of the cross-peaks on the asynchronous map then allows the sequence of events to be deduced by application of the following rules: if the signs of the cross-peaks on the synchronous and asynchronous maps are the same (denoted by +/+ or -/- in the table), then the changes in absorbance at the wavenumber on the x-axis took place at a lower temperature than the changes at the wavenumber on the y-axis, as denoted by the ← symbol; if these two signs are different (denoted by +/- or -/+ in the table), then the changes in absorbance at the wavenumber on the y-axis took place at a lower temperature than the changes at the wavenumber on the x-axis, as denoted by the → symbol; absence of a cross-peak on the asynchronous map (+/0 or -/0 in the table) indicates that the changes in absorbance at the wavenumbers on the x-axis and the y-axis occurred simultaneously, as denoted by the ↔ symbol. However, as features on the asynchronous map may be difficult to distinguish in certain cases, the absence of a cross-peak was not regarded as definitive, particularly under circumstances in which the above rules did not yield an internally

consistent sequence of events. Problems also arise when the changes in intensity at a given wavenumber occur in different directions over the temperature range examined (e.g., a band undergoes an increase in intensity in the early stages of heating but then decreases in intensity as heating continues). For this reason, the VT-FTIR spectra collected at temperatures above 75ºC were excluded from the 2D correlation analysis. Similarly, visual examination of the VT-FTIR spectra collected over the temperature range of 25-75°C indicated that the amide I' band component at 1634-1637 cm^{-1} progressively increased with temperature up to ~65ºC and then decreased. Owing to this change in direction, this band had to be excluded from the 2D correlation analysis but was taken into account in interpreting the results in terms of the sequence of events.

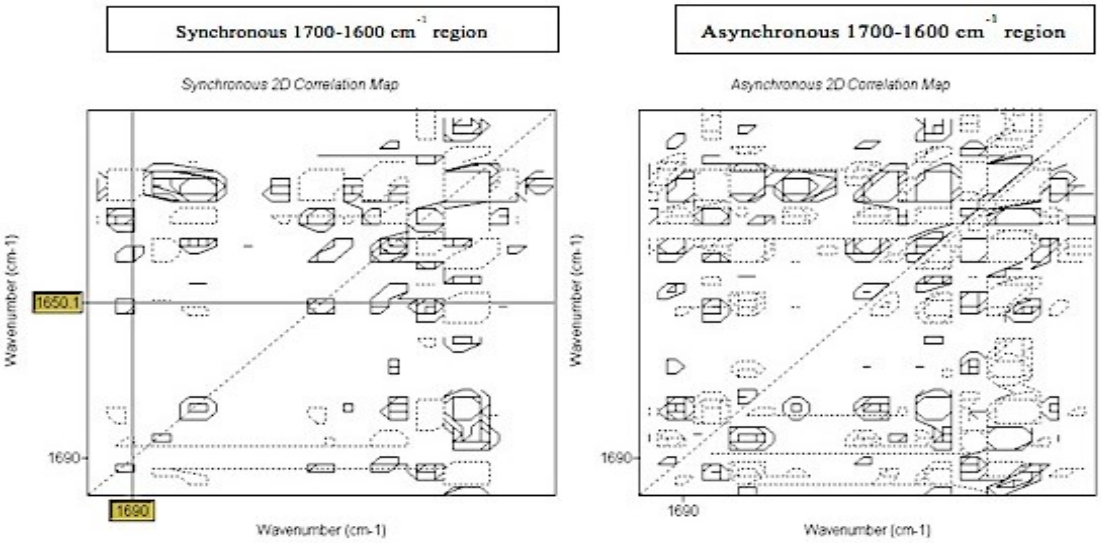

Figure 3.9. Synchronous and asynchronous contour maps obtained by 2D correlation analysis of the amide I´ region in the FSD VT-FTIR spectra of β-lactoglobulin variant A from whole milk over the temperature range of 30-75ºC. The maps were used to generate the correlation table for the sequence of unfolding and aggregation events shown in Table 3.2.

To aid in the interpretation of the 2D results, the spectral changes occurring below 65ºC were highlighted by computing differential and variance spectra from the FSD amide I' band. Figure 3.10 presents the differential spectra obtained for β-lactoglobulin A from whole milk by subtracting the spectrum recorded at the initial temperature from each of the VT-FTIR spectra collected in the early stages of heating (30-60ºC), together with the variance spectrum obtained by computing the variance of these differential spectra. The corresponding plots for β-lactoglobulin

A separated from food-grade β-lactoglobulin AB and for β-lactoglobulin A from the commercial supplier (Sigma) are presented in Figures 3.11 and 3.12, respectively.

The results of the 2D correlation analysis for β-lactoglobulin A isolated from whole milk (Figure 3.9 and Table 3.2) indicated an initial decrease in intensity at 1627 cm^{-1} followed by an increase in intensity at 1621 cm^{-1}; visual examination of the differential spectra in Figure 3.10 indicated that these spectral changes were accompanied by an increase in intensity at 1636 cm^{-1}. The 1621 cm^{-1} band is not resolved in the VT-FTIR spectra although it is observed in the differential spectra of β-lactoglobulin from all three sources, as seen in Figures 3.10, 3.11 and 3.12; its presence on the 2D contour maps exemplifies the enhancement of the effective spectral resolution that 2D-COS can provide by spreading overlapping bands over a second dimension. Subsequent to these initial changes in the "low-frequency β-sheet region" (i.e., below 1640 cm^{-1}), the 2D correlation analysis shows concomitant decreases in intensity at ~1650 and 1692 cm^{-1}. Referring to Table 3.1, the decreasing band at 1650 cm^{-1} is assigned to α-helical structure whereas the decreasing band at 1692 cm^{-1} is a high-frequency β-sheet band assigned to solvent-shielded intramolecular β-sheets. The latter band assignment is based on the FTIR study by Boye *et al.* (1996), in which the spectrum of β-lactoglobulin AB in D_2O solution was monitored as a function of temperature. In that study, a decrease in the 1692 cm^{-1} band was attributed to H-D exchange resulting from exposure of previously buried antiparallel β-sheets to the D_2O solvent and gave rise to an increase in the band at 1684 cm^{-1}, assigned to solvent-exposed intramolecular antiparallel β-sheets. In agreement with the latter study, the 2D-COS analysis indicates that the decrease in the 1692 cm^{-1} band was followed by an increase in the 1682 cm^{-1} band.

As seen in Table 3.3, the 2D-COS analysis for β-lactoglobulin A separated from food-grade β-lactoglobulin AB had the same sequence of events as just described for β-lactoglobulin A isolated from whole milk. In the case of the commercial sample of β-lactoglobulin A (Table 3.4), the sequence of spectral changes differs in that the decrease in intensity at 1621 cm^{-1} precedes the increase in intensity at 1629 cm^{-1}; however, careful examination of the differential spectra for the samples from all three sources suggests that this difference may not be meaningful.

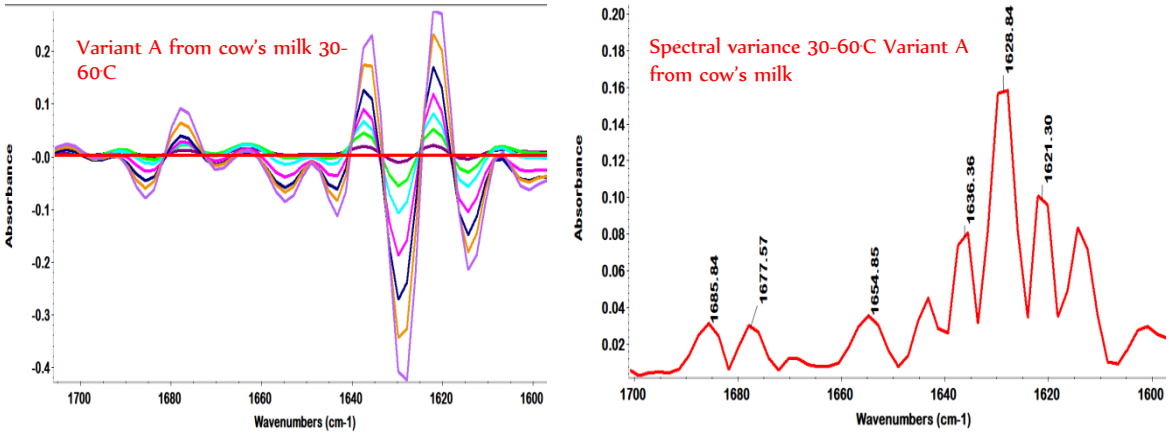

Figure 3.10. Differential spectra (left) and variance spectrum (right) in the amide I´ region of β-lactoglobulin variant A from whole milk. The sample was heated from 25ºC to 60ºC in 5ºC increments, and the differential spectra were generated by subtracting the spectrum recorded at the beginning of the heating cycle from each of the other spectra.

Table 3.2. Correlation table generated by 2D correlation analysis of the FSD VT-FTIR spectra (25-75 °C) of β-lactoglobulin A isolated from whole milk.

cm^{-1}	1692 ↓	1682 ↑	1650 ↓	1636 ↑↓	1627 ↓
1621 ↑	- / + →	+ / - →	- / + →	—[a]	- / - ←
1627 ↓	+ / - →	- / + →	+ / - →	—[a]	
1636 ↑↓	—[a]	—[a]	—[a]		
1650 ↓	+ / 0 ↔	- / + →			
1682 ↑	- / - ←				
Sequence of spectral changes: ↓1627→ ↑1621 → ↓1650 ↔ ↓1692 → ↑1682					

[a] The 1636 cm^{-1} band was excluded from the 2D correlation analysis owing to its bidirectional changes in intensity.

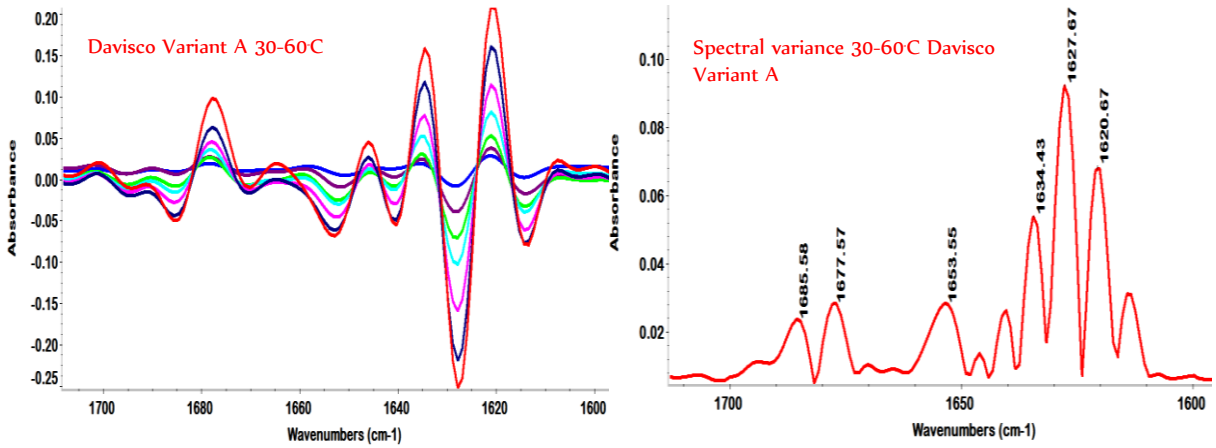

Figure 3.11. Differential spectra (left) and variance spectrum (right) in the amide I′ region of β-lactoglobulin variant A obtained by ion-exchange chromatography of food-grade (Davisco) β-lactoglobulin AB. The sample was heated from 25ºC to 60ºC in 5 ºC increments, and the differential spectra were generated by subtracting the spectrum recorded at the beginning of the heating cycle from each of the other spectra.

Table 3.3. Correlation table generated by 2D correlation analysis of the FSD VT-FTIR spectra (25-75°C) of β-lactoglobulin A obtained by ion-exchange chromatography of food-grade β-lactoglobulin AB.

cm^{-1}	1692 ↓	1682 ↑	1650 ↓	1634 ↑↓	1627 ↓
1621 ↑	- / + →	+ / - →	- / + →	—[a]	- / - ←
1627 ↓	+ / - →	- / + →	+ / - →	—[a]	
1634 ↑↓	—[a]	—[a]	—[a]		
1650 ↓	+ / 0 ↔	- / + →			
1682 ↑	- / - ←				
Sequence of spectral changes: ↓1627→ ↑1621 → ↓1650 ↔ ↓1692 → ↑1682					

[a] **The 1634 cm-1 band was excluded from the 2D correlation analysis owing to its bidirectional changes in intensity**

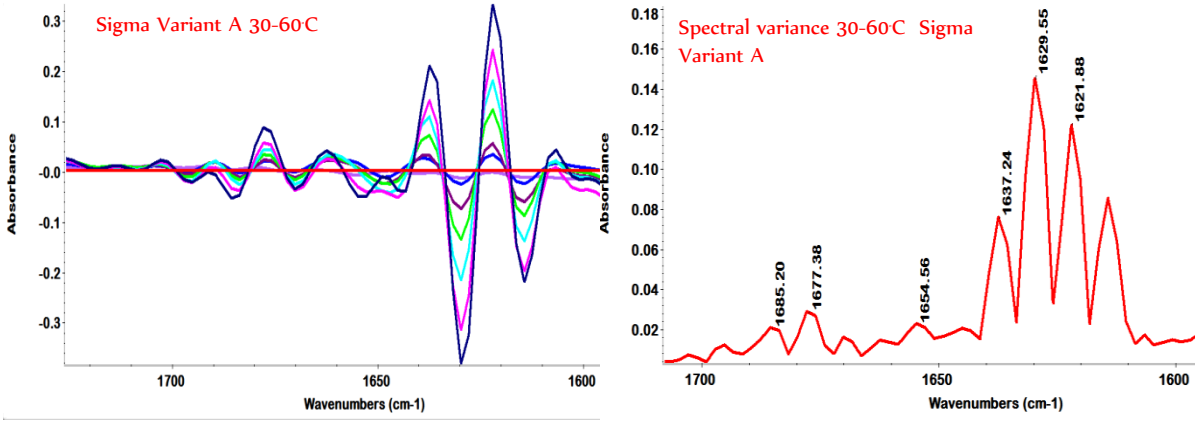

Figure 3.12. Differential spectra (left) and variance spectrum (right) in the amide I´ region of β-lactoglobulin variant A obtained from a commercial supplier (Sigma). The sample was heated from 25°C to 60°C in 5°C increments, and the differential spectra were generated by subtracting the spectrum recorded at the beginning of the heating cycle from each of the other spectra.

Table 3.4. Correlation table generated by 2D correlation analysis of the FSD VT-FTIR spectra (25-75 °C) of β-lactoglobulin A acquired from a commercial supplier.

cm^{-1}	1692 ↓	1682 ↑	1650 ↓	1637 ↑↓	1629 ↓
1621 ↑	- /0 ↔	+ / - →	- / + →	—[a]	-/ + →
1629 ↓	+ / - →	+ / - →	+ / 0 ↔	—[a]	
1637 ↑↓	—[a]	—[a]	—[a]		
1650 ↓	+ / + ←	- / + →			
1682 ↑	- / 0 ↔				
Sequence of spectral changes: ↑1621 → ↓1629 → ↓1692 ↔ ↓1650 → ↑1682					

[a] The 1637 cm^{-1} band was excluded from the 2D correlation analysis owing to its bidirectional changes in intensity

Overall, the above studies using differential spectral analysis and 2D-COS analysis yielded very similar results for the samples of β-lactoglobulin A from the three different sources, despite the differences apparent in their spectra at room temperature in Figure 3.4. As noted above, the latter spectra are characterized by a pronounced decrease in the absorbance ratio A_{1627}/A_{1637} between the spectrum of the sample obtained from Sigma and that of the sample separated from the food-grade β-lactoglobulin AB mixture, with the spectrum of the sample isolated from cow's milk exhibiting an intermediate value of this ratio. Comparison of the latter spectra in light of the

VT-FTIR results, which reveal a progressive decrease in the 1628 cm^{-1} band with increasing temperature accompanied by increases in bands at 1621 cm^{-1} and 1636 cm^{-1}, indicates that the process responsible for these changes has already proceeded substantially at room temperature, at least in the case of the samples derived from food-grade β-lactoglobulin and, to a lesser extent, cow's milk. As noted above, the latter protein had never been subjected to any heat treatment, nor to any denaturing agent. Accordingly, it was concluded that the process in question does not involve any changes in the native secondary structure. Having excluded this possibility, further investigations were undertaken to elucidate whether the process in question is a shift in the dimer-monomer equilibrium in favor of the monomer with increasing temperature. Since the monomer should also be favored in dilute solution, three solutions of β-lactoglobulin A in D_2O were prepared at much lower concentrations [2.5%, 0.5% and 0.25% (w/v)] than employed in the VT-FTIR studies and their spectra acquired at ambient temperature in longer pathlength cells to improve the signal-to-noise ratio (50-μm pathlength for the 2.5% and 0.5% solutions and 75-μm pathlength for the 0.25% solution). These spectra, presented in Figure 3.13, do not exhibit any substantial differences in band positions or relative intensities in the FSD amide I' region. Furthermore, the spectra in Figure 3.13 resemble the upper spectrum in Figure 3.4 (15% solution of β-lactoglobulin A isolated from milk). In view of the spectral similarity over this very broad concentration range, it was concluded that shifts in dimer-monomer equilibrium do not have a major role in the changes observed in the VT-FTIR spectra or in the differences among the three room-temperature spectra in Figure 3.4.

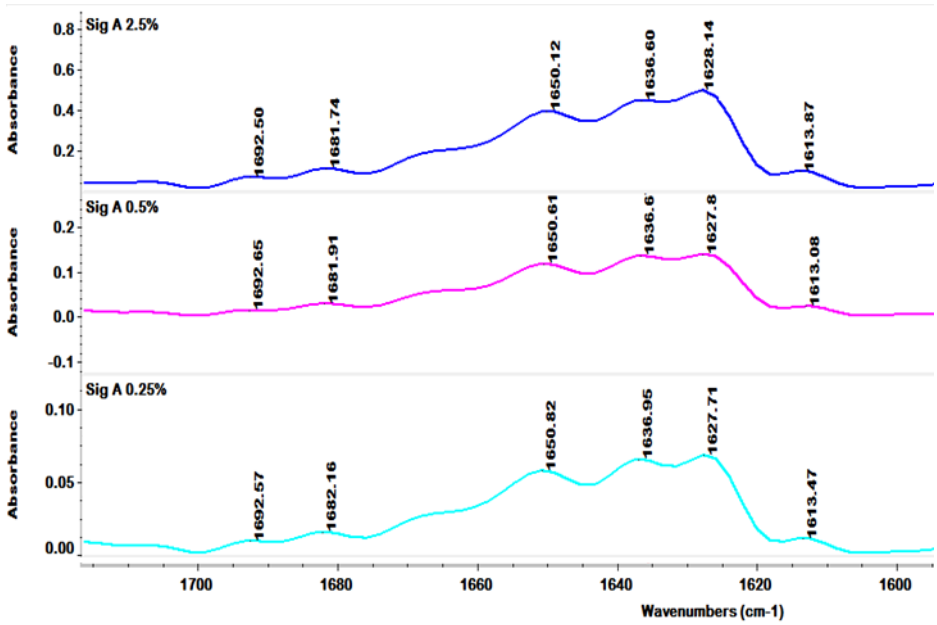

Figure 3.13. Fourier self-deconvolution (FSD) of the amide I´ band of β-lactoglobulin A (Sigma) dissolved in D_2O at a concentration of 2.5%, 0.5% and 0.25% (w/v).

Taken together, the above findings suggest that the changes in the FTIR spectra of β-lactoglobulin A during heating from 25°C to 60°C are primarily associated with progressive H-D exchange of certain amide groups in this temperature range. Evidence supporting this postulate is provided by an FTIR study in which the spectra of β-lactoglobulins A and B were acquired in both H_2O and D_2O solution (Dong *et al.*, 1996). The wavenumber positions of major peaks in the resolution-enhanced amide I region of β-lactoglobulin A in H_2O tabulated by Dong *et al.* (1996), (1683, 1656, 1641, and 1628 cm^{-1}) closely match the positions of the negative peaks in the differential spectra we have presented in Figure 3.10, with the exception of the negative peak at 1613 cm^{-1}; however, the latter wavenumber is below the amide I region and may be associated with side-chain absorptions, as noted by Dong *et al.* (1996). In turn, the positions of the positive peaks in our differential spectra correspond fairly well with wavenumber positions tabulated by Dong *et al.* (1996) for β-lactoglobulin A in D_2O (1676, 1633 and 1623 cm^{-1}). Accordingly, the differential spectra in Figure 3.10 are consistent with H-D exchange of some of the protein's amide groups resulting in the following band shifts: 1683 → 1677 cm^{-1}, 1641 → 1636 cm^{-1} and 1628 → 1621 cm^{-1}. It must be noted, however, that the intensity increase at 1636 cm^{-1} far exceeds the intensity decrease at 1641 cm^{-1} while the intensity increase at 1621 cm^{-1} is lower in magnitude than

the intensity decrease at 1628 cm^{-1}. The resulting apparent redistribution of band intensity in the β-sheet region below 1640 cm^{-1} with increasing temperature is illustrated in Figure 3.14. This phenomenon was also noted by Dong *et al.* (1996) but remains to be explained. Two possible explanations can be suggested: (1) the H-D exchange of the β-sheets results in a conformational change and/or (2) the hydration of the dissolved protein with time results in some rearrangements of the hydrogen bonds to amide carbonyl groups, altering the bandwidth and/or absorptivity of certain amide I' bands. .

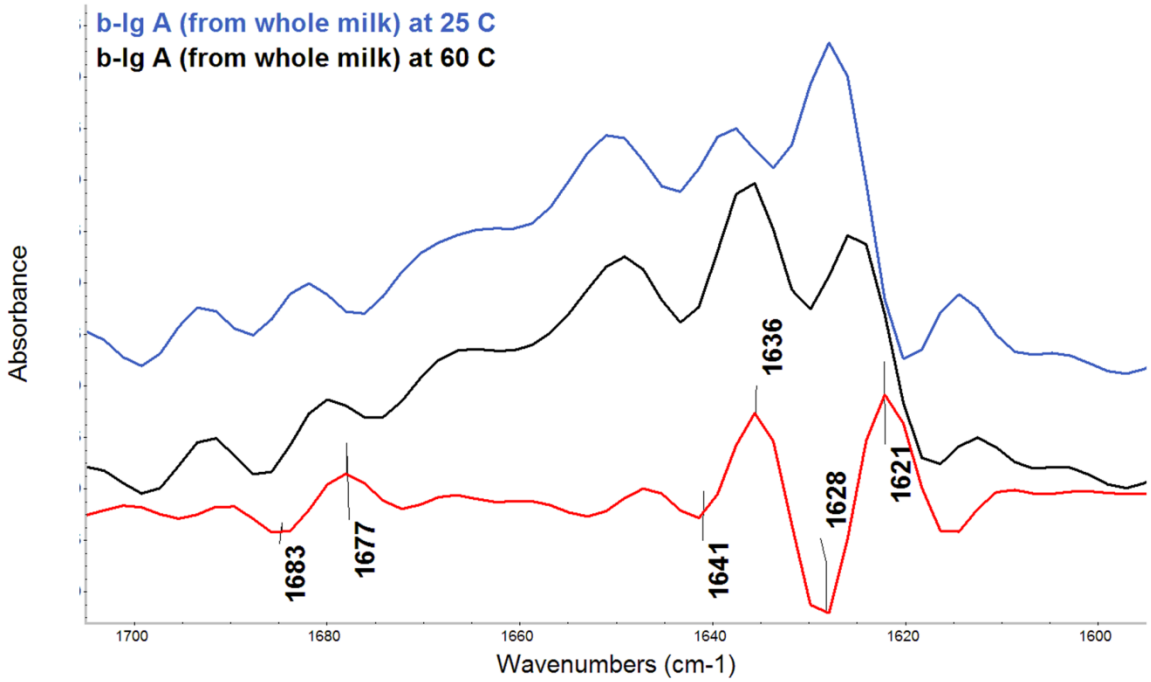

Figure 3.14. Fourier self-deconvolution (FSD) of the amide I´ band of β-lactoglobulin A (isolated from whole milk) in spectra recorded at ambient temperature (top) and at 60°C (middle). The bottom spectrum is the differential spectrum obtained by subtraction of the ambient-temperature spectrum from the 60°C spectrum.

In a study of the thermal denaturation and aggregation of β-lactoglobulins A and B, Boye *et al.* (1997) observed that a decrease in the intensity at 1628-1629 cm^{-1} in the VT-FTIR spectra of β-lactoglobulin A was mirrored by an increase an intensity at 1635-1636 cm^{-1} up to an inflection point at 59-65°C (depending on pH), beyond which the changes in intensity of these two bands

were reversed but continued to mirror each other. Boye *et al.* (1997) attributed the changes observed before the inflection point to an initial stage in the thermal unfolding of β-lactoglobulin A involving an increase in β-sheet structure accompanied by a possible association of the protein molecules. However, as discussed above, the results of our study do not support this conclusion.

In this regard, it is interesting to note that Boye *et al.* (1997) did not observe any increase in intensity at 1635-1636 cm^{-1} during the heating of β-lactoglobulin B, which led them to conclude that the initial increase in β-sheet structure during thermal unfolding referred to above occurs only in the case of β-lactoglobulin A. As described below, the examination of the VT-FTIR spectra of β-lactoglobulin B in the present study confirmed their observations but led to a different interpretation of the spectral differences between variants A and B.

3.3.4. Study of the secondary structure and thermal behavior of β–lactoglobulin B by FTIR spectroscopy

Figure 3.15 shows the Fourier self-deconvoluted amide I' region in the FTIR spectra of β-lactoglobulin B obtained by ion-exchange chromatography of food grade β-lactoglobulin AB (Davisco) as described in Section 3.2.2 as well as β-lactoglobulin B purchased from a commercial supplier (Sigma). The spectra of β-lactoglobulin B from the two different sources are virtually identical, in contrast to the findings reported above for β-lactoglobulin A (Figure 3.4). As in the case of β-lactoglobulin A, the FSD-FTIR spectra of the β-lactoglobulin B samples show six amide I' bands, which have been previously assigned by Boye *et al.* (1996, 1997) (Table 3.1), and the amide I' band profile does not appear to be altered in the spectra of dilute solutions (Figure 3.16).

Comparison of the spectra of β-lactoglobulin B in Figures 3.15 and 3.16 with those of β-lactoglobulin A collected under the same conditions (Figures 3.4 and 3.13, respectively) reveals pronounced differences between the two variants, particularly in terms of the relative intensities of the two bands in the β-sheet region below 1640 cm^{-1}. As concluded in the previous section, these differences in relative intensities may be indicative of different extents of H-D exchange of certain amide groups in β-sheets. Indeed, comparing the spectra in Figure 3.15 with those in Figure 3.14 reveals a strong similarity between the spectrum of β-lactoglobulin B at room temperature and that of β-lactoglobulin A at 60°C. This observation indicates that at least some of the amide

groups in β-sheets undergo H-D exchange with the D_2O solvent much more readily in β-lactoglobulin B, suggesting that the conformational mobility of variant B is much greater that of variant A. It may be noted that Dong *et al.* (1996) reached the opposite conclusion based on their FTIR results; however, the rationale for that conclusion is unclear.

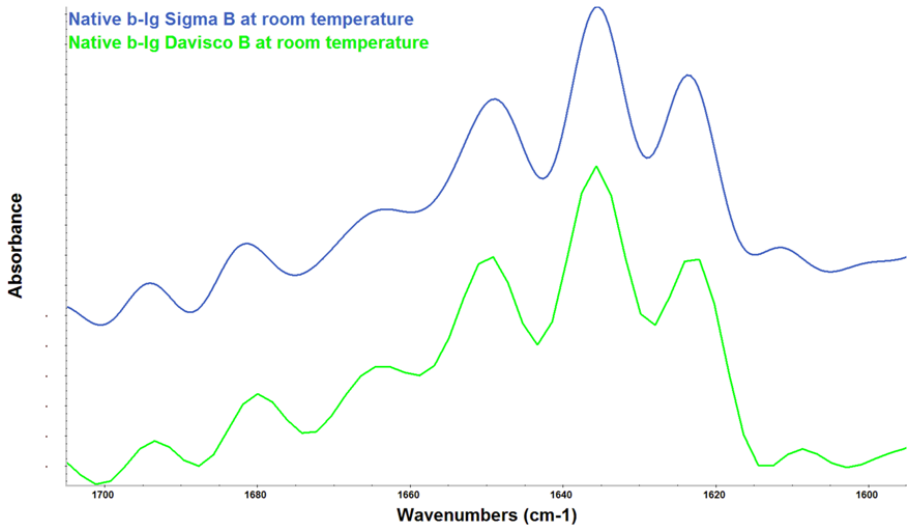

Figure 3.15. Deconvoluted spectra in the amide I´ region of β-lactoglobulin B purchased from Sigma (blue) and separated from variant A by ion-exchange chromatography of food-grade β-lactoglobulin (Davisco) (green) at 25° C.

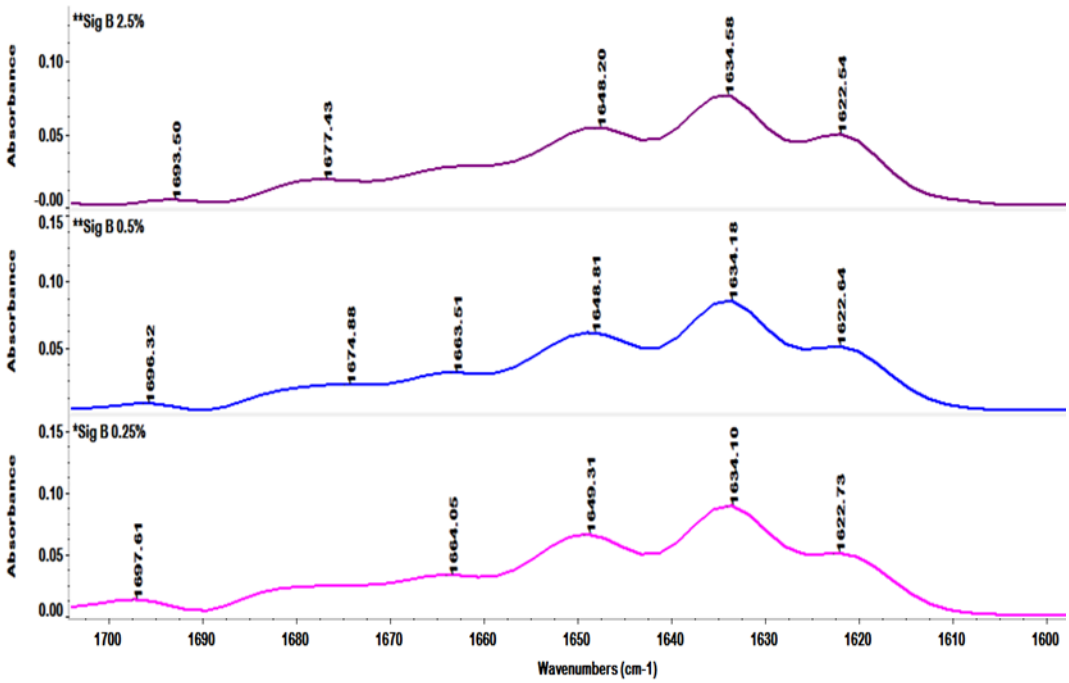

Figure 3.16. Fourier self-deconvolution (FSD) of the amide I´ band of β-lactoglobulin B (Sigma) dissolved in D_2O at a concentration of 2.5%, 0.5% and 0.25% (w/v).

The results of the VT-FTIR experiments conducted with β-lactoglobulin B from the two sources over the temperature range of 30-60°C are presented in Figure 3.17. Overall, the differential spectra of β-lactoglobulin B are more complicated than those of β-lactoglobulin A and also depend on the source of the protein, even though the room-temperature spectra in Figure 3.15 are virtually identical. In particular, whereas all the bands (both positive and negative) in the differential spectra of the A variant (regardless of the source) change progressively with increasing temperature in such a manner that all the differential spectra overlay each other, the differential spectra for the B variant at the two highest temperatures (55-60°C) are distinct from the spectra for temperatures in the range of 30-50°C, which show very minor thermally induced changes. The pronounced spectral changes in the differential spectra at the two highest temperatures differ markedly from those observed for variant A. In particular, the major thermally induced change for the B variant is a decrease in intensity at 1636 cm^{-1} accompanied by a comparable increase in intensity at 1628 cm^{-1}, which is opposite to the trend observed in Figures 3.10-3.12 for the A variant over the same temperature range. In addition, the variance spectra in Figure 3.17 have a peak at 1692-1693 cm^{-1} that is absent in the variance spectra of the A variant. Examination of the differential spectra in Figure 3.17 shows that this variance peak is due to a decrease in intensity

that occurs at the two highest temperatures and is more pronounced in the spectra of the sample from the commercial supplier. Furthermore, much of the intensity decrease at 1636 cm^{-1} and increase at 1628 cm^{-1} occurs at these two temperatures and appears to parallel the decrease in intensity at 1692 cm^{-1}. Boye *et al.* (1996) reported that the 1692-cm^{-1} band in the spectrum of β-lactoglobulin (AB mixture) in D_2O solution decreased slowly over time, consistent with slow H-D exchange and that its disappearance upon mild heating was accompanied by the appearance of bands at 1684 and 1628 cm^{-1}. Based on these observations, they assigned the 1692 cm^{-1} band to the high-frequency component of the amide I absorption of β-sheets buried deep within the protein (Table 3.1). In a subsequent study of the individual A and B variants of β-lactoglobulin, Boye *et al.* (1997) did not report any differences between the two variants with respect to the thermally induced decrease of the 1692 cm^{-1} band. However, in the present study, as described above, a pronounced decrease of this band was observed at 55-60°C in the spectra of β-lactoglobulin B whereas the intensity of this band in the spectra of β-lactoglobulin A was unchanged over the full temperature range examined in Figures 3.10-3.12 (30-60°C) and decreased only above ~70°C (spectrum not shown). These results again indicate that the conformational mobility of β-lactoglobulin B is greater than that of β-lactoglobulin A. It also appears that the sample of β-lactoglobulin B derived from the food-grade AB mixture had somewhat less conformational mobility than the sample from the commercial source, given the more extensive decrease of the 1692 cm^{-1} band in the spectra of the latter.

Upon continued heating of β-lactoglobulin B beyond 60°C, changes in the FSD amide I' band profile associated with protein unfolding and aggregation (appearance of new bands at 1682 and 1618 cm^{-1} characteristic of intermolecular β-sheets) were observed for the samples from both sources. Thus, at these temperatures, the thermal behavior of β-lactoglobulin B was similar to that of β-lactoglobulin A, except in two respects. First, whereas β-lactoglobulin A obtained by ion-exchange chromatography of food-grade β-lactoglobulin was found to have much less propensity for aggregation than the other samples of β-lactoglobulin A examined in this study (as illustrated by Figures 3.5-3.8), the samples of β-lactoglobulin B obtained in the same procedure did undergo extensive aggregation, behaving similarly to the samples of β-lactoglobulin B from the commercial supplier. As such, it appears that the proprietary mild thermal treatment employed in the production of food-grade β-lactoglobulin has a larger effect on the A variant than the B variant in

terms of reducing the propensity for aggregation upon thermal denaturation. Furthermore, for the samples of β-lactoglobulin A from the other two sources, the bands characteristic of intermolecular β-sheets appeared above 75ºC whereas the VT-FTIR spectra of the B variant (irrespective of the source) already exhibited these bands at 70ºC, indicating that the A variant is more thermally stable than the B variant under the conditions employed in these studies. This finding is consistent with those reported in circular dichroism studies, in which it was established that the thermal stability of variants A, B and C decreased in the order C > A > B (Qin *et al.,* 1999; Manderson *et al.,* 1999). The differences in the thermal stability of the variants were mainly attributed to the differences in amino acid composition (Qin *et al.,* 1999; Manderson *et al.,* 1999) (variant A Asp^{64}, Val^{118}; variant B Gly^{64}, Ala^{118}; variant C will not be considered here as it was not included in the present study). The results have also been attributed specifically to the substitution of Asp^{64} in variant A for Gly^{64} in variant B in the CD loop by causing a change in the charge distribution given that Asp^{64}, Glu^{62} and Glu^{65} are negatively charged, and this substitution has a propagating effect on the disulfide bond between Cys^{66} and Cus^{160} (Qin *et al.,* 1999; Manderson *et al.,* 1999). The second substitution is Val^{118} in variant A for Ala^{118} in variant B; this residue is located in the H strand, which is in the second β–sheet in the core of β-lactoglobulin. The latter is covered by the N and C termini and by a three-turn α-helix, making this area the most rigid part of the structure. According to Qin *et al.* (1999), when Val^{118} is substituted by Ala^{118}, the loss of the two methyl groups translates to a decrease of complementarity in the hydrophobic surface causing the loss of five hydrophobic contacts in the B variant compared to the A variant, making variant B more susceptible to thermal denaturation than variant A.

3.3.5. Study of the secondary structure and thermal behavior of β–lactoglobulin AB by FTIR spectroscopy

The substantial differences in the thermal behavior of the A and B variants described above as well as possible effects of A-B interactions, including formation of AB dimers (in addition to AA and BB dimers), may be expected to complicate the interpretation of the VT-FTIR spectra of samples of β-lactoglobulin that contain both variants A and B. This is manifested in Figure 3.18, in which differential and variance spectra over the 30-60ºC range are presented for food-grade

(Davisco) and research-grade (Sigma) samples of β-lactoglobulin (mixtures of variants A and B). In particular, the low-frequency β-sheet region in the variance spectra of the two samples is strikingly different: the spectral variance for β-lactoglobulin from the commercial supplier shows bands of comparable intensity at 1636 and 1628 cm^{-1} and a smaller band at 1621 cm^{-1} whereas the latter two bands are barely discernible in the variance spectrum of food-grade β-lactoglobulin. Although the positions of the other peaks in the variance spectra of the two samples are similar, examination of the differential spectra reveals differences in the temperatures at which these thermally induced spectral changes occur. Overall, these results reflect the variability that is introduced when AB mixtures are studied, which may account for discrepancies between many studies of β-lactoglobulin that have been done in the past by different research groups.

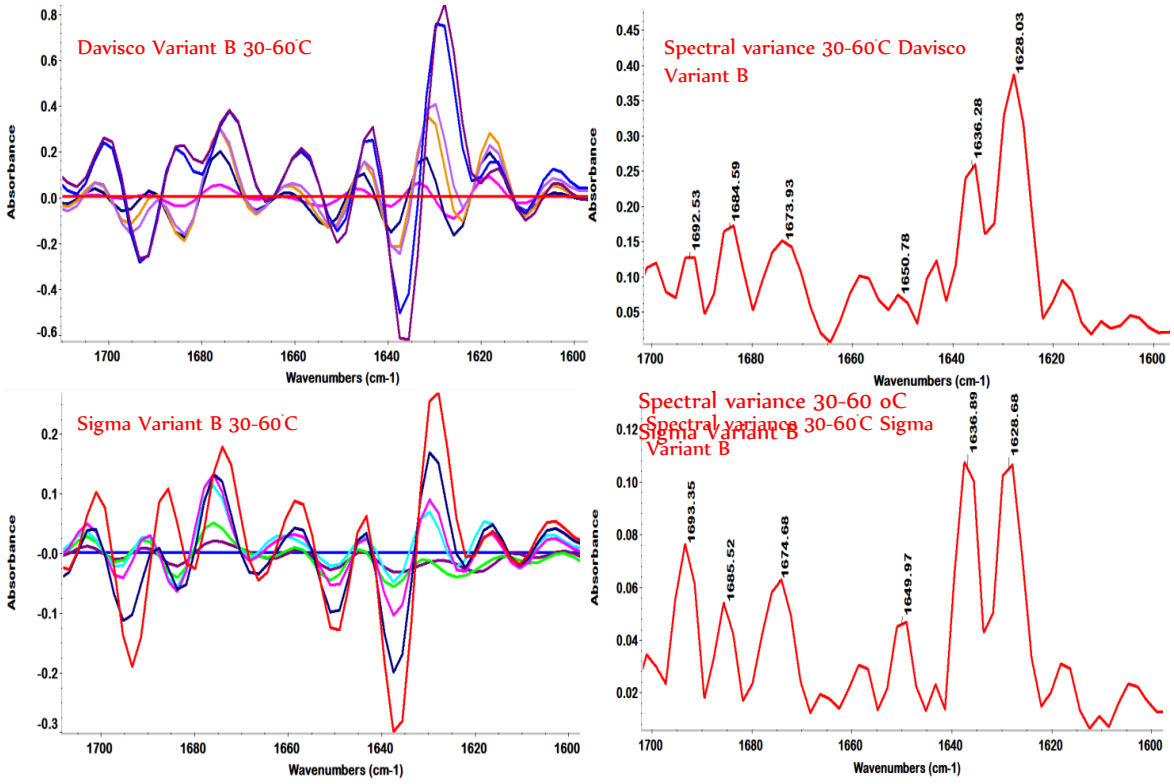

Figure 3.17. Differential spectra (left) and variance spectrum (right) in the amide I´ region of β-lactoglobulin variant B obtained by ion-exchange chromatography of food-grade β-lactoglobulin AB (Davisco) and β-lactoglobulin variant B obtained from a commercial supplier (Sigma). Each sample was heated from 25ºC to 60ºC in 5ºC increments, and the differential spectra were generated by subtracting the spectrum recorded at the beginning of the heating cycle from each of the other spectra.

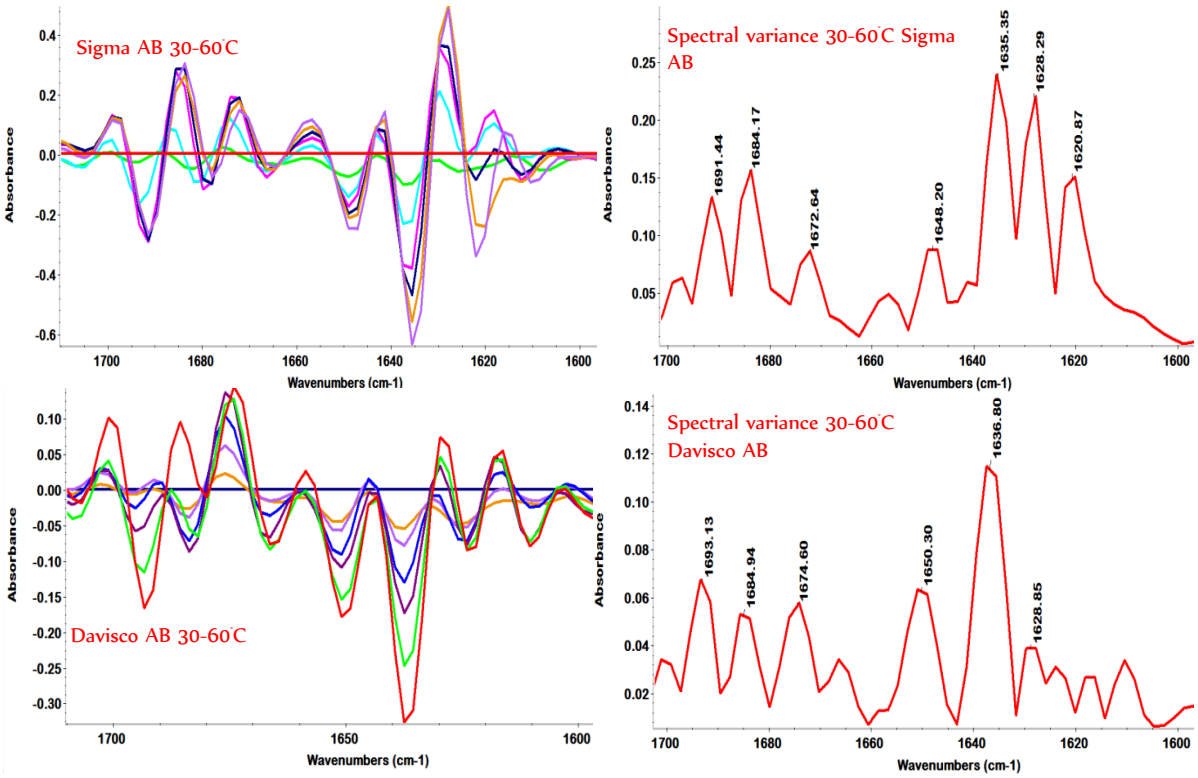

Figure 3.18. Differential spectra (left) and variance spectrum (right) in the amide I´ region of β-lactoglobulin variants AB obtained from a commercial supplier (Sigma) and from a food-grade supplier β-lactoglobulin AB (Davisco). Each sample was heated from 25°C to 60°C in 5°C increments, and the differential spectra were generated by subtracting the spectrum recorded at the beginning of the heating cycle from each of the other spectra.

3.3.6. Study of the H-D exchange of β–lactoglobulin A using ^{1}H NMR spectroscopy

In Section 3.3.4 the VT-FTIR results presented for β-lactoglobulin A indicated progressive H-D exchange of amide groups over the temperature range of 30-60°C. Given that H-D exchange of specific amino acid residues in β-lactoglobulin A as a function of temperature has been monitored by employing 2D ^{1}H NMR techniques (Edwards *et al*., 2002), an investigation was undertaken in the present study to ascertain whether the detailed information provided by 2D ^{1}H NMR could be related to changes in the amide I' band profile attributed to H-D exchange. However, the scope of this investigation was limited because our VT-FTIR studies were conducted under conditions that strongly favor dimer formation whereas 2D ^{1}H NMR studies require that only the protein monomers are present in solution, as is the case in acidic solutions (pH ≤ 3) (Edwards *et al*., 2002). Since our VT-FTIR results could accordingly not be directly

correlated with 2D NMR data, we only conducted a preliminary investigation in which 2D ^{1}H NMR and FTIR spectroscopy were both employed in parallel to examine H-D exchange of β-lactoglobulin A (isolated from cow's milk) at pH 2 over a 48-h period at room temperature.

Following, the procedure employed by Edwards *et al*. (2002), the 2D ^{1}H NMR experiments employed total correlation spectroscopy (TOCSY) to examine H-D exchange by measuring the signals from coupled amide (H_N) and α-carbon (H_α) protons. The results of the TOCSY experiments performed with a freshly prepared D_2O solution and after 48 h are presented in Figures 3.19 and 3.20, respectively. The dark spots in these figures represent the (H_N, H_α) cross peaks from the TOCSY spectra, which correspond to amide protons that have not undergone H-D exchange with the D_2O solvent; upon H-D exchange of amide protons, their H_N signals and hence the corresponding (H_N, H_α) cross-peaks in the TOCSY spectra are lost. The residues for which cross-peaks are observed are listed in Table 3.5. The assignments are based on those reported by Uhrínová *et al.* (1998); in the case of the residues marked with an asterisk in Table 3.5, the assignments are considered tentative because the H_N and Hα chemical shifts do not match those reported by Uhrínová *et al.* (1998), who employed a recombinant variant of β–lactoglobulin A in which some of the amino acids were different from those in the native protein, which in turn may have altered the chemical environment of some other amino acid residues, causing a shift of their resonances. The highlighted rows in Table 3.5 correspond to cross-peaks observed in the TOCSY spectrum of the freshly prepared solution (Figure 3.19) that were absent in the spectrum collected after H-D exchange had been allowed to proceed at 25ºC for 48 h. Table 3.5 shows that the TOCSY spectra allowed the identification of 104 amide groups that had not undergone H-D exchange upon dissolution of the protein in D_2O, 33 of which had undergone H-D exchange after 48 h at 25ºC (Table 3.5). Accordingly, most of the residues remained unexchanged after 48 h, demonstrating the rigidity of the protein´s structure at room temperature under acidic conditions (pD 2). The results in Table 3.5 indicate that the H-D exchange that occurred over time was not localized to any individual segment of the protein's structure but rather occurred at residues located in five of the β-strands (B-F) making up the β-barrel as well as the ninth β-strand (I) and in the C-terminal and N-terminal regions. The most solvent-shielded segments appear to be β-strands A, G, and H, for which there was no evidence of H-D exchange over time, and the main α-helix (denoted as α2), in which a single residue was found to have undergone H-D exchange of its amide proton between time zero and 48 h. These findings are largely in accordance with

those of Edwards *et al*. (2002), who studied H-D exchange as a function of temperature and determined the temperatures at which H-D exchange was complete in various parts of the structure. In particular, they reported that the G-H pair of strands is the most stable segment in the protein, apparently due to its location within the calyx of β-lactoglobulin and also because one of the two disulphide bonds of the protein is located in this region (between Cys106 and Cys119). In addition, the free thiol group located at Cys121 is also in strand H and this residue forms H bonds with two hydrophobic nonpolar residues from strand A (Leu22 and Ala23). Edwards *et al.* (*2*002) also reported that the main α-helix (α2) is thermally stable until temperatures of ≥60ºC owing to its relatively rigid structure, consistent with our findings at room temperature.

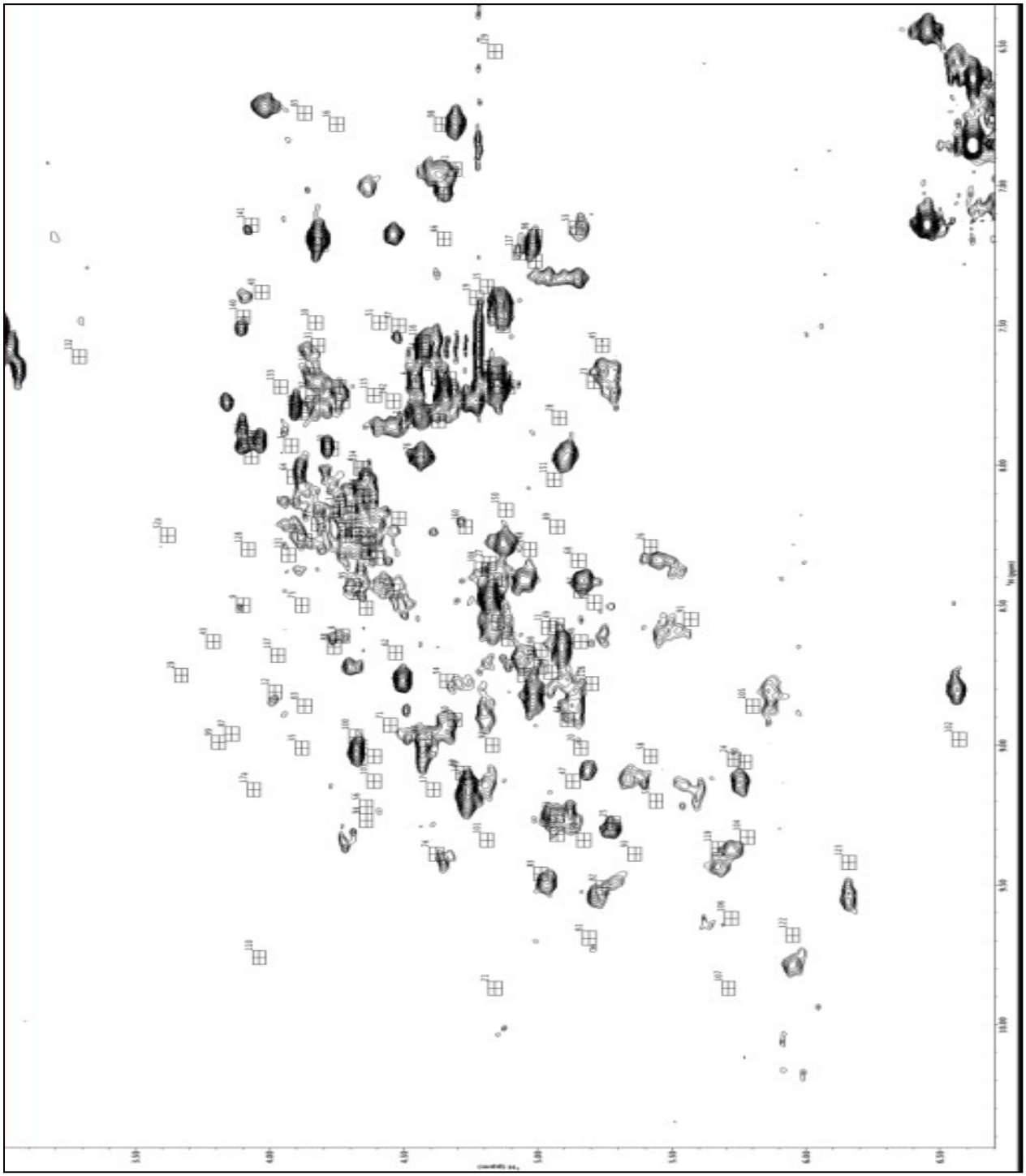

Figure 3.19. H_N-H_α cross-peaks from the TOCSY spectra of β–lactoglobulin freshly dissolved in D_2O (pH 2, 25ºC). The assignments are based on those published by Uhrínová *et al.* (1998). All the dark spots represent residues that have not undergone H-D exchange.

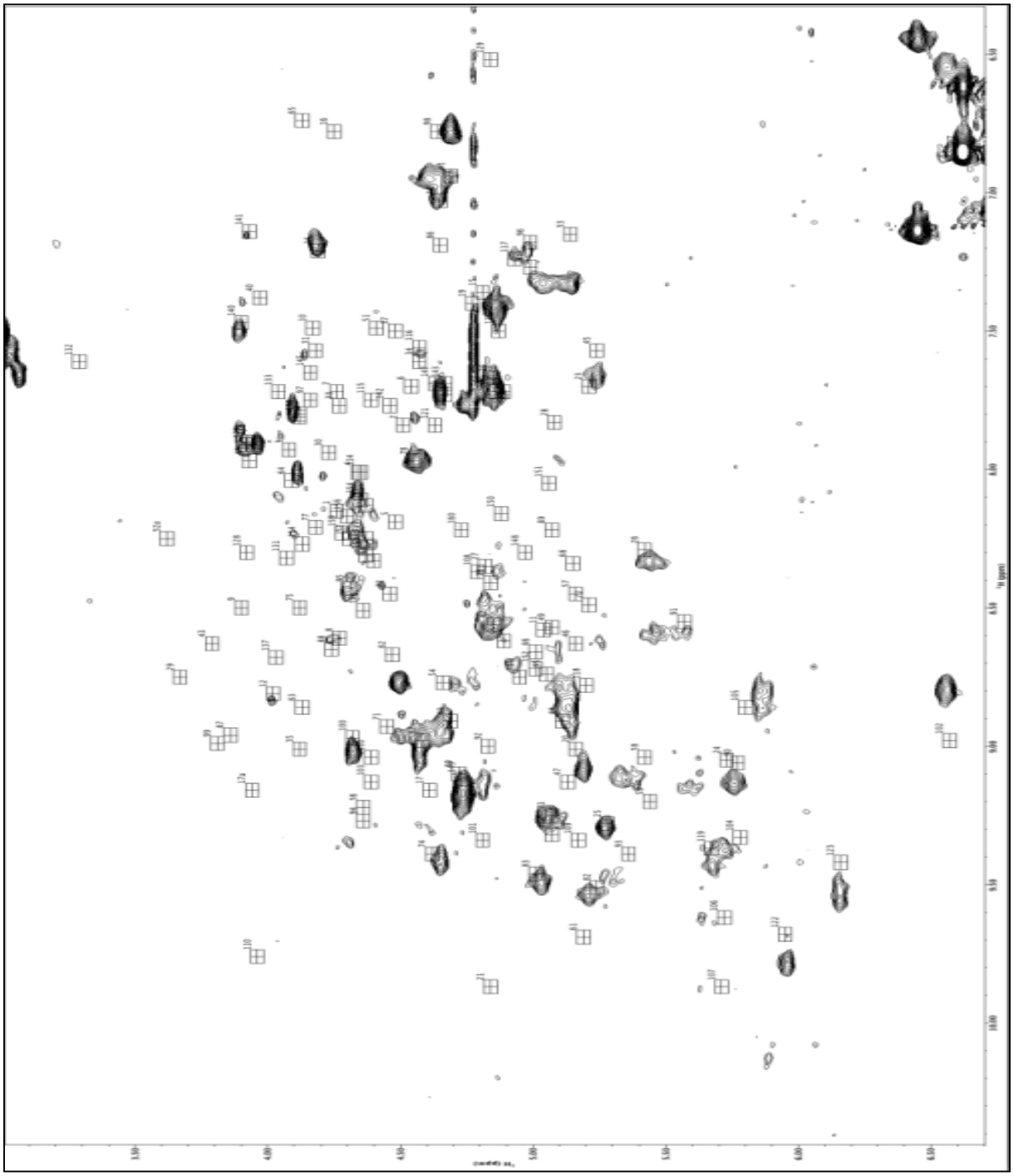

Figure 3.20. H_N-H_α cross-peaks from the TOCSY spectra of β–lactoglobulin A in D_2O after 48 hours (pH 2, 25ºC). The residue assignment was based on Uhrínová *et al*, (1998).

Table 3.5. Deuterium exchange of backbone NH groups of assigned residues (25ºC, pD 2.0). The signals that disappeared after 48 h are marked in yellow.

Residue	Amino acid	Location[a]	Time 0	Time 48 h
1	Leu	N-term	+	-
2	Ile	N-term	+	-
3	Val	N-term	+	+
4	Thr	N-term	+	-
5	Gln	N-term	+	-
6	Thr	N-term	+	-
7	Met	N-term	+	-
8	Lys	N-term	+	+
12	Ile	N-term	+	+
13	Gln	N-term	+	+
14	Lys	N-term	+	+
15	Val	N-term	+	+
19	Trp	A	+	+
20	Tyr	A	+	+
23	Ala	A	+	+
24*	Met	A	+	+
25	Ala	A	+	+
26*	Ala	A	+	+
30	Ser	α1	+	-
31	Leu	α1	+	-
32	Leu	α1	+	+
33	Asp	α1	+	-
34	Ala	A-B loop	+	+
36	Ser	A-B loop	+	+
37	Ala	A-B loop	+	-
39	Lys	A-B loop	+	+
40*	Arg	B	+	+
41	Val	B	+	+
44	Glu	B	+	+
45*	Glu	B	+	-
46*	Leu	B	+	-
47*	Lys	B	+	+ (less intense)
52	Gly	C	+	+
53	Asp	C	+	-

Table 3.5 (Cont.).

Residue	Amino acid	Location[a]	Time 0	Time 48 h
54	Leu	C	+	+
56*	Ile	C	+	-
57	Leu	C	+	+
58	Leu	C	+	+
59	Gln	C	+	+
60	Lys	C	+	+
61*	Trp	C	+	-
62	Glu	C-D loop	+	+
64	Asp	C-D loop	+	+
65*	Glu	D	+	-
66	Cys	D	+	-
67	Ala	D	+	+
69	Lys	D	+	+
71*	Ile	D	+	+
72	Ile	D	+	-
73	Ala	D	+	+
74	Glu	D	+	+
77	Lys	D	+	+
78	Ile	D-E loop	+	+
81	Val	E	+	-
82	Phe	E	+	+
83	Lys	E	+	+
85	Asp	E	+	-
88	Asn	E-F loop	+	+
90	Asn	E-F loop	+	+
91	Lys	F	+	+
92*	Val	F	+	-
95	Leu	F	+	+
96	Asp	F	+	+
97	Thr	F	+	-
98	Tyr	F	+	+
100	Lys	F-G loop	+	+
102*	Tyr	G	+	+
103*	Leu	G	+	+
104*	Leu	G	+	+
105*	Phe	G	+	+
106*	Cys	G	+	+

Table 3.5 (Cont.)

Residue	Amino acid	Location[a]	Time 0	Time 48 h
112	Asp	G-H loop	+	+
114	Asp	G-H loop	+	-
116	Ser	G-H loop	+	-
117	Leu	G-H loop	+	+
118*	Val	H	+	+
119	Cys	H	+	+
120	Gln	H	+	+
121	Cys	H	+	+
122*	Leu	H	+	+
123*	Val	H	+	+
125	Thr	H-α2 loop	+	+
127	Glu	H-α2 loop	+	+
130	Asp	α2	+	+
131	Glu	α2	+	-
134	Glu	α2	+	+
135	Lys	α2	+	+
136	Phe	α2	+	+
140	Leu	α2	+	+
141	Lys	α2	+	+
143	Leu	H-I loop	+	+
145	Met	H-I loop	+	-
146	His	I	+	-
147	Ile	I	+	+
149	Leu	I	+	+
151*	Phe	I	+	-
152	Asn	I	+	+
154	Thr	α3	+	+
156	Leu	α3	+	-
158	Glu	α3	+	+
159	Gln	C-term	+	-
160	Cys	C-term	+	-
161	His	C-term	+	-

[a]The nine β-strands in the structure of β-lactoglobulin are designated by the letters A-I.
*Tentative assignment.

The FTIR spectra of the NMR sample and a fresh D_2O solution of β-lactoglobulin A prepared in the same manner (pH 2.5, 0.5% w/v) were acquired at 25ºC to examine whether changes in the FSD amide I' band profile could be associated with the H-D exchange that occurred during the 48-h NMR experiment. As shown in Figure 3.21, the spectra of these two samples were very similar, demonstrating the stability of β-lactoglobulin A in acidic solution after more than 48 hours at 25ºC. As will be discussed further below, it may also be noted that the amide I' band profile in Figure 3.21 looks substantially different from that obtained for the near-neutral pH (unbuffered) solution of the same concentration presented in Figure 3.13. Comparison of the two spectra in Figure 3.21 indicates that only the bands at 1684 and 1652 cm^{-1} were affected by H-D exchange over the 48-h duration of the NMR experiment, exhibiting red shifts of approximately 6 and 4 cm^{-1}, respectively, consistent with H-D exchange of amide groups in β-sheet and α-helical structure. The position of the single band in the low-frequency β-sheet region is invariant, but H-D exchange of a subpopulation of amide groups in β-sheets might not affect this fairly broad band. In any case, given that the 2D NMR results showed that residues in β-strands B-F and I underwent H-D exchange over the 48-h duration of the NMR experiment (Table 3.5), comparison of the NMR and FTIR results does not allow the H-D exchange associated with the shift of the 1684-cm^{-1} band to be localized to a particular portion of the β-sheet structure. With regard to the α-helical structure, the FTIR band shift indicative of extensive H-D exchange is inconsistent with the 2D NMR results, which revealed H-D exchange of only a single residue located in the main α-helix (Table 3.5). The reason for this discrepancy remains to be ascertained.

As noted above, a distinctive feature of the FTIR spectra of β-lactoglobulin A at pH 2.5 is the presence of only a single amide I' component in the low-frequency β-sheet region. As in the spectra recorded from unbuffered solutions in the present study, two distinct bands in this region were observed for β-lactoglobulin A at pH 3 (Boye *et al.,* 1997), which is the lowest pH examined in the literature. However, in the case of the B variant, the FSD amide I' band profile as a function of pH between pH 2 and pH 13 has been published (Casal *et al.*, 1988) and reveals that the two amide I' components below 1640 cm^{-1} blend into a single asymmetrical band upon reduction of the pH from 3 to 2. Casal *et al*. (1988) attributed this change to dimer → monomer dissociation, known to occur in this pH range, and, more specifically, to its effects on β-strand I, located at the dimer interface. A detailed understanding of this phenomenon was beyond the scope of the present

study, but our findings for the A variant as well as those of Casal *et al*. (1988) for the B variant make it evident that the acidic conditions required for the 2D NMR experiments affect the β-structure of the protein in some manner, thereby invalidating any attempt to relate our VT-FTIR findings to the 2D NMR results.

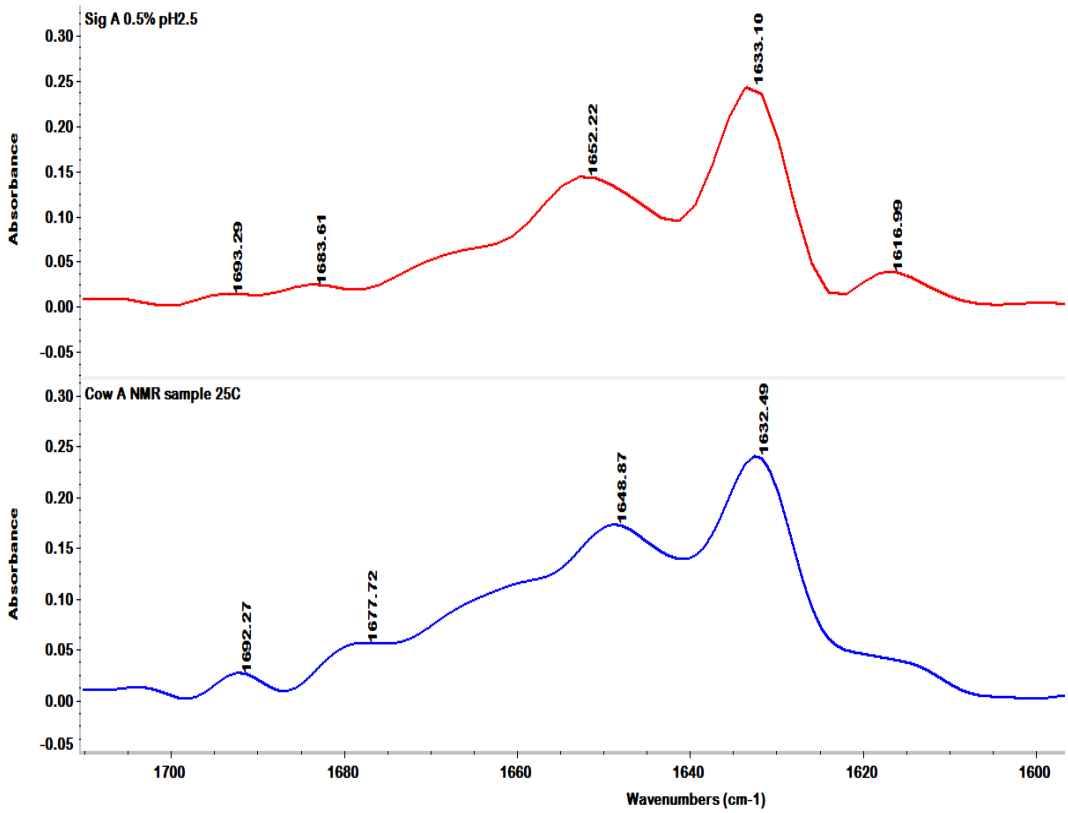

Figure 3.21. FSD of the amide I´ band of β-lactoglobulin A in a freshly prepared solution, in red, and in the NMR sample (after 48 h at room temperature), in blue.

3.4. CONCLUSIONS

The work presented in this chapter entailed studies initially undertaken to characterize food-grade β-lactoglobulin by VT-FTIR spectroscopy to lay the foundation for the research presented in the subsequent chapters of this thesis. For this purpose, samples of the food-grade protein were separated into the individual genetic variants A and B by ion-exchange chromatography for comparison of their FTIR spectra with those of suitable "reference" samples of β-lactoglobulin A

and β-lactoglobulin B, Several spectroscopic trends observed during the course of this work led to some re-examination of the results of previous spectroscopic studies of β-lactoglobulins A and B.

In the case of β-lactoglobulin A, the samples from three different sources compared in this study (i.e., samples isolated from whole milk, separated from food-grade β-lactoglobulin AB by ion-exchange chromatography and purchased from a commercial supplier) showed different relative band intensities in the FSD amide I' region of the FTIR spectra recorded from freshly prepared D_2O solutions at room temperature. We have attributed these differences to varying extents of H-D exchange of certain amide groups involved in β-sheet formation. Given that all D_2O solutions were prepared and analyzed under identical conditions and that the differences in relative band intensity were both substantial and reproducible, we suggest that the different protein isolation methods associated with the samples from the three sources affected the conformational mobility of the protein in solution.

Despite the differences observed in the room-temperature spectra, samples from the three sources behaved very similarly in VT-FTIR experiments over the temperature range of 25-75°C. However, major differences among these samples were observed upon thermal unfolding of the protein above 75°C. In particular, protein aggregation through the formation of intermolecular β-sheets was much less extensive in samples derived from food-grade β-lactoglobulin AB, as evidenced by the lack of the well-defined band at 1618 cm^{-1} observed in the spectra of the other samples of β-lactoglobulin A when heated above 75°C. On the other hand, the β-lactoglobulin B samples derived from the same samples of food-grade β-lactoglobulin AB did not exhibit a reduced propensity for aggregation by comparison with β-lactoglobulin B from a commercial supplier.

The VT-FTIR studies of β-lactoglobulin A (from three sources) and β-lactoglobulin B (from two sources) under identical physicochemical conditions showed that the differences between the two variants far exceeded the differences among samples of the same variant from different sources. Taken together, the results obtained for β-lactoglobulins A and B suggest that the spectral changes occurring over the temperature range of 30-60°C are primarily associated with H-D exchange of different β-sheet populations. In the case of the A variant, H-D exchange results in a progressive increase of amide I' band components at 1621 and 1636 cm^{-1} in the low-frequency β-sheet region as well as a high-frequency component at 1677 cm^{-1}.

In contrast, for the B variant over the same temperature range, H-D exchange results in the increase of an amide I' band component at 1628 cm^{-1} in the low-frequency β-sheet region, with a high-frequency component at 1684 cm^{-1}, and these changes occur primarily above 50°C. These differences between the two variants are attributed in the present study to a greater conformational mobility of the B variant for two reasons: (I) the amide I' band in the FSD spectrum of β-lactoglobulin B at room temperature resembles that of β-lactoglobulin A at 60°C, suggesting that the β-sheet population(s) undergoing H-D exchange between 30 and 60°C in the A variant have already undergone a comparable extent of H-D exchange at room temperature in the B variant and (II) the H-D exchange of β-sheets buried deep within the protein (indicated by the decrease of the 1692 cm^{-1} band) occurs for the B variant in a temperature range in which the secondary structure remains intact, whereas in the A variant this β-sheet population seems to remain inaccessible to the solvent up to a temperature close to the denaturation temperature; indeed, it is difficult to ascertain whether the disappearance of the 1692 cm^{-1} band at ~75°C is due to H-D exchange of the buried β-sheets or loss of secondary structure.

As illustrated by the TOCSY experiments performed with β-lactoglobulin A in the present study as well as the much more extensive studies reported in the literature, 2D ^{1}H NMR spectroscopy allows for identification of specific amino acid residues that undergo slow H-D exchange. However, the detailed information provided by 2D NMR studies ultimately did not advance our description of the H-D exchange phenomena observed in the VT-FTIR studies presented in this chapter for several reasons. First, as recognized at the outset, the acidic pH and lower protein concentration required for the NMR studies in order to prevent self-association of β-lactoglobulin monomers were problematic, particularly because the reduction in pH resulted in a substantial change on the amide I' band profile of β-lactoglobulin A. While it is evident that this limitation could have been overcome by conducting a series of VT-FTIR experiments under these conditions, the results of the 2D NMR and FTIR studies of H-D exchange at room temperature were inconsistent and did not seem to warrant such an undertaking.

On the other hand, the apparent differences in conformational mobility between variants A and B revealed by our VT-FTIR studies certainly appear to warrant further comparison of the thermal behavior of the two variants by 2D ^{1}H NMR spectroscopy. In this regard, it may be

noted that although Edwards *et al.* (1999) alluded to a 2D ^{1}H NMR study of β-lactoglobulin B, the results of that study have not appeared in the literature.

CONNECTING STATEMENT

In the previous chapter, the impact of the isolation/purification method and the conformational mobility of β-lactoglobulin variant A, β-lactoglobulin variant B and β-lactoglobulin variants AB were examined using variable temperature-FTIR and 2D-correlation spectroscopy. The results demonstrated that the isolation method has an impact on the conformational mobility of β-lactoglobulin variant A, and that β-lactoglobulin variant B has a higher conformational mobility than variant A. In the next chapter, binary mixtures of β-lactoglobulin variant A, β-lactoglobulin variant B and β-lactoglobulin variants AB mixtures were examined in the presence of glycomacropeptide (GMP) using variable temperature-FTIR and 2D-correlation spectroscopy to assess the impact of GMP on the conformational mobility of the individual and mixed β-lactoglobulin variants. The effect of varying concentrations of GMP on the denaturation temperature of the protein was examined.

Chapter 4. Study of Binary Mixtures of GMP and β-Lactoglobulin A, B, and AB from Different Sources

4.1. INTRODUCTION

Glycomacropeptide (GMP) constitutes 15–20% of the whey protein in sweet whey. In recent years, the nutritional and biological properties and benefits of GMP have been the focus of much research. However, knowledge about the influence of GMP on the behavior of whey proteins is very limited. There is little data on GMP/β-lactoglobulin mixtures; and the available information mainly pertains to an understanding of the behavior of GMP per se or the behavior of GMP/β-lactoglobulin as a system rather than an understanding of the interactions between GMP and β-lactoglobulin (Martinez *et al.,* 2010; Martinez *et al.,* 2009). Therefore; the research presented in this chapter was undertaken to examine the influence of GMP on the thermal stability of β-lactoglobulin through studies of its impact on the changes in the amide I' band in the FTIR spectra of β-lactoglobulin during heat treatments.

As mentioned in previous chapters; although variants A and B of β-lactoglobulin differ from each other only at two positions (64 and 118, where Asp and Val in the A variant are substituted by Gly and Ala, respectively, in the B variant), these seemingly minor differences have been shown to have a profound effect on the physicochemical properties of the protein (Boye *et al*., 1997). As illustrated in Chapter 3, the FTIR spectra of variants A and B in D_2O solution exhibit substantial differences in their amide I' band profile after the same equilibration time at room temperature as well as during subsequent VT-FTIR experiments. These differences confound FTIR spectroscopic investigations of samples containing both variants (β-lactoglobulin AB) and may lead to inconsistent results, given that such samples have been isolated from milk pooled from homozygous (AA or BB) and heterozygous (AB) cows and contain varying proportions of variants A and B. Accordingly, the present studies were conducted with β-lactoglobulin A, β-lactoglobulin B, and β-lactoglobulin AB from various sources. Binary mixtures of each of these protein samples and GMP at two different ratios (3:1 and 1:1) were employed to examine the effects of GMP on the thermal stability of the protein through the application of variable-temperature FTIR (VT-FTIR) spectroscopy and two-dimensional correlation (2D-COS) spectroscopy.

4.2. MATERIALS AND METHODS

4.2.1. GMP and protein samples

Glycomacropeptide (GMP) and food-grade β-lactoglobulin (consisting of variants A and B) were obtained from Davisco Foods International Inc. (Le Sueur, MN, USA). Some of the β-lactoglobulin obtained from this source was separated into variants A and B by ion-exchange chromatography as described in Chapter 3. β-Lactoglobulin A from whole milk was obtained as described in Chapter 3. β-Lactoglobulin B and β-lactoglobulin AB mixture were purchased from Sigma Aldrich (Oakville, ON, Canada) and used without further purification.

4.2.2. Study of binary mixtures of β-lactoglobulin and GMP by FTIR spectroscopy

Binary mixtures of each of the β-lactoglobulin samples listed above and GMP in ratios of 3:1 and 1:1 were dissolved in D_2O (Cambridge Isotope Laboratories, Inc., Lancaster, MA, USA) at a concentration of 15% (w/w). D_2O solutions of each of the individual components of these mixtures were also prepared at a concentration of 15% (w/w). All solutions were prepared in triplicate. The final pH of the solutions was in the range of 6.0±0.3. FTIR spectra were recorded with an Agilent FTIR spectrometer equipped with a deuterated triglycine sulfate (DTGS) detector and purged with dry air from a Balston dryer (Balston, Lexington, MA) to avoid spectral interferences from water vapor. All spectra were collected by co-addition of 256 scans at a resolution of 2 cm^{-1}. A 10-μL aliquot of protein solution (15% w/v in D_2O) was placed between two CaF_2 windows separated by a 15-μm Teflon spacer in a temperature-controlled cell. Spectra were acquired as the temperature of the sample was elevated from 30°C to 85°C in 5°C increments, with a hold time of 10 min at each temperature. Fourier self-deconvolution (FSD) of the spectra was performed with a correction factor of k = 2.4 and a bandwidth of w = 24 cm^{-1}, and the Fourier self-deconvoluted spectra were baseline-corrected and normalized by using the peak area values of each spectrum. The spectra processed in this manner were subjected to 2D-COS analysis using the software written by Y. Wang (Wang *et al.,* 2006).

4.3. RESULTS AND DISCUSSION

4.3.1. Study of binary mixtures of β-lactoglobulin and GMP by VT-FTIR and 2D correlation spectroscopy

The VT-FTIR spectra in the secondary-structure-sensitive amide I' region of D_2O solutions of β-lactoglobulin A, β-lactoglobulin B, and β-lactoglobulin AB from the various sources examined in Chapter 3 and their mixtures with GMP (β-lactoglobulin:GMP ratios of 3:1 and 1:1) are presented in the following sections. All spectra have been subjected to Fourier self-deconvolution and are thus referred to as FSD spectra. In the case of the mixtures, the FTIR spectrum of GMP (not shown) has been subtracted out by a scaling factor based on the proportion of GMP in the mixture. GMP is a polypeptide that is mainly random coil, has little organized structure (α-helix, β-sheets, β-turns) and lacks disulfide bonds. The spectrum of GMP was unchanged over the full temperature range examined (30-85ºC), which is consistent with the findings of other researchers that GMP showed no denaturation temperature (Martínez *et al.*, 2010; Ono *et al.,* 1987). As such, the contributions of GMP to the VT-FTIR spectra could be removed by subtracting the spectrum of GMP, thereby allowing the effects of different concentrations of GMP on the thermal stability and conformational changes of β-lactoglobulin to be clearly discerned without spectral interference from GMP. The interpretation of these VT-FTIR spectra as well as the elucidation of the sequence of the thermally induced spectral changes through the application of 2D-COS is further aided by isolating the spectral changes occurring at temperatures between 30 and 60ºC from those accompanying the onset of protein aggregation in the temperature range of 65-85ºC. Accordingly, in each of the following sections, an overview of the VT-FTIR spectra is followed by a separate examination of the temperature ranges 30-60ºC and 65-85ºC. The results of 2D-COS analysis of the VT-FTIR spectra of the β-lactoglobulin/GMP mixtures over each of these temperature ranges are then compared with the corresponding results for the β-lactoglobulin sample employed to prepare the mixtures (as summarized in Tables 4.5 and 4.6) in order to ascertain the effects of GMP on the sequence of unfolding and aggregation of the protein.

4.3.1.1. Mixtures of β-lactoglobulin variant A obtained from whole milk and GMP (β-lactoglobulin: GMP ratios of 3:1 and 1:1)

The FSD-FTIR spectra of β-lactoglobulin variant A from whole milk and its binary mixtures with GMP at the beginning and at the end of the heating cycle (30ºC and 85ºC) are overlaid in Figure 4.1. While pronounced changes during heating are evident in these spectra, only small differences among the three samples are apparent; hence, differential and variance spectra were generated to study whether the thermal behavior of β-lactoglobulin is altered by interactions with GMP. The thermally induced changes in the amide I' band of β-lactoglobulin A from whole milk in the 3:1 and 1:1 mixtures with GMP in the temperature range of 30-60ºC are illustrated by the spectra presented in Figure 4.2. The spectral variance over this temperature range shows the same amide I' band components as observed for β-lactoglobulin A by itself in Figure 3.10 and attributed to progressive H-D exchange; however, while the relative intensities of the bands in the variance spectrum of the 3:1 mixture are virtually identical to those in Figure 3.10, those in the spectra of the 1:1 mixture are somewhat different, indicating that the presence of GMP may have altered the conformational mobility of β-lactoglobulin A.

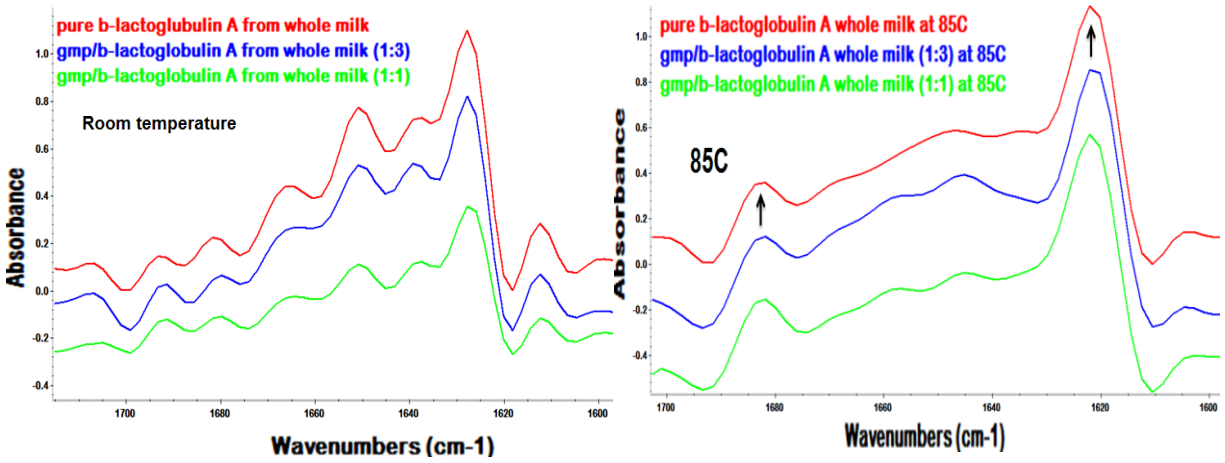

Figure 4.1. Fourier self-deconvolution of the amide I´ band in the spectra of β-lactoglobulin variant A from whole milk and its binary mixtures with GMP (ratios 3:1 and 1:1) at 30ºC and 85ºC

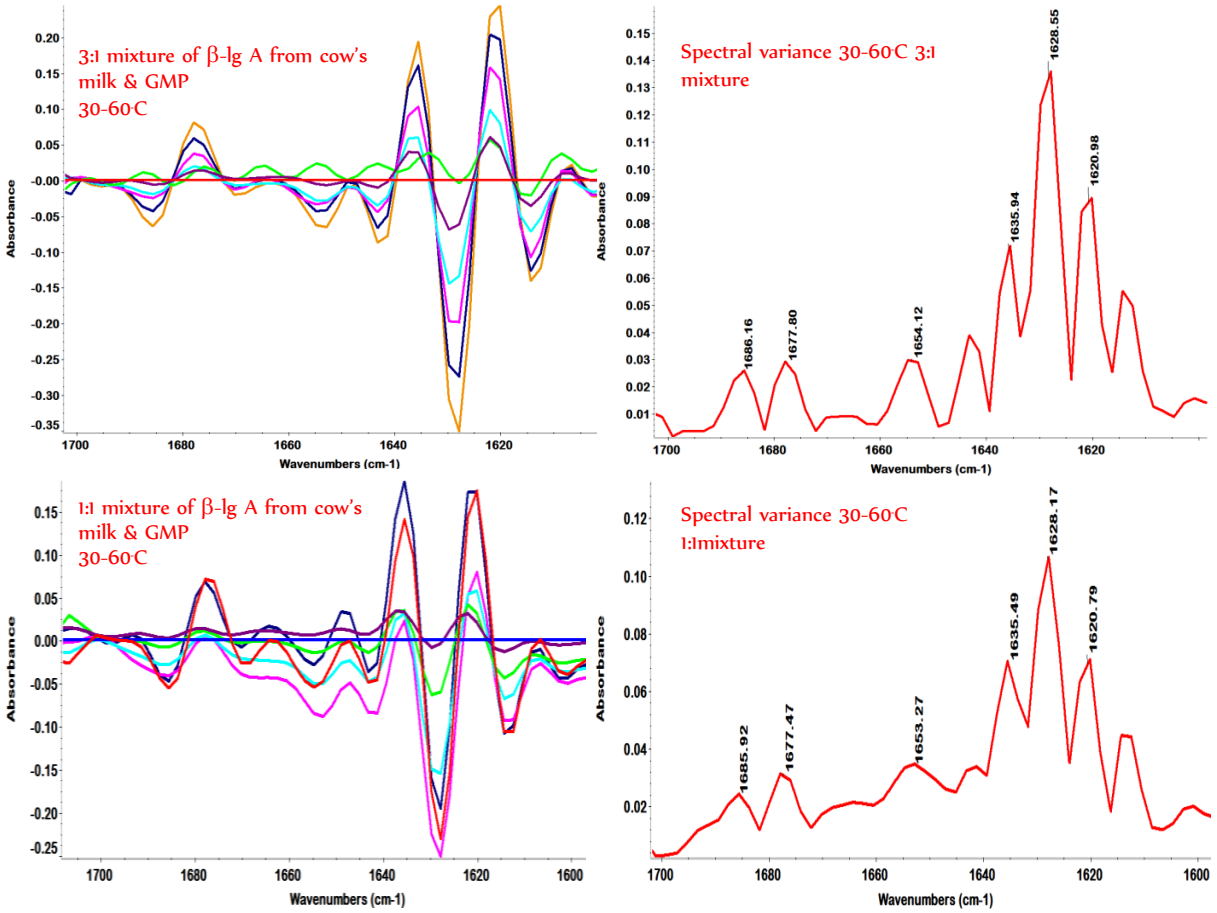

Figure 4.2. Differential spectra (left) and variance spectrum (right) in the amide I′ region of β-lactoglobulin variant A from whole milk in binary mixtures with GMP (ratios 3:1 and 1:1). The samples were heated from 25 ºC to 60ºC in 5ºC increments. The differential spectra were generated by subtracting the spectrum recorded at the beginning of the heating cycle from each of the other spectra.

Tables 4.1 and 4.2 are the correlation tables generated by 2D-COS analysis of the VT-FTIR data for the two mixtures of β-lactoglobulin variant A from whole milk and GMP (ratios of 3:1 and 1:1, respectively) from 30ºC to 60ºC. The results in these tables were employed to elucidate the sequences of spectral changes presented at the bottom of the tables. Combination of the sequence of spectral changes with the results presented for β-lactoglobulin A from whole milk in Chapter 3 yielded the following sequence of events. As the 3:1 β-lactoglobulin A-GMP mixture was heated from 30 to 60ºC, H-D exchange within β–sheets occurred, resulting in a band shift from 1628 to 1621 cm^{-1}, an increase in intensity at 1636 cm^{-1}, and a band shift from 1686 to 1677 cm^{-1} followed by unfolding of the α–helical (1654 cm^{-1}) structure. Comparison of the results of

the 2D correlation analysis with those obtained in the absence of GMP (as summarized in Table 4.5) shows that at a 3:1 protein: GMP ratio, GMP had little effect on the unfolding of β-lactoglobulin A from whole milk. In the case of the 1:1 mixture of β-lactoglobulin A from whole milk and GMP in the temperature range of 30-60ºC (Table 4.2), the 2D correlation analysis indicated that changes in the α–helical structure (1653 cm^{-1}) take place before changes in any of the bands assigned to β–sheet components (1628, 1636, 1621, 1686, and 1677 cm^{-1}). Accordingly, the sequence of unfolding elucidated for the 1:1 mixture differs from that for the protein by itself or in a 3:1 mixture with GMP (Table 4.1), indicating that at a 1:1 ratio, GMP had an important effect on the thermal behavior of β-lactoglobulin A from whole milk.

Table 4.1. Correlation table generated by 2D correlation analysis of the FSD VT-FTIR spectra of a 3:1 mixture of β-lactoglobulin A from whole milk and GMP collected over the temperature range of 30-60ºC.

cm^{-1}	1686 ↓	1677 ↑	1654 ↓	1636 ↑	1628 ↓
1621 ↑	- / + →	+ / - →	- / + →	+ / - →	- / 0 ↔
1628 ↓	+ / - →	- / + →	+ / - →	- / - ←	
1636 ↑	- / + →	+ / - →	- / + →		
1654 ↓	+ / 0 ↔	- / - ←			
1677 ↑	- / + →				
Sequence of spectral changes: ↑1621→↑1636→↓1628→↑1677→↓1654↔↓1686					

Table 4.2. Correlation table generated by 2D correlation analysis of the VT-FTIR spectra of a 1:1 mixture of β-lactoglobulin A from whole milk and GMP collected over the temperature range of 30-60ºC.

cm^{-1}	1686 ↓	1677 ↑	1653 ↓	1636 ↑	1628 ↓
1621 ↑	- / 0 ↔	+ / - →	- / - ←	+ / 0 ↔	- / - ←
1628 ↓	+ / 0 ↔	- / + →	+ / + ←	- / + →	
1636 ↑	- / - ←	+ / - →	- / - ←		
1653 ↓	+ / 0 ↔	- / + →			
1677 ↑	- / 0 ↔				
Sequence of spectral changes: ↓1653→↓1628→↑1635↔↑1621↔↓1686→↑1677					

From 65ºC to 85ºC (Figure 4.3, Tables 4.3 and 4.4), decreases in both the 1636 cm^{-1} band and the 1628 cm^{-1} band were observed for both the 3:1 and 1:1 mixtures as well as a gradual disappearance of the 1692 cm^{-1} band followed by the appearance of bands at 1684 and 1619 cm^{-1}; these two bands are assigned to formation of intermolecular β-sheets and indicate aggregation of the denatured protein. Comparison of the results of the 2D correlation analysis with those obtained for pure β-lactoglobulin A from whole milk (summarized in Table 4.6) showed that at a 3:1 and a 1:1 ratio, once the unfolding and the collapse of the structure of β-lactoglobulin A had taken place, GMP had little effect on the aggregation of the β-sheets.

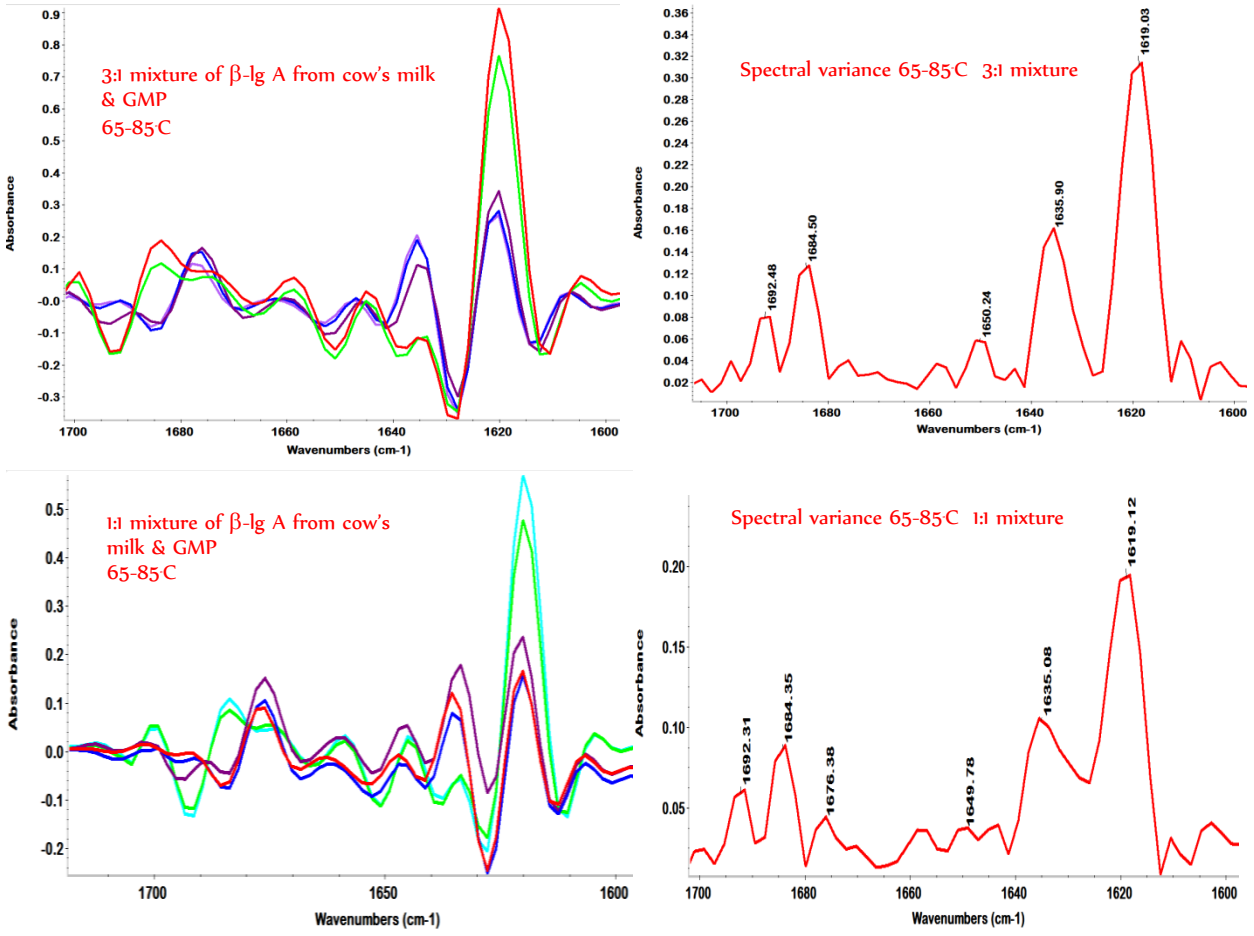

Figure 4.3. Differential spectra (left) and variance spectrum (right) in the amide I´ region of β-lactoglobulin variant A from whole milk in binary mixtures with GMP (ratios 3:1 and 1:1). Spectra were collected as the samples were heated from 65ºC to 85ºC in 5ºC increments, and the differential spectra were generated by subtracting the spectrum recorded at 65ºC from each of the other spectra.

Table 4.3. Correlation table generated by 2D correlation analysis of the VT-FTIR spectra of a 3:1 mixture of β-lactoglobulin A from whole milk and GMP collected over the temperature range of 65-85ºC.

cm^{-1}	1692 ↓	1684 ↑	1650 ↓	1636 ↓
1619 ↑	- / - ←	+ / - →	- / - ←	- / - ←
1636 ↓	+ / + ←	- / + →	+ / + ←	
1650 ↓	+ / - ←	- / + →		
1684 ↑	- / - ←			
Sequence of spectral changes: ↓1692→↓1650→↓1636→↑1619→↑1684				

Table 4.4. Correlation table generated by 2D correlation analysis of the VT-FTIR spectra of a 1:1 mixture of β-lactoglobulin A from whole milk and GMP collected over the temperature range of 65-85ºC.

cm^{-1}	1692 ↓	1684 ↑	1635 ↓
1619 ↑	- / - ←	+ / 0 ↔	- / - ←
1635 ↓	+ / 0 ↔	- / 0 ↔	
1684 ↑	- / 0 ↔		
Sequence of spectral changes: ↓1692↔↓1635→↑1619↔↑1684			

4.3.1.2. Mixtures of β-lactoglobulin A obtained by ion-exchange chromatography of food-grade β-lactoglobulin AB (Davisco AB) and GMP (β-lactoglobulin:GMP ratios of 3:1 and 1:1)

The FSD-FTIR spectra of β-lactoglobulin A obtained by ion-exchange chromatography of food-grade β-lactoglobulin AB (Davisco AB) and its mixtures with GMP (β-lactoglobulin: GMP ratios of 3:1 and 1:1) at 30ºC and 80ºC are presented in Figure 4.4. As in the case of the samples prepared with β-lactoglobulin A from whole milk, the spectra of β-lactoglobulin A and its 3:1 and 1:1 mixtures with GMP recorded at room temperature show the same amide I' band components, but at 80ºC there are major differences among the three spectra. The spectrum of β-lactoglobulin A by itself reveals that much of the secondary structure remains intact at 80ºC whereas the spectra of the mixtures with GMP are indicative of more extensive protein unfolding leading to aggregation, as evidenced by the bands at 1684 and 1619 cm^{-1}. In fact, comparison with

Figure 4.1 indicates that the lower propensity for aggregation exhibited by β-lactoglobulin A derived from food-grade β-lactoglobulin relative to β-lactoglobulin A isolated from cow's milk, as reported in Chapter 3 (Section 3.3.3), is not observed in the presence of GMP.

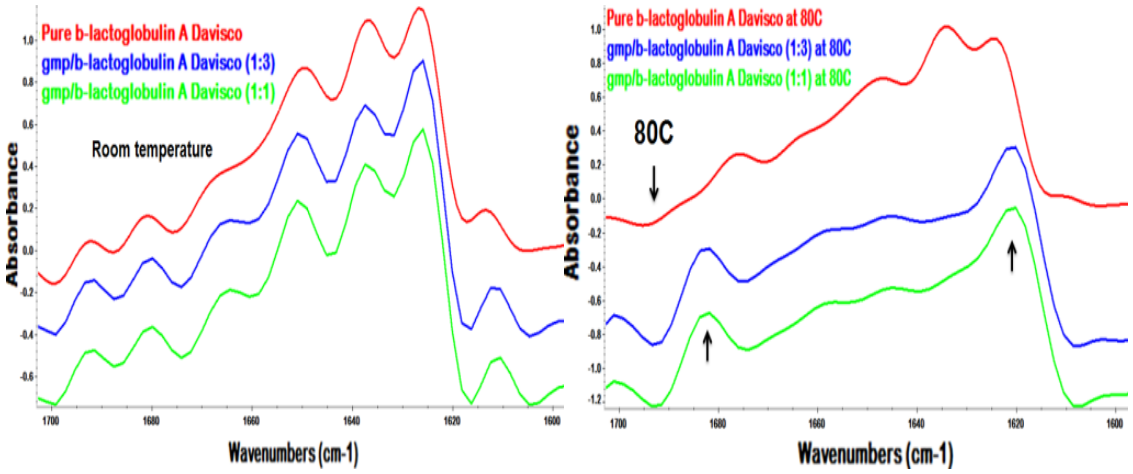

Figure 4.4. Fourier self-deconvolution of the amide I´ band in the spectra of β-lactoglobulin variant A obtained by ion-exchange chromatography of food-grade β-lactoglobulin (Davisco AB) and its binary mixtures with GMP (ratios 3:1 and 1:1) at 30ºC and 80ºC.

The thermally induced changes in the amide I' band in the temperature range of 30-60ºC are illustrated by the differential and variance spectra presented in Figure 4.5 and reveal other effects of GMP on the thermal behavior of β-lactoglobulin A obtained by ion-exchange chromatography of food-grade β-lactoglobulin. The variance spectra over this temperature range show the same amide I' band components as observed in the absence of GMP in Figure 3.11 but with different relative intensities. In particular, by comparison with Figure 3.11 the relative intensities of the bands at both 1677 and 1620 cm^{-1} are disproportionately high in the variance spectra of the 1:1 mixture and, to a lesser extent, the 3:1 mixture. This observation suggests that the bands at these positions are the high-frequency and low-frequency amide I' components associated with a particular antiparallel β-sheet population and that H-D exchange of this population is enhanced in the presence of GMP. In addition, the differential spectrum of the 1:1 mixture at 60ºC reveals a decrease in intensity at 1692 cm^{-1}, suggesting that the presence of GMP also enhances H-D exchange of the more deeply buried β-sheet population associated with the 1692 cm^{-1} band (see Table 3.1). It may be noted that no such effects of GMP on β-lactoglobulin A

from cow's milk were observed in Figure 4.2. Furthermore, whereas 2D-COS analysis of the latter spectra revealed that the thermal stability of the α-helical component was reduced in the presence of GMP (1:1 mixture), the opposite trend was obtained for the 1:1 mixture of GMP with β-lactoglobulin A derived from food-grade β-lactoglobulin, such that the decrease in the α-helical band is the final spectral change in the 2D-COS sequence for the temperature range of 30-60ºC (Table 4.5). It should also be mentioned that the 1692 cm^{-1} band appeared on the 2D contour maps (and hence in the sequence of spectral changes) for this sample but not for the samples in the five rows above it in Table 4.5 owing to the invariance of this band in their spectra.

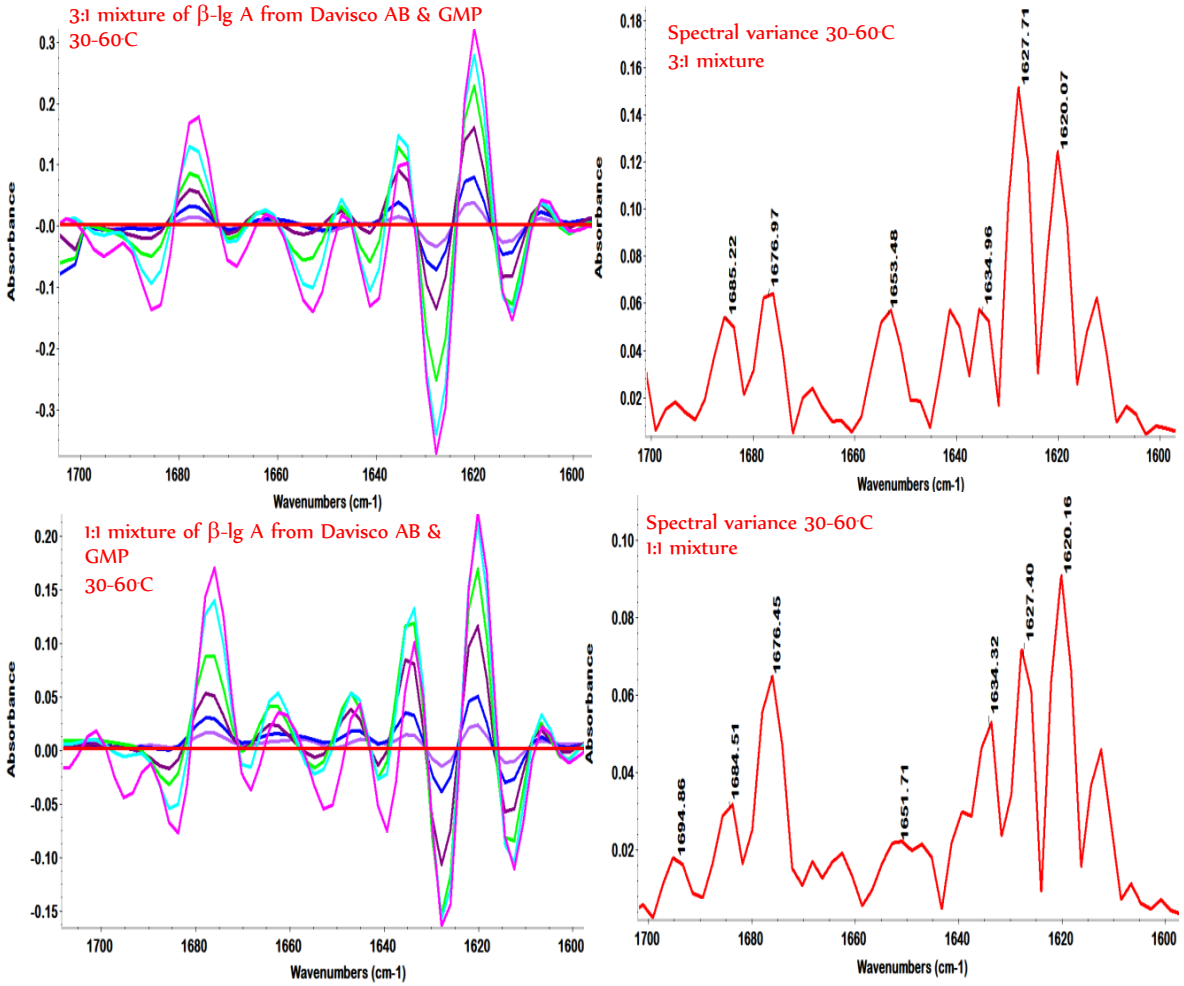

Figure 4.5. Differential spectra (left) and variance spectrum (right) in the amide I´ region of β-lactoglobulin variant A obtained by ion-exchange chromatography of food-grade β-lactoglobulin AB (Davisco AB) in binary mixtures with GMP (ratios 3:1 and 1:1). The samples were heated from 25°C to 60°C in 5°C increments. The differential spectra were generated by subtracting the spectrum recorded at the beginning of the heating cycle from each of the other spectra.

The differential and variance spectra of the 3:1 and 1:1 mixtures for the temperature range of 65-85ºC are presented in Figure 4.6, and the results of 2D-COS analysis of these spectra are summarized in Table 4.6. The beginning of the sequence of events for the 3:1 mixture is the H-D exchange of the deeply buried β-sheet population (1692 cm^{-1}), which had already begun at 60ºC in the case of the 1:1 mixture, followed by the unfolding of the α–helical structure (1654 cm^{-1}). Subsequently, the formation of intermolecular β–sheets (1618 and 1684 cm^{-1}) took place although some intramolecular β-sheet structure remained intact, as indicated by the subsequent decrease in intensity at 1636 cm^{-1}, which was the final event in the sequence, A similar sequence of events was obtained by 2D-COS analysis of the spectra of the 1:1 mixture, except that the unfolding of the intramolecular β-sheet structure occurred earlier in the sequence (Table 4.6). In the absence of GMP, the thermal unfolding of the protein proceeded by a different sequence of events that began with unfolding of the α–helical structure However, it may be noted the results of the 2D-COS analysis do not reflect clearly the effects of GMP on the protein's propensity for aggregation that are evident in Figure 4.6.

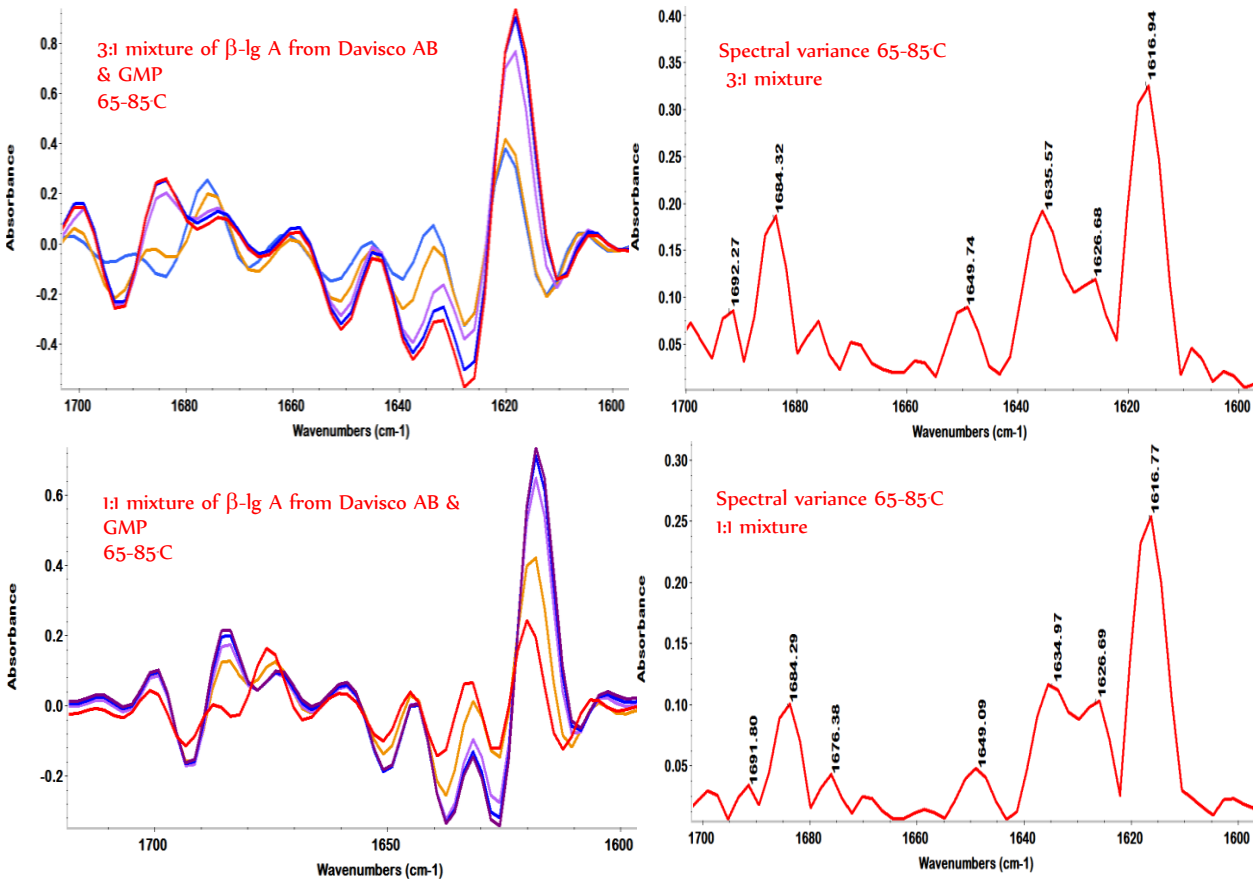

Figure 4.6. Differential spectra (left) and variance spectrum (right) in the amide I´ region of β-lactoglobulin variant A obtained by ion-exchange chromatography of food-grade β-lactoglobulin AB (Davisco AB) in binary mixtures with GMP (ratios 3:1 and 1:1). Spectra were collected as the samples were heated from 65°C to 85°C in 5°C increments, and the differential spectra were generated by subtracting the spectrum recorded at 65°C from each of the other spectra.

4.3.1.3. Mixtures of β-lactoglobulin B obtained by ion-exchange chromatography of food-grade β-lactoglobulin AB (Davisco AB) and GMP (β-lactoglobulin: GMP ratios of 3:1 and 1:1)

The FSD amide I' band in the VT-FTIR spectra of β-lactoglobulin B, obtained by ion-exchange chromatography of food-grade β-lactoglobulin AB (Davisco AB) and its mixtures with GMP (β-lactoglobulin:GMP ratios of 3:1 and 1:1) are presented in Figure 4.7 at 30ºC and at 80ºC. At 30ºC the spectra of both the 1:1 and 3:1 mixtures showed the same amide I' band components as the protein by itself. At 80ºC, the bands at 1682 cm^{-1} and 1618 cm^{-1} were observed in the spectra of

all three samples but with higher intensity in the spectrum of the 3:1 mixture than in the spectrum of β-lactoglobulin B alone and with lower intensity in the spectrum of the 1:1 mixture, showing that GMP affected the unfolding and aggregation of β-lactoglobulin B.

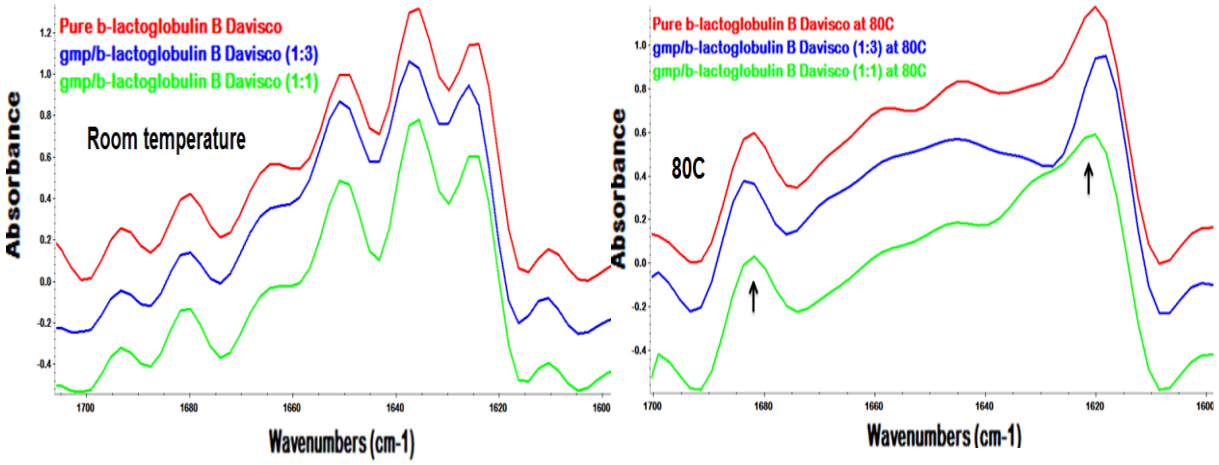

Figure 4.7. Fourier self-deconvolution of the amide I′ band in the spectra of β-lactoglobulin variant B obtained by ion-exchange chromatography of food-grade β-lactoglobulin AB (Davisco AB) and its binary mixtures with GMP (ratios 3:1 and 1:1) at 30ºC and 80ºC.

The differential and variance spectra for the 3:1 and 1:1 mixtures over the temperature range of 30-60ºC are presented in Figure 4.8. The pattern of thermally induced spectral changes for the 1:1 mixture is similar to that observed for the GMP mixtures with β-lactoglobulin A in Figure 4.5 and is indicative of progressive H-D exchange of β-sheet amide groups that results in 1684 →1676 and 1628 →1620 cm^{-1} band shifts. Although the variance spectrum of the 3:1 mixture appears similar to that of the 1:1 mixture, close examination of the differential spectra reveals several significant differences. In the case of the 3:1 mixture, the maximum decrease in intensity at 1628 cm^{-1} is reached at 55ºC whereas at 60ºC the change in intensity reverses direction accompanied by a substantial decrease in intensity at 1692 cm^{-1}. Comparison of the spectra in Figure 4.8 with the corresponding spectra in Figure 3.17 for β-lactoglobulin B derived from food-grade β-lactoglobulin reveals major differences. In particular, in the low-frequency β-sheet region, the largest variance for both GMP mixtures is at 1628 and 1620 cm^{-1} as compared to 1636 and 1628 cm^{-1} in the case of the protein by itself. As discussed in Section 3.3.4, the changes in this region observed for the B variant are attributed to H-D exchange of amide groups in deeply buried β-

sheets that remain largely inaccessible to the solvent in the A variant over the 30-60°C temperature range. Accordingly, the resemblance of the differential spectra of the mixtures of GMP and β-lactoglobulin B to those of β-lactoglobulin A indicate that the presence of GMP has reduced the conformational mobility of the B variant. Indeed, the sequence of spectral changes for the 1:1 mixture of variant B with GMP provided by 2D-COS analysis of the VT-FTIR spectra (Table 4.5) is very similar to that for variant A with GMP (1:1). The sequence of events for the 3:1 mixture differs from that for the 1:1 mixture and shows a greater similarity to that of the protein by itself, indicating that the lower proportion of GMP in this mixture results in a smaller effect on the protein's conformational mobility.

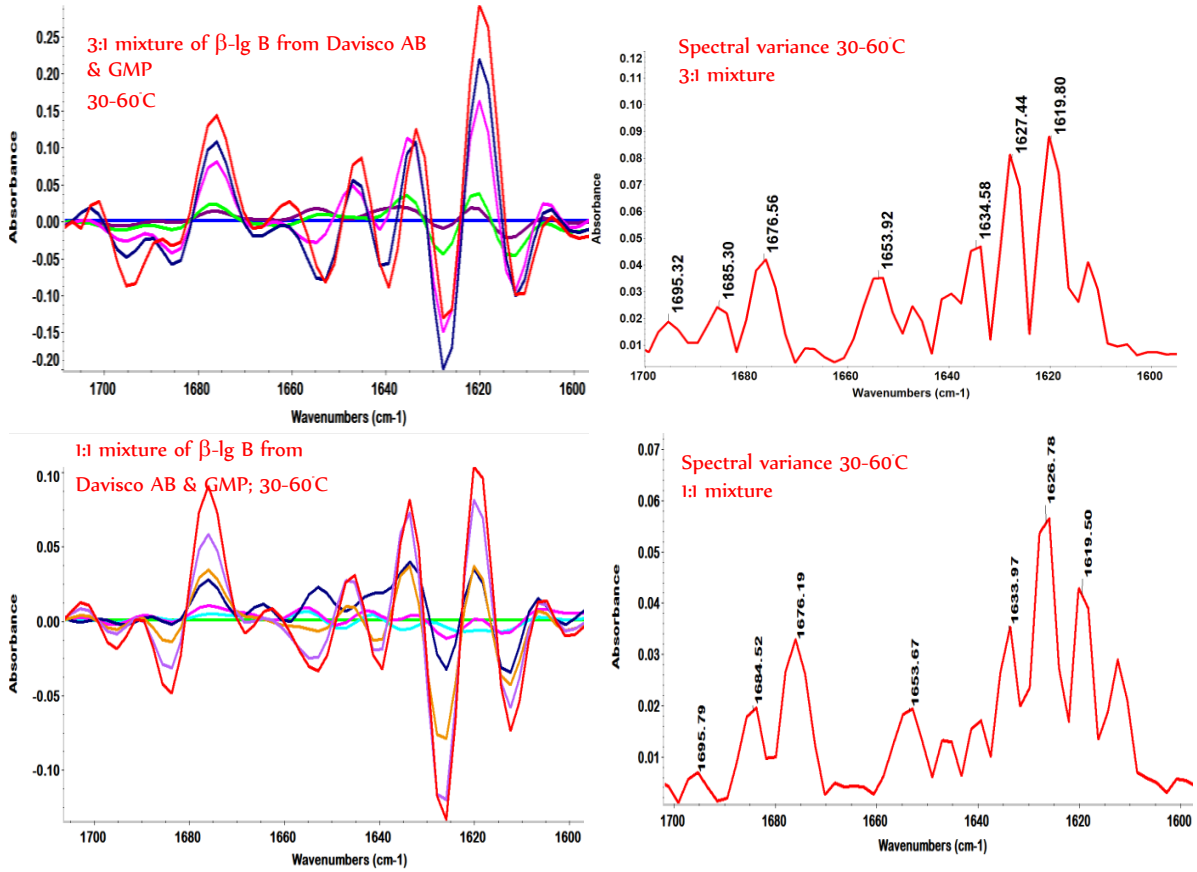

Figure 4.8. Differential spectra (left) and variance spectrum (right) in the amide I´ region of β-lactoglobulin variant B obtained by ion-exchange chromatography of food-grade β-lactoglobulin AB (Davisco AB) in binary mixtures with GMP (ratios 3:1 and 1:1). The samples were heated from 25°C to 60°C in 5°C increments. The differential spectra were generated by subtracting the spectrum recorded at the beginning of the heating cycle from each of the other spectra.

The differential and variance spectra for the upper temperature range examined (65-85ºC), presented in Figure 4.9, and the corresponding 2D-COS results show that the unfolding and aggregation of the protein proceeded by the same pathway in the 1:1 and 3:1 mixtures, although the relative stability of the protein was somewhat greater in the 1:1 mixture. Comparison of the 2D-COS results in this temperature range with those for the protein by itself (Table 4.6) clearly shows that GMP enhances the thermal stability of β-lactoglobulin B derived from food-grade β-lactoglobulin. More specifically, spectral changes associated with intramolecular β-sheets (1692, 1635, and 1627 cm^{-1}) and α–helical structure (1654 cm^{-1}) were discerned in the analysis of the 2D contour maps for the mixtures (and accordingly appear in the 2D-COS sequence of events); in contrast, in the absence of GMP, most of these spectral features were absent in this temperature range and the observed spectral changes were mainly associated with intermolecular β–sheet formation (1618 and 1684 cm^{-1}). Similar trends were observed for β-lactoglobulin B from a commercial source and its 3:1 and 1:1 mixtures with GMP (Table 4.6).

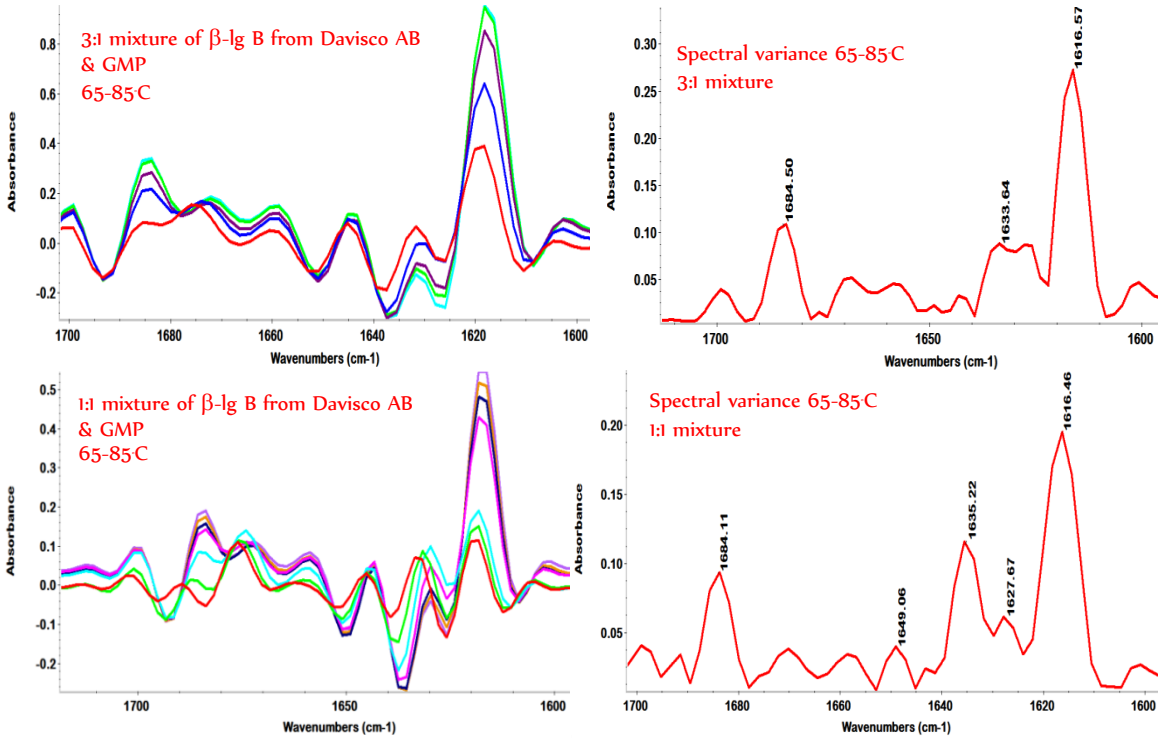

Figure 4.9. Differential spectra (left) and variance spectrum (right) in the amide I′ region of β-lactoglobulin variant B obtained by ion-exchange chromatography of food-grade β-lactoglobulin AB (Davisco AB) in binary mixtures with GMP (ratios 3:1 and 1:1). Spectra were collected as the samples were heated from 65°C to 85°C in 5°C increments, and the differential spectra were generated by subtracting the spectrum recorded at 65°C from each of the other spectra.

4.3.1.4. Mixtures of food-grade β-lactoglobulin AB (Davisco AB) and GMP (β-lactoglobulin: GMP ratios of 3:1 and 1:1)

The FSD amide I' band in the FTIR spectra of food-grade β-lactoglobulin (Davisco AB) and its mixtures with GMP (β-lactoglobulin: GMP ratios of 3:1 and 1:1) at 30ºC and at 80ºC are presented in Figure 4.10. At 30ºC, the 1:1 and 3:1 mixtures showed the same amide I' band components as the protein by itself. At 80ºC, the bands at 1682 cm^{-1} and 1618 cm^{-1} were observed in the spectra of all three samples but with higher intensity in the spectrum of β-lactoglobulin AB alone and with lowest intensity in the spectrum of the 1:1 mixture, showing that GMP affected the unfolding and aggregation of β-lactoglobulin AB.

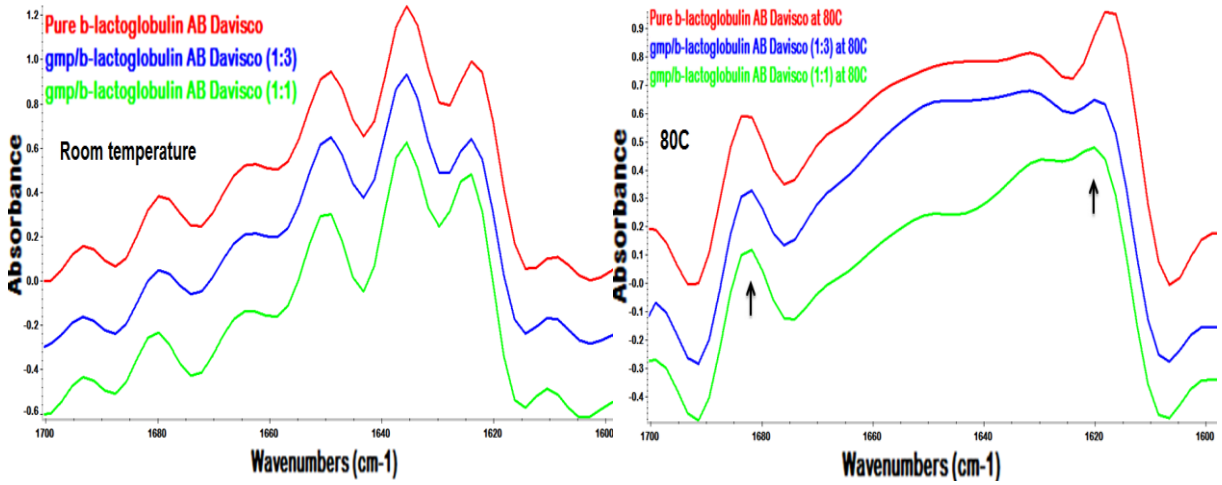

Figure 4.10. Fourier self-deconvolution of the amide I´ band in the spectra of β-lactoglobulin AB (Davisco AB) and its binary mixtures with GMP (ratios 3:1 and 1:1) at 30ºC and 80ºC.

The thermally induced changes in the amide I' band in the temperature range of 30-60ºC are illustrated by the differential and variance spectra presented in Figure 4.11. While the differential spectra for the 3:1 and 1:1 mixtures show the same amide I' band components, the relative intensities of the bands in the corresponding variance spectra differ markedly. In particular, the differences observed in the low-frequency β-sheet region indicate that the extent of H-D exchange associated with the 1628 → 1620 cm^{-1} band shift is substantially higher in the 1:1 mixture than in the 3:1 mixture. The differential spectra of both mixtures reveal gradual and substantive H-D exchange of the more deeply buried β-sheet population associated with the 1692 cm^{-1} band over the temperature range of 30-60ºC, as was also observed for the food-grade β-lactoglobulin in the

absence of GMP (Section 3.3.5). The differential and variance spectra for the temperature range of 65-85ºC presented in Figure 4.12 show that no further decrease in intensity at 1692 cm^{-1} band occurred with continued heating above 60ºC, indicating complete H-D exchange of this β-sheet population. While this finding would be consistent with extensive unfolding of the protein's β-sheet structure at this relatively low temperature, the low-frequency β-sheet region of the spectra in Figure 4.19 and the 2D-COS results in Table 4.6 reveal that unfolding of β-sheets continued beyond 65ºC.

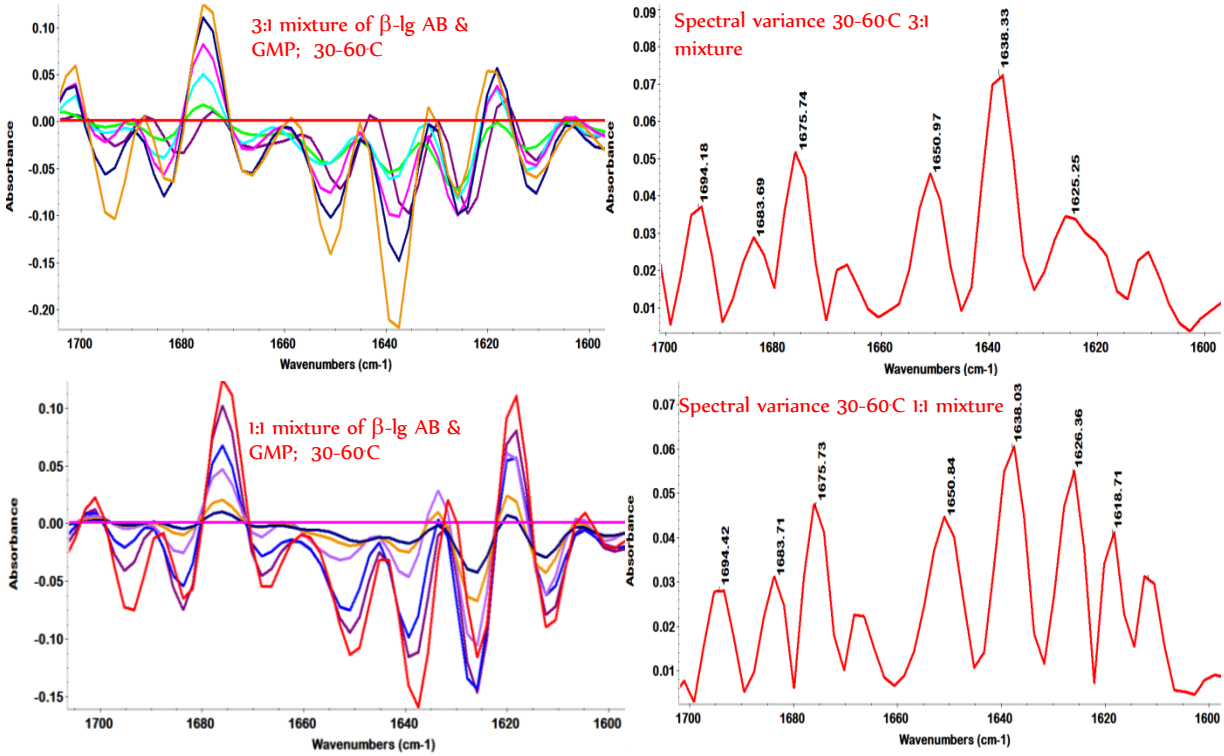

Figure 4.11. Differential spectra (left) and variance spectrum (right) in the amide I′ region of food-grade β-lactoglobulin AB (Davisco) in binary mixtures with GMP (ratios 3:1 and 1:1). The samples were heated from 25ºC to 60ºC in 5ºC increments. The differential spectra were generated by subtracting the spectrum recorded at the beginning of the heating cycle from each of the other spectra.

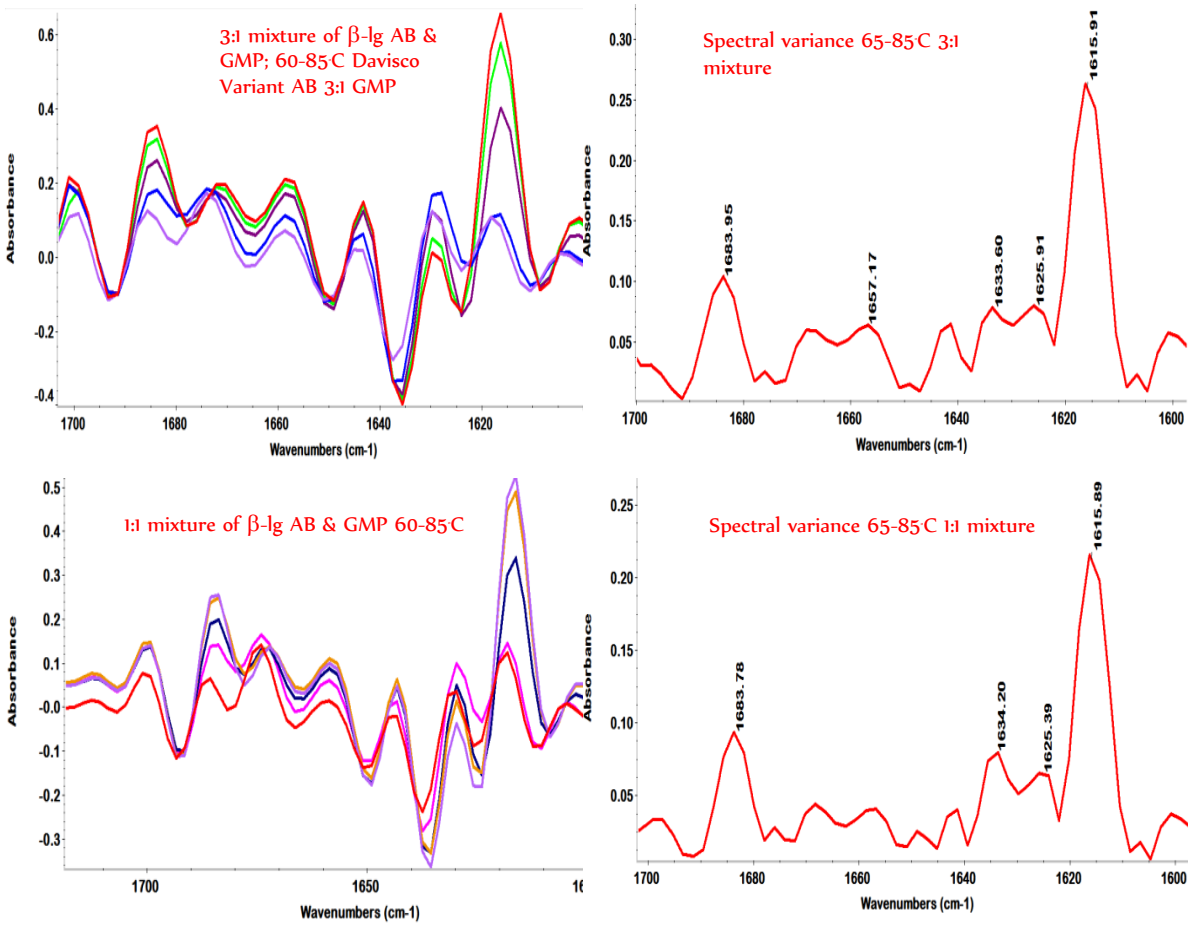

Figure 4.12. Differential spectra (left) and variance spectrum (right) in the amide I′ region of food-grade β-lactoglobulin AB (Davisco) in binary mixtures with GMP (ratios 3:1 and 1:1). Spectra were collected as the samples were heated from 65ºC to 85ºC in 5ºC increments, and the differential spectra were generated by subtracting the spectrum recorded at 65 º C from each of the other spectra.

4.3.2. Summary of effects of GMP on β-lactoglobulin samples from different sources

In Tables 4.5 (30-60ºC) and 4.6 (65-85ºC), the 2D-COS results obtained for β-lactoglobulin samples from different sources and their mixtures with GMP have been summarized. Table 4.7 summarizes the denaturation temperatures of the β-lactoglobulin samples and their mixtures with GMP, as determined by plotting the intensity at 1682 cm^{-1} as a function of temperature for each sample. These tables include results for binary mixtures of GMP with β-lactoglobulin B and β-lactoglobulin AB from a commercial supplier (Sigma) that have not been presented above.

Table 4.5. Sequence of intensity changes of amide I' band components in the VT-FTIR spectra of β-lactoglobulin samples and their mixtures with GMP over the temperature range of 30-60ºC, as deduced by 2D correlation analysis of FSD spectra[a]

Sample	↓1692 cm^{-1}	↓1684 cm^{-1}	↑1676 cm^{-1}	↓1654 cm^{-1}	1635 cm^{-1}*	1627 cm^{-1}*	↓1620 cm^{-1}
Cow A [b]	-	5	4	3	↑6	↓2	1
Cow A : GMP 3:1	-	5	4	6	↑2	↓3	1
Cow A : GMP 1:1	-	3	6	1	↑5	↓2	4
Davisco A	-	5	4	5	↑3	↓1	2
Davisco A : GMP 3:1	-	5	4	5	↑1	↓3	2
Davisco A : GMP 1:1	5	5	4	6	↑1	↓2	3
Davisco B	4	1	2	3	↓5	↑6	-
Davisco B : GMP 3:1	4	-	2	3	↓5	↓1	-
Davisco B : GMP 1:1	4	5	3	6	↑1	↓2	4
Davisco AB	6	1	3	4	↓5	↓2	-
Davisco AB : GMP 3:1	6	2	5	3	↓4	↓1	-
Davisco AB : GMP 1:1	6	2	4	3	↓5	↓1	6
Sigma B	6	1	2	3	↓4	↑5	-
Sigma B : GMP 3:1	1	4	4	1	↓2	↑3	-
Sigma B : GMP 1:1	6	6	5	3	↓4	↓1	2
Sigma AB	1	2	1	2	↓3	↑4	5
Sigma AB : GMP 1:1	6	3	4	5	↓6	↓1	2
Sigma AB : GMP 3:1	7	3	4	5	↓6	↓1	2

[a]Bands that have the same number changed more or less simultaneously.

[b]β-Lactoglobulin A isolated from the milk of a cow identified as homozygous for variant A.

[c]The 1635 cm^{-1} band was excluded from the 2D correlation analysis owing to its bidirectional changes in intensity.

*Direction of the intensity change of this band differed among the different samples; arrows are marked individually in each row.

Table 4.6. Sequence of intensity changes of amide I' band components in the VT-FTIR spectra of β-lactoglobulin samples and their mixtures with GMP over the temperature range of 65-85°C, as deduced by 2D correlation analysis of FSD spectra[a]

Sample	↓1692 cm^{-1}	↑1684 cm^{-1}	↓1676 cm^{-1}	↓1654 cm^{-1}	↓1635 cm^{-1}	↓1627 cm^{-1}	↑1618 cm^{-1}
Cow A[b]	2	4	-	1	2	-	3
Cow A : GMP 3:1	1	5	-	2	3	-	4
Cow A : GMP 1:1	1	3	-	-	2	-	3
Davisco A	3	4	5	1	6	7	2
Davisco A : GMP 3:1	1	3	-	2	6	5	4
Davisco A : GMP 1:1	1	2	2	3	3	5	4
Davisco B	-	1	-		-	3	2
Davisco B : GMP 3:1	3	5	-	3	1	2	4
Davisco B : GMP 1:1	-	2	-	3	1	5	4
Davisco AB		5	2	-	4	1	3
Davisco AB : GMP 3:1	-	2	-	-	1	4	3
Davisco AB : GMP 1:1	-	1	-	-	2	4	3
Sigma B	-	1	-	-	-	1	1
Sigma B : GMP 3:1	-	3	-	1	2	5	4
Sigma B : GMP 1:1		2	-	2	1	4	3
Sigma AB	-	1	-	-	-	3	2
Sigma AB : GMP 3:1	-	1	-		2	4	3
Sigma AB : GMP 1:1	-	1	-	2	2	4	3

[a]Bands that have the same number changed more or less simultaneously.

[b]β-Lactoglobulin A isolated from the milk of a cow identified as homozygous for variant A.

Table 4.7. Denaturation temperatures of β–lactoglobulin (β-lg) samples and their mixtures with GMP

Denaturation temperature (ºC) (±1ºC)[a]						
Sample	Variant A from whole milk	Variant A from Davisco AB	Variant B from Davisco AB	Variant B from Sigma	AB Davisco	AB Sigma
β-lg	81	84	71	73	74	70
3:1 β-lg:GMP	77	73	73	73	75	77
1:1 β-lg:GMP	78	70	78	76	76	77

[a]Experiments were performed in triplicate; the mean standard deviation was 0.1.

As discussed in Chapter 3, the VT-FTIR studies revealed that the denaturation temperature of β-lactoglobulin variant A was higher than that of variant B, consistent with circular dichroism studies, in which it was established that the thermal stability of variants A, B and C decreased in the order C > A > B (Qin *et al.,* 1999; Manderson *et al.,* 1999). The VT-FTIR studies also revealed that the denaturation temperatures of the food-grade β-lactoglobulin AB and the separated A and B variants were in the order B < AB < A, which is in accordance with the order obtained by Gough and Jenness (1962) when they examined the stability of β-lactoglobulin variants A and B (isolated from the milk of homozygous cows for each variant) and β-lactoglobulin AB (obtained from the milk of heterozygous cows) by evaluating thermal denaturation and, sulfhydryl group activity. However, the results obtained for the samples from Sigma were different, with variant B being more thermally stable than the AB mixture, again illustrating the important role of the "mixed populations" effect in AB mixtures.

The VT-FTIR studies of the binary mixtures of GMP with β-lactoglobulin from the different sources and at different ratios showed variable effects of GMP on the denaturation temperature of β-lactoglobulin. In the case of β-lactoglobulin A, its denaturation temperature in the mixtures with GMP was lower than that of the pure protein whereas the opposite trend was observed for β-lactoglobulin B and the AB mixtures.

4.4. CONCLUSIONS

GMP is a 64 amino acid peptide with a molecular weight between 6755 and 6787 Da (depending on the variant) which can go up to approximately 30,000 Da depending on the amount of glycosylation. GMP has no aromatic (Phe,Trp, Tyr) and no Cys amino acids, it is highly negatively charged (two Asp and 7-8 Glu, depending on the variant) and the N-terminus has three positively charged domains (three Lys) with no defined secondary and/or tertiary structure (random coil). GMP is a hydrophilic peptide due to the presence of carbohydrates (sialic acid) bound to three out of five of the possible glycosylation sites ($Thr_{131, 133, 135}$, Ser_{141}, Thr_{142}), located approximately in the middle of GMP´s backbone, the higher the glycosylation, the higher the hydrophilicity. In other words, the functionality of GMP depends on the source and isolation method (Neelima *et al.,* 2013).The GMP used for the present study contains approximately 83% protein and 7% sialic acid, according to the specifications sheet (Davisco Foods International Inc.).

In the present study, pure β-lactoglobulin A (obtained from whole milk) had a higher denaturation temperature than in binary mixtures with GMP (3:1 and 1:1 ratios). In the case of β-lactoglobulin A, β-lactoglobulin B and β-lactoglobulin AB from a food-grade commercial source (Davisco), the thermal stability was in the following order: A < AB < B, with A being the most thermally stable and the AB mixture having a denaturation temperature in between those of the two individual variants; these results were also obtained by previous studies (Gough and Jenness, 1962). However, when comparing pure β-lactoglobulin B and pure β-lactoglobulin AB from a commercial source (Sigma), pure β-lactoglobulin variant B (Sigma) had a higher denaturation temperature than the mixture of β-lactoglobulin AB (Sigma) variants. In the mixed binary systems of GMP with β-lactoglobulin from different sources and at different ratios (β-lactoglobulin: GMP 3:1 and 1:1) it was demonstrated that GMP also had different effects on all β-lactoglobulin´s unfolding and aggregation pathways and that these effects were also different at the different ratios used in this study.

As mentioned previously, there is not much known about GMP itself (Neelima *et al.,* 2013) and much less is known about its interactions with β-lactoglobulin (Martínez *et al.,* 2009 and Martínez *et al.,* 2010). So far, the following hypotheses have been made by previous authors: (i) β-lactoglobulin hinders GMP´s absorption; (ii) a strong synergism between the two molecules occurs (Martínez *et al.,* 2009 and Martínez *et al.,* 2010); (iii) electrostatic repulsion that creates a

compressing effect of the structure of β-lactoglobulin making it more compact and less prone to unfolding; and (iv) hydrophobic and/or ionic interactions between peptides and β-lactoglobulin (Barbeau *et al.,* 1996).

Based on the results of the present study and the literature available we propose that the most likely interactions between GMP and β-lactoglobulin are hydrogen bonds, hydrophobic interactions and electrostatic repulsions, however, we cannot propose an accurate mechanism of the effect of GMP on the tertiary and secondary structure of β-lactoglobulin based on the following statements: (1) different variants and/or mixed variants (β-lactoglobulin AB) will result in different unfolding and aggregation pathways since the mixed variants have different populations of AB, AA and BB dimers, (2) the unfolding and aggregation mechanisms of all the samples of β-lactoglobulin were affected to a different degree when mixed in binary systems with GMP at both ratios (3:1 and 1:1), (3) the source and the isolation method of β-lactoglobulin have an impact on the protein´s behavior which is substantially compounded by the source and isolation method of GMP given that GMP is not found as a pure peptide and the degree of glycosylation will have major effects on its interactions, (4) future studies of pure GMP and/or binary mixtures using GMP will require a quantitative determination of the concentration of sialic acid using a fluorimetric method and (5) future studies using surface plasmon resonance could be used to elucidate the binding affinity between β-lactoglobulin and GMP.

CONNECTING STATEMENT

In the previous chapter, binary mixtures of β-lactoglobulin variant A, β-lactoglobulin variant B and β-lactoglobulin variants AB mixtures in the presence of GMP were examined using variable temperature-FTIR and 2D-Correlation spectroscopy to assess the impact of GMP on β-lactoglobulin's secondary structure and its conformational mobility. The results demonstrated that GMP affects the conformational mobility and the denaturation temperature of β-lactoglobulin. In the next chapter, focal plane array-FTIR microspectroscopy was used to demonstrate the applicability of chemical imaging for the study of a high- β-lactoglobulin AB-based model food system.

Chapter 5. Interactions of β-Lactoglobulin with Other Ingredients in a "High-Protein Cookie" Model Food System

5.1. INTRODUCTION

Within the field of food science, the chemistry of individual food components has been thoroughly studied with the ultimate objective of understanding their properties in food systems. However, the way these components behave individually is often altered when they interact with other food components in a complex food matrix. For instance, the so-called "food protein paradox" refers to the fact that the behavior of a food protein studied in its pure state under strictly controlled conditions is often not the same as its behavior in a complex food formulation. Apart from their nutritional importance, food proteins have a number of important functional properties in food systems, and obtaining desired functional properties is intrinsically linked to the control of protein unfolding and aggregation processes during food processing.

Accordingly, while much research has been directed toward understanding the effects of changes in physicochemical conditions on the structure of individual food proteins and elucidating the relationships between these structural changes and the functional properties of the protein, the results of these investigations often do not translate into the desired outcome. As a consequence, there is an increasing tendency to make use of sophisticated research techniques such as spectroscopic methods to study model food systems (Harper, 2009; Owusu and Apenten, 2004).

Food scientists have a large variety of methods at their disposition for studies of model food systems. Among these methods, vibrational spectroscopy has unique advantages including its suitability for nondestructive analysis of food matrices in liquid, solid or even gaseous state and its applicability to quality assurance and quantitative compositional analysis of food constituents (Sedman *et al*., 2010; Jiang *et al*., 2010; Li-Chan *et al.*, 2010). Furthermore, the capabilities for infrared imaging afforded by FTIR microspectroscopy with the use of multichannel detectors allow for the study of heterogeneous food samples with a spatial resolution on the micron scale. Another technique widely used in studies of heterogeneous food systems is scanning electron microscopy (SEM). This technique has proved to be useful for the elucidation of the internal structure and distribution of ingredients in doughs and baked products (Widjanarko *et al.,* 2011, Ribotta *et al.,* 2004; Zounis *et al.,* 2002).

This chapter addresses the development and study of a "high whey protein cookie" model food system. The "cookie" contained whey protein (β-lactoglobulin; glycomacropeptide; or glycomacropeptide in combination with β-lactoglobulin), carbohydrates, fats, emulsifiers and a small amount of water. While there have been many studies on partial substitution of wheat flour in wheat-based baked products by other types of flour, such as soy flour or rice flour (Pérez *et al.,* 2008; Mohsen *et al.,* 2009; Conforti *et al.,* 2004), there have been no studies focusing on the complete substitution of flour by pure protein. In addition, most research on high-protein food systems has focused on nutritional aspects (Veldhorst *et al*., 2008; Booth *et al*., 1970; Bensaïd *et al.,* 2002; Vandewater *et al*., 1996; Widjanarko *et al.,* 2011) rather than addressing molecular aspects. The present research employs infrared imaging and SEM to examine the model "high whey protein cookie" and applies FTIR spectroscopic techniques to investigate the molecular interactions between β-lactoglobulin and each of the other components in this model food system.

5.2.MATERIALS AND METHODS

5.2.1. Development of a "high whey protein cookie" model system

A "high whey protein cookie" model food system was developed in cooperation with Bariatrix Nutrition (Lachine, Québec, Canada), which is a company that produces weight-loss/weight-management products and food supplements. The attributes targeted in the formulation of the "high whey protein cookie" were: high protein content and high in fiber. All the ingredients were provided by Bariatrix Nutrition and all the formulations were baked at their Research and Development laboratory. The protein ingredients used for the "cookie" model system were β-lactoglobulin and glycomacropeptide from Davisco Foods International Inc. (Le Sueur, MN, USA); other ingredients provided by Bariatrix Nutrition were maltitol syrup, maltitol crystalline powder, polydextrose powder, sucrose, sunflower oil, diacetyl tartaric acid ester of monoglycerides (DATEM), lecithin, xanthan gum, guar gum, low methoxyl (LM) pectin and water. All the ingredients, including water, were food grade. The process used to mix the ingredients was proprietary to Bariatrix Nutrition.

Once the ingredients were mixed and the dough was formed, it was compressed into a cookie gun and cut into slices of an approximate thickness of 5 mm and deposited on a tray which

was sprayed with canola oil to allow better pan release. The cookies were baked for five minutes in a convection oven at 150ºC; once they were taken out of the oven, they were placed on a wire rack for a more efficient cooling process. After approximately 1 hour of cooling down; moisture content, water activity (a_w) and texture analysis tests were performed on the cookies.

5.2.2. Moisture content and water activity (a_w) of the "high whey protein cookie" model system

The moisture content and the water activity of each cookie formulation were determined approximately one hour after the baked cookies had cooled down. The water activity (a_w) was measured using an AquaLab Dew Point Water Activity Meter 4TE Series 3 (Decagon Devices, Pullman, WA, USA), equipped with a chilled mirror Dewpoint. The cookies were ground using a KitchenAid coffee grinder (BCG111OB, KitchenAid, USA), and the ground samples were placed in AquaLab disposable cups (15-mL capacity) and inserted into the "cup holder chamber" for analysis. For the determination of moisture content using a microwave Smart Turbo Moisture/Solid Analyzer (CEM Corporation, Matthews, NC, USA); two square sample pads were tared, and then the ground sample was placed between the pads, forming an approximately 2-mm-thick layer. The tests were performed in duplicate.

5.2.3. Texture analysis of the "high whey protein cookie" model system

The texture analysis was performed using a TA.XT2 Texture Analyzer (Texture Technologies, Hamilton, MA, USA). The tests performed on the cookies were bending tests and the parameters used are shown in Table 5.1. The tests were done in triplicate.

Table 5.1.Texture tests

Sample	Tests	Probe	Crosshead speed
Cookies	Bending	3 point bending rig	3 mm/s (hardness and fracturability)

5.2.4. Examination of the spatial distribution of the ingredients in a model food system by infrared imaging using a focal-plane-array-FTIR (FPA-FTIR) spectrometer

Infrared images were recorded on a Varian Excalibur FTIR spectrometer operating under Varian Resolutions Pro 4.0 software (Agilent Technologies, Melbourne, Australia) and equipped with a UMA-600 infrared microscope and a liquid-nitrogen-cooled 64 × 64 mercury-cadmium-telluride (MCT) focal-plane-array (FPA) detector. A germanium attenuated total reflectance element was affixed to the microscope objective. To acquire spectral images from dough samples, a piece of dough was cut in the shape of a small cube and placed on a metal plate. Baked samples were placed on a metal plate. All experiments were done in triplicate. The spectral data contained within each image (4096 individual spectra) was processed and analyzed using Image Processor Version 0.8.5.1© software (developed in-house by A. Ghetler).

5.2.5. Examination of the distribution of the ingredients in a model food system using variable-pressure scanning electron microscopy (VP-SEM)

Cookie samples were cut into pieces of approximately 10 mm × 10 mm with a thickness of approximately 5 mm and were then placed onto double-sided tape attached to specimen stubs. The mounted specimens were examined using a Hitachi S-3000N Variable Pressure Scanning Electron Microscope (Hitachi High Technologies America Inc., Schaumburg, IL, USA) equipped with a backscatter electron detector (BSE) at 5-nm resolution in a variable-pressure mode with an acceleration voltage of 25 kV and a vacuum of 25 Pa. Micrographs were taken at three different magnifications (60×, 200× and 250×).

5.2.6. Examination of the stability of the native structure of β-lactoglobulin (AB, food grade) in the presence of carbohydrates, fats and emulsifiers before and after heating (baking conditions) using FPA-FTIR spectroscopy

Samples for FTIR examination were prepared in two ways: [1] thin films of food-grade β–lactoglobulin AB (Davisco), on its own and with each of the other individual components in the "high whey protein cookie" were layered on ZnSe crystals as described below in order to study the interactions between the protein and the other components in the formulation and [2] baked cookies were dissolved in D_2O to extract the protein with the dual purpose of ascertaining whether there was still soluble (undenatured) protein after baking and analyzing the secondary structure of the protein.

For the preparation of the films, binary mixtures of food-grade β–lactoglobulin AB (Davisco) and each of the other ingredients of the "high whey protein cookie" model system were prepared in D_2O at the concentrations used in the formulation on a w/w basis (1 gram of total weight); the concentration of β-lactoglobulin was kept constant at 37% as shown in Table 5.2. The solution was then deposited on a ZnSe crystal (60 mm in diameter) and air-dried to produce a thin film suitable for imaging by FPA-FTIR spectroscopy in the transmission mode. Samples were prepared in duplicate. FPA-FTIR spectral images were recorded in the transmission mode using the FPA-FTIR spectrometer described in Section 5.2.4. After the FPA-FTIR spectral images had been recorded, the films on the ZnSe crystals were left overnight in a covered glass Petri dish with a moistened (in D_2O) disposable tissue under the ZnSe crystal in order to transfer moisture to the films. Immediately after being removed from the Petri dish, the films on the ZnSe crystals were heated in a countertop oven (Hamilton Beach®, NC, USA) at 150ºC for five minutes, and their FPA-FTIR images were then recorded as described above.

The FPA-FTIR imaging data was processed using Image Processor Version 0.8.5.1© software (developed in-house by A. Ghetler). Any spectral interference from the non-protein ingredient in each mixture was eliminated by spectral subtraction employing the average of the spectra obtained by FPA-FTIR imaging of a film of the ingredient. Fourier self-deconvolution (FSD) was performed with a resolution enhancement factor of k = 2.4 and a bandwidth of w = 24 cm^{-1} using OMNIC® Version 6.0 software (Thermo Nicolet, Madison, WI). For samples prepared by dissolving baked cookies in D_2O, FTIR spectra were recorded with a Varian FTIR spectrometer equipped with a deuterated triglycine sulfate (DTGS) detector and purged with dry air; 256 scans

at a resolution of 4 cm^{-1} were co-added. A 10-µl aliquot of the D_2O solution was placed between two CaF_2 windows separated by a 15-µm Teflon spacer and placed in a temperature-controlled cell. The temperature was held at 25ºC for 10 minutes prior to collection of the FTIR spectrum of the solution. The FTIR spectra were subjected to Fourier self-deconvolution (k = 2.4, w = 24 cm^{-1}) and baseline corrected.

Table 5.2. Concentrations (w/w) of solutions prepared for the deposition of films on a zinc selenide crystal for imaging by focal-plane-array-FTIR (FPA-FTIR) spectroscopy

Component	Concentration (%, by wt) in solution number:										
	1	2	3	4	5	7	8	9	10	11	12
β-Lactoglobulin	37	37	37	37	37	37	37	37	37	37	37
Sunflower oil	-	8	-	-	-	-	-	-	-	-	-
Sugar	-	-	4	-	-	-	-	-	-	-	-
Maltitol syrup	-	-	-	22.5	-	-	-	-	-	-	-
Maltitol (powder)	-	-	-	-	5	-	-	-	-	-	-
Polydextrose	-	-	-	-	-	15	-	-	-	-	-
Lecithin (powder)	-	-	-	-	-	-	1	-	-	-	-
DATEM	-	-	-	-	-	-	-	1	-	-	-
Xanthan gum	-	-	-	-	-	-	-	-	0.125	-	-
LM pectin gum	-	-	-	-	-	-	-	-	-	0.25	-
Guar gum	-	-	-	-	-	-	-	-	-	-	0.125

*Solutions of each individual component were also prepared and deposited as films for FPA-FTIR imaging.

5.2.7. Sensory evaluation of the cookie model system

A hedonic sensory evaluation test of the model cookies was conducted by 22 panelists. The evaluations were done in triplicate, and a model cookie formulated using BiPRO® whey protein isolate (Davisco Foods International, Le Sueur, MN, USA) was employed as a reference. The experimental design was a complete randomized block design, and an analysis of variance (ANOVA) was done to find out whether there were significant differences (5% significance level) between the WPI cookie model and the β–lactoglobulin cookie model. A Tukey´s honestly significant difference (5% significance level) test (Tukey´s HSD) and a Fisher´s least significant difference (5% significance level) test (Fisher´s LSD) were done to verify a significant difference between means (Foroughbakhch, 2001). The formulation of the sensory test evaluation sheet (instructions, questions, coding and score evaluation) and the evaluation of the data were performed using the software Compusense® (Guelph, ON, Canada).

The panelists were semi-trained volunteers from the Product Development course in the Food Science program at McGill University, and the sensory evaluation was done in the sensory

evaluation laboratory at McGill University (Macdonald Campus). Each panelist was seated in a booth equipped with a computer that displayed the codes of the samples and the attributes to be evaluated, which are presented in Table 5.3. Each attribute was evaluated on a scale from 1 to 7; the descriptors for the extremes and the midpoint of the scale (corresponding to values 1, 4, and 7) for each attribute are presented in Table 5.4.

Table 5.3. Definition of the evaluated attributes for the "cookie model system" (Meilgaard *et al.*, 2007)

Attribute	Definition
Color (Intensity)	The intensity or strength of the color from light to dark
Hardness	Force required to bite through
Cohesiveness	The extent to which the sample deforms rather than ruptures
Crispness	The noise and force with which the sample breaks or fractures
Moistness	The amount of wetness or oiliness (moistness if both) on surface
Adhesiveness	Force required to remove sample from molars
Flavor	Analysis of a product´s perceived flavor characteristics

Table 5.4. Descriptors for the extreme and midpoint values (on the scale of 1 to 7) of each attribute analyzed in the sensory evaluation test

Value	Color (Intensity)	Hardness	Cohesiveness	Crispness	Moistness	Adhesiveness	Flavor
1	Light	Very soft	Breaks	Not crispy	Extremely dry	Extremely non sticky	Milky
4	Medium	Not soft/ not hard	Maintains shape	Crispy	Neither dry nor wet/oily	Sticky	Neither milky nor goaty
7	Dark	Very hard	Deforms	Very crispy	Extremely wet/oily	Extremely sticky	Goaty

5.3. RESULTS AND DISCUSSION

5.3.1. Development of a "high whey protein cookie" model system

Sixteen formulations were developed (Table 5.5) in order to obtain a standardized functional recipe for a "high whey protein cookie" with acceptable texture and appearance characteristics to be used as a model system. With regard to texture, a common problem encountered when using whey protein in baked products is the hardness conferred to the final product. Thus; the use of emulsifiers, humectants, and bulking agents such as sorbitol, polydextrose, glycerin and lecithin is necessary for the development of these types of products (Gallagher *et al*., 2005; Zoulias *et al.*, 2000; Conforti and Lupano, 2004; Ranhotra *et al.*, 1980). Other criteria addressed in the development of the "cookie model system" were compatibility with the use of rotary mold cookie equipment and also dough properties such as dough release, dough binding, mixing, and dough texture and baking properties such as pan release, puffing and moisture release in a uniform way (proprietary work conducted at Bariatrix Nutrition Inc.). The final standardized formulation (based on formulation 14 in Table 5.5) is shown in Table 5.6.

Table 5.5. Formulations developed and tested for the preparation of a "high whey protein cookie" as a model food system.

Formulations ‡	Ingredients (% weight)														
	Protein	Poliol syrup	Sucrose	H_2O	Maltitol powder	Polydextrose	Maltodextrin	Sunflower oil	Lecithin	DATEM *	Tween 80	Mono-glycerides	Pectin gum	Guar gum	Xanthan gum
1	38	22	6	6	-	10	10	6	-	-	1	1	-	-	-
2	38	22	6	6	-	10	10	6	-	-	1	1	-	-	-
3	38	24	6	4	-	10	10	6	-	-	1	1	-	-	-
4	38	24	6	4	-	10	10	6	1	-	1	-	-	-	-
5	37	22	6	6	-	10	10	6	-	1	1	-	-	-	1
6	37	22.5	6	6	-	10	10	6	-	1	1	-	-	-	0.5
7	37	22.5	6	6	5	15	-	6	-	1	1	-	-	-	0.5
8	37	22.5	4	6	5	15	-	8	-	1	1	-	-	-	0.5
9	37	22.5	4	6	5	15	-	8	1	1	-	-	-	-	0.5
10	37	22.5	4	6	5	15	-	8	1	1	-	-	-	0.1	0.4
11	37	22.5	4	6	5	15	-	8	1	1	-	-	0.5	-	-
12	37	22.5	4	6	5	15	-	8	1	1	-	-	0.1	-	0.4
13	37	22.5	4	6	5	15	-	8	1	1	-	-	0.125	0.125	0.25
14	37	22.5	4	6	5	15	-	8	1	1	-	-	0.25	0.125	0.125
15	37	22.5	4	6	5	15	-	8	-	1	-	1	0.25	0.125	0.125
16	37	22.75	4	6	5	15	-	8	-	1	-	1	0.125	0.063	0.063

*Diacethyl tartaric acid esters of monoglycerides (DATEM)
‡Twenty one formulations were done, however five had the same formulation than formulation number 14 differing in the mixing procedure

Table 5.6. Standardized formulation for the preparation of a model high whey protein cookie.

INGREDIENT	%
Protein*	**37**
Maltitol syrup	**22.5**
Polydextrose	**15**
Oil	**8**
Water	**6**
Maltitol powder	**5**
Sucrose	**4**
DATEM	**1**
Lecithin (from soybean oil)	**1**
Low-methoxyl (LM) pectin gum	**0.25**
Guar gum	**0.125**
Xanthan gum	**0.125**

*Either β-lactoglobulin, GMP, or β-lactoglobulin/GMP (1:3).

5.3.1.1. Moisture content and water activity (a_w)

The moisture content and the water activity (a_w) of the baked cookies are presented in Table 5.7. As noted in Table 5.6, the whey protein utilized in the "high whey protein cookie" formulation was either β-lactoglobulin, GMP, or β-lactoglobulin and GMP in a 1:3 ratio. The results in Table 5.7 show that the moisture content and the water activity (a_w) of the baked cookies were higher when GMP or β-lactoglobulin/GMP (1:3 ratio) was employed in place of β-lactoglobulin in the formulation. Given that the water content in the formulation was 6%, the moisture content values indicate that either the moisture was lost during baking or it could suggest that the water was tightly bound to the various hydrophilic constituents, mainly the carbohydrates. In support of this, the low water activity (a_w) values in Table 5.7 indicate that there was little free/unbound water in the baked cookies (Potter and Hotchkiss, 1998). All three cookie models had water activity (a_w) values of ≤0.55, which would inhibit microbial growth and allow for a longer shelf life (Potter and

Hotchkiss, 1998); in fact, after six months of storage at room temperature, the cookies did not present any evidence of microbial growth.

Table 5.7. Moisture content and water activity of baked model cookies formulated with β-lactoglobulin, GMP, or β-lactoglobulin/GMP (1:3)

Protein ingredient	Moisture content	Water activity (a_w)
β-lg	6.25±0.63	0.51±0.05
GMP	8.69±1.03	0.55±0.004
β-lg/GMP (1:3)	8.76±0.52	0.54±0.001

5.3.1.2. Texture analysis of the cookie model food system

The results of texture analysis tests conducted to evaluate the hardness and fracturability of the baked cookies are presented in Table 5.8. Higher values for hardness and fracturability were obtained when GMP or β-lactoglobulin/GMP (1:3 ratio) was employed in place of β-lactoglobulin in the formulation. These differences reflect the notable differences in texture among the baked model cookies: whereas the β-lactoglobulin cookie model had a crispy texture and was therefore easy to break, the other two cookie models had a rubbery texture that made them harder to break. The hardness value of the GMP cookie model was slightly higher than that of the β-lactoglobulin/GMP cookie model while the fracturability values were comparable.

Table 5.8. Texture analysis results for the baked model cookies

Protein ingredient	Cookie hardness (g-force)	Cookie fracturability (mm)
β-lg	240.49±45.41	7.49±0.329
GMP	2199.93±88.01	8.11±0.236
β-lg/GMP (1:3)	1911.67±24.92	8.28±0.94

As mentioned by Phan *et al*. (2008), many sensory properties of a food product, such as crispness, depend on the moisture content and water activity. As noted above and shown in Table 5.7, the GMP and β–lactoglobulin/GMP cookie models had very similar moisture content values,

which are reflected in their similar hardness and fracturability values, whereas the β-lactoglobulin cookie model had the lowest values of moisture content, which helped in conferring it the crispiness and ease of cracking. Both the GMP and the β–lactoglobulin/GMP cookie models had a "harder and rubbery" texture, which is attributable to having water activity values above the threshold (0.50) for a number of crisp snacks (Katz and Labuza, 1981; Labuza and Hyman, 1998), with the rubberiness being a consequence of the high protein content.

5.3.1.3. FPA-FTIR imaging of the spatial distribution of the ingredients in the model cookies

FPA-FTIR imaging of dough samples and baked model cookies and was performed in the attenuated total reflectance (ATR) mode using a germanium ATR crystal affixed to the IR microscope's objective. As discussed in Chapter 2 (Section 2.4.6), an advantage of imaging in the ATR mode is the short effective path length inherent to the ATR technique, which allows samples of any thickness to be imaged without sample preparation. An additional advantage is that higher spatial resolution can be attained in the ATR mode than in the transmission or transmission-reflection mode (Sedman *et al.*, 2010). For the optical configuration employed in the present work, the nominal spatial resolution (given by $0.61\lambda/n \sin\theta$, where n is the refractive index of germanium ($n = 4$) and $\theta = 50^{o}$) is 1.25 μm at 1600 cm^{-1} and 2 μm at 1000 cm^{-1}.

As described in Chapter 2, FPA-FTIR imaging data is displayed in the form of "chemical images" representing the value of a single spectral parameter (such as an absorbance value at a single wavenumber or an integrated intensity of a selected absorption band) in the spectrum associated with each of the pixels making up the image. The values of the spectral parameter are plotted on a color scale ranging from blue (lowest value) to red (highest value). In the present study, chemical images were generated in several ways to visualize the distribution of protein (β-lactoglobulin; cookies formulated with GMP were not imaged), lipid (sunflower oil), and carbohydrates (maltitol, polydextrose) in the dough and in different parts of the baked model cookies.

Figure 5.1 presents an illustrative example of a "chemical image" of a dough sample together with spectra corresponding to pixels in the red, green, and blue areas of the image. This

chemical image has been generated by measuring the maximum absorbance between 1790 and 1700 cm^{-1}, which is the spectral region in which the ester ν(C=O) absorption band of lipids (triglycerides and phospholipids) is observed, and mapping the values for all the pixels in the image to a color scale in the manner described above. Thus, the displayed spectrum from the red area of the image (Figure 5.1a) shows an intense absorption band in this region together with other strong bands in the CH stretching region (3050-2800 cm^{-1}), also characteristic of lipids. In the case of the spectrum representing the blue area of the image (Figure 5.1c), these absorption bands are very weak while absorption bands characteristic of proteins (amide I and II bands at ~1640 and 1540 cm^{-1}, respectively), carbohydrates (below 1200 cm^{-1}), and water (broad band centered at ~3285 cm^{-1}) are prominent. Accordingly, the chemical image in Figure 5.1 shows that the imaged area of the dough sample contains a lipid phase within a protein-carbohydrate matrix. Furthermore, based on the number of pixels constituting the red portion of the image and a spatial resolution at 1750 cm^{-1} at ~1.14 μm, this undispersed lipid covers an area of approximately 25 × 50 μm^2. The size of this lipid "droplet" in the third dimension cannot be estimated owing to the very short effective pathlength of the ATR measurement (<1 μm). This lipid droplet is seen to be surrounded by an interfacial area (green "halo" in Figure 5.1), ~2-3 μm thick, in which protein and carbohydrate as well as lipid absorption bands are observed (Figure 5.1b). Similar results were obtained for several dough samples whereas some images of other dough samples were devoid of any lipid absorptions, indicating that the lipid distribution in the dough was heterogeneous on a scale exceeding the dimensions of the field of view of the IR microscope (on the order of 100 μm).

For the imaging of baked samples, pieces were cut from the top surface, edges, bottom, and center of cookies and imaged to ascertain whether any differences in microstructure could be discerned. In order to compare images acquired from these four pieces of several cookies, a standardized image processing protocol had to be developed for several reasons. First, the color display in a chemical image such as that in Figure 5.1 is set in the image processing software by mapping the values of the measured parameter to colors in such a manner as to span the red-blue color spectrum. While this maximizes image contrast, it does not allow for direct comparison of chemical images from one sample to another. In addition, these images are subject to artifacts due to, for example, variations in sample thickness, signal-to-noise ratio, and baseline tilt. These limitations were addressed in the present study by devising a standardized data processing

procedure within the in-house FPA-FTIR image processing software. The latter provided various pixel filtration, data transformation, and data display options, and these were systematically explored with the FPA-FTIR images acquired from four parts of three baked cookies (bottom, edge, center, and top surface). The protocol that was developed in this manner and the considerations and criteria on which it was based are described below.

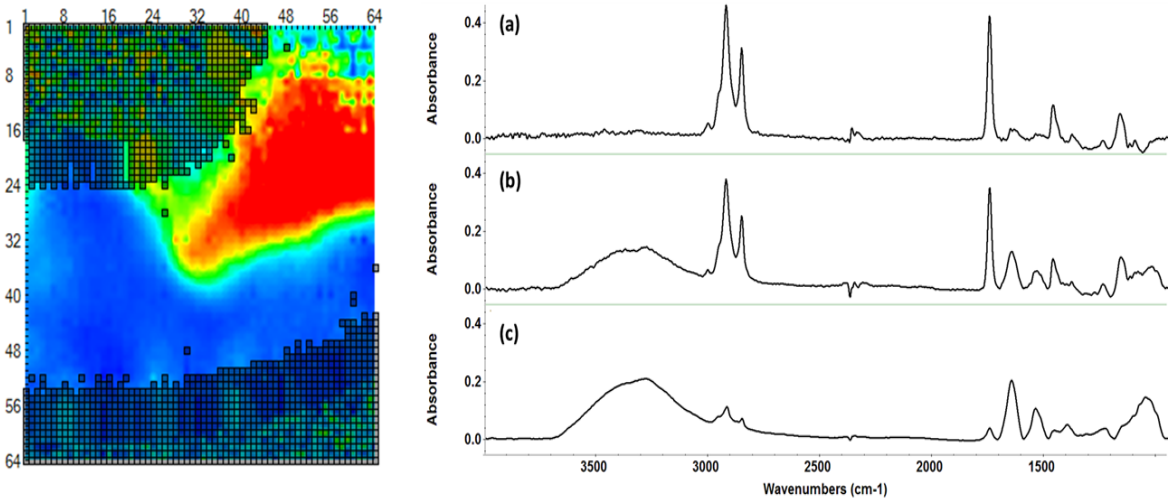

Figure 5.1. Left: "Chemical image" of a dough sample illustrating the distribution of lipid generated by mapping the maximum absorbance between 1800 and 1700 cm^{-1} to a red-blue color scale; right: spectra corresponding to pixels in the (a) red, (b) green, and (c) blue areas of the image. The shaded pixels were rejected as "noisy" pixels (see discussion of Figure 5.2 below).

Step 1. Elimination of "noisy" pixels. In the first step of the image processing routine, a noise filter based on the root-mean-square (rms) noise, measured over a narrow spectral range in which samples would not exhibit any absorption bands, was applied to exclude several types of "noisy" pixels. First, owing to the use of aperturing to define the sampling area within the IR microscope's field of view, pixels in the upper left-hand corner and the bottom rows within each image yielded spectra consisting only of very high levels of noise. Second, some pixels consistently yielded spectra having a poor signal-to-noise ratio. It was established that setting the noise filter with a cut-off of 0.0035 (rms noise) across the range of 1900-900 cm^{-1} was effective in excluding "noisy" pixels (Figure 5.2). This filter excluded approximately 1950 of the 4096 pixels

from each of the 12 images examined, such that the number of pixels remaining following this pixel filtration step was 2272±22 (mean ± standard deviation, computed for 12 images).

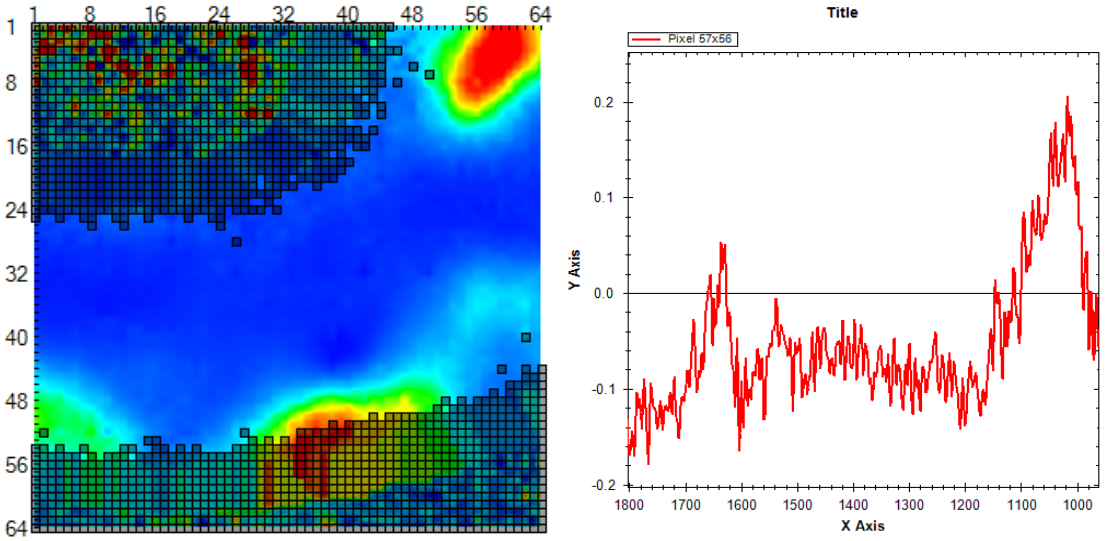

Figure 5.2. Typical image illustrating the results of applying the noise filter. The shaded pixels are those filtered out because the rms spectral noise measured across the range of 1900-900 cm^{-1} exceeded the noise filter cut-off of 0.0035 The spectrum at the right illustrates the high level of noise typical of the filtered-out pixels.

It may be noted that the image processing software also provided the option of pixel filtering based on a maximum absorbance criterion to exclude spectra from samples or portions thereof that are too highly absorbing. However, with the ATR mode of imaging employed in the present study, absorbance values did not exceed 0.5 absorbance units owing to the short effective pathlength associated with the ATR sampling technique and hence no additional pixel filtering beyond that based on rms noise was performed.

Step 2. Baseline correction. A multi-point baseline correction was performed before spectral normalization (Step 3), as recommended by Afseth *et al.* (2006). The baseline anchor points selected were 1800, 1700, 1490, 1200, and 960 cm^{-1}.

Step 3. Spectral normalization. Spectral normalization on a pixel-by-pixel basis provides a means of compensating for variations in sample thickness across the imaged area. The intensities of bands in FTIR spectra acquired with the ATR sampling technique also depend on a number of

other sample-dependent factors, including the sample's refractive index, which affects the depth of penetration of the evanescent wave, and the optical contact between the sample and the IRE. In ATR-FTIR imaging, any variations of these factors between pixels within an image or between different images can be a source of artifacts, but these variations are compensated for when spectral normalization is performed.

Several spectral normalization options are included in the image processing software employed in the present study. Normalization based on the peak height or area of a specified absorption band was not suitable for this study because of the large variability in the relative proportions of all the components present in the samples, as illustrated by the spectra presented in Figure 5.1. Accordingly, total intensity normalization based on vector normalization was the option selected. In vector normalization, spectral data are represented as vectors in an *n*-dimensional data space (where *n* is the number of spectral data points) and converted to vectors of unit magnitude by squaring the intensity values at each data point, summing the squared values, and then dividing each intensity value by the square root of the sum of the squares, Normalization of the spectra maintains the relative band intensities and hence the qualitative information contained within an image as well as quantitative information determined by ratioing the intensities of two bands, while quantitative information based on absolute band intensities is lost. For the purposes of the present study, the latter type of information was not relevant, and hence the use of spectral normalization did not introduce any limitations.

Step 4. Generation of chemical images with predefined display limits (colors). As noted above, chemical images are pseudo-color representations generated by mapping of specific intensity measurements (e.g., peak height or area) to a red-blue color scale. Figure 5.3 presents spectra extracted from the images of baked cookies that were selected by visual pixel-by-pixel examination as representative of areas rich in lipid, protein, and carbohydrate, respectively, although all these spectra contain contributions from more than one of this components. These spectra were employed to select the parameters for construction of chemical images that would best represent the distribution of these components based on the following considerations.

Lipid distribution (Figure 5.3a), The maximum absorbance between 1800 and 1700 cm^{-1}, measured relative to a baseline drawn between these end points, was selected owing to the strong and fairly narrow lipid absorption band centered at ~1745 cm^{-1} [the ester ν(C=O) absorption band] as well as the lack of protein and carbohydrate absorption in this spectral range.

Protein distribution (Figure 5.3b). Measurements of the maximum absorbance in the amide I region (1700-1600 cm^{-1}), the maximum absorbance in the amide II region (1590-1490 cm^{-1}), and the combined band areas of the amide I and amide II bands (1700-1490 cm^{-1}) were considered. The amide I region contains a broad absorption band of water (H-O-H bending vibration) but this interference was not considered to necessarily preclude the use of the amide I band, given the low levels of water in both unbaked and baked cookie samples (Section 5.3.1.1). There is much less spectral interference in the amide II region but signal-to-noise limitations were apparent owing to the lower intensity of the amide II band. Measurement of the total band area between 1700 and 1490 cm^{-1} provided optimal signal-to-noise ratio, and the contribution of water absorption to this measurement would be less (on a percentage basis) than its contribution to the amide I absorbance. Accordingly, this band area was the measure selected for visualization of protein distribution.

*Carbohydrate distribution (Figure 5.3*c*)*. The area between 1200 and 960 cm^{-1} (where the lower limit is dictated by the low-wavenumber cut-off of the FPA detector) was initially considered for the visualization of carbohydrate distribution. However, as seen in Figure 5.3a, lipid absorptions are also observed in this region. Consequently, the measure of carbohydrates was restricted to the narrower range of 1040-960 cm^{-1} so as to minimize the contributions of lipid absorptions, and the measurement of maximum absorbance in this range as opposed to integrated area was selected to minimize the potential contributions of baseline tilt and noise near the detector cut-off.

In principle, carbohydrate distribution could be better visualized by plotting the ratio of the maximum absorbance in the 1040-960 cm^{-1} region to the maximum absorbance in the 1800-1700 cm^{-1} region (which is due exclusively to lipids), thereby effectively ratioing out the lipid contributions in the 1040-960 cm^{-1} region. Although this procedure is not workable in practice, because the denominator in the ratio approaches zero in spectra from areas of the image that are devoid of lipid, the inverse of this ratio can be plotted to produce a chemical image of lipid/carbohydrate ratio, as shown in Figure 5.4. The colors in such an image could be inverted to obtain an image of carbohydrate distribution that would not be distorted in regions devoid of lipid.

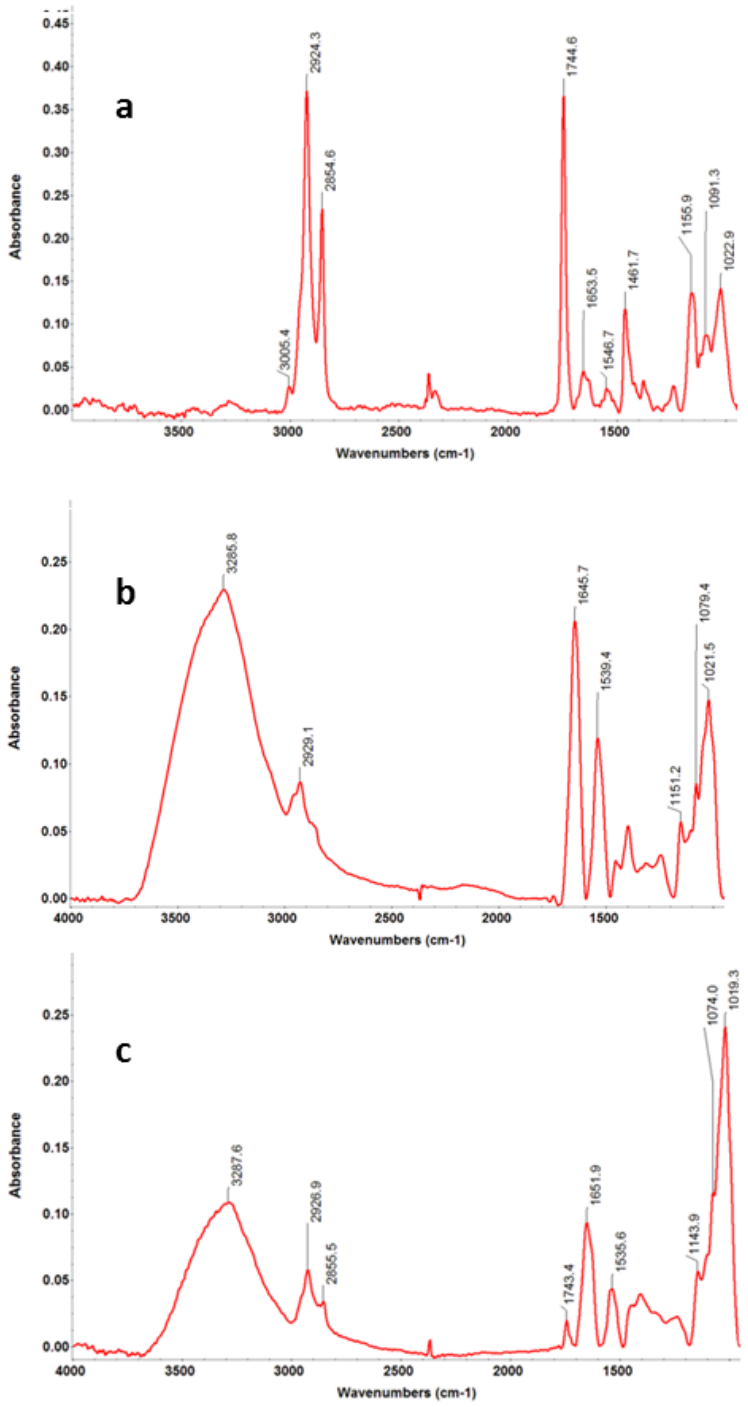

Figure 5.3. Spectra extracted from the images of baked cookies selected as representative of areas rich in lipid (a), protein (b), and carbohydrate (c).

As previously mentioned, direct comparison of chemical images from one sample to another requires that the color display be based on fixed upper (red) and lower (blue) limits of the measurement parameter in question. Judicious setting of these limits is required to maximize the information content of chemical images generated in this manner. In the present study, the limits for each of the measurement parameters, listed in Table 5.9, were established in the following manner. Images acquired from four parts of three baked cookies (the bottom, edge, center, and top surface) were pre-processed in accordance with steps 1-3 described above. For each of these 12 images, the values of each measurement parameter were determined at each pixel (with the exception of those eliminated by pixel filtration in step 1) and plotted in the form of histograms to reduce the size of the data files, typically from approximately 2200 pixels in the image to 60 bins in the histogram. The mean value (μ) and the standard deviation around the mean (σ) of the histogram data were then computed using the formulas for grouped data. For each measurement parameter, the values of $\mu \pm 2\sigma$ obtained in this manner from each of the 12 images were tabulated, and the highest of the $\mu + 2\sigma$ values was set as the upper limit to be used in generating the corresponding chemical image; the lower limit was set to the lowest of the $\mu - 2\sigma$ values but was defaulted to 0 if the latter value was negative (Table 5.9).

.

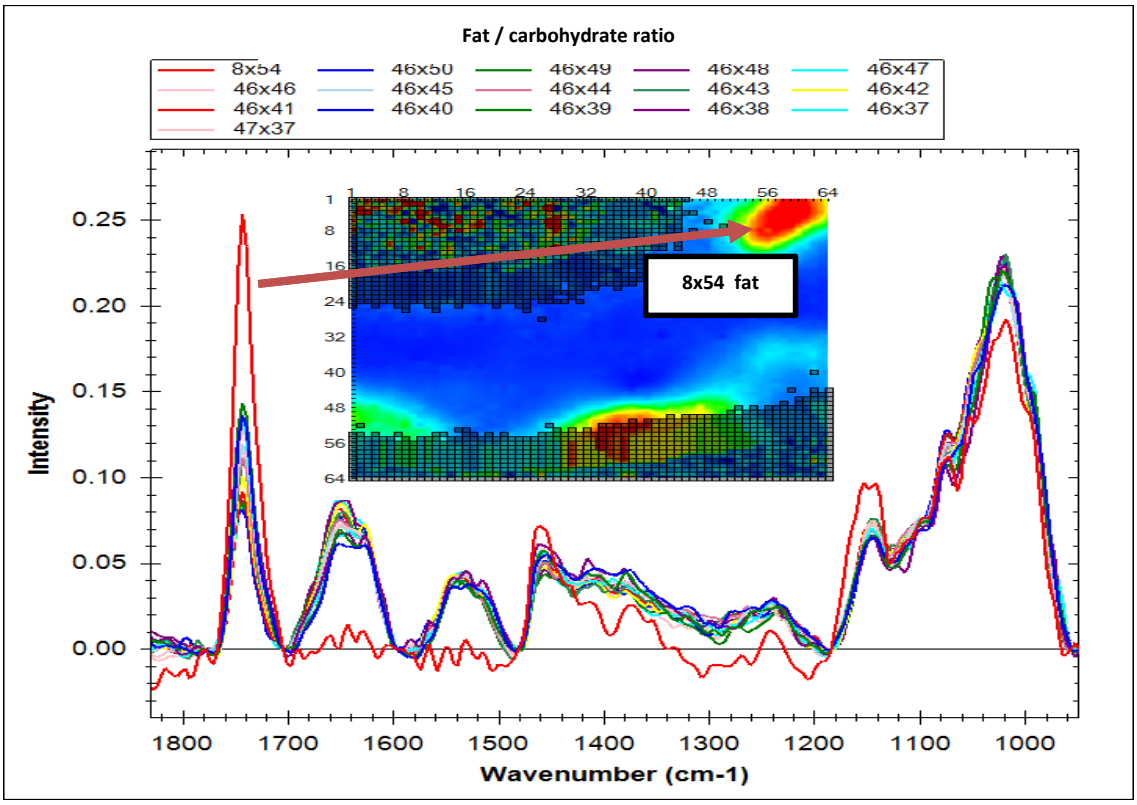

Figure 5.4. "Chemical image" depicting the lipid/carbohydrate ratio at each pixel in the image of a baked cookie sample together with spectra from selected pixels in the image. The spectrum in red corresponds to a pixel in the red portion of the image and represents a fat globule. The remaining spectra correspond to pixels in the blue and green portions of the image and contain absorption bands due to lipids, carbohydrates, and proteins. The intensity of absorption in the 1040-960 cm^{-1} range increases as the lipid absorption band in the 1800-1700 cm^{-1} region decreases owing to the strong carbohydrate absorption in this range.

Table 5.9. Spectral measurements and color-mapping specifications employed to generate chemical images

Component	Spectral region (cm^{-1})	Measurement[a]	Values mapped to red	Values mapped to blue
Lipids	1800-1700	Maximum absorbance	≥0.36	0
Proteins	1700-1490	Area	≥23.8	≤3.5
Carbohydrates	1040-960	Maximum absorbance	≥0.25	≤0.10

[a]Each measurement was made relative to a baseline drawn between the upper and lower wavenumbers of the spectral region.

Illustrative chemical images generated by the standardized protocol described above to examine the spatial distribution of lipid, protein, and carbohydrate in a baked model cookie are presented in Figures 5.5, 5.6, and 5.7, respectively. The four panels in each figure are images of four parts of the cookie: the top surface, the edge, the bottom, and the interior.

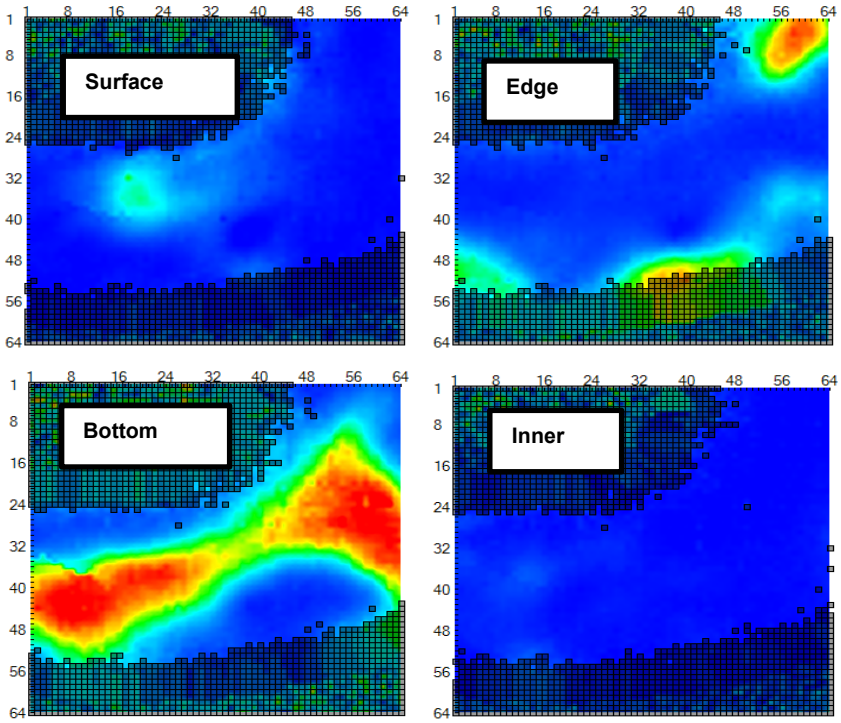

Figure 5.5. ATR-FPA-FTIR chemical image showing the lipid distribution in four parts of a baked model cookie. The parameters used to plot the chemical image are given in Table 5.9.

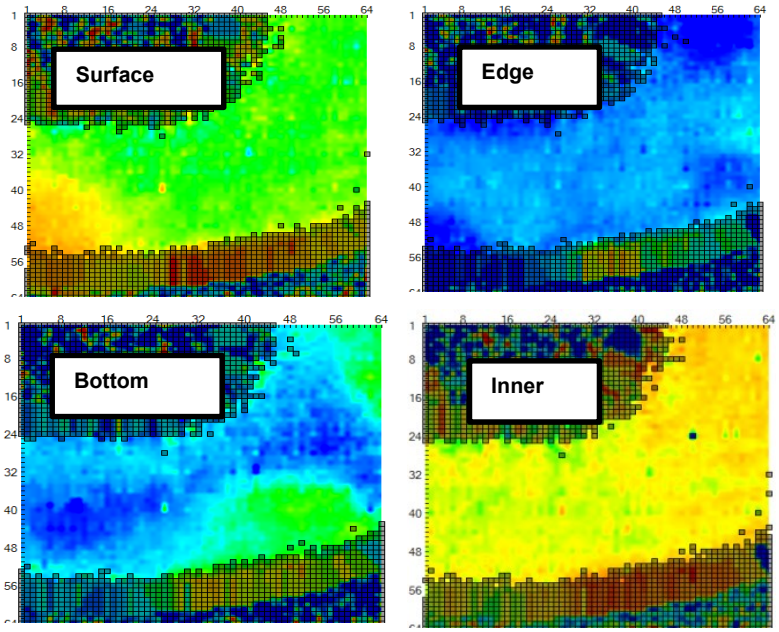

Figure 5.6. ATR-FPA-FTIR chemical image showing the protein distribution in four parts of a baked model cookie. The parameters used to plot the chemical image are given in Table 5.9.

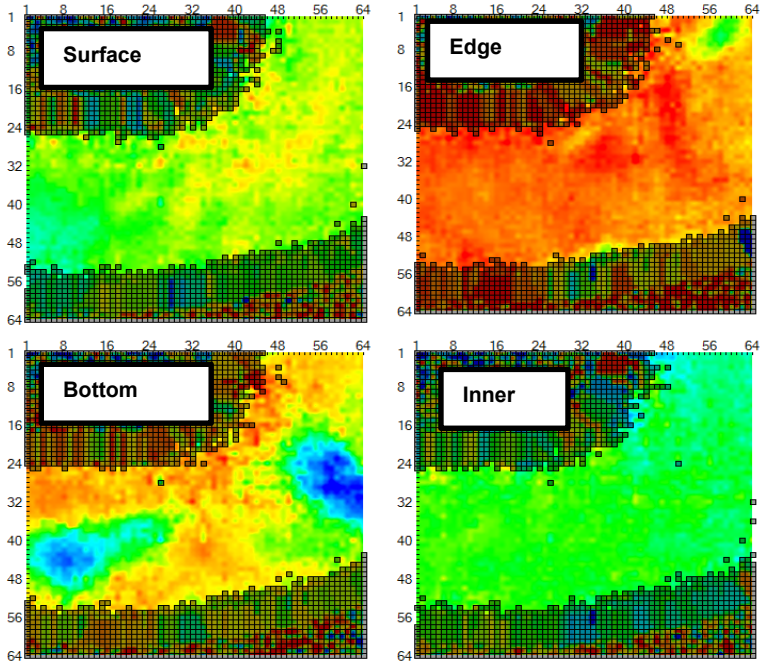

Figure 5.7. ATR-FPA-FTIR chemical image showing the carbohydrate distribution in four parts of a baked model cookie. The parameters used to plot the chemical image are given in Table 5.9.

5.3.1.4. Distribution of the ingredients in a model food system using variable- pressure scanning electron microscopy (VP-SEM)

Variable-pressure scanning electron microscopy (VP-SEM) has been considered by previous authors as an extremely useful technique to characterize the surface of food products in a three-dimensional way. This technique has proven useful to examine the microstructure of products with high moisture content without sample preparation, hence, no sample destruction and/or alteration. Therefore, this technique has been applied in the study of baked products (James, 2009; Zounis *et al.,* 2002) and was applied in the present study of the β–lactoglobulin cookie model system.

VP-SEM micrographs of baked model cookies at three different magnifications (60×, 200×, and 250×) are presented in Figure 5.8. These micrographs show a compact structure and an even and indistinctive distribution of all the components. The small "holes" in the image are small gas voids and the "glued" indistinctive distribution of the components may be the gum "coating/film" "wrapping" the mixture. The presence of small gas voids indicates the incorporation of air bubbles in a homogeneous way into doughs during the mixing stage (Ribotta *et al.*, 2004; Whitehurst, 2004). Most of the carbohydrates used in the formulation of the cookie model system can form films that could be contributing to the "coating" of the whole structure.

Boye *et al.* (1997) studied the microstructure of β–lactoglobulin using SEM and TEM at different pH levels and under heating conditions. Their results showed the globular structures formed by β–lactoglobulin in pure state. Wang and Qvist (2000) studied the interactions of pectin with β–lactoglobulin at different pH values and Dumay *et al*. (1999) studied the interactions between pectin and β–lactoglobulin under heating and pressure conditions; both research groups used scanning electron microscopy in combination with other techniques. Wang and Qvist (2000) showed that the interactions of pectin with β–lactoglobulin are mainly of electrostatic nature and that above the protein´s isoelectric point there is repulsion between them due to the high negative charges they both carry. Wang and Qvist (2000) concluded that because β–lactoglobulin has a globular compact structure it does not contribute significantly to viscosity and that pectins have smaller molecular weight than galactomannans, such as guar, hence they are less efficient in terms of space occupancy.

Dumay *et al*. (1999) demonstrated that the microstructure of β–lactoglobulin/pectin gels under heat treatment is shaped as an alveolar pectin structure with small pillars and small pores, similar to a "honeycomb", and the protein is located inside the pores; they observed that in heat induced gels of β–lactoglobulin/pectin, at neutral pH, large clusters of β–lactoglobulin and higher protein microparticulation were formed when increasing the polysaccharide concentration; they presumed this occurred due to the increase of the negative charges and they concluded that the polysaccharide concentration could be used to control the rate of protein aggregation and/or for microencapsulation purposes. Zasypkin *et al.* (1996) studied β–lactoglobulin/xanthan gum interactions using SEM under heating and pressure treatments and they showed that the microstructure of the β–lactoglobulin/xanthan gum complexes was in the shape of large "spherical-like" aggregates and they concluded that mixing xanthan gum with β–lactoglobulin prevents the interaction of protein aggregates probably by weakening the interactions between β–lactoglobulin aggregates.

Previous studies by Brennan *et al.* (1996) of guar gum using scanning electron microscopy, light microscopy and fluorescence microscopy showed that guar gum acts as a "physical barrier" in bread by "gluing" the overall structure with a mucilage coating. Chaisawang and Suphantharika (2006) reported similar results of tapioca starch granules interaction with xanthan and guar using scanning electron microscopy, viscosity analysis and differential scanning calorimetry; in which they found that xanthan gum acts as a "tight wrapping agent" of the granules and they proposed that the gums are in the continuous phase and they can reinforce the three-dimensional network structure.

Based on the micrographs in Figure 5.8 and the results obtained in the studies mentioned above, we assume that guar gum had a more predominant effect on the microstructure based on the mucilage "coat" observed, although it remains uncertain because most of the carbohydrates used in the formulation of the cookie model system can form films that could be contributing to the "coating" of the whole structure. Further studies should be done using complementary techniques in order to confirm these results, such as confocal laser scanning microscopy.

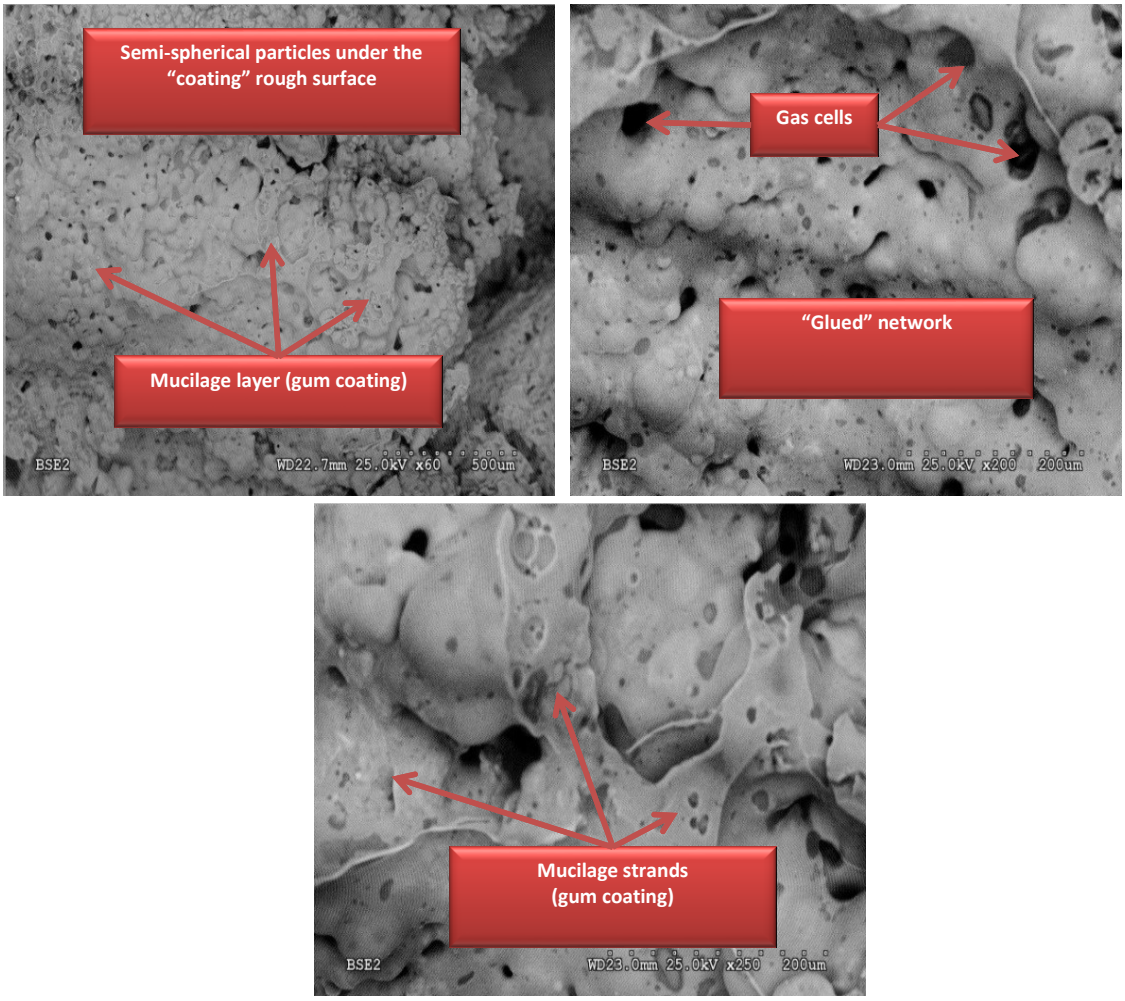

Figure 5.8. Variable-pressure scanning electron microscopy micrographs of baked model cookies at different magnifications: upper left, 60×; upper right, 200×; bottom, 250×. The dotted lines indicate the scale bar in µm.

5.3.1.5. Examination of the stability of the native structure of β-lactoglobulin (AB, food grade) in the presence of carbohydrates, fats, GMP and emulsifiers before and after heating (baking conditions) by FPA-FTIR spectroscopy

Binary mixtures of β-lactoglobulin and each of the other components of the model food system were prepared in D_2O at the concentrations used in the "high whey protein cookie" formulation on a w/w basis (Table 5.2), and each mixture was studied as a thin film deposited on an IR-transparent window (ZnSe), as shown in Figure 5.9. FTIR images of each sample were recorded before and after heating. Processing of the spectra contained within each image as described in Section 5.2.6 indicated that the deposited films were homogeneous on the micron

scale (the diffraction-limited spatial resolution of the FTIR images being on the order of 6 μm). Accordingly, the spectra within each image were averaged to obtain the optimal signal-to-noise ratio.

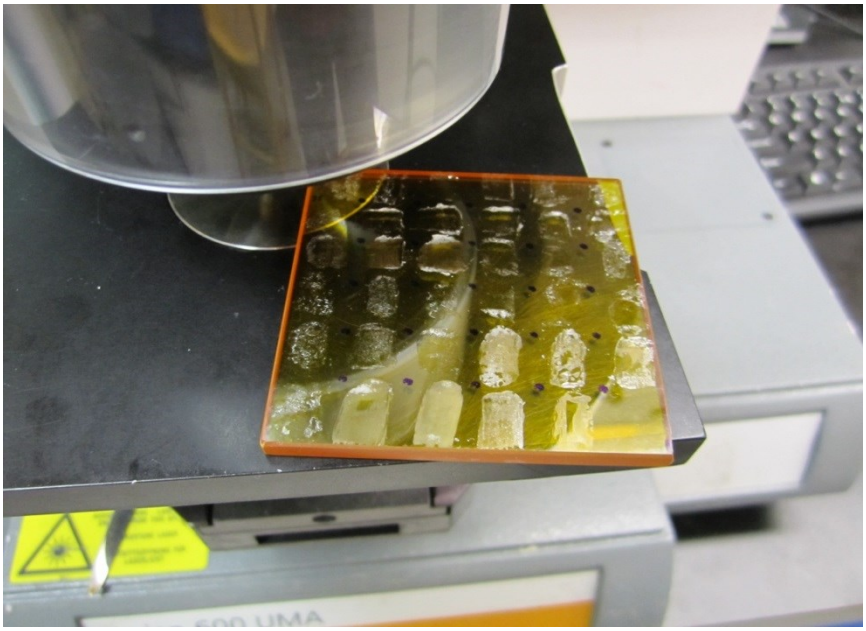

Figure 5.9. Films deposited on a ZnSe crystal under the FPA-FTIR microscope.

Figure 5.10 shows the Fourier self-deconvolved amide I' band in the FTIR spectra of the β-lactoglobulin film before and after heating. It may be noted that these film spectra of the food-grade β-lactoglobulin AB (Davisco) employed in the model food system look quite different from the room-temperature spectrum of the same protein in D_2O solutions. In particular, the amide I' band in the spectra of both the unheated and heated films is dominated by a single intense component at 1628/1636 cm^{-1} whereas the solution spectrum showed two distinct bands at 1634 and 1627 cm^{-1}. This difference was attributed to the high protein concentration (37%) of the solution from which the film was deposited Figure 5.10 also shows that heating of the β-lactoglobulin film resulted in the disappearance of the amide I' band component at 1692 cm^{-1} as well as small peak shifts; as discussed in Chapter 3, a decrease in intensity at 1692 cm^{-1} upon heating of a D_2O solution of β-lactoglobulin has been attributed to H-D exchange of β-sheets that

are buried within the hydrophobic core of the protein and is indicative of disruption of tertiary structure (Boye *et al.*, 1996). It is of interest to note that no evidence of protein aggregation is observed in the spectrum of the heated film; the most likely explanation is that water evaporation occurs faster than aggregation during heating of the films.

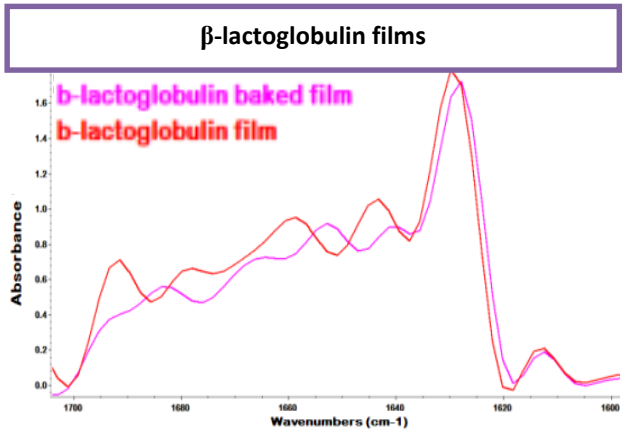

Figure 5.10. Fourier self-deconvolved amide I' band in the FTIR spectra of a β-lactoglobulin film recorded before and after heating.

β-Lactoglobulin/sunflower oil mixture. The first binary mixture examined consisted of β-lactoglobulin and sunflower oil in the same ratio as in the cookie model system (37% protein: 8% sunflower oil) deposited as a film. As shown in Figure 5.11, there were only small and almost imperceptible shifts of the peaks in the amide I' band of β-lactoglobulin upon heating the film. In the case of this film, in contrast to the β-lactoglobulin film, the 1692 cm^{-1} band indicative of a lack of H-D exchange in β-sheets within the hydrophobic core of the protein was not lost upon heating, indicating that the tertiary structure of the protein was stabilized by interaction with the oil.

Evidence from previous studies has demonstrated that β-lactoglobulin can carry hydrophobic molecules such as fatty acids in its core (Yalçin *et al*., 2006), and previous studies by Cornell and Patterson (1989) indicated that the protein conformation did not change significantly in the presence of the lipid while Nylander (2004) reported that protein-protein interactions are disrupted at the lipid-protein interface.

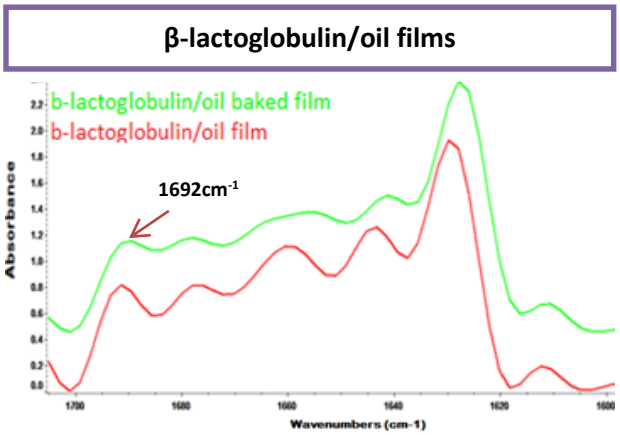

Figure 5.11. Fourier self-deconvolved amide I' band in the FTIR spectra of the β-lactoglobulin/sunflower oil mixture deposited as a film, recorded before and after heating. In both cases the spectrum of the oil has been subtracted from the spectra.

β-Lactoglobulin/lecithin mixture. The film spectra obtained for a 37:1 (w/w) β-lactoglobulin/lecithin mixture, corresponding to the ratio of these ingredients in the cookie model system, are presented in Figure 5.12. These spectra show obvious changes in the amide I band of β-lactoglobulin upon heating of the film. It may be noted that the 1630 cm^{-1} band remains present in the spectrum recorded after heating, indicating that the β-sheet structure was largely retained. Hence, the loss of most of the peaks in the amide I band most probably results from H-D exchange and/or moisture loss of the protein, in the presence of lecithin (soybean oil lecithin).

As is well known, lecithins are obtained mainly from soybean oil (egg yolk lecithin is much more expensive) and are a mixture of different phospholipids (Dalgleish, 2004). Studies by Cornell and Patterson (1989) of the interaction of phospholipids with β-lactoglobulin using CD and UV spectroscopy showed that the protein structure did not change significantly in the presence of the phospholipids. However, the phospholipids studied were obtained in a pure state while lecithin is a mixture of phospholipids and often contains impurities (Dalgueish, 2004). In addition, the oxidation of unsaturated fatty acid chains may give rise to oxidation products that could react with lysine or arginine residues of the protein (Dalgueish, 2004). β–Lactoglobulin has at least seven exposed lysine residues (Lys 1, Lys 32, Lys 39, Lys 46, Lys 54, Lys 57, Lys 58) and one exposed arginine residue (Arg 40) and several more hidden lysine residues in its core (Lys 95, Lys 103,

Lys 104, Lys 122, Lys 140) that could react with the lecithin once the film was heated, resulting in partial unfolding of the protein. Further studies by other techniques would be required to ascertain whether or not any specific residue is reacting with lecithin.

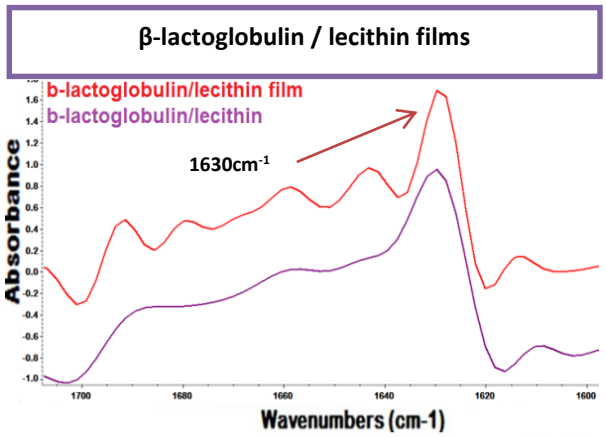

Figure 5.12. Fourier self-deconvolved amide I' band in the FTIR spectra of the β-lactoglobulin/lecithin mixture deposited as a film, recorded before (red) and after heating (purple). In both cases the spectrum of lecithin has been subtracted from the spectra.

β-Lactoglobulin/DATEM mixture. Diacetyl tartaric acid esters of monoglyceride (DATEM) was employed as an emulsifier in the cookie model system at a level of 1%. Accordingly, the film spectra obtained for a 37:1 (w/w) β-lactoglobulin/DATEM mixture are presented in Figure 5.13. The spectrum recorded before heating lacks well-defined peaks other than that at 1630 cm^{-1}, while the spectrum was unchanged upon heating.

It is known that DATEM is an anionic, very hydrophilic and surface-active emulsifier that is only partially soluble in fats and that it interacts very strongly with starch and wheat proteins, reducing their water absorption, increases the starch gelatinization temperature, forms hydrogen bonds with the amide groups of the proteins, and prevents protein denaturation. DATEM molecules interact with starch by "inserting" their hydrophobic part inside the hydrophobic core of the helical structure of amylose, leaving their hydrophilic part to interact with the hydrophilic surface. In the case of proteins, it has also been shown that DATEM can interact with non-charged polar residues, including serine, threonine, cysteine, tyrosine, asparagine, and glutamine (Krog and Sparsø, 2004; Whitehurst, 2004). Accordingly, there are several possibilities of how DATEM

interacts with β-lactoglobulin: [1] the hydrophilic portion of DATEM interacts with the hydrophilic residues on the protein´s surface either by electrostatic repulsion with the acidic residues (Asp, Glu) or by electrostatic attraction (Lys, Arg, His); [2] the hydrophobic portion of DATEM enters the hydrophobic cavity of β-lactoglobulin and forms hydrogen bonds with the non-charged polar residues (Tyr 102, Gln 120, Cys 121, Thr 125, Asn 152). However, DATEM is more hydrophilic, more surface active and a much smaller molecule than β-lactoglobulin; this and the small amount of moisture in the film could translate into lower moisture absorption by β-lactoglobulin, which under these circumstances could be the most likely explanation for the lack of well-defined peaks in the amide I' band.

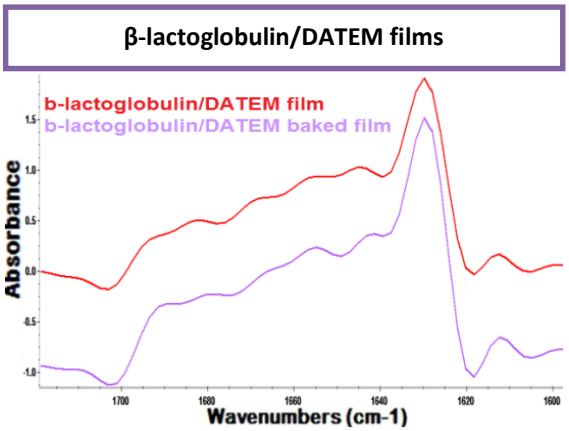

Figure 5.13. Fourier self-deconvolved amide I' band in the FTIR spectra of the β-lactoglobulin/DATEM mixture deposited as a film, recorded before and after heating. In both cases the spectrum of DATEM has been subtracted from the spectra.

β-Lactoglobulin/sucrose mixture. The film spectra obtained for a 37:4 (w/w) β-lactoglobulin/sucrose mixture, corresponding to the ratio of these ingredients in the cookie model system, are presented in Figure 5.14, Comparison of these spectra indicates that heating of the film resulted in broadening of the 1630 cm^{-1} band assigned to β–structures together with shifts of the 1692-cm^{-1} component and other peaks to lower wavenumbers. This again could mean that the 1630 cm^{-1} band corresponds to mixed populations of β–sheets and the changes are due to H-D exchange. In a previous FTIR study, Boye *et al*. (1996) reported that sucrose at a concentration of 10% enhanced the thermal stability of β-lactoglobulin, as revealed by an increase in the transition

temperature measured by differential scanning calorimetry from 55ºC to 75.5 ºC, and also inhibited aggregation of the protein. These authors also noted that all disaccharides are not equally effective in inhibiting aggregation of β-lactoglobulin.

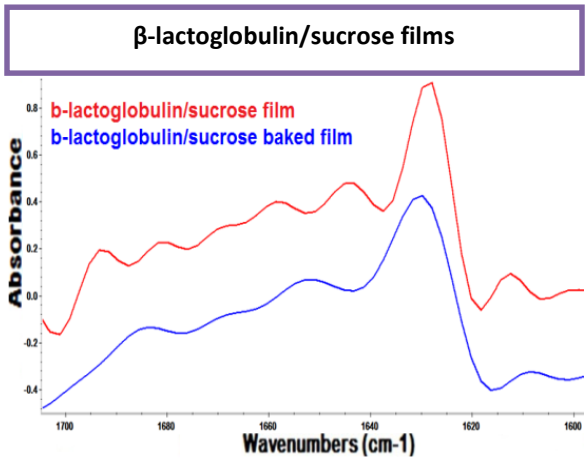

Figure 5.14. Fourier self-deconvolved amide I' band in the FTIR spectra of the β-lactoglobulin/sucrose mixture deposited as a film, recorded before and after heating. In both cases the spectrum of sucrose has been subtracted from the spectra.

β-Lactoglobulin/maltitol mixture. The film spectra obtained for a 1.65:1 (w/w) β-lactoglobulin/maltitol syrup mixture, corresponding to the ratio of these ingredients in the cookie model system, are presented in Figure 5.15. Among the non-protein ingredients in the model system, maltitol syrup had by far the highest concentration on a weight basis. As shown in Figure 5.15, heating resulted in only small shifts in the peaks observed in the amide I' band, and the α–helical and β–sheet structures appear to remain stable. Accordingly, these spectra indicate that the maltitol syrup enhanced the thermal stability of the protein.

Polyols, including maltitol, have the ability to increase the viscosity of a solution and stabilize emulsions by decreasing the collision frequency of the droplets of the dispersed phase. In addition, they increase repulsive colloidal interactions among droplets and reduce internal hydrogen bonding while increasing intermolecular spacing. As a result, polyols can change the conformational stability of globular proteins (McHugh *et al*., 1994; McHugh and Krochta, 1994). As reported by Timasheff (1998), when the interaction between proteins and other ligands such as polyols is weak and nonspecific, these ligands should be used in high concentrations (5-60%) in

order to stabilize the protein. Hence, in the present work we can infer that even though the interactions between maltitol and β–lactoglobulin may be weak and nonspecific, the high concentration of maltitol prevents β–lactoglobulin from unfolding.

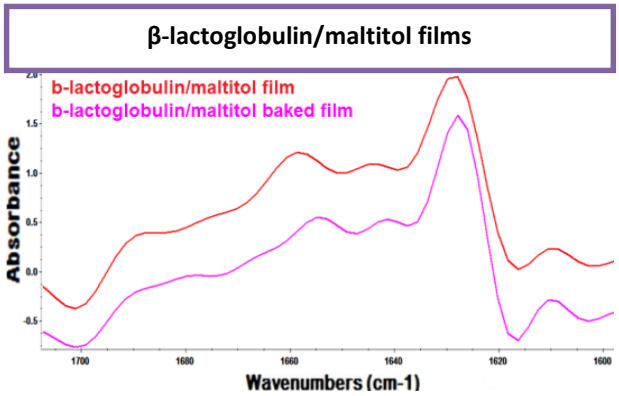

Figure 5.15. Fourier self-deconvolved amide I' band in the FTIR spectra of the β-lactoglobulin/maltitol syrup mixture deposited as a film, recorded before and after heating. In both cases the spectrum of the maltitol syrup has been subtracted from the spectra.

β-Lactoglobulin/polydextrose mixture. The film spectra obtained for a 2.5:1 (w/w) β-lactoglobulin/polydextrose mixture, corresponding to the ratio of these ingredients in the cookie model system, are presented in Figure 5.16. Comparison of these spectra reveals minor changes in the peaks within the amide I' band upon heating of the film. This could also be due to a fast evaporation of D_2O before any denaturation could be possible and the broad peak in the region of 1621-1637cm^{-1} could represent mixed populations of β–sheets.

Polydextrose is basically a randomly linked and highly branched polysaccharide of glucose, sorbitol and citric acid (89:10:1); sorbitol is used in the glucose polymerization reaction with the purpose of giving it plasticity and the citric acid is used as a catalyst; given its low caloric value (1kcal/g) and its physiological effects in human beings, it has been classified as a resistant oligosaccharide; this polysaccharide was created in the mid-1970s by Pfizer Laboratories (Mitchell, 1996; Craig *et al*., 2000). While sucrose is known to bind water molecules easily and confer viscosity, according to previous studies polydextrose can "pick-up" moisture easier and gives a much higher viscosity than sucrose and polyols (Mitchell, 1996). Polydextrose is highly used in the food industry as a sugar replacement because it can give the same textural properties

that sugar does (Mitchell, 1996). Hence, besides the fast evaporation, the high concentration of polydextrose could also prevent β–lactoglobulin from absorbing moisture.

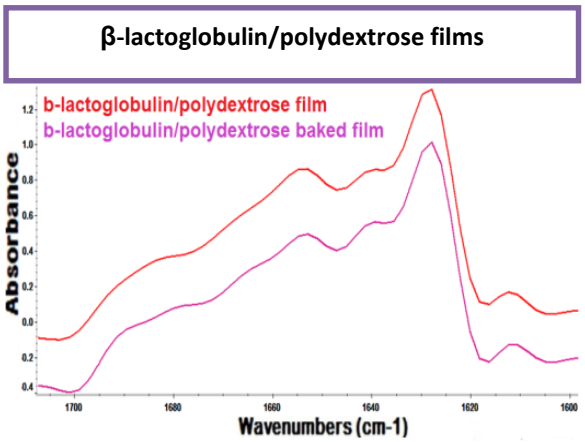

Figure 5.16. Fourier self-deconvolved amide I' band in the FTIR spectra of the β-lactoglobulin/polydextrose mixture deposited as a film, recorded before and after heating. In both cases the spectrum of polydextrose has been subtracted from the spectra.

β-lactoglobulin/gums mixture. The protein/gum mixtures were prepared by employing the same ratios of the components as in the cookie model system. As shown in Figure 5.17; heating resulted in minor changes in β-lactoglobulin's amide I' band, and the 1621-1637 cm^{-1} region remained practically unchanged. As mentioned by Benichou *et al*. (2002), electrostatic complexation between proteins and polysaccharides can improve the thermal stability and increase resistance to food processing treatments. Pectin (negatively charged, random coil in solution, water soluble) and guar gum (neutral charge, random coil in solution, water soluble) are both plant polysaccharides while xanthan gum is a gum of microbial origin (negatively charged; helical structure, water soluble, thermally stable); the three of them are used in the food industry, particularly in the baking industry, for different purposes such as water binding, desirable texture and improvement of shelf life; usually, their concentration does not exceed 1% of the total weight of the formulation (Izydorczyk *et al*., 2005). It has been shown that a synergistic effect is obtained when mixing guar gum with xanthan gum in a 1:1 ratio and the maximum synergism is achieved when heated at 90ºC; being suitable for its application in the baked goods sector (Izydorczyk *et al*., 2005; Sumnu *et al*., 2010; Ozkoc *et al.*; 2009). In the studies of Sumnu *et al*., (2010), Ozkoc *et al.* (2009), and Rosell *et al*. (2007), it was shown that usually when using only one type of gum

there can be negative effects during shelf life while a combination of different types of gums can achieve a favorable/synergistic effect.

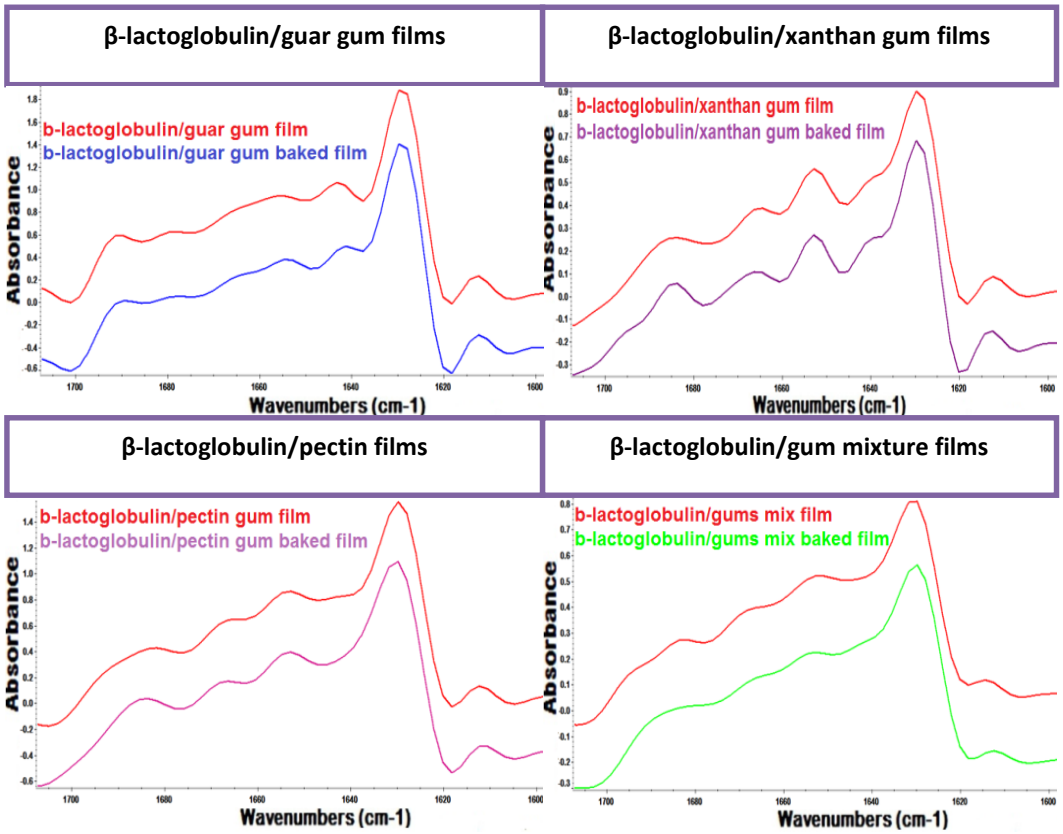

Figure 5.17. Fourier self-deconvolved amide I' band in the FTIR spectra of the β-lactoglobulin/gum mixtures deposited as films, recorded before and after heating: *top left*, β-lactoglobulin/guar gum films; *top right*, β-lactoglobulin/xanthan gum films; bottom left, β-lactoglobulin/pectin gum films; *bottom right*, β-lactoglobulin/gum mixture films.

β-lactoglobulin from the model cookie. The protein was extracted from baked model cookies into D_2O in order to employ FTIR spectroscopy to examine the combined effects of all the ingredients incorporated in this model system on the thermal stability of β-lactoglobulin under baking conditions. Figure 5.18 shows the Fourier self-deconvolved amide I' band in the spectra of

the β-lactoglobulin extracted from the baked model cookies as well as in the spectrum of the pure food-grade β-lactoglobulin (AB from Davisco) used in the formulation as the protein source. These spectra clearly show that the secondary structure of β-lactoglobulin remained intact, such that the spectrum of the protein extracted from the baked β-lactoglobulin model cookie is virtually identical to the original spectrum of this ingredient.

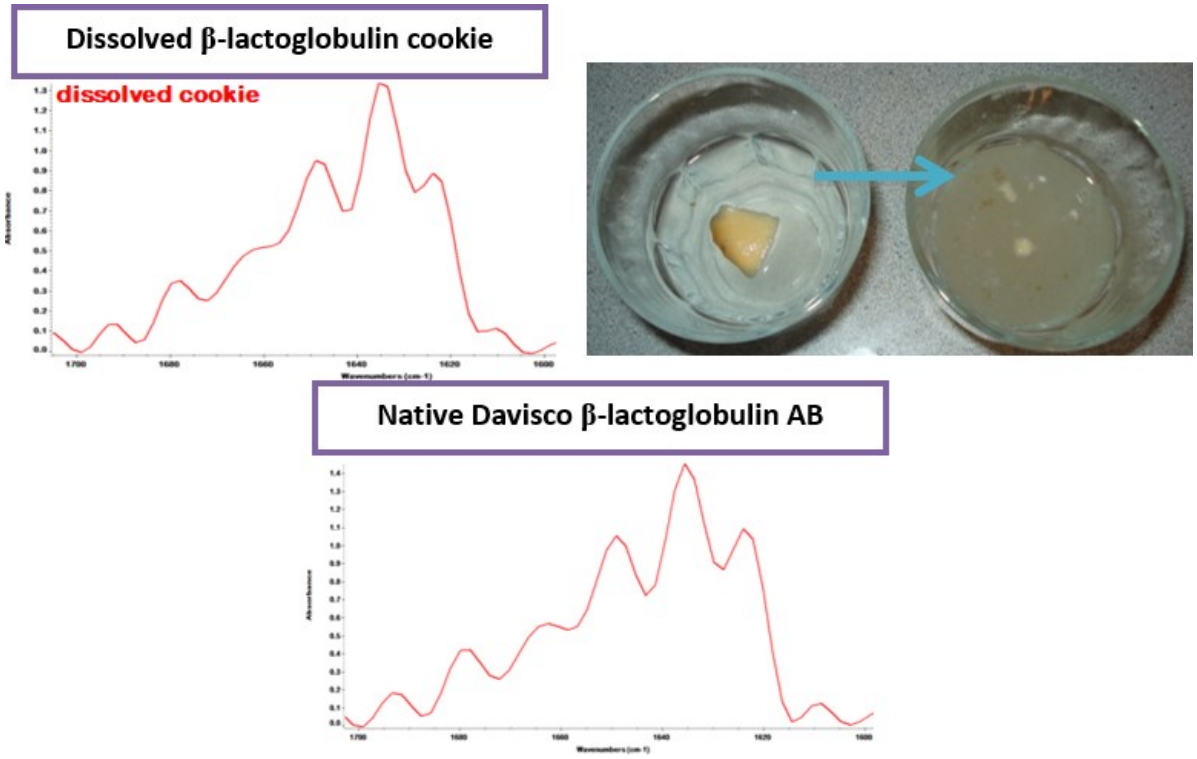

Figure 5.18. Stability of the native structure of β-lactoglobulin extracted (aqueous extraction) from the cookie model system after the baking process and its comparison to the native state of β-lactoglobulin. At the top left is the spectrum of β-lactoglobulin extracted from the β-lactoglobulin cookie model system, at the top right is the image showing how the cookie dissolved in an aqueous medium and at the bottom right is the spectrum of the native β-lactoglobulin AB from Davisco.

5.3.1.6. Sensory evaluation of the β–lactoglobulin cookie model system

The results presented in Table 5.10, show that the β-lactoglobulin cookie model was lighter in color than the whey protein isolate (WPI) cookie model. The WPI cookie model was harder than the β-lactoglobulin cookie model; the β-lactoglobulin cookie model was in the not soft/not hard category and the WPI cookie model was approaching the hard scale. The β-lactoglobulin cookie

model tended to maintain its shape while the WPI cookie model tended to break. The WPI cookie model was crispy while the β-lactoglobulin cookie model was not. Both cookie models had similar moistness tending to the drier side. Finally, while the β-lactoglobulin cookie model tended to have a milkier taste, the WPI cookie model had neither a milky nor a goaty taste.

According to Figure 5.19, using both the Tukey´s and Fisher´s tests, there were four attributes in which the β-lactoglobulin and the WPI cookie models had significant differences: color, hardness, cohesiveness and crispness; however, there were no significant differences in moistness, adhesiveness and flavor.

Table 5.10. Sensory evaluation results for the different factors considered for the model system.

	Color	Hardness	Cohesiveness	Crispness	Moistness	Adhesiveness	Flavor
β-lactoglobulin	**2.56 ± 1.12**	**4.73± 1.24**	**4.54 ± 1.57**	**2.11 ± 1.60**	**3.35 ± 1.43**	**4.67 ± 1.51**	**3.70 ± 1.89**
Whey Protein Isolate	**4.48 ± 1.20**	**4.91 ± 1.58**	**3.39 ± 1.15**	**4.35 ± 1.38**	**3.53 ± 1.46**	**4.11 ± 1.57**	**4.30 ± 1.55**

The results represent the mean ± the standard deviation of the scores obtained for each attribute based on Tables 5.3 and 5.4

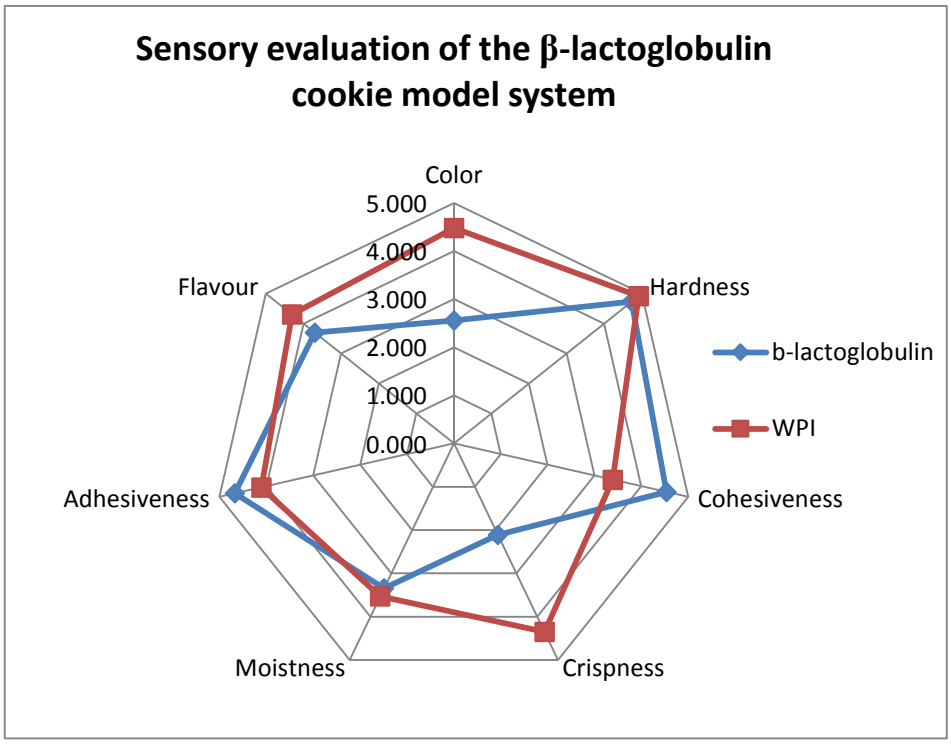

Figure 5.19. Sensory evaluation of the β–lactoglobulin cookie model system. The diagram shows the results from the evaluated attributes for the β-lactoglobulin and the whey protein isolate (WPI) cookie model systems.

The differences observed in color could be attributed to the difference in lysine content; the whey protein isolate (BiPRO®) contains both β-lactoglobulin and α–lactalbumin (the two major whey proteins), hence it contains a higher lysine content than β-lactoglobulin on its own (Davisco Foods, amino acid profile). As mentioned previously (Chapter 2), lysine is generally related to browning in the Maillard reaction. The differences in hardness, crispness and cohesiveness could also be related to the difference in the microstructure and interactions of a blend of proteins such as WPI versus the microstructure of a pure protein such as β-lactoglobulin (Maté and Krochta, 1996). However, it is necessary to also consider that sensory evaluation tests of a product are quite hard to perform because testers are different among themselves, variable over time and prone to bias (Meilgaard *et al*., 2007).

5.4. CONCLUSIONS

This chapter addressed the development and the study of a "high-protein cookie" model food system and the application of fundamental research to elucidate the molecular interactions occurring in it; texture analyses were also performed to complement the molecular studies. Several formulations were elaborated and once an "acceptable" and edible formulation was obtained, it was used as a "template formulation" for three high-protein cookie" model systems differing only in the source of protein: β-lactoglobulin, glycomacropeptide and glycomacropeptide in combination with β-lactoglobulin. Several spectroscopic techniques can be used for the study of food model systems, however two techniques were selected: FPA-FTIR spectroscopy and VP-SEM. FPA-FTIR spectroscopy was selected because it has many advantages over other spectroscopic techniques: [1] it can acquire a "chemical image" of the food product, [2] the acquisition of multiple spectra (4096 spectra) in the same time a single spectrum is acquired by conventional FTIR microspectrometry, [3] its ability to obtain a "snap-shot" of the area that is being sampled, [4] the three different modes on which the images can be acquired: transmission, transmission-reflection or ATR (Sedman *et al*., 2010; Enfield, 2010). Scanning Electron Microscopy was chosen as a complementary technique since it is widely used to elucidate the macromolecular and internal structure of baked products and food products in general (Widjanarko *et al.,* 2010, Ribotta *et al.,*2004; Zounis *et al.,* 2002).

The texture results obtained showed that all the cookie models had water activity (a_w) values around or below 0.5 and moisture content below 20%, which makes them stable for a longer shelf life by inhibiting microbial growth (Potter and Hotchkiss, 1998). Even though they had similar water activity (a_w) and moisture content values, the β-lactoglobulin cookie model had the lowest values which conferred it the crispiness and ease to crack; the GMP cookie model had the highest moisture content and a "hard and rubbery" texture that could be attributed to the presence of carbohydrates in GMP´s structure which have a higher ability to bind moisture than proteins. No spectroscopic analyses were carried out for the GMP cookie system due to its random coil structure and only the β–lactoglobulin was analyzed to study the secondary structure of β-lactoglobulin in a finished cookie model system. In order to understand the effect of each component on the secondary structure of β–lactoglobulin; films of binary mixtures of β–lactoglobulin with each component were studied using FPA-FTIR spectroscopy.

In theory, the possible effects by different components of the formulation on the secondary structure of β-lactoglobulin were: [1] β-lactoglobulin can bind hydrophobic molecules such as the oil fatty acids, hydrophobic emulsifiers and/or the hydrophobic portion of emulsifiers (DATEM) in its hydrophobic core forming either hydrogen bonds with the fatty acids but also through hydrophobic interactions with non-charged polar amino acids buried inside β-lactoglobulin's core (Tyr^{102}, Gln^{120}, Cys^{121}, Thr^{125}, Asn^{152}; Cysteine 106 and Cysteine 119 were excluded since they are already stabilizing the protein through the disulphide bond), [2] the hydrophilic portion of DATEM can interact with the hydrophilic residues of β-lactoglobulin's surface either by electrostatic repulsion or by electrostatic attraction, [3] the hydrophobic portion of DATEM interacts with the hydrophobic cavity of the α–helical portion of β-lactoglobulin, [4] sucrose has a stabilizing effect on β-lactoglobulin by increasing the gelation temperature of its secondary structure, [5] even though, the interactions between maltitol and β–lactoglobulin may be weak and unspecific, nevertheless the high concentration of maltitol prevents β–lactoglobulin from unfolding by impeding it from "moving" and by preventing it from "picking-up" moisture, [6] polydextrose may increase β–lactoglobulin's gelation temperature due to the similar functional properties it shares with sucrose, [7] gums can have synergistic or antagonistic effects on the protein stabilization depending on the electrostatic interactions (attraction and/or repulsion) of protein/polysaccharide, the stability of the gum and the water binding capacity of each gum.

However, under the conditions studied, it is more likely that the more hydrophilic, more surface active and much smaller molecules than β-lactoglobulin (such as the carbohydrates used) bound much more easily the small amount of water that was present in the formulation and this could translate into lower moisture absorption by β-lactoglobulin. This, together with the faster evaporation of water under baking conditions, could be the most likely explanation for the intact structure of β-lactoglobulin. The food model was done using β-lactoglobulin from a food grade commercial source (Davisco AB), however, this source comes as a mixture of A and B variants; much research needs to be done of each individual variant in order to understand the impact of the "lot to lot variability" in food products as a consequence of a mixed populations of each variant. Future studies should be done to elucidate the importance of β-lactoglobulin variant A, variant B and knowing the exact ratio when they are as a mixed population; understanding their differences could have a significant impact in the dairy products industry.

Chapter 6. General Conclusion

The research presented in this thesis is centered on one of the most important food proteins, β-lactoglobulin.

In the first part of this research, variable-temperature FTIR studies were undertaken to characterize food-grade β-lactoglobulin, obtained from its major commercial supplier in North America (Davisco Foods). Given that the two main genetic variants present in the milk of North American dairy cows (variants A and B) have been shown to exhibit differences in their thermal stability, flexibility, and association properties, ion-exchange chromatography was performed to separate variants A and B. Both variants A and B have been extensively studied in the past by FTIR spectroscopy, and so the overall aim of our studies was to examine the differences (if any) between samples derived from food-grade β-lactoglobulin and suitable "reference" samples of β-lactoglobulin A and β-lactoglobulin B. For this purpose, one of the variants (variant A) was isolated from fresh whole milk obtained directly from a homozygous cow, in view of uncertainty about the quality of β-lactoglobulin A purchased from its commercial supplier. Examination of the VT-FTIR and elucidation of the sequence of unfolding events by 2D-COS analysis of the VT-FTIR spectra yielded the same unfolding pathway for β-lactoglobulin A from the three sources, but the denaturation temperature and the extent of aggregation were different. These differences were attributed to the different isolation methods.

The isolation method of the protein proved to be important, however, the major differences were obtained when studying different variants of β-lactoglobulin (β-lactoglobulin A, β-lactoglobulin B and β-lactoglobulin mixture of A and B). The 2D-COS analysis showed to be restricted to the individual variants rather than the mixed variants since the mixed variants have different populations of AB, AA, and BB dimers; also, the initial spectral changes in the sequence of events delineated by the 2D-COS analysis could indicate the progression of H-D exchange of β-structure as the sample was heated.

The 1636 cm^{-1} and 1628/1624 cm^{-1} bands have been attributed to the dimer form of β-lactoglobulin and when a single component appears in this region it has been related to the monomeric form of β-lactoglobulin. However, the 1620-1636 cm^{-1} region represented a conflict because different bands were identified for the different variants and/or the mixture of variants,

plus, the bands increased in some cases and decreased in others. According to our results, the bands cannot be attributed solely to the dimer, the reason for this is that the change in the relative intensity of the 1628/1624 cm^{-1} band does not change significantly in comparison to a rise in the 1636 cm^{-1} and 1621 cm^{-1} bands, therefore: (1) this band could represent multiple populations of antiparallel β-sheets and (2) upon H-D exchange, the absorptivity of the remaining intensity under the 1628 cm^{-1} band has a much lower value. It is not clear why an absorptivity change upon H-D exchange does not manifest itself in a comparable increasing intensity at a lower wavenumber where a higher intensity would be expected. There could be three possible explanations: (1) the bandwidth changes with H-D exchange, (2) the H-D exchange of the β-sheets results in a conformational change and/or (3) the hydration of the protein with time, results in some rearrangements of the tertiary structure. The only way to answer these questions is by isotopic edited future studies where a portion of the protein is labelled with ^{13}C.

Accordingly, these bands were not assigned to the monomer/dimer equilibrium and a significant drop in the β-sheet structure at 1628/1624 cm^{-1} band was not interpreted as a profound change in the secondary structure of the protein since it was not accompanied by an equivalent change in the protein spectra in one of the variants. Hence, with our observations we concluded that the 1636 cm^{-1}, the 1621 cm^{-1} and the 1628/1624 cm^{-1} bands could be a mixed population of β-sheets, to which we referred to as: β-sheet combination 1 (1621 cm^{-1} and 1628/1624 cm^{-1}) and β-sheet combination 2 (1636 cm^{-1}). The NMR studies showed that the residues that underwent H-D exchange were not located in a single portion of the "solvent exposed" part of the structure of β-lactoglobulin but in different locations. This could also confirm that the 1624/1628 cm^{-1}, the 1621 cm^{-1} and the 1636 cm^{-1} bands of β-lactoglobulin in its dimeric form could be attributed to a mixture of multiple populations of antiparallel β-sheets.

When comparing the different variants of β-lactoglobulin, the thermal stability was in the following order: A < AB < B, being A the most thermally stable and AB mixture having a denaturation temperature in between of the two individual variants. The differences in thermal stability of each variant have been mainly attributed to the differences in amino acid constitution; however, there are many hypotheses but there is still not a clear answer.

In the mixed binary systems of GMP with β-lactoglobulin from different sources and at different ratios (β-lactoglobulin:GMP 3:1 and 1:1), it was demonstrated that GMP had different

effects on all β-lactoglobulin´s unfolding and aggregation pathways and that these effects were also different at the different ratios used in this study. GMP is a 64 amino acid peptide with no aromatic (Phe,Trp, Tyr) and no Cys amino acids, hydrophilic due to the presence of carbohydrates (sialic acid) and with no defined secondary and/or tertiary structure (random coil). There are many theories of how GMP interacts with β-lactoglobulin; to begin with, there is not much known about GMP and much less is known about GMP´s interactions with other proteins. So far, many hypotheses have been made about β-lactoglobulin/GMP interactions; however, based on the results of the present study and the literature available we propose that the most likely interactions between GMP and β-lactoglobulin are hydrogen bonds, hydrophobic interactions and electrostatic repulsions, however, we cannot propose an accurate mechanism of the effect of GMP on the tertiary and secondary structure of β-lactoglobulin based on the following statements: (1) different variants and/or mixed variants (β-lactoglobulin AB) will result in different unfolding and aggregation pathways since the mixed variants have different populations of AB, AA and BB dimers, (2) the unfolding and aggregation mechanisms of all the samples of β-lactoglobulin were affected up to a different degree when mixed in binary systems with GMP at both ratios (3:1 and 1:1), (3) the source and the isolation method of β-lactoglobulin have an impact in the protein´s behavior which is exponentially affected by the source and isolation method of GMP given that GMP is not found as a pure peptide and the degree of glycosylation will derive in very different results, (4) future studies of pure GMP and/or binary mixtures using GMP will require a quantitative determination of the concentration of sialic acid using a fluorimetric method and (5) future studies using SPR (Surface Plasmon Resonance) could be used to elucidate the binding affinity between β-lactoglobulin and GMP.

A “high whey protein cookie” model food system was developed and fundamental research techniques were used to elucidate the molecular interactions occurring in it; texture analyses were also performed to complement the molecular studies. Several spectroscopic techniques can be used for the study of food model systems, however two techniques were selected: focal plane array-Fourier transform infrared (FPA-FTIR) spectroscopy and variable pressure-scanning electron microscopy (VP-SEM). FPA-FTIR spectroscopy was selected because it has many advantages over other spectroscopic techniques such as providing “chemical images” of the sample. VP-SEM was chosen as a complementary technique to elucidate the internal structure of the baked food model.

The model was developed using β–lactoglobulin and GMP as protein sources, separately and as a mixture; only the β–lactoglobulin model was analyzed to study the secondary structure of β-lactoglobulin in a finished cookie model system. In order to understand the effect of each component on the secondary structure of β–lactoglobulin; films of binary mixtures of β–lactoglobulin with each component were studied using FPA-FTIR spectroscopy. In theory, the possible effects by different components of the formulation on the secondary structure of β-lactoglobulin could be: β-lactoglobulin can bind hydrophobic molecules such as the oil fatty acids, hydrophobic emulsifiers and/or the hydrophobic portion of emulsifiers in its hydrophobic core while the hydrophilic portion can interact with the hydrophilic residues of β-lactoglobulin's, the carbohydrates used could have a stabilizing effect on β-lactoglobulin by increasing the gelation temperature due to their water binding capacity.

However, under the conditions studied, it is more likely that the more hydrophilic, more surface active and much smaller molecules than β-lactoglobulin (such as the carbohydrates used) bound much more easily the small amount of water that was present in the formulation and this could translate into lower moisture absorption by β-lactoglobulin. This, together with the faster evaporation of water under baking conditions, could be the most likely explanation for the intact structure of β-lactoglobulin. The food model was done using β-lactoglobulin from a food grade commercial source (Davisco AB), however, this source comes as a mixture of A and B variants; much research needs to be done of each individual variant in order to understand the impact of the "lot to lot variability" in food products as a consequence of a mixed populations of each variant. Future studies should be done to elucidate the importance of β-lactoglobulin variant A and variant B and knowing the exact ratio when they are as a mixed population; understanding their differences could have a significant impact in the dairy products industry.

In conclusion, many fundamental studies of pure protein systems have been done in the past as well as studies of food matrices from a nutritional research perspective; the present research is the first one to try to elucidate the behavior of a protein´s secondary structure in a real food matrix and to try to understand the series of events happening to the protein structure under heating conditions. These studies are still very preliminary and many future studies will have to be carried out considering other spectroscopic techniques in combination with FPA-FTIR spectroscopy; however, FPA-FTIR spectroscopy remains as an inexpensive, non-destructive and efficient way to obtain information about food products at a microscopic level. Hence, the real purpose behind

these studies is to be able to apply fundamental research techniques in the food industry in order to understand better the behavior of food components with the purpose of formulating food products with higher quality, better shelf life at a lower cost; the better we understand food at a microscopic level, the better results we will obtain at a macroscopic level.

Recommendations for future work

- H-D exchange studies can be carried out by variable temperature-NMR spectroscopy of the individual β-lactoglobulin variant A and variant obtained from homozygous cows in order to identify the amino acids that are involved in the increased conformational mobility of β-lactoglobulin B variant.
- Variable temperature-FTIR studies of β-lactoglobulin variant A and variant B in the presence of binary and tertiary mixtures of other food ingredients (in place of GMP) could be undertaken to establish the impact of protein-ingredient interactions on conformational mobility, denaturation temperature and unfolding pathway of each β-lactoglobulin variant.
- The impact of varying the amount of moisture on the secondary structure proteins in model single-protein food systems. Correlation of changes in the protein secondary structure to of the functional and sensory properties of the model food can be undertaken.
- Use of β-lactoglobulin variant A and β-lactoglobulin variant B in the preparation of a model food system could be undertaken to exam the changes in the secondary structure of the protein to the functional and sensory properties of the model food system.

Appendix

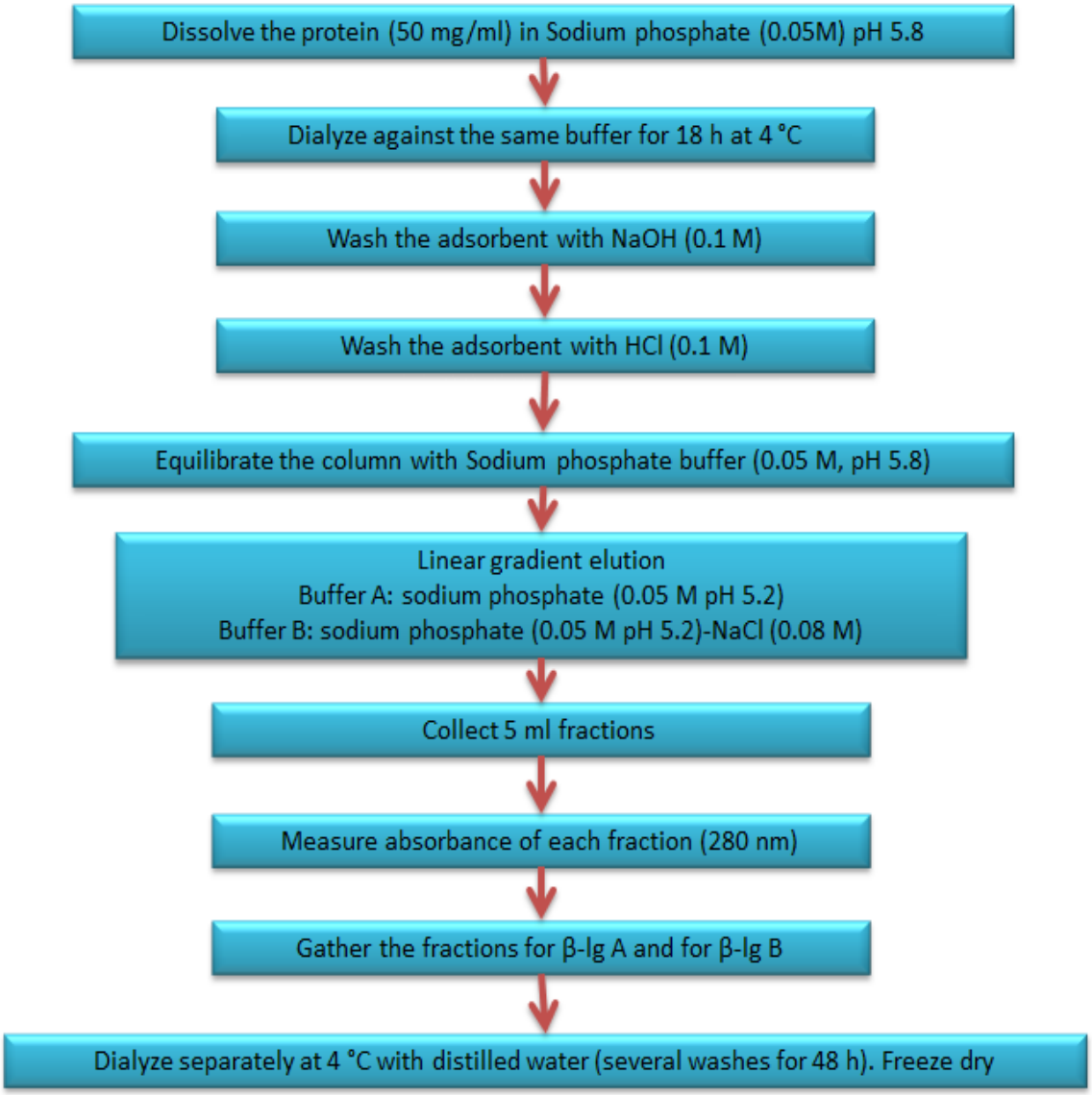

Figure A.1. β-lactoglobulin variants separation using Ion-exchange chromatography. Diagram of the procedure followed to separate a β-lactoglobulin mixture of variants A and B from a commercial source (Davisco AB).

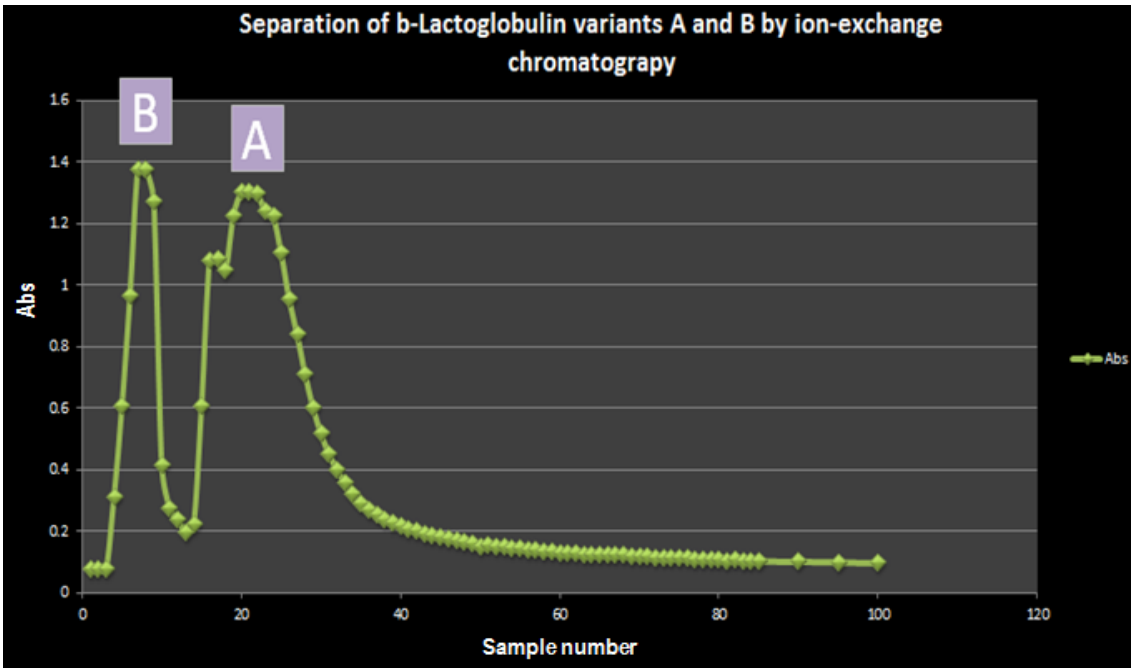

Figure A.2. Results of the separation of β-lactoglobulin variants A and B from a commercial food sample (Davisco AB); results obtained using a UV-visible spectrophotometer.

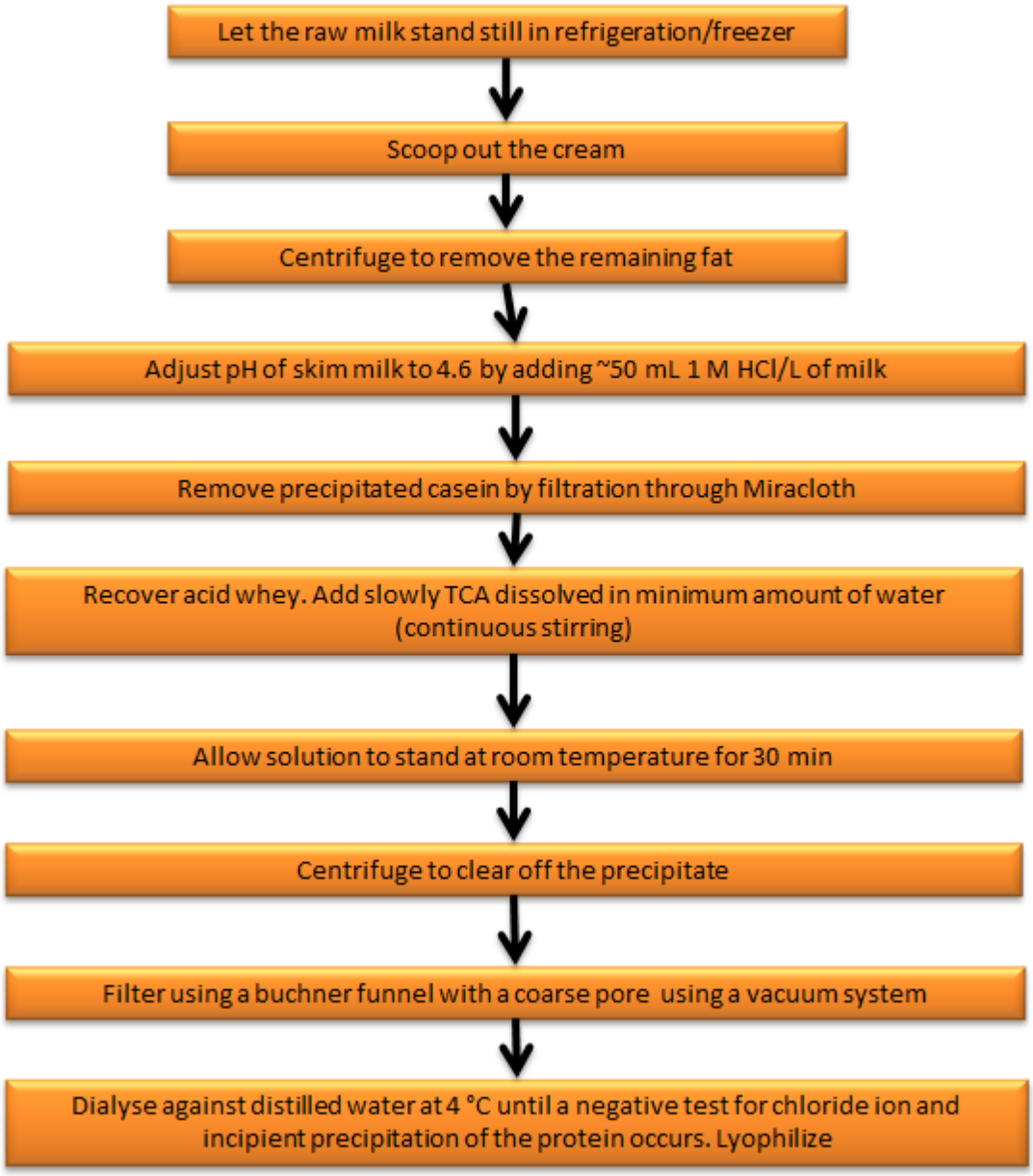

Figure A.3 Diagram of the method followed for the separation of β-lactoglobulin from milk samples using Trichloroacetic acid (TCA) (Fox et al., 1967).

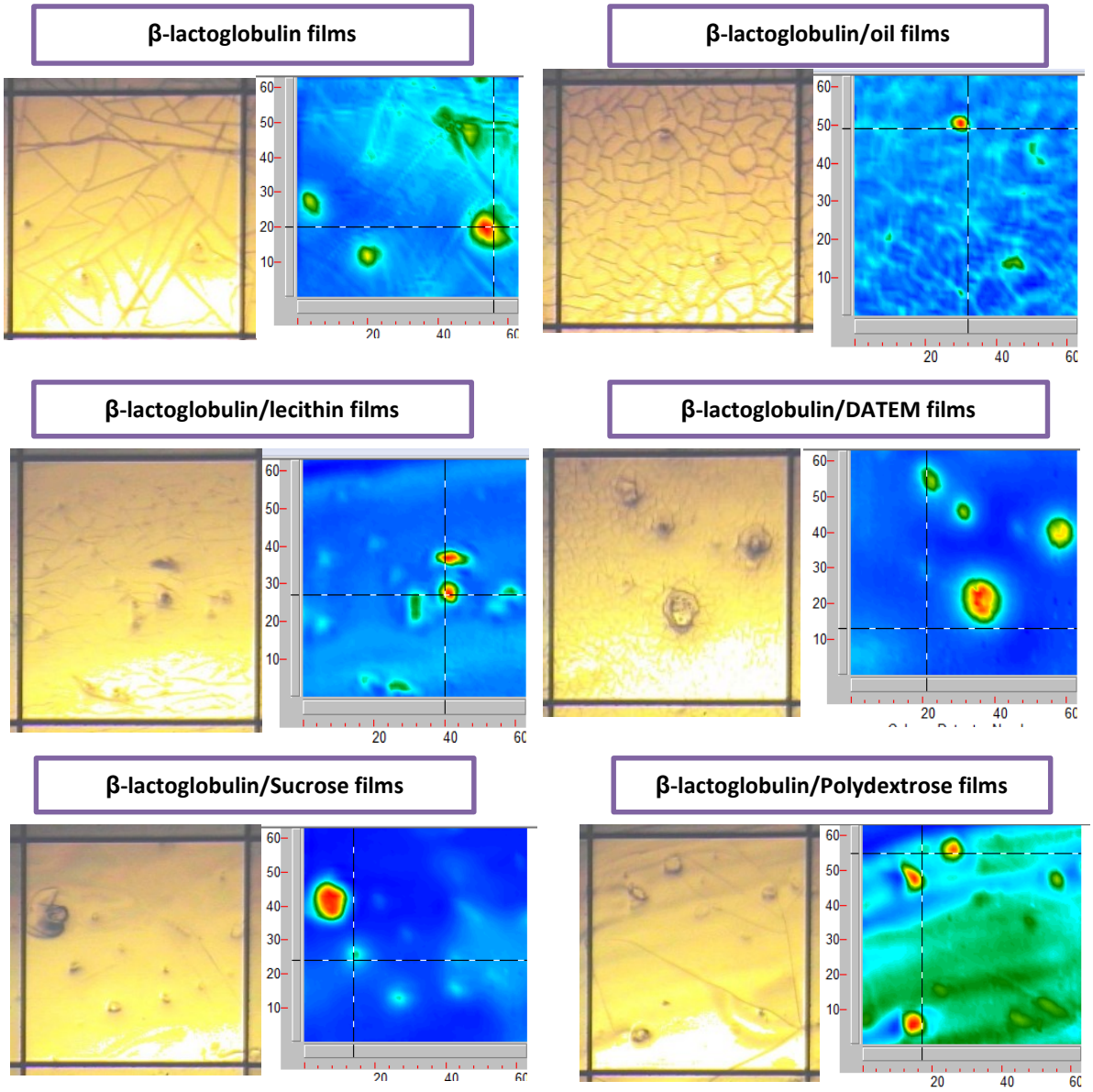

Figure A.4. "Chemical images" of the β–lactoglobulin films using FPA-FTIR microscopy (X axis: Column detector number; Y axis: Row detector number). The left image is the light microscopy image and the right image is the infrared image.

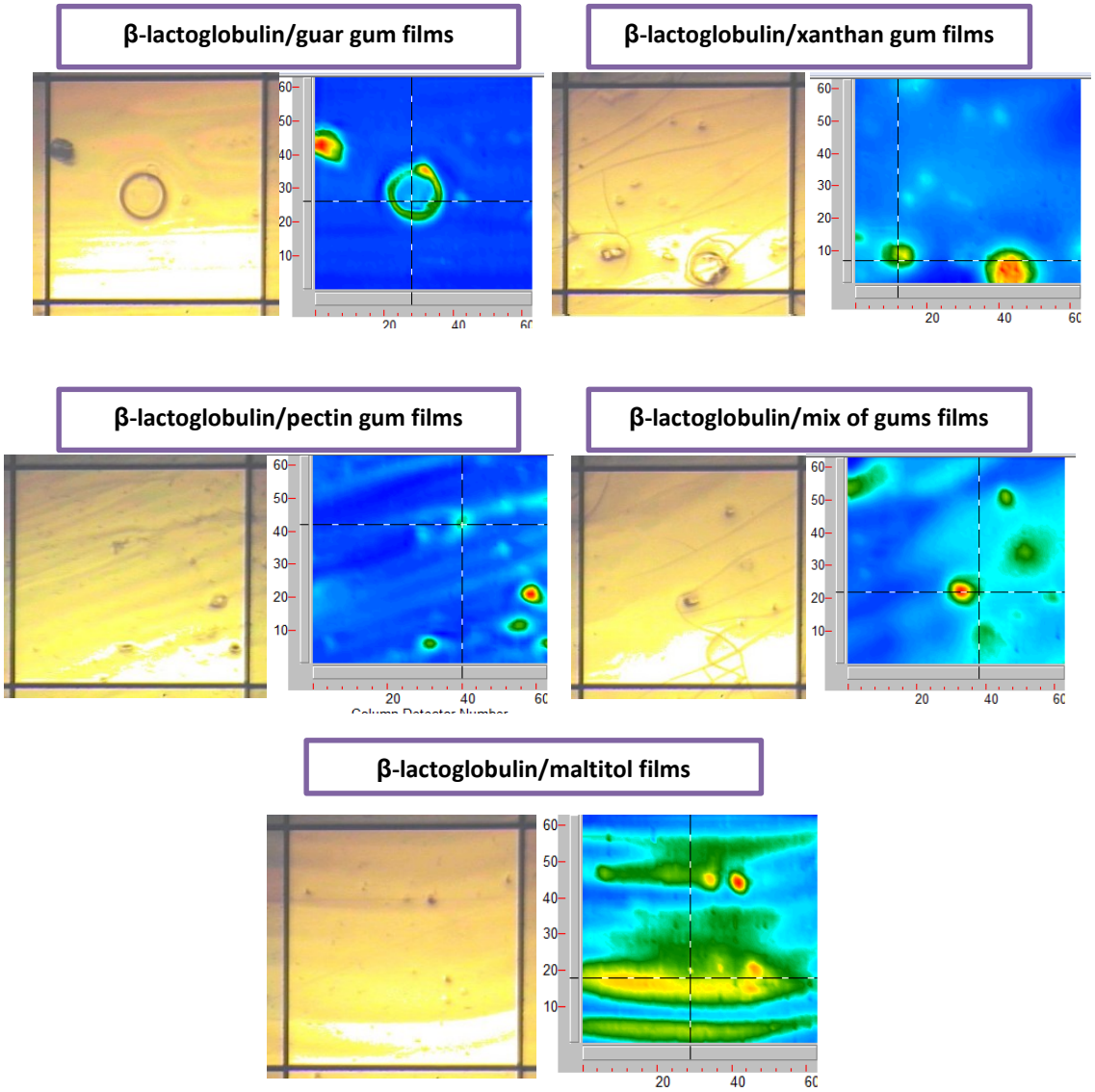

Figure A.4. (Continuation).

REFERENCES

1. Afseth, N. K., Segtnan, V. H., and Wold, J. P. 2006. Raman spectra of biological samples: A study of preprocessing methods. Appl. Spectrosc, Vol. 60(12), 1358-1367.
2. Alhaj, O. A., Kanekanian, A.D. and Peters, A.C. 2007. Investigation on whey proteins profile of commercially available milk-based probiotics health drinks using fast protein liquid chromatography (FPLC). Br. Food J. Vol. 109(6), 469-480.
3. Allain, A.F., Paquin, P. and Subirade, M. 1999. Relationships between conformation of [beta]-lactoglobulin in solution and gel states as revealed by attenuated total reflection Fourier transform infrared spectroscopy. Int. J. Biol. Macromol. Vol. 26(5), 337-344.
4. Alvarez, P.A., Ramaswamy, H.S., Ismail, A.A. 2007. Effect of high-pressure treatment on the electrospray ionization mass spectrometry (ESI-MS) profiles of whey proteins. Int. cDairy J. Vol. 17 (8), 881-888.
5. Alzagtat, A. A. and Alli, I. 2002. Protein-lipid interactions in food systems: a review. Int. J. Food Sci. Nutr. Vol. 53(3), 249-260.
6. Aranyi C. and Hawrylewicz E.J. 1968. A note on scanning electron microscopy of flours and doughs. Cereal Chem. Vol. 45, 500-502.
7. Arrondo, J. L. R. and Goni, F. M. 1999. Structure and dynamics of membrane proteins as studied by infrared spectroscopy. Prog. Biophys. Mol. Biol. Vol. 72(4), 367.
8. Auerbach M. and Dedman A.K. 2012. Bulking agents. In: Multi-Functional Ingredients. Sweeteners and Sugar Alternatives in Food Technology. Second edition (K. O'Donnell and M.W. Kearsley, Eds.). Wiley-Blackwell, West Sussex, UK.
9. Baello B.I., Pancoska P., Keiderling T.A. Baello, B. I., Pancoska, P. and Keiderling, T. A. 2000. Enhanced prediction accuracy of protein secondary structure using hydrogen exchange Fourier transform infrared spectroscopy. Anal. Biochem. Vol. 280 (1), 46-57.
10. Baier, S. and McClements, D. J. 2001. Impact of preferential interactions on thermal stability and gelation of bovine serum albumin in aqueous sucrose solutions. J. Agric. Food Chem. Vol. 49 (5), 2600-2608.
11. Bandekar, J. and Krimm, S. 1979. Vibrational analysis of peptides, polypeptides, and proteins: Characteristic amide bands of β-turns. Proc. Natl. Acad. Sci. USA Vol. 76 (2), 774.

12. Barbeau J., Gauthier S.F. and Pouliot Y. 1996. Thermal stabilization of β-lactoglobulin by whey protein peptide fractions. J. Agric. Food Chem. Vol. 44, 3939-3945.
13. Barron, C., Parker, M., Mills, E., Rouau, X., and Wilson, R. 2005. FTIR imaging of wheat endosperm cell walls in situ reveals compositional and architectural heterogeneity related to grain hardness. Planta. Vol. 220 (5), 667-677.
14. Barth, A. 2000. The infrared absorption of amino acid side chains. Prog. Biophys. Mol. Biol. Vol. 74 (3-5), 141-173.
15. Barth, A. 2000 (a). Fine-structure enhancement–assessment of a simple method to resolve overlapping bands in spectra. Spectrochim. Acta A. Vol. 56, 1223-1232.
16. Barth, A. 2007. Infrared spectroscopy of proteins. Biochim. Biophys. Acta - Bioenergetics. Vol. 1767 (9), 107.
17. Barth, A. and Zscherp, C. 2000. Substrate binding and enzyme function investigated by infrared spectroscopy. FEBS Lett. Vol. 477 (3), 151.
18. Bhattacharjee, C., Saha, S., Biswas, A., Kundu, M., Ghosh, L. and Das, K. 2005. Structural changes of β-lactoglobulin during thermal unfolding and refolding–an FT-IR and circular dichroism study. Prot. J. Vol. 24 (1), 2.
19. Belitz, H. D., Grosch, W. and Schieberle, P. 2009. Milk and dairy products. Food Chem. 498-545.
20. Belloque J. and Smith G.M. 1998. Thermal denaturation of β–lactoglobulin. A 1H NMR study. J. Agric. Food Chem. Vol. 46, 1805-1813.
21. Benichou, A., Aserin, A. and Garti, N. 2002. Protein-polysaccharide interactions for stabilization of food emulsions. J. Disp. Sci. Technol. Vol. 23 (1), 93-123.
22. Bensaïd A., Tomé, D., Gietzen, D., Even, P., Morens, C., Gausseres, N. and Fromentin, G. 2002. Protein is more potent than carbohydrate for reducing appetite in rats. Physiol. Behav. Vol. 75 (4), 577-582.
23. Beullens, K., Kirsanov, D., Irudayaraj, J., Rudnitskaya, A., Legin, A., Nicola, B. M. and Lammertyn, J. 2006. The electronic tongue and ATR-FTIR for rapid detection of sugars and acids in tomatoes. Sensors and Actuators B: Chemical. Vol. 116(1-2), 107-115.
24. Booth, D., Chase, A. and Campbell, A. 1970. Relative effectiveness of protein in the late stages of appetite suppression in man. Physiol. Behav. Vol. 5(11), 1299-1302.

25. Boye, J. I., Ma, C. Y. and Ismail, A. 2004. Thermal stability of β-lactoglobulins A and B: effect of SDS, urea, cysteine and N-ethylmaleimide. J. Dairy Res. Vol. 71(02), 207-215.
26. Boye J.I., Ma C.Y., Ismail A., Harwalkar V.R., Kalab M. 1997. Boye, J., Ma, C. Y., Ismail, A., Harwalkar, V. and Kalab, M. 1997. Molecular and microstructural studies of thermal denaturation and gelation of β-lactoglobulins A and B. J. Agric. Food Chem. Vol. 45(5), 1608-1618.
27. Boye, J. I., Ismail, A. A. and Alli, I. 1996. Effects of physicochemical factors on the secondary structure of β -lactoglobulin. J. Dairy Res. Vol. 63 (01), 97-109.
28. Brennan C.S., Blake D.E., Ellis P.R. and Schofield J.D. 1996. Effects of guar galactomannan on wheat bread microstructure and on the *in vitro* and *in vivo* digestibility of starch bread. J. Cereal Sci. Vol. 24, 151-160.
29. Brody, E. P. 2000. Biological activities of bovine glycomacropeptide. Br. J. Nutr. Vol. 84 (S1), 39-46.
30. Brownlow, S., Cabral, J. H. M., Cooper, R., Flower, D. R., Yewdall, S. J., Polikarpov, I., North, A. C. T. and Sawyer, L. 1997. Bovine β-lactoglobulin at 1.8 Å resolution-still an enigmatic lipocalin. Structure Vol. 5 (4), 481-495.
31. Burstein, E., Vedenkina, N. and Ivkova, M. 1973. Fluorescence and the location of tryptophan residues in protein molecules. Photochem. Photobiol. Vol. 18 (4), 263-279.
32. Burt, D. and Fearn, T. 1983. A quantitative study of biscuit microstructure. Starch Stärke. Vol. 35 (10), 351-354.
33. Bushmarina, N. A., Blanchet, C. E., Vernier, G. and Forge, V. 2006. Cofactor effects on the protein folding reaction: Acceleration of α-lactalbumin refolding by metal ions. Prot. Sci. Vol. 15 (4), 659-671.
34. Byler, D. M. and Susi, H. 1986. Examination of the secondary structure of proteins by deconvolved FTIR spectra. Biopolymers. Vol. 25 (3), 469-487.
35. Careri, M. and Mangia, A. 2003. Analysis of food proteins and peptides by chromatography and mass spectrometry. J. Chromatogr. A. Vol. 1000 (1-2), 609-635.
36. Casal, H. L., Köhler, U., and Mantsch, H. H. 1988. Structural and conformational changes of β-lactoglobulin B: Infrared spectroscopic study of the effect of pH and temperature. Biochim. Biophys. Acta Vol. 957, 11-20.

37. Cauvain, S. and Young, S. L. 2006. Baked Products: Science, Technology and Practice. Blackwell Publishing. Oxford, U.K.
38. Cavallieri, A. L. F. and da Cunha, R. L. 2008. The effects of acidification rate, pH and ageing time on the acidic cold set gelation of whey proteins. Food Hydrocolloids Vol. 22 (3), 439-448.
39. Chaisawang M. and Suphantharika M. 2006. Pasting and rheological properties of native and anionic tapioca starches as modified by guar gum and xanthan gum. Food Hydrocolloids Vol. 20, 641-649.
40. Chevallier, S., Colonna, P., Buléon, A. and Della Valle, G. 2000. Physicochemical behaviors of sugars, lipids, and gluten in short dough and biscuit. J. Agric. Food Chem. Vol. 48 (4), 1322-1326.
41. Childs J.L., Thompson J.L., Lillard J.S., Berry D.T. and Drake, M. 2008. Consumer perception of whey and soy protein in meal replacement products. J. Sensory Studies Vol. 23 (3), 320-339.
42. Chirgadze, Y. N. and Brazhnikov, E. 1974. Intensities and other spectral parameters of infrared amide bands of polypeptides in the helical form. Biopolymers Vol. 13 (9), 1701-1712.
43. Conforti P.A. and Lupano C.E. 2004. Functional properties of biscuits with whey protein concentrate and honey. Int. J. Food Sci. Technol. Vol. 39 (7), 745-753.
44. Cornell D.G. and Patterson D.L. 1989. Interaction of phospholipids in monolayers with β–lactoglobulin adsorbed from solution. J. Agric. Food Chem. Vol. 37 (6), 1455-1459.
45. Craig S.A.S., Holdel J.F. and Khaled M.Y. 2000. Determination of polydextrose as dietary fiber in foods. J. AOAC Int. Vol. 83 (4), 1006-1012.
46. Creamer, L.K., Plowman, J.E., Liddell, M.J., Smith, M.H., anf Hill, J.P. 1998. Micelle stability: κ-casein structure and function. J. Dairy Sci. Vol. 81(11), 3004-3012.
47. Creusot, N., Gruppen, H., Van Koningsveld, G.A., De Kruif, C.G. and Voragen, A.G. J. 2006. Peptide-peptide and protein-peptide interactions in mixtures of whey protein isolate and whey protein isolate hydrolysates. Int. Dairy J. 16(8), 840-849.
48. D'Alfonso, L., Collini, M. and Baldini, G. (2002). Does β-lactoglobulin denaturation occur via an intermediate state? Biochemistry Vol. 41 (1), 326-333.

49. Dalgleish, D. G., van Mourik, L. and Corredig, M. 1997. Heat-induced interactions of whey proteins and casein micelles with different concentrations of α-lactalbumin and β-lactoglobulin. J. Agric. Food Chem. Vol. 45(12), 480.
50. Dalgleish D.G. 2004. Food emulsions: Their structures and properties. In: Food Emulsions, Fourth edition (S.E. Friberg, K. Larsson, and J. Sjöblom, Eds.). Marcel Dekker, New York, Chapter 1.
51. Damodaran, S. and Paraf, A. (Eds.) 1997. Food Proteins and Their Applications. Marcel Dekker, New York.
52. Delaunay, D., Rabiller-Baudry, M., Gozálvez-Zafrilla, J.M., Balannec, B., Frappart, M., and Paugam, L. 2008. Mapping of protein fouling by FTIR-ATR as experimental tool to study membrane fouling and fluid velocity profile in various geometries and validation by CFD simulation. Chemical Engineering and Processing: Process Intensification. Vol. 47 (7), 110.
53. De Jongh, H. H. J., Goormaghtigh, E. and Ruysschaert, J. M. 1996. The different molar absorptivities of the secondary structure types in the amide I region: An attenuated total reflection infrared study on globular proteins 1. Anal. Biochem. Vol. 242 (1), 95-103.
54. Djuric, M., Cari, M., Milanovi, S., Teki, M. and Pani, M. 2004. Development of whey-based beverages. Eur. Food Res. Technol. Vol. 219 (4), 321-328.
55. Donato, L., Guyomarc'h, F., Amiot, S. and Dalgleish, D. G. 2007. Formation of whey protein/κ-casein complexes in heated milk: Preferential reaction of whey protein with κ-casein in the casein micelles. Int. Dairy J. Vol. 17 (10), 1161-1167.
56. Dong, A., Matsuura, J., Allison, S. D., Chrisman, E., Manning, M.C., and Carpenter, J.F. 1996. Infrared and circular dichroism spectroscopic characterization of structural differences between β-lactoglobulin A and B. Biochemistry, Vol. 35 (5), 1450-1457.
57. Doublier, J.L., Garnier, C., Renard, D. and Sanchez, C. 2000. Protein-polysaccharide interactions. Curr. Opin. Colloid Interface Sci. Vol. 5 (3-4), 202-214.
58. Dufour, E., Subirade, M., Loupil, F. and Riaublanc, A. 1999. Whey proteins modify the phase transition of milk fat globule phospholipids. Le Lait. Vol. 79 (2), 217-228.
59. Dumay, E., Laligant, A., Zasypkin, D. and Cheftel, J. C. 1999. Pressure- and heat-induced gelation of mixed β-lactoglobulin/polysaccharide solutions: scanning electron microscopy of gels. Food Hydrocolloids Volume 13 (4), 339-351.

60. Elfagm, A., and Wheelock, J. 1978. Heat interaction between α-lactalbumin, β-lactoglobulin and casein in bovine milk. J. Dairy Sci. Vol. 61 (2), 159-163.
61. Edwards, W. P. 2007. The Science of Bakery Products. Royal Society of Chemistry Publishing. Cambridge, UK.
62. Edwards P.J.B, Jameson G.B., Palmano K.P., and Creamer L.K. 2002. Heat-resistant structural features of bovine β–lactoglobulin A revealed by NMR H/D exchange observations. Int. Dairy J. 331-344.
63. Enfield A. 2010. Investigation of the high-throughput analytical performance of an FPA-FTIR imaging system. M.Sc. thesis, McGill University, Montreal.
64. Fabian, H., Schultz, C., Naumann, D., Landt, O., Hahn, U. and Saenger, W. 1993. Secondary structure and temperature-induced unfolding and refolding of ribonuclease T1 in aqueous solution: A Fourier transform infrared spectroscopic study. J. Mol. Biol. Vol. 232 (3), 967-981.
65. Fabian, H. and Vogel, H. J. 2002. Fourier transform infrared spectroscopy of calcium-binding proteins. Methods Mol. Bbiol. Vol. 173, 173, 57-74.
66. Fairbrother, P., George, W. O. and Williams, J. M. 1991. Whey fermentation: on-line analysis of lactose and lactic acid by FTIR spectroscopy. Appl. Microbiol. Biotechnol. Vol. 35 (3), 301-305.
67. Farrell, H. M., Kumosinski, T. F., Cooke, P. H., King, G., Hoagland, P. D., Wickham, E. D., Dower, H. J. and Groves, M. L. 1996. Particle sizes of purified κ-casein: Metal effect and correspondence with predicted three-dimensional molecular models. J. Prot. Chem. Vol. 15 (5), 435-445.
68. Fertsch, B., Müller, M. and Hinrichs, J. 2003. Firmness of pressure-induced casein and whey protein gels modulated by holding time and rate of pressure release. Innovative Food Science & Emerging Technologies. Vol. 4 (2), 143-150.
69. Filosa, A., Wang, Y., Ismail, A. A. and English, A. M. 2001. Two-dimensional infrared correlation spectroscopy as a probe of sequential events in the thermal unfolding of cytochromes. Biochemistry. Vol. 40 (28), 8256-8263.
70. Fitzsimons, S. M., Mulvihill, D. M. and Morris, E. R. 2007. Denaturation and aggregation processes in thermal gelation of whey proteins resolved by differential scanning calorimetry. Food Hydrocolloids Vol. 21 (4), 638-644.

71. Foroughbakhch Pournavab R. 2001. Estadística aplicada para investigadores. Third edition. Monterrey, N.L. Mexico.
72. Fox, K., Holsinger, V., Posati, L., and Pallansch, M. 1967. Separation of β-lactoglobulin from other milk serum proteins by trichloroacetic acid. J. Dairy Sci. Vol. 50 (9), 1363-1367.
73. Gallagher, E., Kenny, S., and Arendt, E. K. 2005. Impact of dairy protein powders on biscuit quality. Eur. Food Res. Technol. Vol. 221 (3), 237-243.
74. García, G. A., Clavijo, D., Mejía, Ó. R., García, A., Vittorino, M., Casadiego, C. A., Hernández, S., Cobos, C., Tovar, J., and Rey, C. A. 2007. Aspectos biomédicos de la familia de las lipocalinas; biomedical aspects of the lipocalines family. Univ. Med. Vol. 48 (2), 118-128.
75. Gerwert, K. 1993. Molecular reaction mechanisms of proteins as monitored by time-resolved FTIR spectroscopy. Curr. Opin. Struct. Biol. Vol. 3 (5), 769-773.
76. Gomaa A. 2010. An investigation of effects of microwave treatment on the structure, enzymatic hydrolysis, and nutraceutical properties of β-lactoglobulin. Ph.D. thesis, McGill University, Montreal.
77. Gomaa A., Sedman J. and Ismail A.A. 2013. An investigation of the effect of microwave treatment on the structure and unfolding pathways of β-lactoglobulin using FTIR spectroscopy with the application of two-dimensional correlation spectroscopy, Vibr. Spectrosc. Vol. *65*, 101-109.
78. Gough P. and Jenness R. 1962. Heat denaturation of β–lactoglobulins A and B. Sci. J. Series Minnesota Agric. Exp. Station, 1033-1039.
79. Graf E. and Saguy I.S. (Eds.) 1991. Food Product Development: From Concept to the Marketplace, Van Nostrand Reinhold, New York.
80. Grygorczyk A. 2009. Biophysical studies of milk protein interactions in relation to storage deffects in high protein beverages. M.Sc. thesis, McGill University, Montreal.
81. Harper W.J. 2009. Model food systems and protein functionality. In: Milk Proteins: From Expression to Food (A. Thompson, M. Boland and H. Singh, Eds.), Elsevier, Amsterdam, pp. 409-428.

82. Harte, F. M., Gurram, S. R., Luedecke, L. O., Swanson, B. G., and Barbosa-Cánovas, G. V. (2007). Effect of high hydrostatic pressure and whey proteins on the disruption of casein micelle isolates. J. Dairy Res. Vol. 74 (04), 45.
83. Havea P., Singh H. and Creamer L.K. 1998. Electrophoretic characterization of the protein products formed during heat treatment of whey protein concentrate solutions. J. Dairy Res. Vol. 65 (01), 79-91.
84. Havea P., Singh H., and Creamer L. 2001. Characterization of heat-induced aggregates of β-lactoglobulin, α-lactalbumin and bovine serum albumin in a whey protein concentrate environment. J. Dairy Res. Vol. 68, 483-497.
85. Hau J., and Bovetto L. 2001. Characterisation of modified whey protein in milk ingredients by liquid chromatography coupled to electrospray ionisation mass spectrometry. J. Chromatogr. A. Vol. 926 (1), 105–112.
86. Herceg Z., Rezek A., Lelas V., Kresic V., and Franetovic M. 2007. Effect of carbohydrates on the emulsifying, foaming and freezing properties of whey protein suspensions. J. Food Eng. Vol. 79, 279-286.
87. Hiep M.H., Endo T., Kerman K., Chikae M., Kim D.K., Yamamura S., Takamura Y., and Tamiya, E. 2007. A localized surface plasmon resonance based immunosensor for the detection of casein in milk. Sci. Technol. Adv. Mat. Vol. 8 (4), 331-338.
88. Hines M.E. and Foegeding E.A. 1993. Interactions of α-lactalbumin and bovine serum albumin with β-lactoglobulin in thermally induced gelation. J. Agric. Food Chem. Vol. 41 (3), 341-346.
89. Hoffman M.A.M. and Van Mil P. J.J.M. 1997. Heat-induced aggregation of β-lactoglobulin: role of the free thiol group and disulfide bonds. J. Agric. Food Chem. Vol. 45, 2942-2948.
90. Holsinger V.H., Posati L.P., and De Vilbiss E.D. 1974. Whey beverages: A review. J. Dairy Sci. Vol. 57, 849-859.
91. Huppertz T., and De Kruif C.G. 2007. Disruption and reassociation of casein micelles during high pressure treatment: influence of whey proteins. J. Dairy Res. Vol. 74, 194-197.
92. Ikeda S. 2003. Heat-induced gelation of whey proteins observed by rheology, atomic force microscopy, and Raman scattering spectroscopy. Food Hydrocolloids Vol. 17, 399-406.

93. Ikeda S. and Foegeding E.A. 1999. Dynamic viscoelastic properties of thermally induced whey protein isolate gels when added lecithin. Food Hydrocolloids Vol. 13, 245-254.
94. Iloro I. and Pastrana-Rios B. 2006. Simulation of FT-IR spectra and 2D-COS analysis for the H/D exchange of two related ligands. J. Mol. Struct. Vol. 799, 153-157.
95. Indyk H.E. 2009. Development and application of an optical biosensor immunoassay for α-lactalbumin in bovine milk. Int. Dairy J. Vol. 19, 36-42.
96. Iñón F.A., Garrigues S., and De la Guardia M. 2004. Nutritional parameters of commercially available milk samples by FTIR and chemometric techniques. Anal. Chim. Acta Vol. 513, 401-412.
97. Iordache M. and Jelen P., 2003. High pressure microfluidization treatment of heat denatured whey proteins for improved functionality. Innov. Food Sci. Emerging Tecnol. Vol. 4, 367-376.
98. Izydorczyk M., Cui S.W. and Wang Q. 2005. Polysaccharide gums: Structures, functional properties and applications. In: Food Carbohydrates: Chemistry, Physical Poperties and Applications. CRC Press/Taylor and Francis Group, Boca Raton, FL, Chapter 6.
99. James B. 2009. Review: Advances in "wet" electron microscopy techniques and their application to the study of food structure. Trends Food Sci. Technol. Vol. 20, 114-124.
100. Jiang Y. Jiang, Y., Li, Y., Chai, Z. and Leng, X. (2010). Study of the physical properties of whey protein isolate and gelatin composite films. J. Agric. Food Chem. Vol. 58 (8), 5100-5108.
101. Jung C. 2000. Review. Insight into protein structure and protein-ligand recognition by Fourier transform infrared spectroscopy. J. Mol. Recog. Vol. 13, 325-351.
102. Katz E.E. and Labuza T.P. 1981. Effect of water activity on the sensory crispness and mechanical deformation of snack food products J. Food Sci. Vol. 46, 403-409.
103. Kelly S.M, Jess T.J, and Price N.C. 2005. How to study proteins by circular dichroism. Biochim. Biophys. Acta. Vol. 1751 (2), 119-139.
104. Khurana H.K. and Fink A.L. 2000. Do parallel β-helix proteins have a unique Fourier transform infrared spectrum? Biophys. J. Vol. 78, 994-1000.
105. Khurana H.K., Jun S., Cho I.K., and Li Q.X. 2008. Rapid determination of sugars in comercial fruit yogurts and yogurt drinks using Fourier transform infrared spectroscopy and multivariate analysis. Appl. Eng. Agric. Vol. 24, 631-636.

106. Kirkwood J., Al-Khaldi S.F., Mossoba M.M., Sedman J., and Ismail A.A. 2004. Fourier transform infrared bacteria identification with the use of a focal-plane-array detector and microarray printing. Appl. Spectrosc. Vol. 58, 1364-1368.
107. Koffi E., Shewfelt R., and Wicker L. 2005. Storage stability and sensory analysis of UHT processed whey-banana beverages. Food Quality Vol. 28, 386-401.
108. Kötting C, and Gerwert C. 2005. Monitoring protein-ligand interactions by time-resolved FTIR difference spectroscopy. Methods Mol. Biol. Vol. 305, 261-285.
109. Krog N.J. and Sparzø F.V. 2004. Food emulsifiers: Their chemical and physical properties. In: Food Emulsions. Fourth edition. Marcel Dekker, New York, Chapter 2.
110. Kulmyrzaev A.A. and Schubert H., 2004. Influence of KCl on the physicochemical properties of whey protein stabilized emulsions. Food Hydrocolloids Vol. 18, 13-19.
111. Kulmyrzaev A.A., Chanamai R., and McClements D.J. 2000. Influence of pH and $CaCl_2$ on the stability of dilute whey protein stabilized emulsions. Food Res. Int. Vol. 33, 15-20.
112. Kubelka J. and Keiderling D.A. 2001. The anomalous infrared amide I intensity distribution in ^{13}C isotopically labeled peptide β-sheets comes from extended, multiple stranded structures. An ab initio study. J. Am. Chem Soc. Vol. 123, 6142-6150.
113. Kuligowski J., Quintas G., Esteve-Turrillas F.A., Garrigues S., and de la Guardia M. 2008. On-line gel permeation chromatography attenuated total reflectance Fourier transform infrared determination of lecithin and soybean oil in dietary supplements. J. Chromatogr. A Vol. 1185, 71-77.
114. Kumosinski T.F., Brown E.M., and Farrel H.M. 1993. Three-dimensional molecular modeling of bovine caseins: a refined, energy-minimized κ-casein structure. J. Dairy Sci. Vol. 76, 2507-2520.
115. Kundu A. and Kishor N. 2004. 1,1,1,3,3,3-Hexafluoroisopropanol induced thermal unfolding and molten globule state of bovine α-lactalbumin: calorimetric and spectroscopic studies. Biopolymers Vol. 73, 405-420.
116. Kunieda H. and Nakamura K. 1991. Effect of salt on the phase behavior in a water/ionic surfactant/alcohol system. J. Phys. Chem. Vol. 95, 8861-8866.
117. Labropoulus A.E. and Hsu S.H. 1996. Viscoelastic behavior of whey protein isolates at the sol-gel transition point. J. Food Sci. Vol. 61, 65-68.

118. Labuza T.P. and Hyman C.R.1998. Moisture migration and control in multi-domain foods. Trends Food Sci. Technol. Vol. 9, 47-55.
119. Law A. and Leaver J. 2000. Effect of the pH on the thermal denaturation of whey proteins in milk. J. Agric. Food Chem. Vol. 48, 672-679.
120. Lee S.H., Lefèvre T., Subirade M., and Paquin P. 2007. Changes and roles of secondary structures of whey protein for the formation of protein membrane at soy/oil water interface under high-pressure homogenization. J. Agric. Food Chem. Vol. 55, 10924-10931.
121. Lee C.A. and Vickers Z.M. 2008. The astringency of whey protein beverages is caused by their acidity. Int. Dairy J. Vol 18, 1153-1156.
122. Lefèvre T. and Subirade M., 1999. Structural and interaction properties of β-lactoglobulin as studied by FTIR spectroscopy. Int. J. Food Sci. Technol. Vol. 34, 419-428.
123. Li-Chan, E.C.Y. 2010. Introduction to vibrational spectroscopy in food science. In: Applications of Vibrational Spectroscopy in Food Science, Vol. I (E.C.Y. Li-Chan, P.R. Griffiths and J.M. Chalmers, Eds.), Wiley, New York. pp. 3-29.
124. Lim K., Van Calcar S.C., Nelson K.L., Gleason S.T., and Ney D.M. 2007. Acceptable low-phenylalanine foods and beverages can be made with glycomacropeptide from cheese whey for individuals with PKU. Mol. Gen. Metab. Vol. 92, 176-178.
125. Lim S.Y., Swanson B.G., and Clark S. 2008. High hydrostatic pressure modification of whey protein concentrate for improved functional properties. J. Dairy Sci. Vol. 91, 1299-1307.
126. Livney Y.D. 2010. Milk proteins as vehicles for bioactives. Curr. Opin.Colloid Interface Sci. Vol. 15, 73–83.
127. López-Fandiño R. 2006. Functional improvement of milk whey proteins induced by high hydrostatic pressure. Crit. Rev. Food Sci. Nutr. Vol. 46, 351-363.
128. Lucena M.E., Alvarez S., Menéndez C., Riera F.A., and Alvarez R. 2006. Beta-lactoglobulin removal from whey protein concentrates. Production of milk derivatives as a base for infant formulas. Sep. Purif. Technol. Vol. 52, 310-316.
129. Lucey J.A., Tamehana M., Singh H., and Munro P.A. 1998. Effect of interactions between denatured whey proteins and casein micelles on the formation and rheological properties of acid skim milk gels. J. Dairy Res. Vol. 65, 555-567.

130. Madureira A.R., Pereira C.I., Gomes A.MP., Pintado M.E., and Malcata F.X. 2007. Review Bovine whey proteins – Overview on their main biological properties. Food Res. Int. Vol. 40, 1197-1211.

131. Malin E.L., Alaimo L.H., Brown E.M., Aramini J.M., Germann M.W., Farrel H.M., McSweeney P.L.H., and Fox P.F. 2001. Solution structures of casein peptides: NMR, FTIR, CD, and molecular modeling studies of α_{s1}-casein, 1-23. J. Food Chem. Vol. 20, 391-404.

132. Manderson G.A., Creamer L.K. and Hardman M.J. 1999. Effect of heat treatment on the circular dichroism spectra of bovine β–lactoglobulin A, B and C. J. Agric. Food Chem. Vol. 47, 4557-4567.

133. Marchesseau S., Mani J.C., Martineau P., Roquet F., Cuq J.L., and Pugniere M. 2002. Casein interaction studied by the surface plasmon resonance technique. J. Dairy Sci. Vol. 85, 2711-2721.

134. Martínez M.J., Farías M.E. and Pilosof A.M.R. 2010. The dynamics of heat gelation of casein glycomacropeptide - β-lactoglobulin mixtures as affected by interactions in the aqueous phase. Int. Dairy J. Vol. 20. pp. 580-588.

135. Martínez M.J., Carrera Sánchez C., Rodríguez Patino J.M. and Pilosof A.M.R. 2009. Interactions in the aqueous phase and adsorption at the air-water interface of caseinoglycomacropeptide (GMP) and β-lactoglobulin mixed systems. Colloids Surf. B: Biointerfaces. Vol. 68, 39-47.

136. Martins P.A.T., Gomes F., Vaz W.L.C., and Moreno M.J. 2008. Binding of phospholipids to β-lactoglobulin and their transfer to lipid bilayers. Biochim. Biophys. Acta Vol. 1778, 1308-1315.

137. Maté J.I. and Krochta J.M. 1996. Comparison of oxygen and water vapor permeabilities of whey protein isolate and β–lactoglobulin edible films. J. Agric. Food Chem. Vol. 44, 3001-3004.

138. McGuffey M.K., Epting K.L., Kelly R.M., and Foegeding E.A. 2005. Denaturation and aggregation of three α-lactalbumin preparations at neutral pH. Vol. 53, 3182-3190.

139. McHugh, T.H. and Krochta, J.M. 1994. Sorbitol- vs glycerol-plasticized whey protein edible films: integrated oxygen permeability and tensile property evaluation. J. Agric. Food Chem. Vol. 42 (4), 841-845.

140. McHugh, T.H., Aujard, J.F. and Krochta, J. 1994. Plasticized whey protein edible films: water vapor permeability properties. J. Food Sci. Vol. 59 (2), 416-419.

141. Meilgaard M.C., Vance Civille G. and Carr B.T. 2007. Sensory Evaluation Techniques. Fourth edition. CRC Press/Taylor and Francis Group, Boca Raton, FL.

142. Meza-Nieto M.A., Vallejo-Córdoba B., González Córdova A.F., Félix L., and Goycoolea F.M. 2007. Effect of β-lactoglobulin A and B whey protein variants on the rennet induced gelation of skim milk gels in a model reconstituded skim milk system. J. Dairy Sci. Vol. 90, 582-593.

143. Mitchell H.L. 1996. The role of the bulking agent polydextrose in fat replacement. In: Handbook of Fat Replacers. CRC Press, Boca Raton, FL. Chapter 11.

144. Miyawaki O. 2007. Hydration state change of proteins upon unfolding in sugar solutions. Biochim. Biophys. Acta Vol. 1774, 928–935.

145. Mizuguchi M., Nara M., Ke Y., Kawano K., Hiraoki T., and Nitta K. 1997. Fourier-transform infrared spectroscopic studies in the coordination of the side-chain COO^- groups to Ca^{2+} in equine lysozyme. Eur. J. Biochem. Vol. 250, 72-76.

146. Mohsen S.M., Fadel H.M., Bekhit M.A., Edris A.E. and Mohamad Y.S.A. 2009. Effect of substitution of soy protein isolate on aroma volatiles, chemical composition and sensory quality of wheat cookies. Int. J. Food Technol. Vol. 44, 1705-1712.

147. Moros J., Iñón F.A., Garrigues S., and De la Guardia M. 2005. Determination of the energetic value of fruit and milk-based beverages through partial-least-squares attenuated total reflectance-Fourier transform infrared spectrometry. Anal. Chim. Acta Vol. 538, 181-193.

148. Moros J., Iñón F.A., Khanmohammadi M. Garrigues S., and De la Guardia M. 2006. Evaluation of the application of attenuated total reflectance-Fourier transform infrared spectrometry (ATR, FTIR) and chemometrics to the determination of nutritional parameters of yogurt samples. Anal. Bioanal. Chem. Vol. 385, 708-715.

149. Muller-Renaud S., Dupont D., and Dulieu P. 2004. Quantification of β-casein in milk and cheese using an optical immunosensor. J. Agric. Food Chem. Vol. 52, 659-664.

150. Nara M. and Tanokura M. 2008. Infrared spectroscopic of the metal-coordination structures of calcium-binding proteins. Biochem. Biophys. Res. Commun. Vol. 369, 225-239.

151. Ngarize S., Adams A., and Howell N. 2004. Studies of egg albumin and whey protein interactions by FT-Raman spectroscopy and rheology. Food Hydrocolloids Vol. 18, 49-59.
152. Ngarize S., Adams A., and Howell N. 2005. A comparative study of heat and high pressure induced gels of whey and egg albumen proteins and their binary mixtures. Food Hydrocolloids Vol. 19, 984-996.
153. Noyelle K. and Van Dael H. 2002. Kinetics of conformational changes induced by the binding of various metal ions to bovine α-lactalbumin. J. Inorg. Biochem. Vol. 88, 69-76.
154. Nylander T. 2004. Interactions between proteins and polar lipids. In: Food Emulsions. Fourth edition. Marcel Dekker, New York, Chapter 4.
155. Oho E., Asai N. and Itoh S. 2000. Image quality improvement using helium gas in low voltage variable pressure scanning electron microscopy. J. Electron Microscopy. Vol. 49 (6), 761-763.
156. Oldfield D.J., Singh H., Taylor M.W., and Pearce K.N. 1998. Kinetics of denaturation and aggregation of whey proteins in skim milk heated in a Ultra-high temperature (UHT) pilot plant. Int. Dairy J. Vol. 8, 311-318.
157. Ono T., Yada R., Yutani K. and Nakai S. 1987. Comparison of conformations of κ–casein, para-κ-casein and glycomacropeptide. Biochim. Biophys. Acta Vol. 911, 318-325.
158. Onwulata C.I., and Huth P.J. 2008. Whey Processing, Functionality and Health Benefits. IFT Press Wiley-Blackwell, Iowa. Pp.101.
159. Owusu-Apenten, R.K. 2004. Testing protein functionality in model food systems. In: Proteins in Food Processing. CRC Press,Washington, D.C. Boca Raton FL. Chapter 10.
160. Ozkoc S.E., Sumnu G., Sahin S. and Turabi E. 2009. Investigation of physicochemical properties of breads baked in microwave and infrared-microwave combination ovens during storage. Eur. Food Res. Technol. Vol. 228, 883-893.
161. Parris N., Anema S.G., Singh H., and Creamer L.K. 1993. Aggregation of whey proteins in heated sweet whey. J. Agric. Food Chem. Vol. 41, 460-464.
162. Pelegrine D.H.G. and Gasparetto C.A. 2005. Whey proteins solubility as function of temperature and pH.Lebensm.-Wiss. Technol. Vol. 38, 77-80.
163. Perez M.D. and Calvo M. 1995. Interaction of β-lactoglobulin with retinol and fatty acids and its role as a possible biological function for this protein: a review. J. Dairy Sci. Vol. 78, 978-988.

164. Pérez S.R., Osella C.A., de la Torre M.A., and Sánchez H.D. 2008. Efecto del mejoramiento proteico sobre los parámetros de calidad nutricional y sensorial de galletitas dulces (cookies). Arch. Latinoamer. Nutritionales Vol. 58 (4), 403-410.

165. Permyakov E.A. and Berliner L.J. 2000. Minireview: α-lactalbumin: structure and function. FEBS Lett. Vol. 473, 269-274.

166. Phan The D., Debeaufort F., Luu D. and Voilley A. 2008. Moisture barrier, wetting and mechanical protperties of shellac/agar or shellac/cassava starch bilayer bio-membrane for food applications. J. Memb. Sci. Vol. 325, 277-283.

167. Piez K.A., Davie E.W., Folk J.E. and Gladner J.A. 1961. β-lactoglobulins A and B: I. Chromatographic separation and amino acid composition. J. Biol. Chem. Vol. 236 (11), 2912-2916.

168. Potter N.N. and Hotchkiss J.H. 1998 Food Science. Fifth edition. Kluwer Academic/Plenum Publishers, New York.

169. Prabakaran S. and Damodaran S. 1997. Thermal unfolding of β-lactoglobulin: characterization of initial unfolding events responsible for heat-induced aggregation. J. Agric. Food Chem. Vol. 45, 4303-4308.

170. Qi L.X., Brownlow, S., Holt, C. and Sellers, P. 1995. Thermal denaturation of β-lactoglobulin: effect of protein concentration at pH 6.75 and 8.05. Biochim. Biophys. Acta Vol. 1248 (1), 43-49.

171. Qi L.X., Holt C., McNulty D., Clarke D.T., Brownlow S., and Jones G.R. 1997. Effect of the temperature on the secondary structure of β-lactoglobulin at pH 6.7, as determined by CD and IR spectroscopy: a test of the molten globule hypothesis. Biochem. J. Vol. 324, 341-346.

172. Qin B.Y., Bewley M.C., Creamer L.K., Baker E.N. and Jameson G.B. 1999. Functional implications of structural differences between variants A and B of bovine β–lactoglobulin. Prot. Sci. Vol. 8, 75-83.

173. Rahmelow K., Hubner W., and Ackermann T. 1998. Infrared absorbances of protein side chains. Anal. Biochem. Vol. 257, 1-11.

174. Ranhotra G.S., Lee C., and Gelroth J.A.N. 1980. Nutritional characteristics of high-protein cookies. J. Agric. Food Chem. Vol. 28, 507-509.

175. Rich L.M. and Foegeding E.A. 2000. Effects of sugars on whey protein isolate gelation. J. Agric. Food Chem. Vol. 48, 5046-5052.
176. Ribotta P.D., Pérez G.T., León A.E. and Añón M.C. 2004. Effect of emulsifier and guar gum on micro structural, rheological and baking performance of frozen bread dough. Food Hydrocolloids Vol. 18, 305-313.
177. Robbins P.T., Elliott B.L., Fryer P.J., Belmar M.T., and Hasting A.P.M. 1999. A comparison of milk and whey fouling in a pilot scale plate heat exchanger: implications for modeling and mechanistic studies. Food Bioproducts Process. Vol. 77, 97-106.
178. Rosell C.M., Collar C. and Haros M. 2007. Assessment of hydrocolloid effects on the thermo-mechanical properties of wheat using the Mixolab. Food Hydrocolloids Vol. 21, 452-462.
179. Rule G.S. and Hitchens T.K. 2006. Fundamentals of Protein NMR Spectroscopy. Springer. Dordrecht. The Netherlands.
180. Saadati Z. and Bordbar A.K. 2008. Stability of β-lactoglobulin A in the presence of sugar osmolytes estimated from their guanidinium chloride-induced transition curves. Prot. J. Vol. 27, 455–460.
181. Sabanis D., Lebesi D., and Tzia C. 2009. Effect of dietary fibre enrichment on selected properties of gluten-free bread. Food Sci. Technol. Vol. 42, 1380–1389.
182. Sakuno M.M., Matsumoto S., Kawai S., Taihei K. and Matsumura Y. 2008. Adsorption and structural change of β-lactoglobulin at the diacylglycerol-water interface. Langmuir Vol. 24, 11483-11488.
183. Samant S.K., Singhal R.S., Kulkarni R.S., and Rege D.V. 1993. Protein-polysaccharide interactions: a new approach in food formulations. Int. J. Food Sci. Technol. Vol. 28, 547-562.
184. Samhouri M., Abu-Ghoush M., Yaseen E., and Herald T. 2009. Fuzzy clustering-based modeling of surface interactions and emulsions of selected whey protein concentrate combined to κ-carrageenan and gum Arabic solutions. J. Food Eng. Vol. 91, 10-17.
185. Sánchez C., Mekhloufi G., Schmitt C., Renard D., Robert P., Lehr C.M., Lamprecht A., and Hardy J. 2002. Self-assembly of β-lactoglobulin and acacia gum in aqueous solvent: structure and phase-ordering kinetics. Langmuir Vol. 18, 10323-10333.
186. Schultz C.P. 2000. Illuminating folding intermediates. Nature Struct. Biol. Vol. 7, 7-10.

187. Sedman J., Ghetler A., Enfield A., and Ismail AA. 2010. Infrared imaging: princples and practices. In: Applications of Vibrational Spectroscopy in Food Science, Vol. I (E.C.Y. Li-Chan, P.R. Griffiths and J.M. Chalmers, Eds.), John Wiley & Sons, New York, pp. 109-131.

188. Semenova M.G., Antipova A.S., and Belyakova A.S. 2002. Food protein interactions in sugar solutions. Curr. Opin. Colloid Interface Sci. Vol. 7, 438-444.

189. Seol Yuk J., Yi S.J., Lee H.G., Kim Y.M., and Ha K.S. 2003. Characterization of surface plasmon resonance wavelength by changes of protein concentration on protein chips. Sensors and Actuators B. Vol. 94, 161-164.

190. Sibel A.A., Karagözlü C. and Ünal G. 2008. Rheological properties of reduced-fat and low-fat ice cream containing whey protein isolate and inulin. Eur. Food Res. Technol. Vol. 227. 889-895.

191. Siebert F. 1995. Infrared spectroscopy applied to biochemical and biological problems. Methods Enzymol. Vol. 246, 501-526.

192. Sivakesava S., Irudayaraj J.M.K. and Korach R.L. 2001. Detection of adulteration in apple juice using mid infrared spectroscopy. Appl. Agric. Eng. Vol. 17. 815-820.

193. Slayton R.M. and Anfinrud P.A. 1997. Time-resolved mid-infrared spectroscopy: methods and biological applications. Curr. Opin. Struct. Biol. Vol. 7, 717-721.

194. Singha R., Radha C., Prakash J., and Kaul P. 2007. Whey protein hydrolysate: Functional properties, nutritional quality and utilization in beverage formulation. Food Chem. Vol. 101, 1484-1491.

195. Smith B.C. 1996. Fundamentals of Fourier Transform Infrared Spectroscopy. CRC Press, Boca Raton, FL pp. 139-155.

196. Smith E.A., Erickson G.M., Ulijasz A.T., Weisblum B., and Corn R.M. 2003. Surface plasmon resonance inaging of transcription factor proteins: interactions of bacterial response regulators with DNA arrays on gold films. Langmuir Vol. 19, 1486-1492.

197. Smithers G.W. 2008. Whey and whey proteins-From gutter to gold. Int. Dairy J. Vol. 18, 695-704.

198. Sørensen L.K., Lund M., and Jull B. 2003. Accuracy of Fourier transform infrared spectrometry in determination of casein in dairy cows´ milk. J. Dairy Res. Vol. 70, 445-452.

199. Sumnu G., Koksel F., Sahin S., Basman A. and Meda V. 2010. The effects of xanthan and guar gums on staling of gluten-free rice cakes baked in different ovens. Int. J. Food Sci. Technol. Vol. 45, 87-93.

200. Susi H., Timasheff S.N., and Stevens L. 1967. Infrared spectra and protein conformations in aqueous solutions I. The amide I band in H_2O and D_2O solutions. J. Biol. Chem. Vol. 242, 5460-5466.

201. Taulier N., and Chalikian T.V. 2001. Characterization of pH-induced transitions of β-lactoglobulin: ultrasonic, densimetric, and spectroscopic studies. J. Mol. Biol. Vol. 314, 873-889.

202. Tcholakova S. Denkov N., Sidzhakova D., and Cambell B. 2006. Effect of thermal treatment, ionic strength, and pH on the short-term and long-term coalescence stability of β-lactoglobulin interactions. Langmuir Vol. 22, 6042-6052.

203. Temelli F., Bansema C., and Stobbe K. 2004. Development of an orange-flavored barley β-glucan beverage with added whey protein isolate. Sens. Nutr. Qual. Food. Vol. 69, S237-S242.

204. Tilleman K., Deforce D. and Elewaut D. 2005. Review, Rheumatology: a close encounter with proteomics. Rheumathology. Vol. 44, 1217–1226.

205. Timasheff S.N., Susi H., and Stevens L. 1967. Infrared spectra and protein conformations in aqueous solutions II. Survey of globular proteins. J. Biol. Chem. Vol. 242, 5467-5473.

206. Timasheff S.N. 1998. Control of protein stability and reactions by weakly interacting cosolvents: the simplicity of the complicated. Adv. Prot. Chem. Vol. 51, 355-432.

207. Troullier A., Reinstädler D., Dupont Y., Naumann D., and Forge V. 2000. Transient non-native secondary structures during the refolding of α-lactalbumin detected by infrared spectroscopy. Nat. Struct. Biol. Vol. 7, 78-86.

208. Turgeon S.L. and Beaulieu M. 2001. Improvement and modification of whey protein gel texture using polysaccharides. Food Hydrocolloids. Vol. 15, 583-591.

209. Turgeon S.L., Beaulieu M., Schmitt C., and Sanchez C. 2003. Protein-polysaccharide interactions: phase-ordering kinetics, thermodynamic and structural aspects. Curr. Opin. Colloid Interface Sci. Vol. 8, 401-414.

210. Uhrínová S., Uhrín D., Denton H., Smith M., Sawyer L., and Barlow P.N. 1998. Complete assignment of ^{1}H, ^{13}C and ^{15}N chemical shifts for bovine β–lactoglobulin: secondary

structure and topology of the native state is retained in a partially unfolded form. J. Biomol. NMR. Vol. 12, 89-107.

211. Vandewater K. and Vickers Z. 1996. Higher-protein foods produce greater sensory-specific satiety. J. Physiol. Behav. Vol. 59 (3), 579-583.

212. Van der Ven C., Muresan S., Gruppen H., De Bont D.B, A., Merck K.B., Voragen A.G.P. 2002. FTIR spectra of whey and casein hydrolysates in relation to their functional properties. J. Agric. Food Chem. V. 50. pp 6943-6950.

213. Vardin H. Tay A., Ozen B., Mauer L. 2001. Authentication of pomegranate juice concentrate using FTIR spectroscopy and chemometrics. Food Chem. V. 108. pp 742-748.

214. Vasbinder A.J., De Kruif .CG. Chapter 6: Acid-induced gelation of heat-treated milk studied by Diffusing Wave Spectroscopy. J. Colloid. Surf. B 21 (2001) 245.

215. Veldhorst M., Smeets A., Soenen S., Hochstenbach-Waelen A., Hursel R., Diepvens K., Lejeune M., Luscombe-Marsh N., Westerterp-Plantenga M. 2008. Review Protein-induced satiety: Effects and mechanisms of different proteins. Physiology & Behavior. Vol. 94. pp 300–307.

216. Vigano C., Manciu L., Buyse F., Goormaghtigh E., Ruysschaert J.M. 2001. Attenuated total reflection IR spectroscopy as a tool to investigate the structure, orientation and tertiary structure changes in peptides and membrane proteins. Biopolymers (Peptide Sci). V. 55. pp 373-380.

217. Walstra et al. 1999. Dairy technology. Principles of milk properties and processes. Marcel Dekker.

218. Walstra P., Wouters J.T.M., Geurts T.J. 2006. Dairy science and technology. Second edition. CRC/Taylor and Francis.

219. Wang, Y., Gao, W., Noda, I., &Yu, Z. (2006). A modified mean normalization method to reduce the effect of peak overlap in two-dimensional correlation spectroscopy. Journal of Molecular Structure, 799(1-3), 128-133.

220. Whitehurst R.J. 2004. Emulsifiers in food technology. Blackwell Publishing. Pp 204.

221. Widjanarko S.B., Nugroho A., Estiasih T. 2011. Functional interaction components of protein isolates and glucomannan in food bars by FTIR and SEM studies. Afr. J. Food Sci. Vol. 5(1), 12-21.

222. Yada R.Y., Jackman R.L. and Smith J.L. 1994. Protein structure-function relationships in foods. Blackie Academic & Professonal. Glasgow. UK.

223. Yalçin A.S. 2006. Emerging therapeutic potential of whey proteins and peptides. Current Pharm. Design. V. 12. pp 1637-1643.

224. Yan H., Frielinghaus H., Nykanen A., Ruokolainen J., Saiani A., Miller A.F. 2008. Thermoreversible lysozyme hydrogels: properties and an insight into the gelation pathway. Soft Matter. V. 8. pp 1313-1325.

225. Zaleska H. Ring S., Tomasik P. 2000. Apple pectin complexes with whey protein isolate. Food Hydrocolloids. V. 14. pp 377-382.

226. Zhang X. and Keiderling T.A. 2006. Lipid-induced conformational transitions of β-lactoglobulin. Biochemistry. V. 45. pp 8444-8452.

227. Zhuo P., Liu X., and Labuza T.P. 2008. Effects of moisture-induced whey protein aggregation on protein conformation, the state of water molecules, and the microstructure and texture of high-protein-containing matrix. J. Agric. Food Chem. V. 56. pp 4534-4540.

228. Zoulias E.I., Oreopoulou V. and Tzia C. 2000. Effect of fat mimetics on physical, textural and sensory properties of cookies. Int. J. Food Prop. Vol. 3(3). pp 385-397.

229. Zounis S., Quail K.J., Wootton M. and Dickson M.R. 2002. Effect of final dough temperature on the microstructure of frozen bread dough. J. Cereal Sci. Vol. 36, 135-146.